Antibodies against Neuromuscular Blocking agents in allergic patients : from mechanisms to therapeutics

Alice Dejoux

Sorbonne Université

Ecole doctorale Physiologie, Physiopathologie et Thérapeutique

Unit of Antibodies in Therapy and Pathology | UMR 1222 INSERM

Antibodies against Neuromuscular Blocking agents in allergic patients

From mechanisms to therapeutics

By Alice Dejoux

To obtain a PhD degree from Sorbonne Université in Immunology

Supervised by Dr Pierre Bruhns and Dr Aurélie Gouel-Chéron

Defense date: 21st June 2024

Jury Members

Dr Mauro Gaya | Centre d'Immunologie de Marseille-Luminy	Rapporteur
Pr Sinisa Savic | University of Leeds	Rapporteur
Dr Nathalie Heuze Vourc'h | Université de Tours	Présidente
Pr Dan Longrois | Hôpital Bichat-Claude Bernard	Examinateur
Dr Sophie Sibéril | Sorbonne Université	Examinateur
Dr Sylvie Chollet-Martin | Université Paris-Saclay	Membre Invitée

« La liberté commence là où l'ignorance finit »

Victor Hugo | Océan Prose | 1854

« La science consiste à passer d'un étonnement à l'autre »
« S'étonner c'est reconnaître sa propre ignorance »

Aristote | Métaphysique

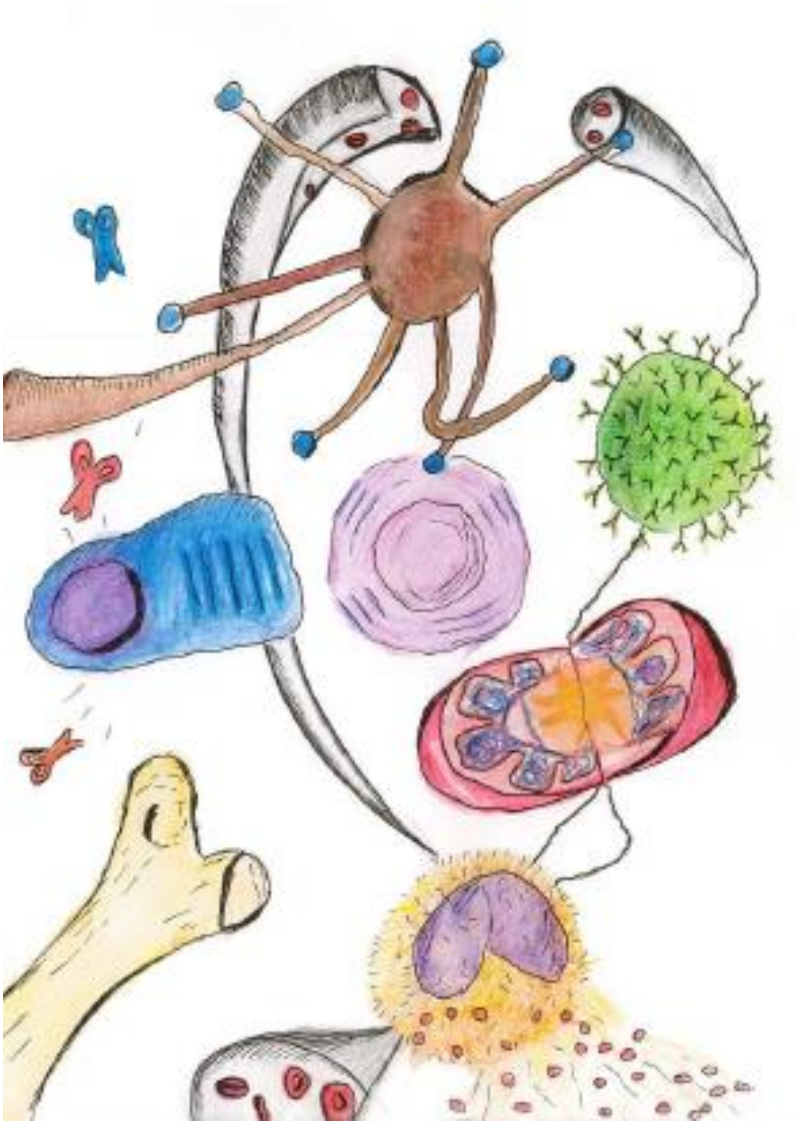

A ma famille, mes amis, mes collègues
Et toutes les belles rencontres faites durant ces quatre années : Merci.

ACKNOWLEDGMENTS

First, I would like to thank all the jury members for accepting their roles. Thank you**, Dr Gaya** and **Pr Savic,** for agreeing to give me feedback on the manuscript. Thank you **Dr Heuze Vourc'h**, **Pr Longrois**, and **Dr Sibéril for** coming on the 21st of June to discuss this work with me.

On a more personal note:

Pierre, je voudrais te remercier pour m'avoir donné la chance de vivre cette magnifique aventure scientifique et humaine. Merci de m'avoir fait confiance il y a plus de quatre ans et d'avoir vu en moi le potentiel pour mener à bien ce projet qui initialement correspondait à ma formation de chimiste. Puis, ce projet a pris une autre ampleur : j'ai appris à l'aimer et j'ai tenté de le mener le plus loin possible. Je pense que l'on partage cela. Tu as su créer un environnement où la recherche n'avait pas de limite à mes yeux. Tout était possible. Ton optimisme et ton dévouement pour ce projet m'ont portée dans cette aventure. Ton excellence scientifique et ta créativité ont permis d'embarquer ce projet encore plus loin. Chaque semaine se jalonnait de nouveaux défis : « allons produire des grammes d'anticorps pour des singes », « tentons d'immuniser des lamas », « faisons des cristaux », « produisons TOUS les anticorps pour lesquels nous avons des séquences », « nous avons un nouveau patient ! Bon, le sang arrivera à 17H de Belgique, mais il est frais ! », que nous avons réussi à relever. Tu as su me donner les clefs pour devenir une chercheuse et tu m'as transmis cette passion, merci infiniment pour tout cela.

Aurélie, ton encadrement m'a été d'un grand soutien humain et scientifique. Ton calme et ta présence m'ont permis de continuer à avancer sereinement dans ce projet quand j'ai pu faire face à des obstacles. Ton enseignement va bien au-delà de mes premiers couplages, tu m'as fait me rendre compte de l'importance que la recherche travaille main dans les mains avec la clinique. Ton implication et ton dévouement pour le projet ont permis de leur donner une tout autre dimension : grâce à toi nous avons eu des échantillons humains, tu as réussi à translater tes compétences sur des singes. Tu as parcouru plus d'une fois Paris à vélo pour m'apporter du matériel. Jamais tu ne t'es avouée vaincue face aux difficultés et j'espère avoir grandement appris de ta résilience. Merci pour ton soutien, ta présence et ton écoute.

Parmi les membres d'ATP je voudrais remercier tous ceux que j'ai pu croiser lors ces quatre années, même ceux qui sont partis. Tout d'abord je pense que toi, **François** tu as eu un impact décisif sur ce projet. Tu m'as toujours soutenue, accompagnée lorsqu'il fallait lancer des manips de tri (même de nuit). Au-delà de ton expertise en cytométrie, tu as su partager avec-moi ton amour pour les cellules B, les centres germinatifs et nos échanges scientifiques sans compter les heures font partie des beaux moments que j'aime tant dans ce que l'on fait. Juste échanger sur les sciences, faire partager le savoir. Merci de m'avoir fait découvrir cet aspect de la recherche qui m'est très cher. **Freddie**, merci de m'avoir prise sous ton aile au début de ma thèse. Tu as été la première personne à me former en biologie moléculaire, production d'anticorps, hybridomes. Tu as non seulement permis cette passation de flambeaux, mais durant toute ma thèse tu auras été d'un vrai soutien scientifique et humain. Je me souviendrais toujours de toi, qui venait me voir pour me demander comment j'allais, comment le projet avançait. **Ophélie**, sans toi la vie au labo serait différente. Tu as su me faire aimer les plus petites tâches du quotidien grâce à ta joie de vire, ton humour, ton écoute. Tu m'as appris mon premier ELISA (qui s'est terminé à 23H la veille d'un confinement), tu as répondu à toutes mes questions (scientifiques ou pas). Ta présence met une ambiance chaleureuse au labo qui rend le

quotidien plus léger. Merci pour ton sourire, merci pour ton oreille, merci pour les conseils et merci pour tout le reste (les commandes café, les soirées jeux, les congélateurs, et j'en passe). **Vanessa** et **Lise**, vous étiez initialement des collègues, puis vous êtes devenues des amies. Nos conversations sur la vie, nos moments en dehors du labo, vos conseils, votre soutien ont rendu cette expérience riche humainement. Je sais que ce n'est que le début d'une longue amitié et je vous souhaite de continuer à devenir ces magnifiques femmes scientifiques, courageuses et persévérantes dont le monde de la recherche a tant besoin. Vous m'avez montré que notre métier dépassait les manips pour remettre l'amitié au cœur de tout cela. **Bruno**, malgré nos points de vue divergents sur certains sujets, tu as su être là pour moi à ta manière et surtout tu as grandement contribué à la réussite du projet grâce à ta production MASSIVE de m1B6. Merci pour toutes ces purifs, j'espère que tu vas continuer à t'AKT(A)iver de la sorte. **Odile**, merci pour ta grande aide pour toutes les manips souris, les cultures cellulaires, tu as aussi grandement contribué à l'avancée du projet. Merci aussi pour ton dévouement dans la gestion du travail commun du labo. Dans cette même note je voudrais vous remercier, **Laetitia** et **Yidan**, pour votre aide pour les manips *in vivo,* mais aussi pour les discussions extra-professionnelles et ces moments de partage. Merci à toi **Gaël** pour avoir accepté de co-superviser ma thèse et pour ta contribution non-négligeable sur l'analyse bioinformatique des répertoires. Tu t'es toujours rendu disponible pour moi, et tu as été d'un vrai support moral et technique. J'espère que ce travail permettra aussi d'aider de futurs projets. Dans la continuité bioinformatique merci **Fred** pour cette collaboration et ton expertise en phylogénie, merci pour ton efficacité. Merci **Luc** non seulement pour ton aide sur avec les manips d'activations de basophiles, mais aussi pour tes idées foisonnantes et ton enthousiasme pour les sciences. **Matteo** et **Lorenzo**, mes chers co-doctorants, je suis heureuse d'avoir partagé ces quelques années avec vous. Merci pour ces moments aussi en dehors du labo. **Emma** (I will switch in French even though I know you speak well), thank you for the laughter and and your chill attitude. **Marion**, merci pour nos discussions et un grand grand merci pour les moments théâtraux! **Thomas**, je suis très heureuse de te transmettre le flambeau, merci pour ton support dans les manips lors de la dernière ligne droite, merci pour ton écoute et ton calme. C'était un plaisir de te transmettre ce que j'ai pu et je te souhaite le meilleur pour la suite. **Thibault** and **Alicia**, it was a pleasure to welcome you guys in the teams, I wish you the best for your projects. **Qian**, we barely met in person but thank you for the work you have undertaken on this project before me and for your quick responses to my emails. Merci à vous **Quitterie** et **Clémentine** pour votre coup de pouce sur le projet et votre dynamisme. Merc Amandine pour nos échanges et les cours de Yoga. Thank you to the other members of ATP: **Angga**, **Venkat**, **Paul**. Thank you for the previous members I did not have the chance to meet but who also greatly contributed to this project.

Merci à vous **Sophie** Sibéril et **Encarnita** Mariotti-Ferrandiz d'avoir accepté les rôles de tutrice et d'experte scientifique, respectivement. Vos retours scientifiques et méthodologiques lors des comités de suivi de thèse m'ont permis d'avancer sereinement dans ce projet. Merci à la Sorbonne Université et l'ED394 pour avoir financé ce travail. Merci aux directeurs de l'Ecole Doctorale : **Xavier** Houard et **Catherine** Monnot pour votre investissement et notamment l'organisation des journées doctorales. Merci à la **Fondation Recherche Médicale** pour avoir financé l'extension de huit mois de thèse.

Les collaborations lors de ce projet ont été riches et j'espère n'avoir oublié personne. Tout d'abord merci à toi **Sylvie** Bay, ce projet ne serait rien sans sa première pierre qui consiste à concevoir et synthétiser les dérivés de curares. Merci de m'avoir accueillie dans ton labo pour que je vienne faire des couplages. Ton soutien et tes conseils (aussi bien scientifiques que personnels) ont été très riches. Merci à toi **Christelle** pour ta grande aide sur le projet, pour ton grain de folie et nos

papoteries qui ont rendu les moments de chimie encore plus agréables. Merci à toi **Frédéric** Bonhomme pour m'avoir initiée au Maldi-Tof, que je n'ai plus quitté par la suite!
Je compte remercier toute l'équipe de la plateforme PFBMI pour leur expertise et leur gentillesse. Je pense à toi **Patrick**, avec qui j'ai passé une bonne partie de ma thèse devant le Biacore et l'Octet. Merci de m'avoir si bien formée avec patience et rigueur. Merci à vous **Bertrand** et **Sébastien** non seulement pour vos conseils qui ont permis d'améliorer le protocole de couplage en début de thèse, mais aussi pour les clefs du Maldi (que j'ai essayé de ne pas perdre plus d'une fois) et surtout pour votre gentillesse et les échanges teintés de rigolades. Merci à vous **Sylviane** et **Maelenn** pour votre disponibilité lorsque j'ai eu des soucis (surtout avec le Biacore !) et votre gentillesse.
Ahmed, je pense que tu es une de mes plus belles découvertes scientifiques et humaines de ces quatre années. J'apprécie énormément ton dévouement et ta façon si unique de m'avoir soutenue tout en me challengeant. Merci de m'avoir inclue dans toutes les étapes de la crystallo, de m'avoir amenée au Synchrotron. J'espère réellement que nos collaborations scientifiques dépasseront le cadre de ma thèse. Je veux aussi remercier toute ton équipe : **Fred**, **Cédric** et **Patrick** pour votre professionnalisme et votre bonne humeur.
Les plateformes au sein de l'Institut Pasteur contribuent grandement à la richesse scientifique des projets. Je compte donc remercier celle de CBUTechs qui m'a permis de profiter du P2+ afin de faire des tris ainsi qu'**Alix** Bourchalat pour avoir profité de la plateforme PF-CCB.
Je voudrais aussi grandement remercier l'équipe de **Felix** Rey et en particulier **Delphine** Brun pour m'avoir aidée à produire des scFv du 1B6, sans lesquels nous n'aurions pas résolu la structure cristallographique. Après avoir essayé pendant deux ans de cristalliser des Fab sans succès, cette collaboration a grandement bénéficié au projet. Merci à tous les gens de cette équipe avec qui j'ai pu travailler, je pense à vous **Ignacio**, **Atousa** et **Annalisa**.
Merci aussi **Thierry** Rose non seulement pour ton aide avec le LuLISA mais aussi pour nos échanges et ta bienveillance. Merci **Laurent** et **Cyprien** pour votre aide avec les expériences sur les mastocytes et l'organisation des congrès.

Les collaborations en dehors du cadre de l'Institut Pasteur ont aussi été très nombreuses et ont permis à ce projet de prendre un tournant décisif. Tout d'abord je compte chaleureusement remercier l'équipe de **Matthieu** Mahévas de l'Institut Necker pour m'avoir formée au tri Kelsoe. Merci à toi **Aurélien** pour avoir effectué le premier tri du patient humain qui a fonctionné dans ce projet et qui a ouvert la voie à tous les autres. **Alexis**, je ne saurais jamais suffisamment te répéter combien tu as été le pivot de ce projet. Tu m'as formée comme si j'étais l'une des vôtres, en faisant primer l'avancée des sciences et le partage des connaissances. Tu es un magnifique exemple de recherche collaboratrice et de rigueur professionnelle. Infiniment merci. Merci à toi **Pascal** pour tes conseils sur les analyses de répertoires et nos riches échanges scientifiques. **Manon**, nous avons collaboré pour un autre projet, mais ça a été un plaisir de travailler avec toi sur la Covid-19.
L'autre majeure collaboration a été avec le CEA de Fontenay-aux-Roses et l'équipe de **Roger** Legrand. Merci à tous pour votre dévouement pour le projet et votre résilience pour mener à bien les expériences. J'espère que ce n'est que le début d'une belle collaboration. Merci donc à vous **Hélène** et **Julien** pour votre résilience qui a permis de faire les premiers monitorages de curarisation chez les macaques. Et merci de faire partager avec nous votre travail et de nous inviter à observer les expériences.
I would also like to thank all the clinicians with whom we collaborated and without whom the project would not have been possible. Thank you Pr **Didier** Ebo for providing us with human samples.

Mon séjour à Pasteur a été riche en belles rencontres. Merci à mes amis co-doctorants avec qui j'ai pu passer de beaux moments au coin café, lors des JDI ou même en dehors de Pasteur. Je pense à vous **Billie**, **Ana**, **Timéa**, **Mathieu.** I am glad to have you around **Efgyny** and **Jessica**. I enjoy our breaks on the 4th floor of Metchnikoff and the nice climbing (and more) moments spent outside the lab. Merci à vous **Isma**, **Colin**, **Maxime** pour les moments de grimpe matinaux qui m'ont permis de démarrer de bonne humeur les journées au labo.

Maintenant je voudrais remercier les personnes qui ont donné toutes les couleurs à ces quatre années en dehors du cadre professionnel.

Maman, sans toi je n'aurais pas fait de thèse. Tu es mon modèle de réussite en tant que femme et chercheuse. Ton soutien infaillible et ton amour m'ont portée tout au long de cette expérience, mais aussi bien avant que je commence la thèse et je le sais aussi pour l'après. Merci d'être là pour moi, merci de me comprendre, merci pour tout. J'ai de la chance de t'avoir comme mère. Tu m'inspires grandement et je t'aime fort.
Papa, mon amour pour les sciences vient très clairement de toi. Depuis mon plus jeune âge, petite on fait des maths, de la physique, de la chimie ensemble. Tu m'as transmis cette approche ludique et rigoureuse des sciences, merci pour cela. Mais pas seulement. Merci pour ton soutien et ta présence dans toutes les étapes de ma vie. Merci pour ton amour inconditionnel. Mes parents, je sais que vous êtes mes plus grands supporters et j'ai de la chance de vous avoir.
Marinou, tu es une sœur en or. Toujours là pour moi, même quand je suis inaccessible. Merci pour ta générosité, pour nos moments de complicité, pour tes conseils sur la vie. Merci d'être ma sœur et d'être là pour moi.
Mamie, notre connexion est éternelle. J'ai tant appris de toi : à aimer la vie et aimer à apprendre. En faisant de la biologie et de la recherche médicale je sais que c'est une partie de toi qui m'accompagne. Je t'aime fort. Merci pour ton amour.
A ma famille entière : **Mimi**, **Bruno**, **Julien**, mon **parrain**, **Papoum**, **Lulu** (future chercheuse?), **Jasmine**, **Alexandre**, **Laetitia**, **Tata Régine** (ancienne pasteurienne!), **Axelle** et **Solène**. Je suis chanceuse de vous avoir parmi mes proches, on forme une belle famille que je l'espère, va continuer d'être soudée.

Puis il y a la famille que l'on choisit. Mes amis, merci à vous de m'avoir sortie de la thèse, de m'avoir ramenée à l'essentiel lorsque j'ai pu l'oublier. Merci pour les beaux moments. Je vous aime.

Je pense à toi **Ariane**, merci d'avoir été là pour moi lorsque j'en avais besoin. Merci de m'avoir ouvert les yeux quand j'étais aveuglée. Merci pour nos moments de rires, d'art, de voyages (de sport un peu aussi). J'ai de la chance de t'avoir comme amie et je sais que l'on a tant d'autres moments à vivre toutes les deux. **Laure**, mon cher binôme de grimpe, toujours disponible et présente. Merci pour nos beaux moments sportifs et musicaux. Ma chère **Clem**, en écrivant ces mots je vois ta tête qui rigole (et j'entends ton rire...). Tu es un petit rayon de soleil. Merci pour nos discussions sur la vie, pour ton écoute, pour les beaux moments. Merci à toutes les trois pour cette magnifique amitié.
Mes amies du lycée : **Camille**, **Mathilde**, **Evang**, **Stridou**, **Laliquou**, **Rerette** et **Tiph**. Merci à vous pour cette amitié qui perdure, pour les beaux moments passés ensemble qui m'ont sortie de la thèse (je pense à la Franchaie, à Bruxelles, à Munich, à Marseille et j'en passe). Petite pensée pour toi ma Cam qui m'a épaulée pendant la dure période du confinement. Je vous aime fort.
Ma **Neness** et ma **Lolo**, merci pour cette belle amitié, les dîners et les déjeuners qui donnent du baume au cœur. Merci **Adèle** pour nos discussions, ton soutien et les activités sportives. Merci à vous

Raph et **Habibou** de m'avoir accueillie chez vous le soir (malgré les couvre-feux) pendant ma première année de thèse
Merci à toi **Gaga** pour les moments de complicité autour de pique-nique, de dîners, ou de jeux. Merci à toi **Dodo** pour m'avoir fait découvrir Zurich et cette amitié improbable.
Merci à tous mes amis de grimpe qui m'ont permis de m'évader les soirs de la semaine, je pense à vous **Jéjé**, **Alex**, **Niels**, **Nolan**. Je suis heureuse de t'avoir rencontré **Pietro**, tu fais partie des belles rencontres de ma dernière année de thèse, merci de m'avoir fait découvrir un tout nouvel univers de la grimpe. Merci pour ton écoute, les rires, les photos et ton assurage irréprochable (contrairement au mien).
Merci **Alexandre** Nicolas de m'avoir accompagnée dans mes premiers pas de chercheuse en encadrant mon M1, puis de m'avoir conseillée tout du long et encore aujourd'hui. Tu es un peu mon mentor d'immunologie et je compte continuer à te demander des conseils
Loulou, mon cher parrain (et bien plus), merci pour ton amitié, tes conseils et nos longues conversations sur la vie. **PJ**, je chéris notre amitié. Merci pour les moments cinéphiles, mais aussi nos discussions.
Ma **Coco**, merci pour les rires, les voyages londoniens et pour cette amitié qui perdure d'abord depuis l'autre bout du monde et maintenant depuis l'autre côté de la Manche.
Clem, merci pour les moments sportifs (spike, grimpe) et ta vision du monde. Continue de la partager avec moi s'il te plait.
Elena, thank you for our friendship that started in London and that will probably continue in another continent...

A toi **Alice**, qui t'es beaucoup cherchée et qui finira par te trouver. J'espère que l'Alice du futur qui relira ces mots saura être fière d'elle.

TABLE OF CONTENTS

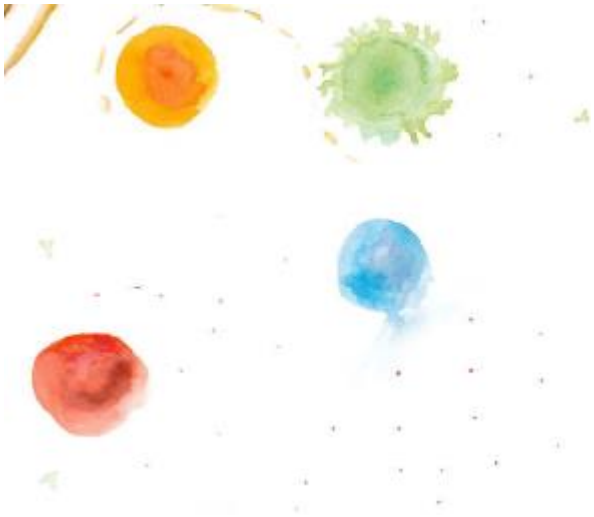

FIGURES

TABLES

ACRONYMS

AHR: Acute Hypersensitive Reaction
AID: Activation-Induced Cytidine Deaminase
AIRR: Adaptive Immune Receptor Repertoire
ASC: Antibody Secreting Cells
BCR: B Cell Receptor
Bmem: memory B cells
BSA: Bovine Serum Albumin
CD-: Cluster of Differentiation-
CD40L: CD40 Ligand
CDR: Complementarity-Determining Region
CFA: Complete Freund's Adjuvant
DNP: 2,4-dinitrophenyl
EDC: 1-Ethyl-3-(3-dimethyl aminopropyl) carbodiimide
ELISA: Enzyme-Linked Immunosorbent Assay
Fab: Fragment antigen binding
Fc: Fragment crystallizable
FcεR: Fragment crystallizable epsilon Receptor
FcγR: Fc gamma Receptors
FR: Framework Regions
HSA: Human Serum Albumin
IFA: Incomplete Freund's Adjuvant
Ig(A/G/D/E/M): Immunoglobulin (A/G/D/E/M):
IL-: interleukin -
KLH: Keyhole Limpet Hemocyanin
NHS: N-Hydroxysuccinimide
NP: 4-hydroxy-3-nitrophenyl)acetyl
mAb: monoclonal Antibody
MRGPRX2: Mas-Related G-Protein coupled Receptor member X2 on mast cells
NMBA: Neuromuscular Blocking Agent
PAF: Platelet-Activating Factor
PBMC: Peripheral Blood Mononuclear Cells
QA: Quaternary Ammonium
RAG: Recombination-Activating Gene
scFvs: Single-Chain Fragment Variable
sIgE: specific IgE
SPT: Skin Prick Test
TCR: Tell Cell Receptor
TdT: Terminal deoxynucleotidyl Transferase
TFA: Trifluoroacetic acid
Th: T helper
TOF: Train of Four
$\mathbf{T_{regs}}$: regulatory T cells
VDJ: Variable (V), Diversity (D), and Joining (J) gene fragments
VH: Variable Heavy
VHH: Variable Heavy chain antibodies
VL: Variable Light

THESIS SUMMARIES

French Summary

Le rocuronium est un curare de 530Da utilisé lors des interventions chirurgicales afin de bloquer la jonction neuromusculaire des muscles striés squelettiques, facilitant ainsi l'intubation et la chirurgie. Les curares ont deux effets secondaires graves : l'hypersensibilité aiguë (1:10,000 procédures d'anesthésie) et la curarisation résiduelle après la fin de l'intervention chirurgicale en l'absence de suivi adapté. Le rocuronium est un curare non dépolarisant largement utilisé, induisant un blocage neuromusculaire de durée intermédiaire et possédant l'incidence d'anaphylaxie la plus élevée. La cause la plus plausible d'anaphylaxie aux curares demeure l'existence d'anticorps anti-curares chez les patients, impliquant des lymphocytes B spécifiques. Cependant, aucun anticorps spécifique anti-rocuronium n'a été décrit et aucun outil biologique n'existe pour les détecter. Un seul médicament approuvé, le sugammadex, peut inverser le blocage neuromusculaire profond induit par le rocuronium, mais ce médicament provoque aussi des effets secondaires allergiques. Ce travail a donc étudié les répertoires d'anticorps IgG des patients allergiques aux curares afin de comprendre leurs (poly)clonalités et d'identifier des anticorps susceptibles d'antagoniser le blocage neuromusculaire profond.

Le rocuronium étant une petite molécule non immunogène et dépourvue de groupements chimiques réactifs, de nouveaux bioconjugués de rocuronium ont d'abord été produits par couplage sur une protéine porteuse (phénomène d'hapténisation). Le répertoire d'anticorps des lymphocytes B de patients présentant une hypersensibilité suspectée au rocuronium a ensuite été étudié à l'aide d'un système de culture cellulaire différenciant les lymphocytes B mémoires spécifiques en cellules B sécrétrices d'anticorps. Les anticorps ont été caractérisés par mesures d'affinité et de spécificité et, à l'aide d'outils bioinformatiques, les répertoires d'anticorps ont été analysés chez trois patients. Des anticorps spécifiques au rocuronium provenant de souris immunisées ont également été générés par des méthodes distinctes: hybridomes et tri microfluidique.

Les résultats montrent que les répertoires d'anticorps IgG anti-rocuronium des patients allergiques sont polyclonaux, avec une grande diversité parmi les gènes V(D)J codant pour les régions variables sans preuve d'existence de groupes clonaux. Les anticorps montrent une affinité moyenne à faible, mais celui ayant la plus forte affinité est parvenu à activer les mastocytes et à déclencher une anaphylaxie passive chez des souris transgéniques sous forme d'isotype IgE. Les anticorps isolés de souris immunisées étaient cependant d'une meilleure affinité et les répertoires oligoclonaux avec des familles V(D)J prédominantes. Exprimés sous forme d'IgE humains, les anticorps ont déclenché la dégranulation des mastocytes, des basophiles et ont induit une anaphylaxie systémique passive avec de très faibles doses

d'anticorps et d'antigène. Leurs modes de fixation avec le rocuronium ont été décryptés par cristallographie, permettant d'identifier l'ammonium quaternaire comme l'épitope allergénique potentiel. Un modèle prophylactique de prévention du blocage neuromusculaire a été établi chez la souris pour tester la capacité des anticorps à capturer le rocuronium *in vivo*. L'anticorps avec la plus grande affinité pour le rocuronium a réussi à inhiber le blocage neuromusculaire profond dans un modèle de primates avec un temps d'antagonisation compétitif avec le sugammadex.

Nous rapportons pour la première fois les répertoires humains d'anticorps dirigés contre un curare et décrivons les premiers anticorps monoclonaux anti-rocuronium en termes de spécificité, d'affinité, de structure et d'efficacité thérapeutique. Ce travail devrait permettre d'élucider les causes sous-jacentes des réactions d'hypersensibilités aigues aux curares, d'améliorer les outils de diagnostic et d'étudier de nouvelles stratégies thérapeutiques pour l'antagonisation du blocage neuromusculaire.

English Summary

Rocuronium is a 530 Da Neuromuscular Blocking Agent (NMBA) used to paralyze skeletal muscles during surgery, hence facilitating surgery and permitting intubation. NMBAs have two severe side effects: rare cases of Acute Hypersensitivity Reactions (AHR) caused by anti-NMBA antibodies in patients (1:10,000 anesthesia procedures), and residual neuromuscular blockade after the end of surgery. Rocuronium is a common non-depolarizing NMBA, inducing among the longest residual neuromuscular blockade and the highest anaphylaxis incidence. The most probable cause of anaphylaxis to NMBA remains the existence of anti-NMBA antibodies in patients, implying NMBA-specific B cells. However, no anti-rocuronium-specific antibodies have ever been described, and no biological tool is available. Only one approved drug, the cyclodextrin sugammadex, can reverse rocuronium-induced deep neuromuscular blockade but also cause allergic side effects. This work therefore investigated the IgG antibody repertoires of NMBA-allergic patients to understand their (poly)clonality and identify high-affinity antibodies that could reverse deep neuromuscular blockade.

Since rocuronium is non-immunogenic, small, and does not possess chemically reactive groups, novel rocuronium bioconjugates were first produced by haptenization on a carrier protein to perform downstream experiments. Then, the memory B cell antibody repertoires of patients with suspected hypersensitivity to rocuronium were investigated using a cell culture system differentiating rocuronium-specific memory B cells in antibody-secreting cells. The human rocuronium-specific IgG antibodies were characterized by affinity and specificity measurements and using bioinformatic tools, the repertoires of B cell receptors were analyzed in three patients, including one sample with nine years interval. Rocuronium-

specific antibodies from immunized mice were also generated with distinct methods: hybridoma technology and microfluidic sorting.

The results showed that the anti-rocuronium IgG antibody repertoires of AHR patients were polyclonal, with a high diversity among V(D)J genes coding for the antibodies' variable regions without evidence of clonal groups. The human rocuronium-specific IgG antibodies had medium to low affinity but the one with the highest affinity could activate human mast cells and trigger passive systemic anaphylaxis in transgenic mice, once switched to a human IgE antibody isotype. The antibodies isolated from immunized mice were, however, of higher affinity and the IgG antibody repertoires were oligoclonal with identical predominant V(D)J families represented in the repertoires of distinct mice. Expressed as human IgE antibodies, the antibodies isolated from immunized mice triggered mast cell, and basophil degranulation, and induced passive systemic anaphylaxis in transgenic mice with very low doses of antibody and antigen. Their binding modes with rocuronium were deciphered by X-ray crystallography, allowing the identification of the quaternary ammonium as the potential allergenic epitope. A prophylactic model of prevention of neuromuscular blockade was established in mice to test the ability of the antibodies to capture rocuronium *in vivo.* The antibody with the highest affinity for rocuronium could reverse rocuronium-induced deep neuromuscular blockade in non-human primates *in vivo* with a reversal time competitive with sugammadex.

We reported for the first time antibody repertoires to an NMBA in humans and mice, and described the first anti-rocuronium mAbs in terms of specificity, affinity, structure, and therapeutic efficacy. This work should help to elucidate the underlying causes of AHR reactions to NMBAs, to improve diagnostic tools following NMBA-mediated allergy, and to validate novel potential therapeutic strategies for the reversal of neuromuscular blockade.

Lay Summary (French)

Le rocuronium est un curare, médicament administré lors des anesthésies générales afin d'inhiber la contraction musculaire, permettant ainsi l'intubation avant la chirurgie. Il existe deux effets secondaires très graves : 1) la forme la plus sévère de réaction allergique, un choc anaphylactique souvent chez des patients n'ayant jamais été exposés à cette molécule, 2) un effet résiduel qui perdure 30-90 minutes après l'injection, conduisant à des risques de dommages de la trachée et d'infections. Ces travaux ont pour objectif de comprendre l'origine de ces allergies qui demeure inconnue et de trouver un anticorps thérapeutique qui pourrait capturer le rocuronium tel un antidote. Les premiers anticorps humains anti-rocuronium ont été isolés à partir du sang de patients allergiques. Nous avons aussi généré des anticorps de fortes affinités en immunisant des souris et révélé leurs structures cristallographiques. Un de ces anticorps a réussi à capturer le rocuronium en moins d'une minute dans des modèles de primates, offrant de nouvelles perspectives aux pistes d'immunothérapies.

Lay Summary (English)

Rocuronium is a neuromuscular blocking agent, which are drugs administered during general anesthesia to inhibit muscle contraction, thus allowing intubation before surgery. Rocuronium causes two severe side effects: 1) the most severe form of allergic reaction (anaphylaxis) often in patients who have never been exposed to the molecule, and 2) a residual action that lasts 30-90 minutes after the injection, leading to risks of tracheal damage and infections. This work aims to understand the origin of these allergies, which remains unknown, and to find a therapeutic antibody that could capture rocuronium as an antidote. The first human anti-rocuronium antibodies were isolated from the blood of allergic patients. By immunizing mice, we also generated high-affinity antibodies and revealed their crystallographic structures. One of these antibodies was able to capture rocuronium in less than a minute in non-human primates, opening novel perspectives for immunotherapy.

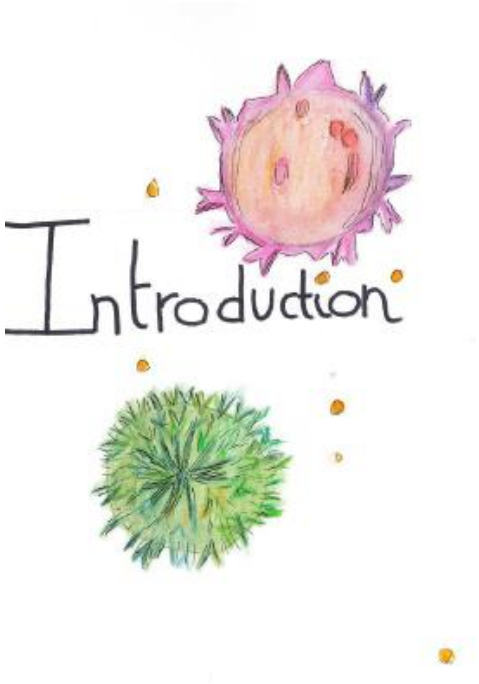

1. NMBAs and their use in perioperative care

1.1 The origin and mode of action of NMBAs

1.1.1 Why and when are NMBAs used in perioperative care?

The use of Neuromuscular Blocking agents (NMBAs) in the clinical context has revolutionized the practice of anesthesia and improved the success rate of emergency medicines[1-2- 3]. By triggering **muscle paralysis** of the skeletal striated muscles (but not of the smooth and cardiac muscles), NMBAs help to assist mechanical intubation, facilitate endotracheal intubation, and perform surgery. They are administered with a cocktail of narcosis and analgesia to also induce sleep and ease pain. The choice of the NMBA varies according to the type of procedure and the profile of the patient. Indeed, for a patient requiring rapid sequence induction, a fast-acting NMBA such as suxamethonium (Celocurine®) or rocuronium (Esmeron®) might be preferred while for a patient without any risk of tracheal inhalation, a long-lasting drug like atracurium (Tracrium®) or cisatracurium (Nimbex®) should be favored. NMBAs are administered intravenously either in controlled boluses or with continuous infusion with a dose depending on the NMBA used: either with the real body weight of the patient for suxamethonium, atracurium, or cisatracurium or with the ideal body weight (theoretical weight calculated according to the height of the patient). Each NMBA possesses distinct features with a different onset time, duration of action, and mode of elimination (Table 1).

	NMBA	Onset time (min)	Recovery time (min)	Dose (mg/kg)	Elimination mode	Side effects
Depolarizing	**Suxamethonium**	<1	~10	1.5	Hydrolysis by cholinesterase in plasma/liver	Muscle pain, malignant Hyperthermia, Hyperkalemia Bradycardia, Renal failure
Non Depolarizing	**Rocuronium**	1-2	~45	0.6	Liver uptake (70%) Kidney excretion (30%)	Bradycardia, Bronchospasm, Dyspnea, Hypotension, Laryngospasm, Tachycardia
	Vecuronium	3-4	~45	0.08	Metabolization in the liver and excreted in the bile	
	Atracurium	2	~40	0.6	Hofmann degradation to laudanosine Ester hydrolysis (80%) Renal elimination (20%)	
	Cisatracurium	5	~40	0.15		

Table 1: Summary table of the key features of NMBAs from different families including onset time, recovery time, dose, elimination route, and side effects[4-5].
Hyperthermia refers to an increase in body temperature, Hyperkalemia to the increase of potassium levels, Bradycardia to a decrease in heart rate contraction, Dyspnea to a shortness of breath, Laryngospasm to spams in the vocal cords and tachycardia to an increase in heart rate contraction.

1.1.2 The evolution of NMBA synthesis

The earliest record of NMBAs goes back to the XVIth century when European explorers discovered a poisoned arrow used for hunting by South Americans[6]. In 1850, Claude Bernard showed that this poison caused muscle paralysis by inhibiting the activity at the neuromuscular junction, and in 1942, **tubocurarine**, isolated from the plant *Chondodendron tomentosum* was the first NMBA used in the clinics to treat tetanus[7-6] (Fig 1. A). Since then, other synthetic blockers have been designed by modifying the original structure such as the distance between the ammonium pharmacophore or the hydrophobicity[8]. Even though in 2011 NMBAs were published as essential medicines by the World Health Organization, the optimal NMBA (rapid onset, existence of a reversal agent, and absence of side effects) does not exist yet[9]. Therefore, patients are often exposed to several NMBAs, either during the same surgery, for example with the co-administration of suxamethonium for rapid intubation followed by a long-lasting NMBA such as atracurium/cisatracurium[10], or months/years apart for distinct procedures.

1.1.3 The mode of action at NMBAs at the neuromuscular junction

NMBAs inhibit muscle contraction by operating at the **neuromuscular junction** by competing with a neurotransmitter, **acetylcholine**. In the absence of NMBAs, skeletal muscle contraction is induced by the transmission of an action potential from the axon of a neuron to muscle fibers. The neuromuscular junction is composed of 1) a presynaptic membrane located at the axon terminal of the neuron, 2) a postsynaptic membrane found at skeletal muscle fibers, and 3) a synaptic cleft (Fig 1.B). The presence of an action potential stimulates the production of calcium ions on the axon terminal. The binding of calcium ions to vesicles enables the release of acetylcholine in the synaptic cleft. Two acetylcholine molecules are required to activate a nicotinic receptor, a ligand-gated ion channel that allows sodium ions to enter the skeletal muscle fiber once opened. When this increase of positive charges, also called **depolarization**, reaches a threshold of -60mV (resting potential of -100mV) it causes the muscle fiber to contract (Fig 1.D). This process is cyclic since molecules of acetylcholine remaining in the synaptic cleft are degraded (hydrolyzed) by an enzyme (acetylcholinesterase) in choline and acetate. The choline produced from the hydrolysis process is recycled in the axon terminal to generate new acetylcholine molecules.

Nicotinic acetylcholine receptors belong to the Cys-loop superfamily of cell surface receptors. This pentameric ligand-gated ion channel is composed of five subunits symmetrical around the central channel axis: α, γ, α, β, δ[11]. Each subunit is divided into three domains: an extracellular ligand binding domain, a membrane binding pore, and an intracellular domain[11-12] (Fig 1.C). Nicotinic receptors are cationic members of the family and exist in two types: muscle-type receptors located at the motor located at the neuromuscular junction and neuronal nicotinic receptors expressed in the central and nervous systems [13]. This work will focus only on the acetylcholine receptors present at the skeletal neuromuscular junction, and not in the central nervous system, since they are the ones responsible for muscle contraction. The existence of this receptor in natural sources can be found by purifying the electrolytes of electric fish such as *Torpedo californica* which allowed its extensive study and the determination of its structure[14 -15].

To compete with acetylcholine at the neuromuscular junction, NMBAs possess a chemical structure that mimics the acetylcholine molecule, all having in common a **charged Quaternary Ammonium (QA)** at physiological pH, the **critical pharmacophore** responsible for the binding of the NMBAs to the nicotinic receptors[16-17]. NMBAs fall into two categories according to their mode of action: depolarizing and non-depolarizing.

Depolarizing NMBAs are **agonists** because they stimulate the nicotinic receptors thus holding open the ion-gated channels which causes first muscle contraction and second, muscle paralysis. The muscle fiber

is then resistant to further stimulation by acetylcholine and they can bind only to the post-synaptic receptors. The only depolarizing NMBA is **suxamethonium**, which has a rapid onset (~1 minute) and short duration (~10 minutes). Suxamethonium is metabolized by enzymes named plasma pseudocholinesterase in the bloodstream, which explains its short-acting block[18-19]. Due to their short duration of action, depolarizing NMBAs are favored when the patient displays an elevated risk of pulmonary inhalation, such as for emergency surgeries when fasting rules were not followed, and for patients with special risks, such as previous bariatric surgeries or gastric reflux. In this setting, an immediate blockade is required to prevent any mechanical ventilation before intubation. Nonetheless, the use of suxamethonium has been decreasing dramatically in the past years and is even counter-indicated or banned from certain countries because of several factors[20]. First, it is associated with hyperkaliemia (high level of potassium in the plasma), because of the generalized muscle contraction induced, which can be of major issue, especially for septic patients or patients with kidney failure. The other explanations (allergic reactions and the lack of antagonist) will be explained in more detail in section §2 of the introduction.

Non-depolarizing NMBAs are **antagonists** since they block the acetylcholine receptors on the pre- and post-synaptic receptors. Binding to the post-synaptic receptors on muscle fibers inhibits the binding of acetylcholine and prevents muscle contraction. This competitive effect relies on the relative affinity and concentration of NMBAs for each acetylcholine receptor. Two factors favor NMBA binding during this competition: 1) the cleavage of acetylcholine molecules by acetylcholinesterase in the synaptic cleft, and 2) the binding of a single NMBA molecule on two receptor binding sites unlike, acetylcholine that requires two molecules to block the receptors. Their long-lasting effect can be explained by 1) their capacity to bind to the presynaptic receptors on the motor neuron, hence blocking the feedback loop where choline is recycled, thus reducing the acetylcholine reservoir, 2) the fact that they are not metabolized by pseudocholinesterase, unlike suxamethonium.

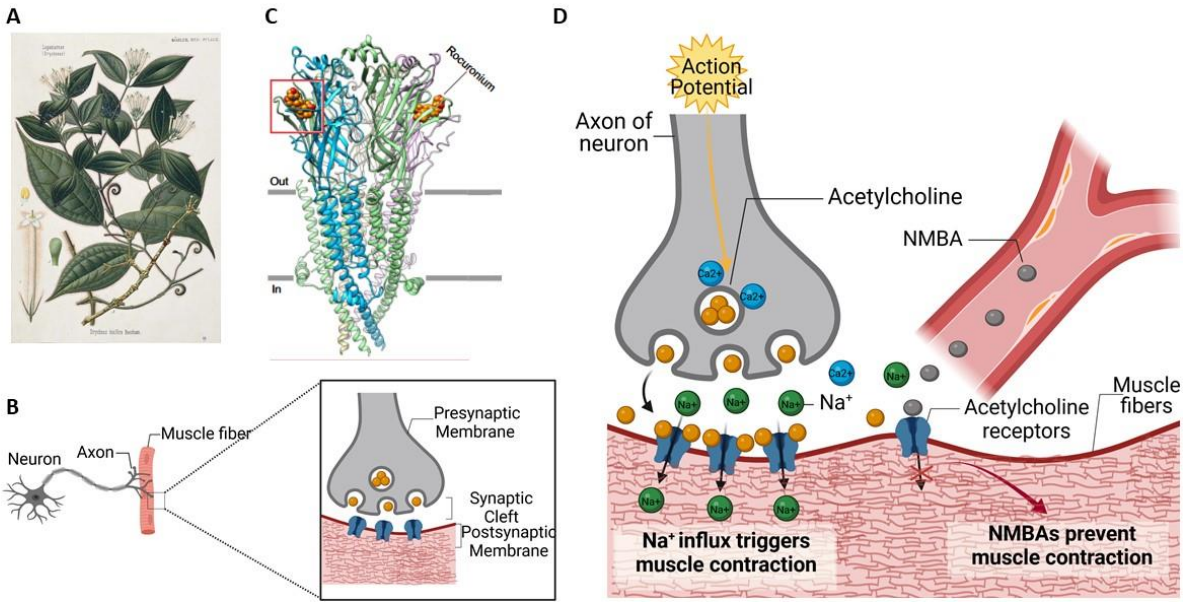

Figure 1: Mode of action of neuromuscular blocking agents at the neuromuscular junction.
(**A**) Drawing of the plant *Chondodendron tomentosum* from which the first NMBA, tubocurarine was isolated[21]. (**B**) Schematic representation of the neuromuscular junction composed of a presynaptic and a postsynaptic cleft (Biorender). (**C**) The co-crystal structure of rocuronium (in orange) bound to nicotinic receptors[22]. (**D**) Mode of action of NMBAs at the neuromuscular junction that compete with acetylcholine to bind to nicotinic receptors, hence preventing ionic influx and muscle contraction. NMBA, Neuromuscular Blocking agents. (Biorender).

Non-depolarizing NMBAs are classified into two distinct families according to their chemical structures:

- **Aminosteroids** (rocuronium and vecuronium): they possess an amino-substituted steroid scaffold and are metabolized in the liver (hepatically)[21]. Their four steroid rings make the molecules hydrophobic/lipophilic (Fig 2).

- **Benzylisoquinolinium** (atracurium, cisatracurium): they possess a benzyl group and an ammonium derived from a quinoline. They are spontaneously degraded through Hofmann elimination in plasma and tissues or by ester hydrolysis[22]. Hofmann elimination breaks down the reversed ester linkages, hence removing the ammonium critical moiety and generating two molecules of laudanosine and an acrylate derivatives from a single molecule of atracurium[23] (Fig 2).

Of note, the term "QA" that will be used in the rest of the manuscript is a misnomer since it will be used to also refer to the tertiary ammonium that becomes quaternary at physiological pH. One should keep in mind that there is a subtle distinction between a "real" QA and a tertiary amine becoming a quaternary ammonium due to pH change.

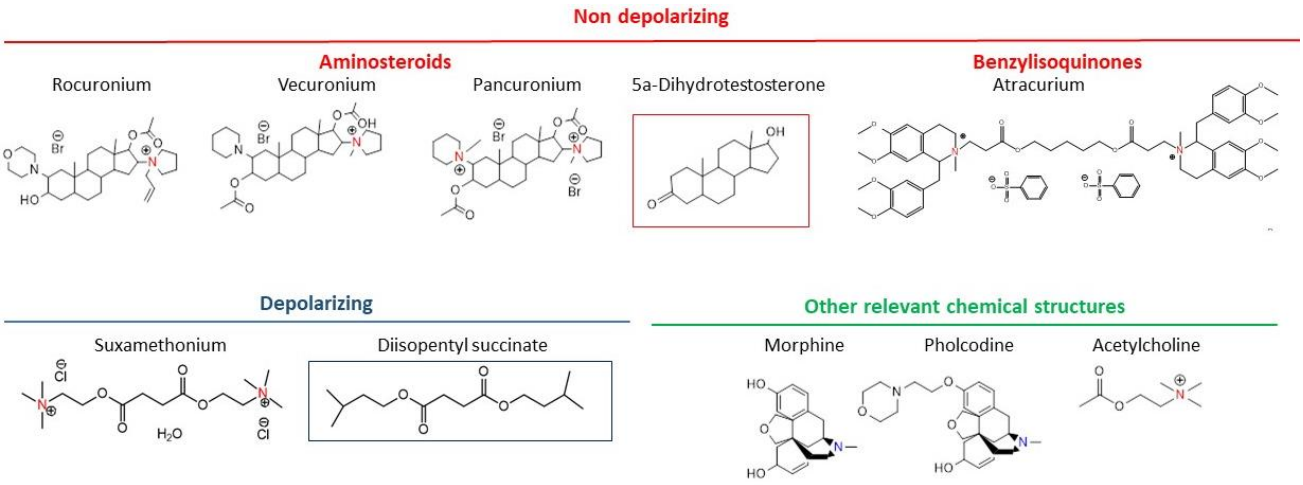

Figure 2: Structural formulas of NMBAs from distinct chemical families, chemical structures of molecules that mimic NMBAs devoid of the QA (boxed), and other relevant chemical structures containing a QA.
"Real" quaternary ammonium atoms are colored in red and tertiary amines that become quaternary in physiological pH are colored in blue.

1.2 The structure-activity relationship of NMBAs from a chemical perspective

1.2.1 The chemical structure of NMBAs

Researchers have been trying to design novel curarizing molecules since the discovery of tubocurarine by modifying the initial chemical structure (the distance between the QA, the substitution of the QA, the polarity, etc.)[7]. All these studies on structure-activity relationships led to the identification of several criteria that need to be respected for NMBAs to possess an optimal effect:

(1) Necessity of having a least one **charged QA** at a physiological pH since the ammonium mimics the natural molecule acetylcholine, with a preference for bisquaternary derivatives that are usually more potent than monoquaternary ones[7]. An optimal separation length between the charged quaternary onium heads of 1.4nm which corresponds to a chain length of ~ ten carbon atoms.

(2) The importance of having at least one **methyl group** on the quaternary nitrogen for potency whilst minimizing the steric hindrance since bulkier groups can interfere with the receptor response[24]. The lipophilic-hydrophilic balance in the NMBAs structure needs to be found with lipophilic groups increasing the affinity to the receptor by favoring Van der Waals bonding but potentially increasing the steric hindrance.

(3) The presence of the **ester** bound that plays an important role in their degradation.

1.2.2 The importance of the stereochemistry: example of atracurium

The 3-dimensional conformation and **stereochemistry** of NMBAs are critical in the NMBAs potency which can be illustrated by the family of benzylisoquinolinium possessing 4 asymmetric centers (2 N^{IV} and 2 C^{IV}), therefore 16 (4^2) potential stereoisomers, and finally only 10 due to the symmetry of the molecule[25-26]. For instance, the benzylisoquinolinium atracurium is a **mixture of ten isomers** and only six out of the ten isomers of atracurium have been studied individually since the others could not be isolated from the mixture. In cats, five among the six isomers had a similar neuromuscular blocking activity to the mixture except for **cisatracurium**, the 1R, 2-R cis isomer of atracurium which was more potent than the others[27]. These results were confirmed in patients with cisatracurium having a similar duration of action to atracurium, but a slower onset time and fewer side effects which can be explained by the fact that it does not trigger histamine release (unlike atracurium), thus minimizing hypotension and bradycardia[28-27]. The impact of the stereochemistry on the binding to nicotinic receptors can also be observed in rodent models since atracurium can induce neuromuscular blockade in mice[29] whilst no study curarizing mice with cisatracurium can be found in the literature.

This project investigates two side effects caused by NMBAs that will be the focus of the next sections: hypersensitivity to NMBAs (§2) and residual neuromuscular blockade (§3).

2 Hypersensitivity reactions in perioperative care and NMBA involvement

2.1 Clinical manifestation and medical management of hypersensitivity reactions

2.1.1 Definition, etiology, and occurrence of perioperative hypersensitivity reactions

The term "**anaphylaxis**" was coined by Nobel prizewinner Charles Richet and Paul Portier in 1902 who were working on the toxicity of jellyfish filaments[30]. They found that dogs that recovered from a primer injection of the toxin experienced fatal reactions after a second injection at a weaker dose. They called this phenomenon "ana" and "phulaxis": the contrary of protection in Greek. Nowadays, anaphylaxis is the most severe form of acute hypersensitive reaction (AHR) and is defined as "a serious allergic reaction that is rapid in onset and may cause death"[31]. In this work, we will refer to the term AHR and not allergy since the term hypersensitivity implies reactions that can be triggered by different pathways whereas the term "allergy" is connoted to describe the classical Immunoglobulin E (IgE)-mediated route of activation, which will be explained in more details in §2.2. The incidence and severity of anaphylaxis have been growing over the past 20 years. For instance, the incidence rate of anaphylaxis has increased at an average rate of 5%

annually since 2001 in Taiwan[32] and food-induced anaphylaxis increased by 214% in the USA from 2005 to 2014[33]. More than a third of anaphylaxis occurs during peri-operative care[34] with an incidence that usually varies between **1:5,000 to 1:25,000 anesthetics procedures** in Europe but with a huge variability according to the geography[35 -36]. Indeed, in a hospital in Pamplona (Spain), the incidence of anaphylaxis was 1:385 surgeries, and in Ohio (USA) the incidence was 1:677 surgeries in 2015 whereas, in France and the United Kingdom, it is estimated around 1: 10,000 anesthesia procedures. The discrepancy between these figures can be explained by different practices in each country concerning the type of NMBA used and the methodology to report a peri-operative AHR. The true incidence of perioperative AHR is also potentially 70% higher than the numbers reported due to diverse challenges: reporting delays, incomplete data, and poor diagnosis [37]. Perioperative AHR can lead to a **fatal outcome in 4.1%** of cases and can generate severe sequelae[38 -39-40]. In the perioperative context, drug-induced anaphylaxis is responsible for the majority of anaphylaxis-related deaths and drugs have become an increasingly identified culprit agent[41]. NMBAs are the most common cause of perioperative anaphylaxis in **France** (58%), followed by latex (20%) and antibiotics (13%)[36]. These numbers vary in each country with the most common causes of perioperative allergies being antibiotics in most countries which can be explained by distinct procedures such as the eviction of latex in certain care units, but mostly because of different anesthesia and/or antibiotic prophylaxis protocols[42].

Across several studies, **suxamethonium** and **rocuronium** have been reported to be the most allergenic NMBAs whereas pancuronium and cisatracurium have the lowest risk of generating an AHR. In an Australian cohort that calculated the rate of anaphylaxis by referring to the number of reactions according to the number of vials sold, the incidence was 1:2079, 1:2498, and 1:7680–109,000 for suxamethonium, rocuronium, and atracurium, respectively. These results depend on the usage frequency of NMBAs in each country that administrates more extensively some NMBAS than others. For instance, in the United Kingdom atracurium is mostly injected (49.1%, followed by rocuronium 40.6%) whereas suxamethonium and cisatracurium are less frequently used (11.2% and 1.6% respectively)[37]. Therefore, it is coherent that in the United Kingdom, the 6th National Audit Project (NAP6) study reported a more even distribution of the proportion of NMBA being the culprit agent: rocuronium (42% of cases), atracurium (35%), succinylcholine (22%), and mivacurium (1.5%) compared to other countries using extensively a single NMBA[37]. In France, suxamethonium was the most predominantly used NMBA, 98% for rapid sequence induction in the south-east of France in 2011[43], until a pharmacovigilance study was performed in 2012 and this NMBA was advised to be used under limited conditions by the *Agence Nationale de sécurité du médicament* (ANSM) in 2018[44]. In a study performed in Japan, rocuronium was the only culprit NMBA

which can be explained by its extensive use in this country[45-46]. In Australia as well, rocuronium was responsible for half (56%) of perioperative anaphylaxis[47]. These epidemiological figures, based on vial usage are fraught with difficulty since vials may be drawn up but never used, or split up between patients, or might go out of date and never be used. So far, the denominator data is notoriously difficult to obtain to compare the epidemiological figures varying in each country and hospital.

In the context of anaphylaxis, the main difficulty is to correlate the **phenotype** (clinical symptoms) to the biological **endotype** (underlying pathological mechanism) since several endotypes can share the same phenotype and *vice versa*. This difficulty will be elaborated in the following section.

2.1.2 Clinical symptoms and therapeutic care

Since there is no universal agreement on the criteria for diagnosis of anaphylaxis, the National Institute of Allergy and Infectious Disease and Food Allergy and Anaphylaxis Network proposed an objective description of the criteria to clearly diagnose an anaphylactic event[48]. According to their report, anaphylaxis is likely when the following criteria are fulfilled:

Acute onset of an illness (minute to hours) with involvement of the **skin and/or mucosal tissues** and at least one of the following:

(1) Respiratory compromise (bronchospasm)
(2) Reduced blood pressure
(3) Persistent gastrointestinal symptoms

A grading system was proposed by Ring and Messmer in 1977 to scale the severity of an anaphylactic reaction from I (low) to IV (severe), this classification is nowadays commonly used to rank the severity of AHR[49] (Table 2).

Grade	Clinical symptoms (adapted from Dewatcher, 2019)[50]
I	Mucocutaneous signs: generalized erythema, extensive urticaria with or without angioedema
II	Moderate multi-visceral signs: mucocutaneous signs, moderate hypotension, tachycardia, or both with or without moderate bronchospasm or gastrointestinal symptoms
III	Life-threatening mono- or multi-visceral signs: life-threatening hypotension, tachycardia or bradycardia with or without cardiac arrhythmia, mucocutaneous signs, severe bronchospasm or gastrointestinal symptoms
IV	Cardiac arrest

Table 2: Clinical symptoms used to grade the severity of an AHR according to Ring and Messmer classification [49-50].

Anaphylaxis diagnosis uncertainty is emphasized by the impossibility of sometimes detecting the **mucocutaneous signs** because of the surgical dressing and by the fact that major clinical signs such as hypotension/tachycardia can also be provoked by the anesthesia and/or the surgery. Therefore, another criterion has been proposed: **a low end-tidal CO2** which has been shown to correlate with the severity of anaphylaxis[51]. This clinically universally available parameter reflects a decrease in cardiac output and can precede arterial hypotension. So far the use of low end tidal CO2 measurements as a way of detecting anaphylaxis is still under debate since there is no evidence showing that it is specific for anaphylaxis as opposed to any cause of low blood pressure. This uncertainty regarding the diagnosis of a perioperative AHR can have serious consequences on the therapeutic management of the patient and can lead to incorrect/delayed therapy. In the first review attached at the end of the introduction (Appendix 3) we give a more thorough update on the current diagnostic tools and we propose a diagnostic work-up to facilitate clinicians in decision-making following an AHR to NMBAs[52].

It is sometimes almost impossible to prevent an anaphylactic reaction since some patients have a shock after the **first exposition** to the causative agent, which is usually the case with NMBAs. Nonetheless, there are certain reflexes to acquire when an anaphylactic reaction is suspected in hopes of decreasing the chances of mortality. If, the **suspected culprit agent needs to be removed** immediately, even though it is not always easily identified. When the causative drug has been administered intravenously (such as NMBAs), it is impossible to eliminate rapidly without a capture molecule. The administration of **adrenaline** is the first-in-line approach to rescue the patient. Adrenaline is not curative but acts by thwarting the symptoms caused by anaphylaxis by provoking bronchodilation, vasoconstriction, reduction of vascular permeability, and edema reduction, it also induces a down-regulation of mast-cell mediator release. A rapid administration of adrenaline is essential to improve the outcome of the patient[53] and a delayed administration has been associated with enhanced mortality in food allergies. Other treatments can complement the injection of adrenaline in case of refractory anaphylaxis, depending on the phenotype of the patient (cardiac failure, vascular failure)[54-55].

2.1.3 The biological and clinical tests routinely conducted after suspicion of perioperative AHR

After a suspected AHR, the patient needs to benefit from an immediate investigation in a specialized center to determine the type of allergic reaction. Since the classical pathway of allergies is commonly hypothesized to be **IgE-mediated**, the biomarkers routinely tested are related to the activation of this pathway. These methods rely on the detection effectors cells responsible for the symptoms of an AHR: **mast cells** niching within tissues or **basophils** circulating in the blood.

First, biomarkers of these effector cells can be measured: they include **histamine** and **tryptase** concentrations. The plasma histamine concentration needs to be measured as quickly as possible since the histamine peak is observed within the first minutes following the AHR and their elimination half-life is 15-20 minutes. High levels of histamine (>10nmol/L) often correlate with the severity of the symptoms[56] but routine histamine measurements are not widely available. Then, the serum tryptase is usually controlled by sampling 30-120 minutes (to measure the concentration at the peak) and 12-24 hours after the shock (to determine the baseline level) since the tryptase half-life is 2 hours. Then, the tryptase threshold is calculated using the formula: 2µg/mL + 1.2 x baseline level, which is compared to the peak concentration.[57] (Table 3).

Since the total IgE level has no diagnostic value, the presence of **allergen-specific IgE (sIgE)** antibodies is confirmed *in vitro* and *in vivo.* Concerning NMBAs, the most used *in vitro* diagnosis approach consists of detecting sIgE antibodies against **morphine**. Indeed, tests routinely available to detect anti-NMBA IgEs are available only for suxamethonium, so the tests for the other NMBAs rely on the detection of the tertiary ammonium of morphine that becomes tertiary at physiological pH, the QA being hypothesized to be the allergenic epitope of NMBA-induced anaphylaxis[58]. These tests using morphine grafted on a solid phase ImmunoCAP or enzyme-linked immunosorbent assay (ELISA) are nonetheless unreliable to diagnose anaphylaxis to benzylisoquinolinium[59] and should be complemented with a specific inhibition test with the full NMBA molecule to ensure the specificity of the antibodies. The timing of blood sampling is important since blood taken shortly after anaphylaxis might be negative for sIgE due to their consumption during the event. Ideally, investigations need to be done within 4-8 weeks after the event but can be undertaken later in time since anti-NMBA sIgE can also be detected years after the reaction. The most frequently used *in vivo* methods to detect sIgE antibodies are the **skin prick test** (SPT) and **intradermal tests** with SPT having a lower sensitivity (49%) than the intradermal one (73%)[60]. During a SPT, a drop of the allergen extract is introduced in the upper layers of the skin using a needle whereas an intradermal test consists of injecting

a 1/1000 dilution of the NMBA in the dermis[61]. After 20 minutes, the diameter of the wheal is measured and if the diameter is 3mm greater than the negative control, the test is considered positive. Another method to detect the activation of effector cells is the **basophil activation test**. This method, not commercially available neither in every country nor in every center, should not replace skin tests and should only be used as an additional tool[62]. It has been shown to be a useful technique to detect cross-reactivity among different NMBAs. This test relies on the quantification of basophil activation markers, the cluster of differentiation (CD)63 upon its activation using flow cytometry. It has shown promising results for the diagnosis of atracurium-mediated AHR with a sensitivity of 63%, an absolute positive predictive value, and a negative predictive value of 70%[63]. The final method often used to investigate an IgE-mediated AHR is the **drug provocation test** that consists of injecting an increasing dose of the NMBA that can reach 1/10 of the therapeutical dose to prevent respiratory paralysis that would necessitate an intubation. This test is controversial in the field of allergy and anesthetics and must be performed at least one month after the AHR. It is carried out under strict supervision in specialized centers with resuscitation facilities due to the associated risk. Despite the potential risk for the patient, they are sometimes the only source available to draw conclusions when all the previous tests are negative (Table 3).

2.2 The IgE-dependent pathway

2.2.1 The mechanism involved in IgE-mediated allergy at the cellular level

IgE antibodies are found in small quantities in the blood (50-200ng/mL) due to their short half-life in circulation (few days) explained by the fact that they are not recycled by the neonatal Immunoglobulin G (IgG) recycling receptor FcRn[64]. The production of IgE antibodies occurs in two steps (Fig 3):

1) **The sensitization phase**: the allergen is taken up by antigen-presenting cells (**dendritic cells**) that internalize it, digest it into peptides, and present it on their major histocompatibility complex II molecule (MHC) (for extracellular antigen, thus allergens) to further interact with specific **T-cell receptor** (TCR). In the case of NMBAs, the antigens are very small (<1KDa), also called **hapten** so they are hypothesized to be grafted on a carrier protein (a process referred to as haptenization) to be presented on a MHC II molecule. Immature dendritic cells patrol the tissues and once they encounter an antigen and receive a danger signal, they migrate to secondary lymphoid organs (such as **lymph nodes**) where they present the antigen to T lymphocytes. In the context of an allergy, the cytokine environment is **T helper (Th) 2** mediated with the presence of interleukin (IL)-4, IL-5, and IL-13 that allow the differentiation of CD4+ T lymphocytes in auxiliary Th. In the lymph nodes as well, **B cell receptors** (BCR) recognize the hapten/protein complex, and can take up and

process the allergen to present it to its cognate by Th2 lymphocytes, which in turn secrete cytokines that allow the differentiation of B lymphocytes in plasma cells secreting IgE antibodies[65]. The IgE antibodies bind to **high-affinity receptors** for the fragment crystallizable (Fc) portion of IgE (**FcεRI**) on effector cells which allows them to remain months and years, even though their half-life as free circulating molecules is only a few days. The effector cells include tissue-resident mast cells and blood basophils, and other cell types involving neutrophils, eosinophils, and platelets[66-67].

2) **The effector phase**: The second phase occurs when the **allergen is reintroduced**. During this second exposure, the antigen will rapidly be recognized by sIgE already fixed on the surface of effector cells. The **cross-linking** of two FcεRI-bound IgEs by the allergen will allow the activation of effector cells, provoke their degranulation and synthesis of **inflammatory mediators** including histamine, tryptase, platelet-activating factor (PAF), prostaglandin D2 and leukotrienes. These mediators are responsible for the symptoms of anaphylaxis such as **vasodilatation** and **bronchoconstriction** by increasing vascular permeability, and heart rate and by promoting airway remodeling.

Evidence supporting the role of sIgE antibodies in anaphylaxis has been demonstrated by several studies showing that the **transfer of purified antigen-specific IgE** from a sensitized patient to a naïve host could induce skin reactivity[68]. It has also been shown that following **bone marrow transplantation** from allergic donors to non-allergic recipients, drug hypersensitivity was transferred from the donor to the recipient with an increase in total IgE levels[69]. In rodent models, it has been proven that in mice lacking FcεRI or mast-cell deficient mice, IgE-mediated anaphylaxis was abolished[70 -71]. This work is also supported by the development of an **anti-IgE therapeutic antibody**, omalizumab, a humanized murine monoclonal antibody (mAb) that forms complexes with free IgE in the serum. Omalizumab has been shown to reduce the risk of anaphylaxis in clinical trials[72 -73] and can be used to treat unprovoked anaphylaxis in patients with mastocytosis, a disease associated with an increase in mast cell number and activity[74]. The origin of IgE-producing B cells in humans remains speculative, as most of the work has been performed on animal models. Even though it has been shown that IgE antibodies are derived from previously antigen-experience B cells rather than naïve B cells, there are still a lot of open questions concerning the type of B cells: if they are circulating and none-secreting memory B cells (Bmem) or non-circulating and secreting (plasma cells). In Appendix 4, we propose to discuss the current use and limitations of animal models in IgE-mediated anaphylaxis[75].

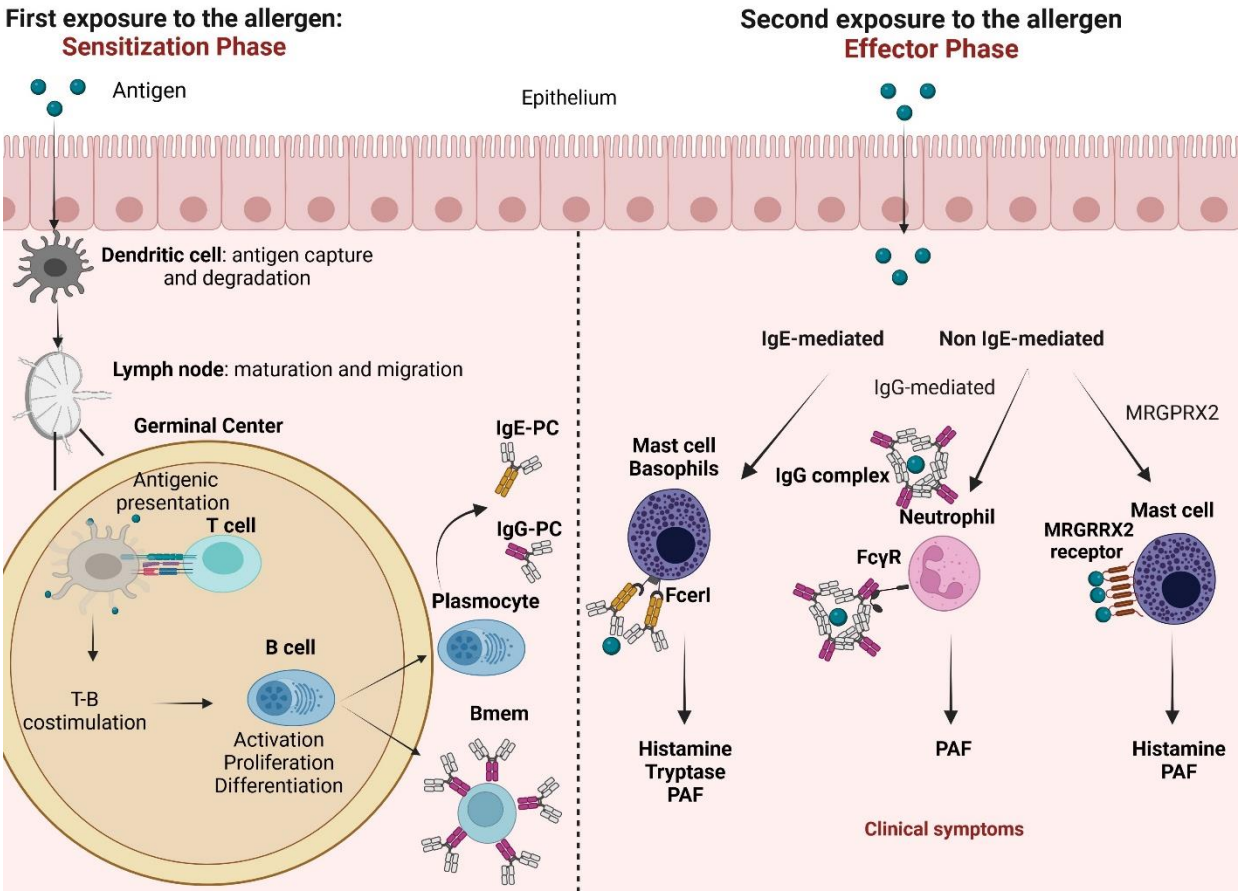

Figure 3: Mechanisms of sensitization and effector phases in anaphylaxis.
During the sensitization phase, the individual is exposed for the first time to the allergen that is captured by dendritic cells. The dendritic cells migrate to the lymph nodes where they mature and process the antigen to expose it to a naive T cell with a MHC molecule. The T cell differentiates in a T helper cell, upon interaction with a B cell, it activates it, leading to its proliferation and differentiation either in a Bmem or an antibody-secreting cell such as a plasmocyte. During the second antigen exposure, the effector phase is initiated. Through the canonical IgE-dependent pathway, the sIgE pre-bound on effector cells (mast cells or basophils) cross-link FcreRI in the presence of the antigen which leads to the degranulation of the effector cells and mediator release (histamine, tryptase, PAF) responsible for the clinical symptoms. The IgG-dependent pathway is activated through the formation of antigen-antibody aggregates termed "immune complexes" that can activate FcγR expressed on myeloid cells: macrophages, neutrophils, and basophils, in turn producing PAF. The antibody-independent pathway is activated through the receptors MRGPRX2 expressed on mast cells. Bmem, memory B cells; MRGPRX2, Mas-related G-protein coupled receptor member X2; PAF, platelet-activating Factor; PC, plasma cells. (Biorender).

2.2.2 The diagnosis of the IgE-mediated pathway and its limitations in the clinics

The gold standard to validate an IgE-mediated AHR relies on **positive skin tests and/or sIgE antibody assay** consistent with the clinical history of the reaction and the anesthetic protocol. In this ideal case when the pathway and culprit agent have been identified, the strategy is straightforward. The difficulty lies when the routine clinical diagnostic results are incoherent with the phenotype and when the results are discordant/negative.

All these methods face various limitations as data on the predictive value of SPT, basophil activation test, and sIgE are limited or non-available. The **drug provocation** test is highly debated among allergists since there is no consensus on the **dose** that should be administered, it is uncertain if it could sensitize the patient and potentially be responsible for a future AHR, and if is insecure to administer drugs that require general anesthesia with no chirurgical purpose. **Skin tests** and **basophil activation** tests have excellent **negative predictive values**, but some argue that the sIgE serology is less clinically predictive than the functional investigations relying upon the activation of mast cells or basophils. Indeed, a **positive sIgE** to rocuronium with **negative skin tests/basophil activation** test does not necessarily reflect a rocuronium IgE-mediated allergy according to certain studies[76]. False positives in the sIgE detection test are also biased by the fact that the prevalence of QA sIgE antibodies is detected in 10% of the population[77]. False positive tryptase levels or skin test can also be generated by patients with a non-diagnosed mast cell disorder such as **mastocytosis** which is characterized by a massive and systemic activation of mast cells[78]. The sensitivity and specificity of the skin tests are also limited by **false positives** that can be triggered by skin trauma, dermographism, contaminated allergen extract, or **false negatives** if the dose is too low. Overall, there is also a huge variability across countries, hospitals, and professionals on the technical methodology and interpretation of these results[79] even though some methodological standardization and strategies are proposed by a consortium of experts[57]. In up to 30% of cases, the results of those tests remain inconclusive due to all the limitations stated above[52] but this incoherency also hints that by searching for sIgE antibodies solely, clinicians might be overlooking another biological mechanism: the IgG-mediated pathway.

Test	Markers detected
Plasma histamine concentration	Histamine levels produced by mast cells/basophils
Serum tryptase concentration	Tryptase levels produced by mast cells/basophils
ImmunoCAP	sIgE antibodies against morphine
Skin Prick Test	sIgE bound to the surface receptors on mast cells
Intradermal Test	
Basophil activation test	Quantification of basophil activation markers
Drug provocation test	Reproduction of the allergic symptoms regardless of the underlying mechanism

Table 3: Current diagnostic tools routinely used after a peri-operative AHR and markers detected.

2.3 The alternative pathways

2.3.1 The IgG-dependent pathway

The existence of an alternative pathway was supported by the evidence that anaphylaxis can occur in mice in the absence of IgE, FcεRI, or mast cells[80-81]. In humans, intravenous administration of histamine in volunteers reproduces most signs and symptoms of anaphylaxis but anti-histamines are not efficient in controlling anaphylaxis in humans so histamine release might not be the sole mediator[82]. IgG antibodies are the most abundant immunoglobulins in serum (concentration ≃ 10mg/mL) with the longest biological half-life (14-21 days). They exist under 4 subclasses differing in their heavy chains and based on their relative concentration in the serum: IgG1 (65%), IgG2 (25%), IgG3 (6%) and IgG4 (4%)[83]. Humans express **nine IgG Fc receptors** named Fc gamma Receptors (FcγR): 7 activators (FcγRI, FcγRIIa, FcγRIIc, FcγRIIIa, FcγRIIIb, TRIM21, and FcRL5), one inhibitor (FcγRIIb) and the FcRn, the latter being responsible for the recycling of IgG thus increasing their half-life. The receptors all bind the constant region of the antibody heavy chain on the cell surface except TRIM21 and FcRn which bind internalized IgG. The receptors express differential affinities for antibody binding and their expression varies for each cell type[84] (Fig 4). The main IgG subclasses predominantly depicted in anaphylaxis are **IgG4** and **IgG1**. The IgG4 subclass is commonly described as the "protective" antibody since it has been shown that successful allergen-specific immunotherapy (also called desensitization) correlates with the induction of allergen-specific IgG4[85]. This therapy consists of exposing the patient to low doses of allergen and the method was discovered by passively transferring blood from a patient exposed to ragweed extract to a naive recipient, which improved the latter's sensitivity to the allergen[86]. IgG4 antibodies are hypothesized to compete with IgE, thus inhibiting the formation of allergen-IgE complexes by neutralizing the antigen and engaging the inhibitory receptor FcγRIIb. Nonetheless, a more recent study has shown that IgG1 had a comparable role to IgG4 in blocking human basophil activation in allergies[87]. The role of the IgG subclasses in the pathways of anaphylaxis has only been shown in mice where it was demonstrated that three IgG subclasses (IgG1,

IgG2a, and IgG2b) induce three different pathways of anaphylaxis that are all primarily activated by a single low-affinity IgG receptor (murine FcgRIII)[88].

Human IgG receptors									
Name	**FcγRI**	**FcγRIIA**	**FcγRIIB**	**FcγRIIC**[5]	**FcγRIIIA**	**FcγRIIIB**	**FcRn**	**TRIM21**	**FcRL5**
CD	CD64	CD32A	CD32B	CD32C	CD16A	CD16B	-	-	CD307
	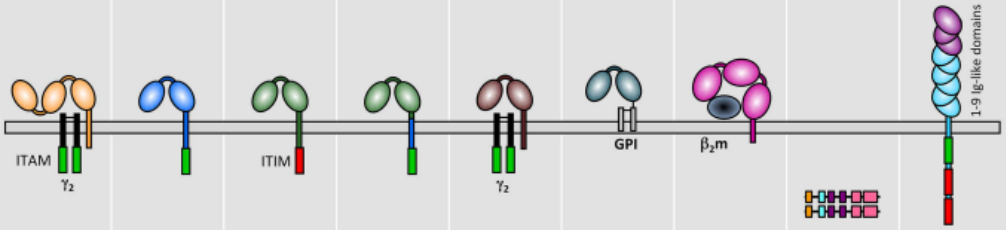								
B cell	-	-	+	-	-	-	-	+	+
T cell	-	-	-	-	-	-	-	+	-
NK cell	-	-	-[4]	+[3]	+	-	-	+	-
Mono/Macro	+	+	+/-	+[3]	+	-	+	+	-
Neutrophil	(+)	+	+/-	+[3]	-	+	+	+	-
Dendritic Cell[§]	+	+	+	-	-	-	+	+	-
Basophil	-	+	+	-	-	+/-	-	+	-
Mast cell	(+)	+	-	-	-	-	NA	+	-
Eosinophil	-	+	-	-	-	-	-	+	-
Platelet	-	+	-	-	-	-	NA	NA	-
Endothelium	-	-	-	-	-	-	+	+	-

Figure 4: Human IgG receptor expression pattern.
+, indicates expression; (+) inducible expression; ±, very low percentages; -, no expression; and NA, not analyzed. Mono/macro, monocytes/macrophages. Extracted from Gillis et al.,[84]

The alternate mechanism relies on allergen-specific IgG antibodies binding to an allergen, forming **IgG-allergen immune complexes** that can activate **FcγR** expressed on myeloid cells: macrophages, neutrophils, and basophils, in turn producing PAF. The existence of this pathway has been extensively shown in mice models in which IgG-induced anaphylaxis was elicited by intravenous injection of allergen-specific IgG following antigen challenge and monitoring of rectal temperature drop, termed passive **systemic anaphylaxis**[88]. It was also reported that histamine and PAF could reproduce the symptoms of anaphylaxis when injected in mice[89]. This pathway has also been validated in mice using **active systemic anaphylaxis** (direct immunization of the mice before challenging them with the same antigen) and this method was not affected in mice deficient in IgE[80 -90 -91]. IgG-dependent anaphylaxis in mice models has been reported to rely on PAF mediator[88] and high PAF concentrations can be observed in the serum of patients after anaphylaxis[82]. Passive and active systemic anaphylaxis in mice was also validated on a novel mouse strain expressing the low-affinity human FcγRs: 3 activating (hFcgRIIA, hFcgRIIIA, and hFcgRIIIB) and one inhibitory (hFcgRIIB). In this knock-in mice model, neutrophils were shown to contribute to anaphylaxis

and basophils to a lesser extent and anaphylaxis was inhibited by PAF receptor or histamine receptor blockade[92] (Fig 3).

My laboratory has shown for the first time that the IgG-dependent pathway is also activated in NMBA-allergic patients. A study with 86 allergic patients was conducted and revealed that the severity of anaphylaxis correlated with anti-NMBA IgG, FcγR activation, PAF release, and neutrophil activation[93]. It is still unclear if both pathways are activated in parallel or not since some patients displayed the IgE and IgG endotypes whereas others showed activation of only one pathway. Nonetheless, both pathways were concomitantly activated in the most severe patients.

2.3.2 Activation of the MRGPRX2

An entirely different, **antibody-independent** pathway of anaphylaxis has also been reported involving Mas-related G-protein coupled receptor member X2 on mast cells (**MRGPRX2**) (Fig 3). The existence of MRGPRX2 was first established in human mast cells[94] and further characterized in mice using its mouse orthologue (Mrgprb2) which had a higher affinity for the drugs tested[95]. In mice, it was shown that this pathway was mostly activated by cationic small-molecule drugs and they found that all NMBA families except suxamethonium could activate Mrgprb2 at concentrations as low as 0.5% of the clinical injection concentration[95]. These results were also confirmed in human **skin** using dermal micro-dialysis to deliver the relaxants to the skin[96]. The study showed that suxamethonium and cisatracurium had the lowest potency of mast cell activation whereas **atracurium** was very potent. Concerning NMBAs from the aminosteroid family, the activation of mast cells was less pronounced with a delayed release of tryptase compared to histamine[96]. The activation of MRGPRX2 in human **blood** gave similar results where it was demonstrated that atracurium but not suxamethonium could induce activation and degranulation of human peripheral blood mononuclear cells (PBMCs) via MRGPRX2 activation. Concerning rocuronium, the mast cell MRGXPRX2 expression and function were similar in patients with an IgE-dependent or independent anaphylaxis and the activation of this receptor by rocuronium is unlikely, given its low-affinity for the receptor [97].

Even though this pathway is considered as pseudo-allergic (or anaphylactoid reaction) since it is antibody-independent, in the case of NMBA-mediated reactions it should not be overlooked, and it is potentially activated for some NMBAs (very likely atracurium) despite tangible evidence lacking so far. One important question remains: how do individuals become sensitized by NMBAs and produce IgE and/or IgG against NMBA?

2.4 The hypothesized allergenic epitopes of NMBAs

Given that some patients who experience an NMBA-mediated AHR have never been exposed to NMBAs previously (40-50% in Australia and 19% in France), the route of sensitization is hypothesized to be induced through **environmental** factors[98 - 99]. The main hypothesis supported today was established by Baldo and Fisher in 1983 who showed that alcuronium-specific IgE in patient serum could cross-react with other NMBAs, having only in common the **QA**[100]. They replicated these results with other molecules containing a quaternary or tertiary amine and they could all inhibit the binding to alcuronium-sepharose[100]. Therefore, they hypothesized the QA to be the allergenic epitope of NMBAs. This hypothesis could also explain the cross-reactivity among different NMBAs since up to 44% of patients are sensitized by at least one other NMBA than the one provoking the AHR[101]. Only 50% of the patients are mono-sensitized[102]. The cross-reactivity between different NMBAs is more important between NMBAs of the same chemical family, especially aminosteroid with patients who did a rocuronium-induced AHR cross-reacting with vecuronium in 81.6% of cases[103].

In 2005, an epidemiological survey was undertaken in Sweden and Norway since the incidence of anaphylaxis to NMBAs was **six times higher in Norway** than in Sweden. A comparison of environmental factors containing QA was undertaken (household and hair care products, skincare ointments, toothpaste, and cough syrup). Interestingly, most of these products inhibited binding to IgE anti-suxamethonium or IgE-morphine but no difference in exposure was found between the two countries except for cough syrop containing a QA molecule, **pholcodine** (Fig 2). In the same cohort, it was shown that in Norway 64.5% of patients with NMBA-mediated AHR were sensitized to pholcodine and none of the Swedish patients possessed anti-pholcodine IgE[104]. These findings were supported by an additional study showing that in 17 patients sensitized during one week to pholcodine, their IgE levels specific to pholcodine, morphine, and suxamethonium were highly boosted but also slightly increased for inhalants and food allergens which points out the production of non-specific IgEs[105]. Following these studies, pholcodine was **withdrawn from the Norwegian market in 2007**, and the reporting of perioperative allergy in which NMBA was used decreased from 66.2% ± 7.4 to 43.8% ± 9.9 in eight years[106]. In France, a similar study on pholcodine named the ALPHO[107] multicenter national survey was undertaken from 2014 until 2020 including 167 patients who experienced an NMBA-induced AHR and one-year exposure to pholcodine with their matching controls without perioperative anaphylaxis. This analysis revealed that pholcodine consumption and **professional exposure** to QA (cleaning professionals and hairdressers) were associated with NMBA-related anaphylaxis, which suggests that other environmental factors play a role in NMBA sensitization. Nonetheless, the low predictive value of QA-sIgE and pholcodine-sIgE preclude them from identifying a

risk population to NMBA-related AHR. As a result, cough syrups were withdrawn in France from sale since September 2022[108] and in the European market since December 2022.

The hypothesis that other environmental factors might be involved is supported by the fact that in some countries where pholcodine is not sold (the United States and the Netherlands), there is also a high incidence of NMBA-mediated AHR and a prevalence of IgE antibodies to pholcodine of 2% and 4.9% respectively. Furthermore, the incidence of NMBA-mediated AHR is more elevated among females than males, a population more frequently exposed to compounds containing QA (cosmetics, households, cleaning products)[36]. **Hairdressers**, a population professionally exposed to QA ions were shown to possess a 4.6-fold higher frequency of positive IgE against QA ions compared to baker/pastry makers and control groups. The results were not biased by the higher predominance of women in the exposed group since the frequency remained higher when comparing females from both groups. A main limitation of the study was the lack of evidence that these sIgE imply an AHR to NMBAs since no skin test/challenge was performed on these populations to evaluate the risk [109].

The main limitation of all these studies that could explain that QA sIgE levels do not always correlate in patients who did an NMBA-mediated AHR could be explained by the fact that the IgG-dependent mechanism was neglected and that the tests are based on NMBA mimics. Despite all the evidence that supports the hypothesis that the allergenic epitope of NMBAs is the QA, reasonable doubt remains since it may not be the only molecular moiety involved such as the adjacent scaffold that could play a role. To date, there is no structural evidence that proves the QA allergenic epitope hypothesis.

3 Residual Neuromuscular Blockade in perioperative care

3.1 Monitoring and clinical management of neuromuscular blockade

A second side-effect associated with the use of perioperative NMBAs is **residual neuromuscular blockade** which consists of prolonged symptoms of muscle weakness after the administration of NMBAs, which reflects the incapacity of the body to naturally eliminate the NMBAs in the absence of an antagonist capture molecule. This side effect was first reported in 1953 in a randomized study over 6 years which showed that the use of NMBAs was associated with a 6-fold increase of anaesthesia-related mortality[110]. The symptoms associated with residual blockade include **postoperative pulmonary complications**, unpleasant symptoms of muscle weakness, longer postanesthesia care unit stays, increased risk of infection, and delayed tracheal extubation with rare fatal consequences [111]. The incidence of residual paralysis is estimated to occur in 40%-60% of patients with variations according to the type of NMBA administered, in the absence of neuromuscular blockade monitoring. For instance, according to a study the incidence is slightly lower with rocuronium (44%) than with cisatracurium (57%)[112] and patients receiving pancuronium have higher risks of facing postoperative pulmonary complications than those intubated with vecuronium or atracurium[113]. This large proportion of patients presenting residual neuromuscular blockade comes with a serious financial burden for the hospitals. Indeed, a recent study performed in the United States demonstrated that if the residual neuromuscular blocks were eliminated, postoperative complications would be reduced by 66%, hence **saving $4.6 million annually** for the hospital [114-115].

Monitoring neuromuscular blockade is a useful tool used during an anesthetic procedure to determine the depth of muscle relaxation and, therefore, to decrease the risks of the associated adverse clinical outcomes mentioned above. Monitoring of neuromuscular blockade can be qualitative (subjective assessment by visual or tactile means) or quantitative (objective real-time measurements). Quantitative measurement is the gold-standard[116] and can be monitored using peripheral nerve stimulators (usually the ulnar nerve on the forearm)[117-118] and assessing the response of the stimulated muscle. After four consecutive 2 Hertz stimuli, the **train of four (TOF)** ratio is determined by dividing the amplitude of the fourth twitch (T4) on the first one (T1). In the absence of neuromuscular blockade, the four twitches are of equal amplitude (TOF ratio between 0.9 and 1), whereas when the neuromuscular blockade is induced, the TOF ratio is reduced. The accepted TOF ratio at which patients are considered under deep neuromuscular blockade is 0 and extubation is recommended if this ratio is higher than **0.9**[119] (Fig 5.C). Every international guideline recommends the systematic use of neuromuscular blockade monitoring for

several reasons: to guide the dosing of NMBAs and to know when and how to antagonize them[116]. This monitoring should start at the induction of anesthesia to facilitate tracheal intubation until the end of recovery and extubation. These recommendations were for example supported by the French Anesthesia Society in 2020 and the Association of Anaesthetists of Great Britain and Ireland in 2021[120-121]. Indeed, evidence supports that quantitative monitoring **enhances recovery** from anesthesia and **decreases postoperative morbidity**. For instance, a multicenter study in Spain revealed that in the post-anesthesia care unit, patients with residual neuromuscular blockade had an increased incidence of respiratory events and tracheal reintubation [122]. Quantitative monitoring also reduces the incidence of airway obstruction (14% in patients assessed quantitatively compared to 45% for those assessed clinically)[123] and of muscle weakness (incidence of 14.5% of muscle with 55% of subjects noted general weakness in the control group versus 32.6% in the group with quantitative monitoring)[124].

3.2 The existing reversing blocking agents and their limitations

Currently, two types of NMBA reversal drugs are available: anticholinesterases and the selective reversal agent sugammadex (Bridion®). **Anticholinesterases** are inhibitory drugs that extend the life span of acetylcholine at the neuromuscular junction by **inactivating cholinesterases** (enzymes that metabolize acetylcholine in choline and acetic acid). The increase in acetylcholine levels displaces NMBA molecules from the nicotinic receptors, hence reducing neuromuscular blockade. Anticholinesterases are QA compounds that do not penetrate the blood-brain barrier and reverse non-depolarizing blockers, depolarizing blockers being more resistant to this drug. The most used anticholinesterase drug is **neostigmine** which is reversible since it makes non-covalent bonding with the enzyme acetylcholinesterase. However, anticholinesterases are not effective in reversing deep neuromuscular blockade[125], which was nicely demonstrated in several studies such as one with 40 patients showing that two doses of neostigmine do not hasten recovery from profound-induced neuromuscular blockade[126]. Even more surprising, with atracurium-induced neuromuscular blockade, administration of neostigmine at profound degrees of blockade extends reversal time[127]. Another striking example is that despite an accelerated recovery by 40% with the use of neostigmine, the reversal of rocuronium and vecuronium with neostigmine still remains less rapid (37.1 and 29.7 minutes respectively) than spontaneous recovery after succinylcholine administration (9.4 minutes)[128]. The limited effect of anticholinesterases can be explained by their competitive nature with non-depolarizing NMBAs (and not destructive). Indeed, once anticholinesterases have targeted all the cholinesterase enzymes present at the neuromuscular junction, administrating more inhibitors has no further effect while the concentration of NMBAs can continue to increase, depending on the dose administered by the clinicians[129]. Therefore, it is recommended to use

neostigmine only if the TOF ratio is higher than **0.4**, to perform extubation within 10 minutes after neostigmine administration (the maximal effect of neostigmine occurs within 10 minutes), and with a single dose lower than 50µg/kg since higher doses are not effective[130]. Anticholinesterases are also associated with various adverse events in multiple organ systems due to their undesired activation of muscarinic receptors that are found in smooth muscles which which mainly include cardiovascular complications (bradycardia), bronchoconstriction, nausea, and vomiting[131].

Sugammadex, another reversal neuromuscular agent specific to the family of aminosteroids NMBAs (rocuronium and vecuronium), was first shown to reverse profound rocuronium-induced blockade in 2006 in rhesus monkeys[132] and became commercially available in 2008. This molecule is a modified gamma cyclodextrin with a lipophilic cavity and a hydrophilic external domain therefore able to encapsulate and interact with the lipophilic NMBAs[133] (Fig 5.A-B). The negatively charged groups of the side chains of sugammadex also reinforce the strength of the complex by interacting with the positively charged QA. Once injected, sugammadex binds rocuronium/vecuronium in the plasma with a 1:1 molar ratio; removal of free NMBA in the plasma actually creates a concentration gradient that draws the NMBAs outside the neuromuscular junction. Sugammadex competes advantageously with acetylcholinesterase drugs because it has fewer side effects (due to its absence of activation of the muscarinic receptors) and can reverse rocuronium/vecuronium moderate blockade in 1.4 min while 17.6 min is required for neostigmine. It can also be used to reverse deep blockade in 2.7 minutes when 49 minutes are needed with the same dose of NMBA with neostigmine[134]. Several case studies suggest that sugammadex can be used to treat rocuronium-induced AHR with rapid and selective elimination of circulating rocuronium antigenic activity[135-136]. However, neither the United Kingdom nor France guidelines recommend its use for the treatment of rocuronium-induced AHR. In fact, it is therefore recommended to use sugammadex over neostigmine for moderate (TOF ratio<0.4) and deep blockade (TOF=0) induced by rocuronium/vecuronium[130].

Despite its relatively safe profile and efficacy, sugammadex was reported to induce systemic **anaphylactic reactions**, particularly in Japan where this drug is extensively used. Indeed, 44% of the sugammadex-induced AHR are reported in Japan[137] a country in which 10% of the total population has been exposed to sugammadex[138]. These cases of anaphylaxis remain rare with an incidence varying between 0.7-10% according to the dose of sugammadex[139-140]. Very surprisingly, after a rocuronium-sugammadex-induced AHR, the clinical tests cannot identify anti-sugammadex IgG/IgE antibodies, basophil, and mast cells do not seem activated and the skin tests are very predominantly negative[140]. Ebo et al. described a clinical

case of a patient with a sugammadex-rocuronium-induced AHR who experienced an IgE-mediated anaphylaxis to the complex sugammadex-rocuronium with the lack of evidence of an IgE-mediated AHR to **sugammadex or rocuronium alone** using basophil activation tests[141]. This change in IgE recognition can be explained by a shape alteration of sugammadex during the complex formation, hence creating a **neoepitope** responsible for the AHR[141].

Since the perfect drug to reverse rocuronium-induced neuromuscular blockade does not exist, how could we identify novel drugs? Could biologics, like antibodies found in allergic patients, be used for this purpose? The first therapeutic mAb Orthoclone OKT3 was approved in 1986 and is currently used to reduce the risks of organ transplant rejection by targeting a T cell receptor [142]. Since then, more than 100 mAbs have been used as therapeutics. Indeed, the very high specificity and affinity of antibodies for their target (dissociation constants ranging in the femto/picomolar) combined with the progress made regarding their engineering, position them as very interesting therapeutic candidates. First, they possess few off-target effects and reduced immunogenicity with the development of chimeric, humanized, or fully human mAbs[143]. Moreover, their half-life can be adapted (extended or shortened) by mutating residues in their constant regions. For example, in the context of a capture molecule to reverse neuromuscular blockade, a short half-life is required if the patient needs a prompt re-administration of an NMBA, which is possible by generating mutants that do not bind to FcRn with the following mutations: I253A, H310A, H435A=. Finally, antibody fragments, such as variable heavy-chain antibodies (VHH) or single-chain fragment variables (scFvs) can be engineered, facilitating their penetration into tissues and elimination. Research to improve antibody affinities through mutagenesis combined with machine learning continues to advance, making these approaches even more attractive[144]. The final section of the introduction will focus on the identification of antibodies to develop a therapeutic antibody as an effective NMBA capture molecule.

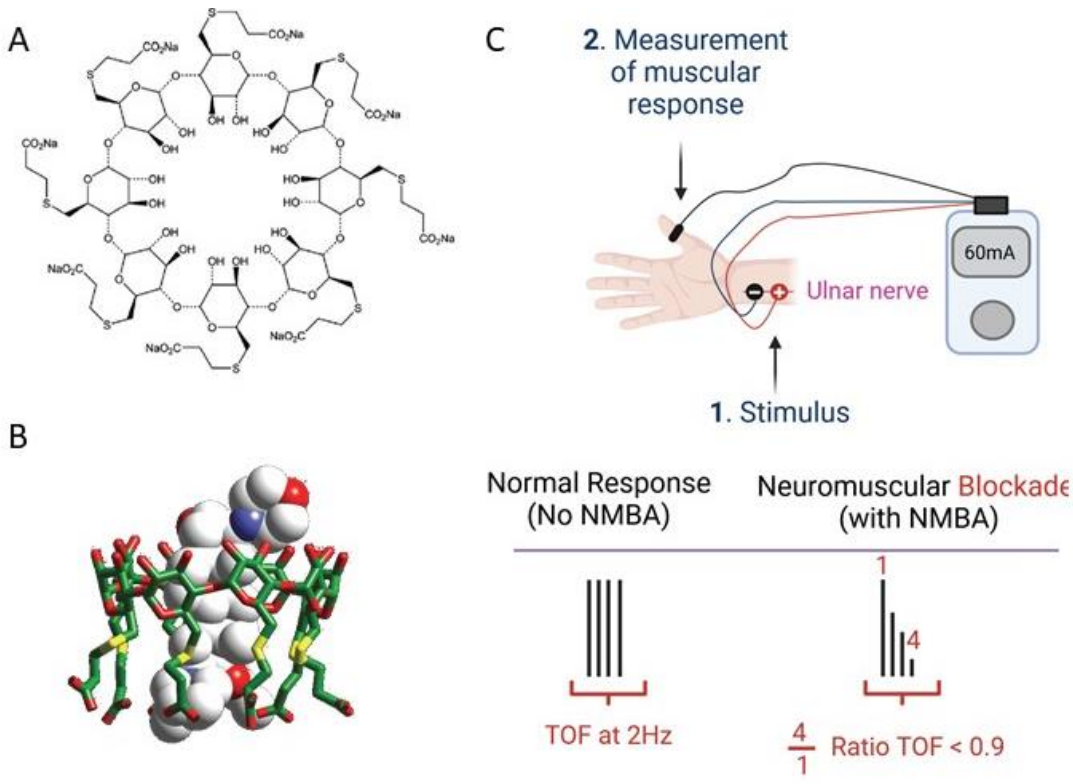

Figure 5: Monitoring reversal of rocuronium-induced neuromuscular blockade using sugammadex.
(**A**) Structure of sugammadex sodium[145]. (**B**) Complex formation of sugammadex and rocuronium as obtained by X-ray diffraction. The rocuronium molecule (model with spheres) is completely encapsulated by sugammadex (model with sticks in green)[146]. (**C**) Monitoring of neuromuscular blockade using TOF. Muscles on the ulnar nerve are electrically stimulated 4 times (twitches). The amplitude of the muscular responses is monitored and the ratio of the fourth response divided by the amplitude of the first response is measured and referred to as the TOF ratio. A TOF ratio lower than 0.9 is a reference threshold of neuromuscular blockade. TOF, Train of Four. (Biorender)

4 Identification of antibodies of interest from B cells

4.1 What are antibodies?

Antibody production by B cells and the mechanisms involved in increasing their affinity and specificity require complex steps that will be presented in this section.

First, it is important to note that antibodies exist in two forms: either they are found anchored to the B cell membrane as **BCRs** or they are water soluble proteins **secreted** by the B cells and patrolling in extracellular fluids such as the bloodstream, lymph nodes, skin, lungs, saliva, breast milk… Antibodies are 180,000 dalton symmetrical proteins composed of two identical **heavy** and a **light** chain connected by disulfide bonds possessing a **variable** (at their N-terminal) and the **constant** region (at their C-terminal). The variable regions are responsible for antigen recognition and are composed of hyper-variable subregions named complementarity-determining regions (CDR1, CDR2, and CDR3) flanked by less variable subregions referred to as framework regions (FR1, FR2, FR3, and FR4). The six CDRs (three in the heavy and three in the light chains) are polypeptide loops with hypervariability anchored in the framework's beta-sheets (Fig 6). The light chain in human and mice falls in two classes: kappa or lambda, with a higher ratio of kappa versus lambda (kappa: lambda ratio of 60:40 in humans and 95:5 in mice)[147].

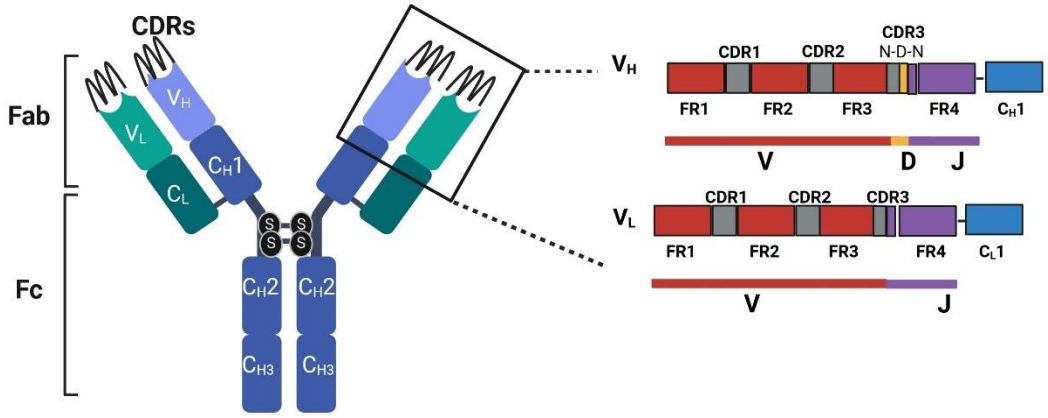

Figure 6: Antibody structure and variable chains genetic coding.
Antibodies are composed of two identical heavy and light chains (kappa or lambda) connected by covalent disulfide bridges. The lower region is the Fc fragment and the upper is the Fab fragment. Each chain is composed of a variable and constant region. The variable region binds the antigen and is coded by V(D)J gene segments that encode the CDR3 loop which is the region with the highest diversity. The constant region confers the function of the antibody by allowing its binding to receptors on effector cells. CDR, Complement Determining Regions; CL, Constant Light; Fab, Fragment antigen binding; Fc, Fragment crystallizable; FR, Framework; S, sulfide; VH, Variable heavy; VL, Variable Light. (Biorender).

The constant region of the heavy chain confers its **effector function** to the antibody by binding to receptors on white blood cells and complement. This constant region also defines the class of the antibody: IgM, IgD, IgA, IgG, and IgE with IgG, IgA, and IgD possessing three constant domains (C_H1, C_H2, and C_H3) whereas IgE and IgM have four (Fig 7B). The light chain also possesses a constant region and the association of the Variable heavy (VH), variable light (VL) and CH1 forms two identical fragment antigen binding (Fab) regions that can recognize an antigen. Each antibody class possesses distinct roles and is mainly located in different regions of the body. Briefly, IgM have generally a low-affinity but their ability to form pentameric structures confers them high avidity. Their multimeric structure facilitates their ability to activate the complement and to bind to multivalent pathogens such as bacteria[148]. IgG is the most predominant isotype in the blood and extracellular fluids, representing up to 75% of the antibodies class[149]. They are mostly present as monomers but their ability to form immune complexes when binding to multivalent antigens allows them to bind with avidity to FcyRs[150]. IgA can form dimers and are mostly present in the epithelium of the intestinal and respiratory tracts[151]. IgE antibodies are present at the lowest concentration of the five isotypes in circulation in the blood but can remain bound to effector cells such as mast cells under the skin or mucosa, and basophils. Finally, IgD isotypes are less characterized but are suspected to play a role in the initiation of the immune response. They are of low-affinity and found in higher concentrations than IgE but lower than the other isotypes because they are mainly attached to B cells and rarely found in their soluble form[152]. In the next section, we will explain the antibody formation process.

4.2 The antibody repertoire formation

Ideally, we would need 100 million different antibodies to protect us against the wide range of potential pathogens. However, there are 25,000 genes in human cells, and even by combining the genetic diversity of the VH and VL, not enough combinations could be generated. Therefore, another mechanism different from the classical genetic information transmitted from one mother cell to two daughters needs to exist. This process discovered by Tonegawa[153] consists of **somatic recombination** of the genes coding for the variable region of a naive B cell. The entire scope of BCRs in an individual will be referred to as the **antibody repertoire** and the mechanism to generate this variety of antibodies will be depicted in the following paragraphs.

Indeed, the VH and VL present on the BCRs of human B cells are coded by three chromosomes (chromosome 14 for the VH, 2 for the VL of the kappa chain, and 22 for the VL of lambda)[154] that possess **copies of DNA modules**, called gene segments: one Variable (V), one Diversity (D) and one Joining (J) for the heavy chain, only VJ for the light one. The first two hypervariable loops of the heavy chain (CDR1 and

CDR2) are encoded by the V_H gene segment. The **CDR3** is the most diverse since it is formed by amino acids coded by the V_H, D, and J_H gene segments, thus additional insertions of random nucleotides are required to make the V_H-D and D-J_H junction[155]. The V_H -D and D-J_H junctions can also be nibbled away and replacement nucleotides named N-nucleotide can be inserted, hence increasing the diversity (Fig 6). The D gene segment is present only on the VH locus and is lacking in the VL. In humans, there are about 50 gene fragments for the V segment, 27 for the D, and 6 for the J segment[156]. To assemble in a mature heavy and light chain, the B cells select randomly these gene segments and assemble them together, a process termed **V(D)J** recombination monitored by Recombination activating genes (**RAG**) proteins[157]. V(D)J recombination occurs in an early differentiation stage of B cells in the bone marrow therefore all the progeny of a B cell expresses the same V genes. It is important to note that each B cell has identical BCRs expressed on its surface (approximately 50 000-100 000).

The BCR of a naive B cell that did not encounter an antigen is referred to be in its **germline configuration** but to increase the genetical diversity, the variable regions of the Ig can be later modified in the germinal centers (GC). Upon contact with its cognate antigen, the variable region of the immunoglobulin undergoes **mutations** in a relatively **stochastic** manner since this process is biased by some DNA motifs. Indeed, in the process of joining the V(D)J gene segments together, additional DNA bases are replaced, added, or deleted by enzymes, a mechanism called **somatic hyper-mutation**. With this sophisticated "lottery-like" process, a small amount of genetic information is required to create a broad antibody diversity. During this operation, single strands of DNA are broken and repaired by random nucleotide additions at the end of the gene segments, a process referred to as **non-homologous end joining** that increases the junctional diversity[158]. Non-homologous end joining can happen in the bone marrow on naive B cells and in the GC, and for each location, different enzymes are involved. In the bone marrow, this process depends on RAG proteins that induce the single-strand breaks while terminal deoxynucleotidyl transferase (TdT) randomly adds nucleotides. In the GC, this mechanism involves the enzyme activation-induced cytidine deaminase (**AID**) that converts cytosines in uracil bases which introduces single-strand DNA breaks at the end of the selected V, D, and J gene segments[159]. Nonetheless, it has been shown that mutations are not fully random and appear to be more frequent on certain DNA motifs, named **hotspots** that are predominant in the V region of Ig genes. Indeed, hypermutations are preferentially found in the DGYW/WRCH motif (G:C is the mutable position; D=A/G/T, H=T/C/A)[160]. The **CDR3** is notable for its high diversity, thus considered to determine the antibody specificity since it is coded by the **junctional** random mutations from associating the V and J gene segments. The recombination of the heavy chain is performed before the one of the light chains and the isotype kappa of the light chain before the lambda. At each step, the recombined heavy

and light chains undergo a selection process to ensure the functionality of the antibody since non-functional BCRs are eliminated. Even though the relative abundance of kappa and lambda light chains is 66% versus 34% in humans (whereas 95% kappa versus 5% lambda in mice), some antigens such as the human immunodeficiency virus have been shown to trigger a biased selection towards lambda light chains [161-162]. All in all, this mechanism allows the generation of approximately 10^{11} antibody recombination[163].

The antibody class that depends on the constant region of the heavy chain of the antibody can also be modified during B cell maturation and proliferation. A B cell always starts by expressing an IgM and/or IgD on its surface that can later switch in the GC as an IgG, IgA, or IgE once the B cell has been stimulated by an antigen. The IgH locus first expresses the exon δ (for IgD), followed by μ (for IgM), γ (for IgG), α (for IgA), and or ϵ (for IgE). A naïve B cell can co-express IgM and IgD due to the alternative splicing on the exons of the μ and δ heavy chains. Unlike the δ gene fragment, the other isotypes possess a **switch region** that explains that this mechanism happens in a unilateral direction (an antibody cannot switch back to its precedent isotype). Indeed, **isotype switching** consists of replacing the exon δ and μ of the constant heavy chain regions with the exon γ, α, or ϵ using **double-strand** DNA breaks in the switch region located upstream of each constant heavy gene region (except for the IgD constant region) by the same enzyme as the one involved in somatic hypermutation: **AID**[164] (Fig 7.A). The cytokine environment favors certain isotype switches. For instance, the presence of **IL-4 / IL-13** and the reduction of interferon-gamma facilitates the switch to IgE antibodies[165]. The cytokines are produced by **Th cells** that recognize the antigen exposed on the B cell surface and are presented to the T cell via an MHC molecule. During anaphylaxis, Th2 response and IL-4 stimulate the isotypes to switch to IgG1, IgG2, IgG4, and IgE. It was also shown that the IgE isotype switch is enhanced by the absence of IL-21 in mice[166]. In humans, the switch to an IgE can happen via two routes: either a direct switch from IgM to an IgE or the indirect route from an IgM to an IgG switching in an IgE. In the first route, the IgM+ precursor B cell is immature whereas, with the indirect switch, the IgG+ B cells can experience the GC process (somatic hypermutation, affinity maturation, and Bmem development)[167].

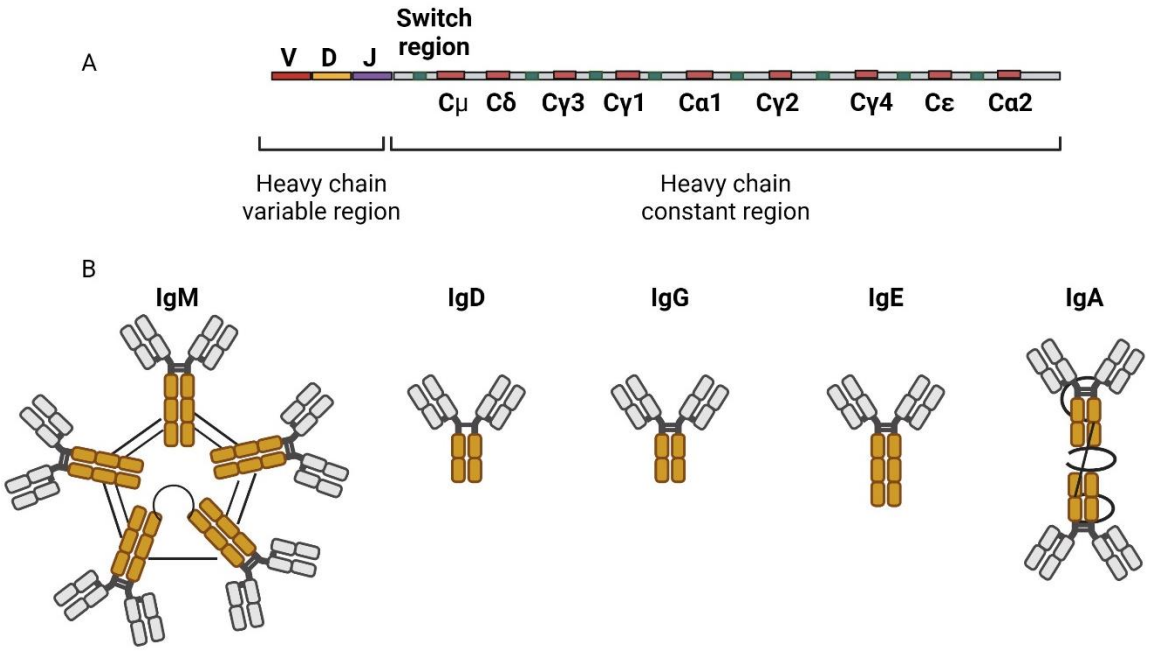

Figure 7: Generation and structure of the different classes of antibodies.
(**A**) Antibody class switch. Different classes of antibodies are generated with identical variable regions and distinct constant domains with the class switch recombination mechanism. Double strand breaks are generated in DNA at conserved nucleotide motifs called switch regions (in green) located upstream of a gene fragment (in red). IgM antibodies are the first ones to be produced, followed by IgD, IgG that can be subdivided into four subclasses, IgE and IgA. (**B**) The five main classes of antibodies are classified according to the type of heavy chain constant region. IgM antibodies have a pentameric structure, hence a high avidity for antigens, IgA form dimers, and the other classes of monomers. (Biorender).

4.3 B cells activation and differentiation in antibody-secreting cells

B cells are produced during hematopoiesis in the **bone marrow** where V(D)J rearrangement occurs. Following the Ig gene rearrangement, immature B cells undergo negative selection to confirm **self-tolerance**, therefore to delete auto-reactive B cells with the help of follicular dendritic cells presenting self-antigens and regulatory T cells[168].

Then, naive B cells migrate to **secondary lymphoid organs** (lymph nodes, spleen, and mucosal tissue) where they can encounter an antigen presented by dendritic cells. Some B cells can directly secrete low-affinity IgM and IgA after this presentation, they are called short-lived T-independent antibody-secreting cells (**ASC**s). Other subsets of the B cell can interact with a T cell via important molecular players: 1) presentation of antigen on an MHC class II from the B cell to the T cell; 2) co-stimulation of CD40 on B cells that binds CD40 Ligand (**CD40L**) and the T cell; 3) T cell cytokine expression of cytokines such as IL-4 and IL-21. During this T cell:B cell interaction, the Ig class-switch recombination occurs[169] and leads to the proliferation and differentiation of the B cells in 3 subtypes: GC-independent Bmems, GC B cells, or short-lived plasma cells[170]. This non-canonical pathway occurring outside the GC is referred to as **extrafollicular** response and tends to generate predominantly lower affinity IgM+ Bmems[171-172]. Alternatively, the B cell can enter a **GC**, this transient structure is necessary to generate higher affinity B cells since it is the localization of the highly selective process depicted in the previous paragraph. Indeed, in the GC, the B cell undergoes **proliferation** and **somatic hypermutation** in the dark zone before exiting in the light zone where they can encounter the antigen presented on dendritic cells and present it to T follicular helper cells to either differentiate in long-lived Bmems, or long-lived plasma cells or re-enter the dark zone in a recursive process (Fig 8). Higher affinity BCR mutants capture more antigens, leading to a higher density of peptide MHC-complexes, resulting in a greater share of Th cells, turning in positive selection. Following a positive selection, the B cells are expanded whereas B cells with low-affinity BCRs capture less antigen and go through apoptosis or anergy. This migration from the dark zone to the light zone can be repeated several times to generate higher affinity of Bmems/plasma cells, a process referred to as **affinity maturation** that is made possible with the somatic hypermutation mechanism.

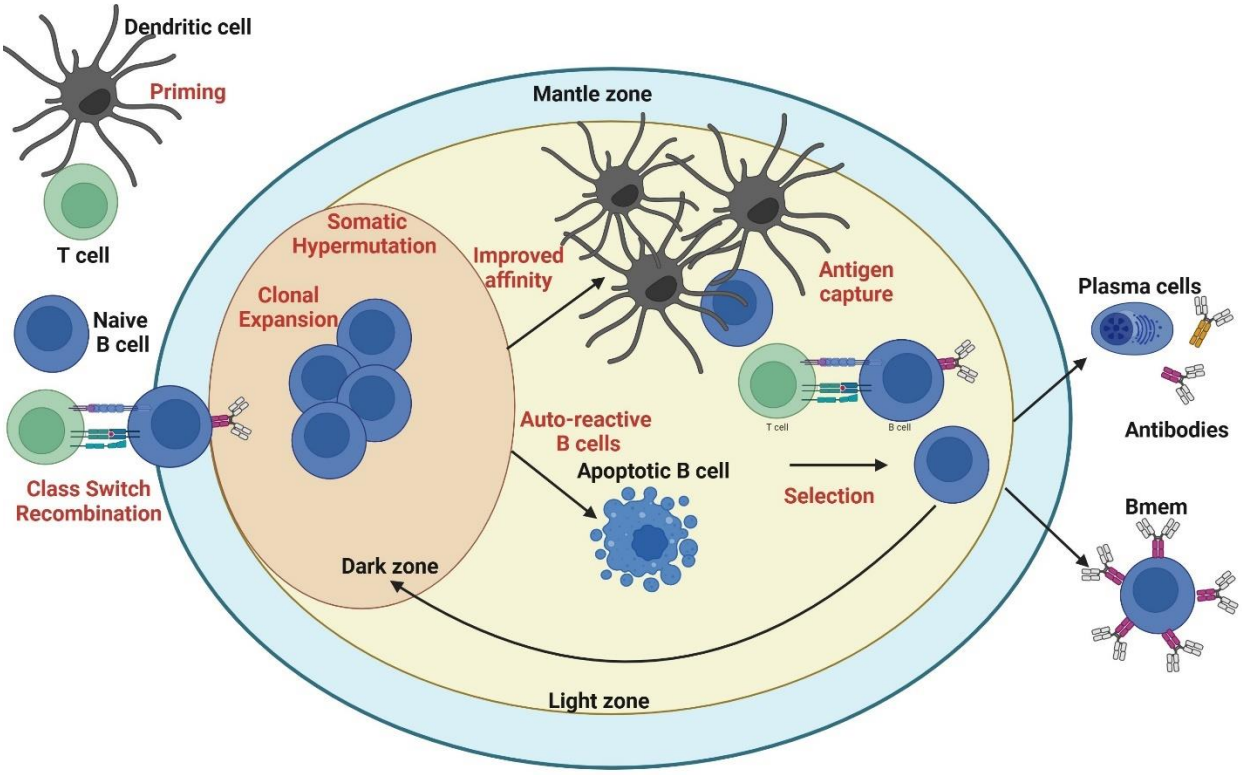

Figure 8: Affinity maturation of B cells in the GC.
After priming and class-switch recombination occurring outside the GC, naive B cells undergo clonal expansion and somatic hypermutations in the dark zone of a germinal center before entering the light zone where they are subjected to selection by follicular T helper cells in the presence of dendritic cells to improve affinity to the immunizing antigen. Auto-reactive B cells or B cells with unfavorable BCR undergo apoptosis. Selected B cells either differentiate in Bmem or plasma cells or re-enter the dark zone to repeat the process. Bmem, memory B cells; GC, Germinal Center. (Biorender)

4.4 How to identify a B cell repertoire: plasmabast/plasma B or Bmems?

To identify a B cell repertoire, i.e. the range of BCRs expressed by an individual B cell population specific to a given antigen, various subsets of B cells can be investigated: plasmablast, plasma cells, or Bmems. **Plasmablasts** are very short-lived ASC B cells producing low-affinity antibodies that usually arise from an extrafollicular response. They are dividing cells with high migratory properties and are known to be the precursors of plasma cells that can secrete antibodies [173]. **Plasma cells** are terminally differentiated ASCs that cannot divide and are traditionally described as short-lived. Bmems are very long-lived B cells, they can survive for decades to be easily reactivated to produce ASCs when exposed to an antigen[173]. The persistence of humoral response in time can be explained by the activation of **Bmem** or with the presence of a recently identified subset of ASC, referred to as **long-lived plasma cells**. These cells have been shown to survive for long periods in niches located in the bone marrow and are reported to be motile[174]. The

origin of this cell subset remains elusive and it is still unclear if they preferentially originate either from GC plasmablast, Bmem, or short-lived plasma cells[174]. Bmem and long-lived plasma cells express high-affinity antibodies that are modified by class-switch recombination and somatic hypermutation, a hallmark of GC reaction, even though those two mechanisms can occur in B cells activated outside of GC.

A lot of questions remain concerning the persistence of Bmems and the definition of "true" **memory**. Indeed, are Bmems conserved for decades after a single antigen-encounter and can be re-activated activated years later by an intermittent stimulation or does memory require the continuous presence of antigen or can a Bmem be activated years later by an intermittent stimulation? The concept of **vaccination** relies on the second hypothesis stating that consistent antigen exposure is required to maintain memory since it is necessary to boost several times to obtain long-lasting vaccinal protection. The antigen-stimulation-dependent memory dogma was also supported by adoptive transfer experiments (transfer of B and T cells from antigen-primed mice) that showed a memory decay in the antigen-free mice[175]. These results were reinforced by experiments using different viruses with distinct replication rates, hence generating different reservoirs of antigens that revealed that memory cytotoxic T lymphocytes were short-lived and needed stimulation by persisting antigens to confer long-term protection[176]. Nonetheless, contradictory results reveal that dormant Bmem can persist in the absence follicular of dendritic cells, with however a reduction of antibody production, hence of plasma cells[177]. Complementary experiments on T cells deprived mice (before, during, or after immunization) showed that preliminarily established Bmem can persist for at least 6 weeks in the absence of antigen-mediated T helper cells. A genetically modified mice model using a genetic switch with Cre recombinase that can induce targeted mutagenesis in the BCR to generate B cells exposed to an antigen that produces a BCR that does not bind the inducing antigen elegantly supported the hypothesis that Bmems retain their original antigen-binding specificity and **did not require persistent antigen exposure**[178]. Both hypotheses were demonstrated using models with limitations (artificial systems with genetically modified mice), therefore today it is impossible to state which mechanism reflects reality, even though both pathways are probably not exclusive. Another question resides: can cross-reactive environmental antigens activate Bmems and, in this case, are the same Bmem reactivated or do they form new GC? Investigating the evolution of the B cell repertoire upon antigen re-exposure or not could provide insights into these elusive mechanisms.

The identification of a B cell repertoire requires the isolation of either Bmem or long-lived plasma cells. Since Bmems express Ig at their surface unlike plasma cells that secrete them, it is easier to identify the **repertoire** of Bmem in the first place. Indeed, using flow cytometry these cells can be single-cell sorted

and sequenced in a relatively simple manner[179]. The BCR repertoire of antigen-specific ASC requires more advanced technologies such as microfluidic droplets that can entrap a single ASC in an aqueous drop. Sequencing can be performed after sorting in a multi-well plate or in the presence of bar-coded primers[180]. Another recent technology to study the antibody repertoire of ASCs in human serum relies on high-resolution mass spectrometry that consists of the enzymatic digestion of the mAbs into peptides, followed by liquid chromatography-mass spectrometry analysis and proteogenomic/bioinformatics for CDR3/VHV/VL identification[181]. Great progress has been achieved concerning the sequencing and analysis of the collection of BCRS in an individual against an antigen (called its adaptive immune receptor repertoire (AIRR)). Indeed, the AIRR Community proposes bioinformatics tools to describe the BCR repertoire according to the V-J gene usage, CDR3 length, and CDR3 amino acid sequence[182- 183].

HYPOTHESIS & AIMS

In this work we aimed to tackle two severe side effects caused by the extensively used NMBA, rocuronium: 1) NMBA-mediated AHR in patients who undergo anesthetic procedures, 2) residual neuromuscular blockade after the end of surgery. The first side effect is poorly understood since some patients who were never exposed to the molecule can suffer from an NMBA-mediated AHR and the diagnostic follow-up often does not permit to elucidate the mechanism with contradictory results in the detection of sIgE antibodies. Concerning residual neuromuscular blockade, one drug sugammadex can reverse rocuronium-induced deep neuromuscular blockade but its use is controversial due to the presence of allergic side effects.

Therefore, we hypothesized that:

1) Investigating the **Bmem IgG+ repertoires** would give us insights into the mechanisms of NMBA-mediated allergies, based on the previous findings by Jönsson et al.,[93] showing that circulating anti-NMBA IgE and IgG antibodies were involved in NMBA-mediated AHR, and relying on the immune memory of the patients. Indeed, the most plausible cause of anaphylaxis to NMBA remains the existence of anti-NMBA antibodies in patients, implying NMBA-specific B cells.

2) The isolation of rocuronium-specific mAbs either in patients or mice would help us to elucidate the mechanisms of NMBA-mediated anaphylaxis by performing *in vitro* and *in vivo* experiments with the recombinant mAbs to test their efficacy in **activating effector cells** and **inducing anaphylaxis** in their IgE and IgG isotypes.

3) Establishing a murine model by immunizing mice with rocuronium grafted on an immunogenic carrier protein, would allow us to generate high-affinity **rocuronium-specific IgG antibodies**.

4) The generation of high-affinity mAbs would permit the design of a therapeutic molecule that could capture rocuronium and **reverse deep neuromuscular blockade**.

Therefore, **Aim 1** of my thesis was to mine and profile the rocuronium-specific IgG+ Bmem repertoires of allergic patients to NMBAs. Three patients with positive levels of rocuronium-specific IgG antibodies in their serum were sampled and one with a nine-year interval. Using a cell culture system, single cells Bmem expressing rocuronium-specific IgG were sorted and differentiated in antibody-secreting cells *in vitro*. This allowed the identification of the Bmem rocuronium-specific repertoire by sequencing the variable regions of the BCRs and performing a bioinformatic analysis. The human antibodies were characterized in terms of specificity and affinity. Their potency to trigger anaphylaxis was also evaluated by switching them in

their IgE isotype, by performing experiments on effector cells (mast cells,) and by inducing passive systemic anaphylaxis in mice expressing a humanized IgE receptor.

Aim 2 was to generate a therapeutic antibody that could reverse rocuronium-induced neuromuscular blockade. Since the human mAbs isolated were medium to low affinities, we generated high-affinity mAbs by immunizing mice with rocuronium grafted on the immunogenic keyhole limpet hemocyanin (KLH) and using the hybridoma technology. Two high-affinity mAbs: 1B6 and 2B1 were characterized (affinity and specificity) and their crystal structures in complex with rocuronium were revealed. The capture potency of the mAb with the highest affinity (1B6) was first evaluated using a prophylactic model of prevention of neuromuscular blockade in mice. Then, the reversal efficacy of 1B6 was validated in non-human primates for which deep neuromuscular blockade was induced (monitored using a TOF) and reversed by injecting mAb 1B6 in a competitive timeframe (1-2 minutes) compared to the standard of care, sugammadex.

Aim 1 and 2 are summarized in the article under revision in *Science Translation Medicine*: Dejoux A and Qianqian Zhu et al., Drug-specific antibody repertoires unravel mechanisms of perioperative anaphylaxis and identify novel therapeutics.

Aim 3 was first to study the anti-rocuronium IgG-secreting cell repertoires of two mice using a microfluidic droplet-based screening, sorting, and sequencing pipeline previously reported[184]. Second, to elucidate the underlying mechanisms of NMBA-mediated AHR by investigating the IgE and IgG-dependent pathways. The high-affinity mAbs could activate effectors cells (mast cells and basophils as IgE antibodies and neutrophils as IgG) and could induce passive systemic anaphylaxis with very low antibody/antigen doses in mice expressing humanized IgE receptors.

Aim 3 is gathered in an article in preparation for submission: Dejoux A and Qianqian Zhu et al., Plasma cell repertoires identify high-affinity anti-rocuronium antibodies that recapitulate anaphylaxis *in vivo*.

Of note, two other projects were undertaken during the PhD, but the data will not be presented in this manuscript due to confidential issues and for the sake of clarity.

Article 1: Drug-specific antibody repertoires unravel mechanisms of perioperative anaphylaxis and identify novel therapeutics

In this article, under revision in *Science Translational Medicine*, we took advantage of the existence of anti-NMBA antibodies in allergic patients to unravel the mechanisms of NMBA-mediated AHR. Indeed, NMBA-mediated AHR is justified by the current dogma that proposes that IgE antibodies with reactivity towards NMBAs lead to mast cell and basophil activation in NMBA-allergic patients, but my team has previously reported that circulating anti-NMBA IgE and IgG levels correlate with the severity of anaphylaxis[93]. However, no anti-NMBA antibody has ever been identified and described to ascertain this dogma. We also developed an antibody-based reversal drug for residual neuromuscular blockade, using rocuronium and non-human primates as a proof of concept.

First, we characterized the Bmem antibody repertoires of patients with suspected hypersensitivity to rocuronium and identified anti-rocuronium mAbs with exquisite specificity for rocuronium and the ability to induce mast cell activation and passive systemic anaphylaxis in mice. The antibodies isolated in humans were of too low-affinity for rocuronium to reverse neuromuscular blockade *in vivo*, therefore we generated high-affinity antibodies by immunizing mice. We selected the mAb with the highest affinity for rocuronium, to demonstrate that an anti-rocuronium antibody expressed as an effector-less human IgG can reverse rocuronium-induced neuromuscular blockade in non-human primates with kinetics competitive with sugammadex. Additionally, we solved the co-crystal structures of rocuronium in a complex with two different high-affinity antibodies.

Our work reports on the underlying causes of anaphylactic reactions to NMBAs and paves the way to improve diagnostic tools for rocuronium hypersensitivity and for developing antibodies as drugs for neuromuscular blockade reversal. Not only do these findings substantially increase our understanding of the antibodies in drug allergy, but they also provide a rationale for the design of strategies targeting NMBAs to reverse neuromuscular blockade.

Title: Drug-specific antibody repertoires unravel mechanisms of perioperative anaphylaxis and identify novel therapeutics.

One Sentence Summary: Rocuronium reversal agents identified from rocuronium-specific Ab repertoires.

Authors: Alice Dejoux[1,2,†], Qianqian Zhu[1,3,†], Christelle Ganneau[4], Odile Richard-Le Goff[1], Ophélie Godon[1], Julien Lemaitre[5], Francis Relouzat[5], François Huetz[1], Aurélien Sokal[6,7], Alexis Vandenberghe[6], Cyprien Pecalvel[8], Lise Hunault[1,2], Thomas Derenne[1,2], Caitlin Gillis[1], Bruno Iannascoli[1], Yidan Wang[1], Thierry Rose[9], Christel Mertens[10], Pascale Nicaise-Roland[11], *NASA study group*, Patrick England[12], Matthieu Mahévas[6], Luc de Chaisemartin[3,11], Roger Le Grand[5], Hélène Letscher[5], Frederick Saul[13], Cédric Pissis[13], Ahmed Haouz[13], Laurent L. Reber[8], Pascal Chappert[6], Friederike Jönsson[1,14], Didier G. Ebo[10], Gaël A. Millot[1,15,§], Sylvie Bay[4,§], Sylvie Chollet-Martin[3,11,§], Aurélie Gouel-Chéron[1,16,17,§,*] and Pierre Bruhns[1,18,§,*].

Affiliations:

[1]Institut Pasteur, Université Paris Cité, INSERM UMR1222, Antibodies in Therapy and Pathology, 75015 Paris, France.

[2]Sorbonne Université, Collège Doctoral, 75005 Paris, France.

[3]Inflammation Chimiokines et Immunopathologie, INSERM UMRS996, Faculté de Pharmacie, Université Paris-Sud, Université Paris-Saclay, Châtenay-Malabry, France.

[4]Institut Pasteur, Université Paris Cité, CNRS UMR3523, Chimie des Biomolécules, 75015 Paris, France.

[5]Université Paris-Saclay, INSERM, CEA, Center for Immunology of Viral, Autoimmune, Hematological and Bacterial Diseases (IMVA-HB/IDMIT), Fontenay-aux-Roses & Le Kremlin-Bicêtre, France.

[6]Institut Necker Enfants Malades, INSERM U1151/CNRS UMR 8253, Action thématique incitative sur programme-Avenir Team, Auto-Immune and Immune B cells, Université Paris Cité, Université Paris Est-Créteil, Créteil, France; INSERM U955, équipe 2. Institut Mondor de Recherche Biomédicale (IMRB), Université Paris-Est Créteil (UPEC), Créteil, France.

[7]Service de Médecine interne, Hôpital Beaujon, Assistance Publique-Hôpitaux de Paris (AP-HP), Université de Paris Cité, Clichy, France

[8]Toulouse Institute for Infectious and Inflammatory Diseases (Infinity), INSERM UMR1291, CNRS UMR5051, University Toulouse III; Toulouse, France.

[9]Institut Pasteur, Université Paris Cité, INSERM UMR1224, Biologie Cellulaire des Lymphocytes, Ligue Nationale Contre le Cancer, Équipe Labellisée Ligue 2018, 75015 Paris, France.

[10]Faculty of Medicine and Health Science, Department of Immunology-Allergology-Rheumatology, Antwerp University Hospital and the Infla-Med Center of Excellence, University of Antwerp, Antwerp, Belgium; Department of Immunology and Allergology, AZ Jan Palfijn Ghent, Ghent, Belgium.

[11]Département d'Immunologie et d'Hématologie, UF Auto-immunité et Hypersensibilités, HUPNVS, Hôpital Bichat, Paris, France.

[12]Institut Pasteur, Université Paris Cité, CNRS UMR3528, Molecular Biophysics Core Facility, Paris, France.

[13]Institut Pasteur, Université Paris Cité, CNRS UMR3528, Plate-forme Cristallographie-C2RT, Paris, France.

[14]CNRS, F-75015 Paris.

[15]Institut Pasteur, Université Paris Cité, Bioinformatics and Biostatistics Hub, Paris, France.

[16]Anaesthesiology and Critical Care Medicine Department, DMU Parabol, Bichat-Claude Bernard Hospital, AP-HP, 75018 Paris, France.

[17]Université Paris Cité, 75010 Paris, France.

[18]INSERM 1152, DHU FIRE, Labex Inflamex, Université Paris Diderot Paris 7, Paris, France.

[†]: Equal contribution.

[§]: Co-senior authorship.

*To whom correspondence should be addressed: **Pierre Bruhns**, Unit of Antibodies in Therapy and Pathology, Department of Immunology, Institut Pasteur, 25 rue du Docteur Roux, 75015 Paris, France. Phone: +33-145688629. E-mail: bruhns@pasteur.fr; **Aurélie Gouel-Chéron**, Anaesthesiology and Critical Care Medicine Department, DMU Parabol, Bichat-Claude Bernard Hospital, AP-HP, 75018 Paris, France. Phone : +33-140258355. E-mail: aurelie.gouel@aphp.fr

Abstract:

NeuroMuscular Blocking Agents (NMBA) relax skeletal muscles to facilitate surgeries and ease intubation but lead to adverse reactions: in most cases complications due to postoperative residual NeuroMuscular Blockade (rNMB), and in rare cases severe acute hypersensitivity reactions (anaphylaxis). Both adverse reactions vary between types of NMBAs with rocuronium, a widely used non-depolarizing NMBA, inducing among the longest rNMB durations and highest anaphylaxis incidence. Rocuronium-induced anaphylaxis is proposed to rely on pre-existing rocuronium-binding antibodies, but no such antibody has ever been identified. Deep blockade induced by rocuronium can be reversed by the synthetic γ-cyclodextrin sugammadex that provokes however rare anaphylaxis cases. Herein, we investigated the memory B cell antibody repertoire of patients with suspected hypersensitivity to rocuronium. We identified polyclonal antibody repertoires with a high diversity among V(D)J genes without evidence of clonal groups. Recombinantly expressed, these antibodies demonstrated specificity and low affinity for rocuronium without cross-reactivity for other NMBAs. Expressed as human IgE they triggered human mast cell activation and passive systemic anaphylaxis in transgenic mice. Their affinities were insufficient, however, to capture rocuronium *in vivo* and serve as reversal agents. Rocuronium-specific, high-affinity antibodies were thus isolated from rocuronium-immunized mice and their binding modes with rocuronium deciphered by X-ray crystallography. The highest affinity antibody reversed rocuronium-induced neuromuscular blockade in non-human primates with kinetics like those of sugammadex. This work reports on the underlying causes of anaphylactic reactions to NMBAs, and paves the way to improve diagnostic tools for rocuronium hypersensitivity and for developing antibodies as drugs for neuromuscular blockade reversal.

INTRODUCTION

Neuromuscular Blocking agents (NMBAs) are used in the clinic to paralyze skeletal muscles during surgery conducted under general anesthesia (*1, 2*). They help to assist airway management in programmed or emergency anesthesia by facilitating endotracheal intubation. NMBAs operate at the neuromuscular junction by competing with acetylcholine to bind nicotinic receptors. All NMBAs possess two tertiary and/or quaternary substituted ammonium groups at physiological pH that enable NMBAs to compete with the quaternary ammonium group of acetylcholine for binding to nicotinic receptors. NMBAs have two major side effects: acute hypersensitivity reactions or anaphylaxis that can be life-threatening (*3, 4*) and, in the absence of appropriate monitoring, residual NeuroMuscular Blockade (rNMB) that can lead to tracheal damage and infections (*5*).

The most common adverse reaction following NMBA exposure is due to prolonged presence of NMBA after the end of its infusion, *i.e.* residual neuromuscular blockade. This complication is frequent in the absence of appropriate neuromuscular function monitoring that, despite international recommendations (*1, 2*), is not applied to more than 20% of the patients. Residual neuromuscular blockade can lead to postoperative pulmonary events, pharyngeal dysfunction, urgent tracheal reintubation and prolonged stay in post-anesthesia care units and hospitals that lead to a high economic burden (*6*). The first option for pharmacological neuromuscular blockade reversal, neostigmine (Prostigmine®; used for atracurium reversal), is restricted to situations where half of the spontaneous reversal is effective – thus inefficient on deep neuromuscular blockade (*7*). The second one is the synthetic γ-cyclodextrin sugammadex (Bridion®) (*8*) that encapsulates the aminosteroid NMBAs rocuronium and vecuronium *in vivo* within minutes following injection, and is efficient on deep neuromuscular blockade. Instant blockade reversal might also be necessary, as in difficult intubation scenarios, explaining that it has been considered economically advantageous to administer sugammadex despite a cost of $100-200 per patient, leading to a $400-3,000 economy per patient (*6*). Yet, multiple cases of anaphylaxis induced by sugammadex or by the sugammadex-rocuronium inclusion complex (S-R-Cx) have been reported (*9-12*) leading to restrictions of its use in several countries (*11*).

Rocuronium is the most used NMBA worldwide for full-stomach rapid sequence induction, and has become almost exclusive in countries like Japan, due to the existence of sugammadex for deep neuromuscular reversal (*13*).

The most dramatic adverse event following NMBA exposure is anaphylaxis, the most severe form of allergic reactions that can lead to fatalities, even after rapid recognition and correct management. In some countries, half of perioperative anaphylaxis are caused by NMBAs with a global mortality rate of 4.1% (*14*). The current dogma proposes that IgE antibodies with reactivity towards NMBAs lead to mast cell and basophil activation in NMBA-allergic patients (*15*), and we reported earlier that, indeed, circulating anti-NMBA IgE levels, but also anti-NMBA IgG levels, correlate with the severity of anaphylaxis (*16*). In our view, two pathways are involved in NMBA-induced anaphylaxis separately or concomitantly depending on the patient: the IgE pathway leading to mast cell and basophil activation with histamine release as a major mediator, and the IgG pathway leading to neutrophil and monocyte activation with Platelet-activating Factor (PAF) release as a major mediator (*15, 17*). Both histamine and PAF induce vasodilation, bronchoconstriction, cardiac and pulmonary failure, with probable cumulative or potentiating effects when both mediators are released (*18*). Routinely, only anti-NMBA IgEs are quantified in clinical practice, using a morphine group (termed "Quaternary Ammonium Molecule"; QAM) as a surrogate for NMBA in ImmunoCAP detection as its molecular structure resembles ammonium groups present in some aminosteroid NMBAs (*19, 20*). Morphine ImmunoCAP demonstrates acceptable specificity and sensitivity for aminosteroids (e.g., rocuronium) and suxamethonium, but not for benzylisoquinolines (e.g., atracurium) (*21*).

The tertiary and quaternary substituted ammonium groups present in NMBAs have been proposed to be part of the epitope recognized by anti-NMBA antibodies in patients, as patient sera reacting with one or several NMBAs (*22*) cross-react with unrelated molecules possessing a quaternary ammonium (*23, 24*). Since anti-NMBA mAbs have never been identified, neither from patients nor animals, molecular or structural evidence lacks to ascertain these hypotheses. Importantly, anaphylaxis occurs at the first exposure to aminosteroid NMBAs in half of the patients (*25*), excluding NMBA ammonium groups as primary sensitizing epitopes in the patient's history. NMBAs are small compounds (Molecular Weight ≈ 300-1,000 Da) with unknown

properties in terms of immunogenicity; several families of compounds are however considered to sensitize towards NMBAs, including cosmetics, cleaning and bleaching products, as well as cough syrups containing morphine-based compounds (*22, 26*). Among the latter, studies proposed pholcodine, an opioid cough suppressant with two tertiary ammonium groups at physiological pH, to be a culprit molecule responsible for NMBA hypersensitivity (*27, 28*). Large variations in serum reactivity profile to NMBAs are found between individuals, from a single NMBA to NMBAs belonging to the same chemical family, and even to all NMBAs in 4% of the cases (*22*), suggestive of B cell responses with one or multiple monospecificities each toward a particular compound, and/or cross-reactive B cell responses towards different NMBAs.

To investigate for the first time the antibody fine specificity and affinity for NMBAs in patients who experienced NMBA-induced anaphylaxis, we analyzed single memory B cells with rocuronium reactivity. Antibody repertoires were polyclonal with high V(D)J diversity, exclusive for rocuronium among NMBAs and anaphylactogenic when expressed as human IgE *in vitro* and *in vivo* in mice. Because patient-derived anti-rocuronium mAbs were of low-to-medium affinity and incapable to capture clinical doses of rocuronium *in vivo*, we generated high affinity rocuronium-specific mAbs from immunized mice that reversed rocuronium-induced neuromuscular blockade in non-human primates with similar kinetics as sugammadex. These latter mAbs captured rocuronium in a hydrophobic cleft in which the quaternary ammonium group is completely buried and involved in the binding. High affinity anti-NMBA mAbs represent therefore a novel potential therapeutic avenue for the reversal of neuromuscular blockade.

RESULTS

Identification of rocuronium-specific memory B cells from NMBA allergic patients

Patients with presumed anaphylaxis to NMBAs during general anesthesia were included in two clinical studies (France, registered under NCT05420935, and Belgium) to obtain large volumes of blood for PBMC isolation. Among these, three patients experienced fast occurring symptoms (< 5 min) of anaphylaxis and were admitted to the intensive care unit (ICU) afterwards (Table 1). Patient#1 developed a mild Ring & Messmer grade 2 anaphylaxis to atracurium in 2012 and was sampled for peripheral blood mononuclear cells (PBMCs) in 2014 and 2023. Patient#2 and Patient#3 developed a severe grade 3 and 4 anaphylaxis, respectively, to rocuronium (Fig. 1A) in 2020, and were sampled a few weeks later. QAM IgE ImmunoCAP were positive only for Patient#2, although Patient#1 and Patient#3 had been previously exposed to NMBAs (Table 1). Anti-rocuronium IgE ImmunoCAP was positive only for Patient#3 (Fig. 1B). Skin prick tests and basophil activation tests with rocuronium were negative for Patient#1 but positive for Patient#2 and Patient#3 (Table 1). Anti-rocuronium IgG levels were, however, elevated compared to controls in all three patients, and in both serum samples of Patient#1 at 9 years difference (Patient#1_2014 and Patient#1_2023) using ELISA (Fig. 1C), LuLISA and ImmunoCAP (Supp. Fig. 1). We have previously reported that both IgE and IgG pathways exist with potentially additive/synergistic effects in human NMBA-induced anaphylaxis, and that Patient#1 had elevated serum anti-rocuronium IgG levels even if presenting with a grade 2 atracurium-induced anaphylaxis (*16*). In agreement with these findings, Patient#3 that developed a grade 4 anaphylaxis upon rocuronium infusion presents with elevated levels of both anti-rocuronium IgE and IgG (Fig.1B-C).

IgE memory B cells remain elusive and their existence is still questioned/disputed (*29*), as their survival may be extremely limited (*30-33*). As it has been proposed that IgE plasmablasts (and plasma cells) are continuously derived from IgG memory B cells (*34*), we decided to explore the IgG memory B cell compartment as a surrogate for the IgE B cell compartment to define the rocuronium-specific antibody repertoire in these patients. We single-sorted $CD27^{+}$ memory B cells from frozen PBMCs from these three patients based on expression of memory B cell markers

(IgD$^-$ CD19$^+$ CD27$^+$) using fluorescently-labeled monomeric human serum albumin-rocuronium conjugate (HSA-roc) as a bait for B cell receptor (BCR) with affinity for rocuronium, and exclusion of markers of other immune cells (CD3$^-$, CD14$^-$, CD35$^-$) and affinity for HSA alone (Fig.1D). The percentage of HSA-roc$^+$ HSA$^-$ among CD27$^+$ IgD$^-$ memory B cells varied between patients with a mean of 4.6% (2.74 and 6.5%) for both sorts of Patient#1_2014, 1% for Patient#1_2023, 2% for Patient#2 and 3.6% for Patient#3 (Supp. Fig. 2A-B). Of note, the percentage of CD27$^+$ cells among antigen-specific CD3$^-$ CD14$^-$ CD19$^+$ CD38$^-$ CD27$^+$ IgD$^-$ cells varied from 58 to 89% (Supp. Fig. 2C).

Characteristics of anti-rocuronium memory B cell repertoires from NMBA allergic patients

In order to test the specificity towards rocuronium of the antibodies corresponding to the BCRs expressed by these memory B cells before V(D)J sequencing of their VH-VL, we cultured these single cells in an optimized *in vitro* culture assay allowing their differentiation in antibody-secreting cells (*35, 36*). After 25 days of culture, supernatants with detectable amounts of IgG were further tested for rocuronium specificity by ELISA using HSA-rocuronium as an antigen in the absence or presence of free rocuronium (competitive inhibition ELISA). We obtained 57 supernatants with rocuronium specificity from the CD27$^+$ memory B cell cultures of Patient#1_2014, 128 for Patient#1_2023, 45 for Patient#2 and 23 for Patient#3 (Supp. Table 1). These represented only a minor fraction of the monoclonal cultures, from 1.3% to 16.7%, indicating poor selectivity of the allophycocyanin-labeled HSA-roc used as a bait for sorting. This selectivity did not increase with sorts using antigen labeled with two different fluorophores (HSA-rocuronium-APC versus HSA-rocuronium-FITC), and/or when selecting atypical CD45RB+ memory B cells (*37*) instead of CD27+ memory B cells (Supp. Fig. 3). As expected from serum reactivity to rocuronium in humans (*16*), higher numbers of rocuronium-specific memory B cells and stronger binders were identified when comparing antigen-specific sorts of PBMCs from Patient#1_2023 with PBMCs from a healthy donor (Supp. Fig. 4).

RNA of the 240 monoclonal cell cultures (listed in Supp. Table 2) was extracted to perform V(D)J sequencing of their VH-VL domains. Using the *repertoire-profiler* bioinformatic pipeline (refer to the Methods section) (*38*), we established the anti-rocuronium antibody repertoire

profile of the three patients. We obtained a total of 211 VH and 191 VL sequences (Fig. 1E) with a mutational load compared to germline showing gaussian distributions for Patient#1 and Patient #2 with an average of ~14 nucleotide mutations in the VH and ~7 in the VL (Supp. Fig. 4). The distribution of mutations among VH and VL sequences of Patient#3 was not gaussian with a majority of non- or poorly-mutated sequences.

Analyses of V-J gene usage identified highly diverse and polyclonal repertoires, both intra- and between patients, for both the VH and VL sequences. Indeed, the proportion of B cells with VH sequences coded by identical V-J genes was lower than 11% for all patients. The VL sequences were as diverse, with identical V-J genes lower than 9% except for Patient#3 for whom 23% of the sequences (5 out of 22) were coded by KV3-20*01_J1*01 (Fig. 1E). The amino acid sequence alignment of the 211 VH revealed 22 groups of at least 3 members with identical V-J genes but dissimilarities in their sequences and CDRs (Supp Fig. 5A). Because of this very high diversity, attempts to identify clonal groups inside a patient defined by at least 3 distinct complementary determining region 3 (CDR3) of identical length and identical V-J gene usage, failed (Supp Fig. 5B). We found, however, identical VH sequences in seven instances in Patient#1_2023, one in Patient#2 and one in Patient#3 (Table 2). As we obtained PBMC samples 9 years apart from Patient#1, we compared her antibody repertoires over time in the absence of any exposure to NMBAs between the samplings. Surprisingly, the repertoires of Patient#1_2014 and Patient#1_2023 were very distinct, with only rare similarities of V-J gene usage, V4−39*01_J4*02 being the most predominant for the VH representing 4 out of 49 (~10%) and 8 out of 98 (~8%) of the rearrangements, respectively (Fig. 1E), and six clonal groups for the VL were identified with sequences coming from 2014 and 2023 (KL2-11_KJ1, KV3-20_KJ2, KV1-39_KJ4 and KV2-28_KJ4). However, the amino acid sequence alignment of the VH coded by these identical V-J genes revealed dissimilarities in their sequences and CDRs (Supp Fig. 6).

Among the 211 VH and 191 VL sequences identified (Fig. 1E), 152 were paired VH-VL sequences, including 25 VH-VL pairs from Patient#1_2014, 76 from Patient#1_2023, 32 from Patient#2 and 19 from Patient#3 (Supp. Tables 1-2). Amino acid alignments led to the identification of five B cells clones identified at least twice i.e., with identical VH-VL amino acid sequences. The sequences of the shared mAbs had a large diversity in mutation load compared

to the germline (up to 41 amino acid mutations in the VH and 20 in the VL) and some possessed long CDR3 motifs (Table 2). Only one paired VH-VL with identical V-J usage (V3-7*01-J4*02 and KV4-1*01_KJ1*01) was identified from the two repertoires of Patient#1 (2014 and 2023). The amino acid alignment of those two mAbs revealed >80% homology in the VH and in the VL with mutations in the frameworks and CDRs (Supp. Fig. 7).

Altogether these four anti-rocuronium repertoires are highly diverse, with neither predominant gene usage nor evidence of clonal groups.

Anti-rocuronium antibodies from patients are highly specific, low affinity and anaphylactogenic.

To further characterize the VH-VL pairs identified from single-cell sorting of rocuronium-binding memory B cells, we recombinantly expressed those corresponding to monoclonal cell cultures with the highest anti-rocuronium signal as aglycosylated effector-less (Fc engineering heavy chain mutation $N_{297}A$) human IgG1 mAbs. Anti-rocuronium ELISA using HSA-rocuronium as antigen enabled a first ranking of the antibodies with mostly poor binding except mAb h1F10 (Fig.2A, Supp. Fig. 8A and Table 3). Competitive inhibition ELISA demonstrated their exquisite specificity for rocuronium as only free rocuronium, but not by free molecules with the same aminosteroid scaffold *i.e.*, the closely-related homologue vecuronium, the 5α-dihydrotestosterone that lacks quaternary ammonium groups, nor pholcodine, or irrelevant antigens (ovalbumin, amoxicillin, peanut extract) could inhibit their interaction with HSA-rocuronium (Fig. 2B and Supp. Fig. 8B-C). Of note, from the memory B cells sorted initially based on their binding to HSA-rocuronium-APC, only 1.3-16% expressed antibodies that proved to bind free rocuronium, suggesting a frequency of antigen-specific B cells ranging from 0.04-0.2% in PBMC samples from the three patients (Supp. Tables 1-2). The avidity of the mAbs towards HSA-rocuronium (molar ratio rocuronium:HSA of 15-1) was measured using Bio-layer interferometry (BLI) with the conjugate covalently bound to the sensors. All antibodies had similar profiles with a fast association and a biphasic dissociation. The Dissociation constants (K_D) of these mAbs ranged from 21 to 922 nM, with half the antibodies in the 21-50 nM range (Table 3 & Supp. Fig. 9A), and mAb h1F10 displaying the best avidity (Fig. 2C). The very small size of rocuronium (530

Da) is incompatible with the relatively poor sensitivity of BLI, but at the lower limit of detection for Surface Plasmon Resonance (SPR). Using SPR with the mAbs captured onto the chip, we confirmed that among the mAbs with the highest avidity for HSA-rocuronium, five mAbs bound free rocuronium in solution, in a transitory mode with a very fast association and dissociation (Table 3 and Supp. Fig. 9B), with mAb 1F10 displaying the best affinity for rocuronium with a K_D of 140 μM (Fig. 2D).

Next, we produced h1F10 as a human IgE to investigate if this VH-VL rearrangement represents an allergy-related B cell clone in Patient#1_2014 i.e., promote human mast cell activation and/or induce anaphylaxis in the presence of rocuronium. Human mast cells and basophils express the high-affinity IgE receptor FcεRI that allows them to be sensitized (pre-armed) with IgE *in vivo* for immediate cell activation following IgE engagement with allergens, leading to rapid anaphylactogenic mediator release. Human mast cells derived from PBMCs of healthy donors sensitized with h1F10 IgE dose-dependently degranulated in the presence of HSA-rocuronium but not, as expected (*39*), unsensitized mast cells (Fig. 2E). To test the anaphylactogenic potential of IgE h1F10, we used mice expressing human FcεRI, sensitized them with h1F10 and challenged them with HSA-rocuronium in a classical model of passive systemic anaphylaxis. IgE h1F10-senstized mice, but not unsensitized mice, displayed a pronounced drop in central body temperature (Fig. 2F), a hallmark of anaphylaxis in mice (*40*). Thus, although identified from an IgG-expressing memory B cell, the h1F10 VH-VL rearrangement generates a rocuronium-specific antibody of medium-low affinity that nevertheless demonstrates potential as a human IgE for human mast cell activation and induction of anaphylaxis in mice humanized for FcεRI.

As h1F10 was of sufficient affinity to measure its interaction with free rocuronium by SPR, and capable of inducing mast cell activation and passive systemic anaphylaxis when expressed as an IgE, we wondered if it could also capture circulating rocuronium and promote reversal of neuromuscular blockade. This possibility would represent an alternative to sugammadex for cases of sugammadex or sugammadex-rocuronium hypersensitivity (*9-12*). We first established the lethal dose of rocuronium in wt C57BL/6 mice at 160 μg/kg (Fig. 2G). established a prophylactic model to prevent neuromuscular blockade in mice which consists in pre-treatment with a

rocuronium capture molecule, followed by intravenous injection of a lethal dose of rocuronium and vitality assessment. In this model, only sugammadex protected mice from rocuronium-induced neuromuscular blockade, but not h1F10 or any other of the sixteen anti-rocuronium mAbs (Table 3) that we produced as fully human IgG1 ($N_{297}A$) antibodies (Fig. 2G). We hypothesize that the affinity of these antibodies is too weak to exert capture functions in vivo that might lead to reversal of neuromuscular blockade, as sugammadex does.

Generation of high-affinity anti-rocuronium mAbs

To investigate the potential use of mAbs as capture reagents for rocuronium, we decided to immunize mice against rocuronium and identify high-affinity mAbs. As we failed to raise anti-rocuronium antibody responses in mice using free rocuronium in adjuvant, we immunized mice with rocuronium coupled to keyhole limpet hemocyanin (KLH), as a large size carrier protein that favors bystander activation. Hybridomas were generated from the mice displaying the highest anti-rocuronium titer (Fig. 3A), and their variable domains sequenced, leading to the identification of only two different VH-VL pairs. Both used KV2-112*KJ2 VLs but different VHs (mAb m1B6 IGVH1-63*J4; mAb m2B1 IGVH1-81*J2). Using ELISA and competitive inhibition ELISA, we confirmed that mAb m1B6 (IgG1,κ) and mAb m2B1 (IgG1,κ) bound specifically rocuronium but not any other NMBA, including analogues vecuronium and pancuronium, suxamethonium, but also dihydrotestosterone, diisopentyl succinate and pholcodine (Fig. 3B-C). Both mAbs had a very high avidity for HSA-rocuronium measured by BLI (Supp. Fig. 10A), 800 and 57-times better, respectively, than mAb 1F10. Whereas mAb m2B1 had only a 140-times better affinity for free rocuronium measured by SPR than mAb 1F10 (K_D=1 μM versus 140 μM), mAb m1B6 displayed a 25,000-times better affinity (K_D=5.5 nM versus 140 μM) (Supp. Fig. 10B & Table 3).

To understand how anti-rocuronium mAbs m1B6 and m2B1 bind rocuronium, we produced monovalent formats of mAb m2B1 and m1B6 as Fab fragment and single-chain variable fragment (scFv), respectively, and generated their co-crystals with rocuronium. We solved the X-ray structures of Fab-m2B1 and scFV-m1B6 in complex with rocuronium at a 1.65 Å and 1.70 Å resolution, respectively, with electron density for rocuronium observed in the binding sites in the

two solved structures (Fig. 4A, Supp. Fig. 11 and Supp. Table 3). Both antibodies make extensive hydrophobic interactions i.e., van der Waals bonds, with rocuronium involving the VH and VL in each antibody. The Fab-m2B1-rocuronium contacts involve residues Glu50, Tyr52, Ser54, Tyr56, Gly96, Val97, Ans98, and His100 of the antibody heavy chain and Tyr27, Tyr32, Leu91, Val92, Glu93, Tyr94, and Tyr96 of the light chain (Fig. 4B). The scFv-m1B6-rocuronium contacts involve residues Trp33, Try52, Ser54, Tyr56, Trp99, Ser100, Tyr100A and Tyr100B of the heavy chain and Tyr27, Tyr32, Leu91, Val92, Glu93, Tyr94, Tyr96 of the light chain in the crystal structures of cyclodextrin complexes (Fig. 4B). The ring A of rocuronium has been reported to exist in twist-boat and chair conformations (*41*). In the structure of the scFv-m1B6-rocuronium complex, rocuronium ring A adopts the chair conformation but in the Fab-m2B1-rocuronium complex is not sufficiently well defined within the electron density maps to be determined. Of note, the rocuronium hydroxyl group is fully exposed to solvent, in agreement with the use of this group as attachment point to the rocuronium-carrier proteins used herein for immunization and screening, whereas the acetoxyl group is buried inside the binding pocket of both antibodies. Finally, both co-crystal structures revealed that the allylpyrrolidine substituent containing the quaternary ammonium is completely buried and makes numerous van der Waals contacts with the antibody light chain (Fig. 4), emphasizing the important role of this group in the rocuronium binding mode, in agreement with hypotheses extrapolated from serum cross-reactivity in patients (*22, 42*). The specificity for rocuronium and not vecuronium or pancuronium could be explained by the fact that no space remained in the hydrophobic pocket formed by the VH and the VL of either antibody to accommodate the methylpiperidine substituent of vecuronium and pancuronium, and by numerous hydrophobic contacts made by the allyl group of rocuronium.

High-affinity anti-rocuronium antibodies protect from and reverse neuromuscular blockade in mice and non-human primates.

Rocuronium capture may serve two purposes: (i) binding and sequestration of rocuronium to prevent interaction with IgE on mast cell and basophil to reduce or stop anaphylaxis, as suggested by some case reports (*43-45*), and (ii) reversion of neuromuscular blockade to shorten

patient's recovery time and associated complications (*6*). To test the efficacy of the high affinity anti-rocuronium mAbs isolated from mice on rocuronium capture, we first used the prophylactic model of rocuronium-induced neuromuscular blockade (scheme in Fig. 2G) with a fixed dose of rocuronium of 4 μg per mouse inducing lethality in less than 2 min. Both mAb 1B6 and mAb 2B1 protected mice for neuromuscular blockade in a dose dependent manner. mAb 1B6 was more efficient at lower antibody doses, as expected when considering the affinities of mAb 1B6 and mAb 2B1 for free rocuronium (Fig. 5A).

Neuromuscular blockade is monitored in anesthetized and intubated patients in clinical practice using the Train-Of-Four (TOF) method that compares the twitch response (T1, T2, T3, T4) to four consecutive electric impulses applied by a TOF apparatus on the ulnar nerve through electrodes. Deep neuromuscular blockade corresponds to the absence of response at any of the stimulus, and recovery from neuromuscular blockade to a TOF ratio (T4/T1) >90%. Loss and recovery of spontaneous ventilation is also recorded to calculate the time to retrieve spontaneous ventilation. Because of the very small size of mice, TOF devices were not adaptable even using pediatric equipment, and we moved to non-human primates i.e., cynomolgus macaques, to evaluate the efficacy of mAb 1B6 to reverse deep neuromuscular blockade induced by rocuronium in a therapeutic model that closely reflects the clinical setting. We first established the lowest dose of rocuronium to induce a profound myorelaxation (200 μg/kg) in macaques and the lowest sugammadex dose for fast recovery (<1 minute; 2 mg/kg) as a control. Animals were anesthetized, placed under mechanically assisted ventilation and the myorelaxation status was assessed by TOF monitoring (measured using two TOF instruments, each connected to one upper-limb) and time to retrieval of spontaneous ventilation (Fig. 5B) (*46*). At 200 μg/kg rocuronium injected as a bolus, the spontaneous reversal of neuromuscular blockade happened at 28.5min when monitoring TOF ratio and spontaneous ventilation at 15.5 min (Fig. 5C). Injecting of mAb 1B6 to macaques under deep neuromuscular blockade induced by rocuronium dose-dependently decreased the time to complete neuromuscular blockade reversal. 2.5 mg/kg of mAb 1B6 were sufficient to reduce from 28.5 min to 16 min the recovery of TOF ratio>90% and to reduce from 15.5 min to 5 min recovery of spontaneous ventilation (Fig. 5D). To obtain the same speed of TOF ratio and spontaneous ventilation recovery than obtained with 1 mg/kg sugammadex, 10 to 15

mg/kg of mAb 1B6 were required (Fig. 5E and Supp. Fig. 12). Physiological parameters and blood counts remained unaltered during the experiments (Supp. Fig. 13), indicating that mAb 1B6 does not induce obvious adverse events, even at high doses. These results validate the therapeutic effect of rocuronium-specific mAb 1B6 on rocuronium-induced neuromuscular blockade. They serve as a proof of concept that antibodies or antibody-like molecules may be potential new drugs for the reversal of neuromuscular blockade of NMBAs that have no reversal agent, and as it has been suggested for sugammadex (*43-45*) may mitigate or even reverse anaphylaxis.

DISCUSSION

This study reports on the first investigation of anti-NMBA antibody repertoires from NMBA-allergic patients. Memory B cell antibody repertoires of patients with suspected hypersensitivity to NMBA and evidence of anti-rocuronium antibodies in their serum demonstrated high polyclonality, with no evidence of clonal groups, suggestive of diverse sources of immunization against compounds chemically or structurally related to rocuronium. Surprisingly, no crossreactivity for other NMBAs or structurally related molecules could however be detected, and the affinities for rocuronium were rather poor with K_D around hundred micromolar for free rocuronium. These affinities were sufficient to trigger in vitro mast cell activation and in vivo anaphylaxis, indicating that some of these antibodies may contribute to rocuronium-induced anaphylaxis in patients. Two high-affinity anti-rocuronium mAbs generated from rocuronium-immunized mice also demonstrated selectivity for rocuronium, explained by the structure of their paratope, and demonstrated ability for rocuronium capture in vivo. The highest affinity mAb provided a proof of concept for antibodies as reversal agents for rocuronium-induced deep neuromuscular blockade that may provide an option for patients with allergy to sugammadex.

Rocuronium represents an advantageous study model of NMBA as it is widely used for standard endotracheal intubation and for rapid sequence induction, although it has one of the longest residual neuromuscular blockade durations and among the highest anaphylaxis incidences (*4, 47-49*). This aminosteroid non-depolarizing NMBA was designed as a mono-quaternary ammonium compound (allylated pyrrolidinium group attached to the D ring), unlike its bis-quaternary closely related analog pancuronium (*50*). It is therefore a weaker antagonist at the neuromuscular junction than pancuronium, making rocuronium easier to outcompete for reversal of neuromuscular blockade. With vecuronium, rocuronium is the only NMBA on the market possessing a reversal reagent for deep neuromuscular blockade (*8*), and has been adopted as sole NMBA in countries like Japan due to this drug-antidote pair, despite the cost of the antidote. How rocuronium induces anaphylaxis remains unclear, as IgE receptors on mast cells and basophils require aggregation to enable cell activation and degranulation; the most probable

hypothesis proposes that rocuronium haptenizes onto a large molecule upon infusion (*51*). A previous study using IgE-stripped human basophils sensitized with patient serum containing anti-rocuronium IgE indeed reported that only haptenized rocuronium but not free rocuronium induced basophil activation *in vitro* (*52*). To evaluate IgE-mediated anaphylaxis, allergy work-up mostly includes degranulated biomarkers from mast cells and basophils, specific IgE measurements (during the anaphylaxis and later work-up), and skin tests and basophil activation tests (BAT) to all molecules suspected as the culprit agent (6-8 weeks after the anaphylaxis) (*53*). Rocuronium-specific IgEs are still explored with the morphine antigen surrogate in clinical practice (QAM ImmunoCAP) although anti-rocuronium IgE ImmunoCAP is commercially available, but not yet validated for clinical practice. Exploration of anti-rocuronium IgE antibodies in patients' sera relies on the hypothesis that its quaternary ammonium is part of the epitope bound by anti-QAM antibodies with, however, poor structural and chemical resemblance between rocuronium and the morphine antigen. Anti-QAM ImmunoCAP are also used for screening for hypersensitivity against widely different chemical structures as suxamethonium and atracurium with, however, poor sensitivity and specificity (*21, 24, 54-58*). To avoid this caveat, we used in this study rocuronium derivatives by extending the OH group with a functionalized linker for grafting on carrier proteins e.g., KLH, BSA, HSA, that were used for memory B cell sorting, ELISA, avidity measurements and functional assays. This strategy allowed for identification of anti-rocuronium antibodies with no crossreactivity for other NMBAs, not even vecuronium and pancuronium and dihydrotestosterone, the rocuronium mimetic devoid of ammonium groups. Validated by other groups, some of these rocuronium-based assays could become novel diagnostic tools in NMBA-suspected allergies.

B cells with rocuronium reactivity were sorted from two patients with a history of rocuronium-induced anaphylaxis and from one with atracurium-induced anaphylaxis. For several reasons, we chose to sort IgG-expressing memory B cells and not IgE-expressing B cells to identify anti-rocuronium antibody repertoires: all three patients had evidence of anti-rocuronium IgG in their sera but only one had anti-rocuronium IgE; IgE-expressing memory B cells elude identification in blood samples (*30, 32*); IgE antibody-expressing cells have been reported to result from an intermediary switch to IgG rather than directly from IgM-expressing B cells (*59*). Very

recently, type 2–polarized memory B cells defined either as $CD23^{+}$ $IgG1^{+}$ (*60*) or as IgG1 or IgG4-expressing $CD23^{hi}$, IL-$4R\alpha^{hi}$, and $CD32^{low}$ (*61*) have been identified from allergic patients to hold the allergen-specific IgE memory. Rocuronium haptenized on HSA allowed for the sorting and culture of single memory B cells from all three patients into IgG-secreting cells coupled to screening for both rocuronium reactivity and specificity by competitive ELISA in their culture supernatant. The latter consideration is primordial as >80% of the cultures were excluded because of low reactivity and specificity, thereby curating the repertoire data from all its false positives. The false positive fraction was similar when sorting atypical $CD45RB^{+}$ memory B cells (*37*), and when sorting memory B cells binding HSA-rocuronium labeled with two different fluorochromes. Thus, the highly polyclonal anti-rocuronium antibody repertoires we describe herein, with a high diversity among V(D)J gene usage, corresponds only to *bona fide* anti-rocuronium antibodies. It remains unclear however if the memory B cell sorting method, using monomeric carrier proteins coupled to ~15 rocuronium molecules, might have biased or not B cell selection towards higher avidity B cell clones.

Surprisingly no evidence of common gene usage nor of clonal groups could be found within and between these patients, even between the repertoires of the same patient sampled 9 years apart with no exposure to any NMBA during this period. The underlying reason for the high polyclonality of anti-rocuronium antibody repertoires might be the absence of exposure to rocuronium before the initial anaphylactic episode in the perioperative setting in all these patients, with exposure to other compounds present in cough syrup, cosmetics, hair dyes, household cleaning products or drugs at the probable initiation of the immune reaction towards rocuronium (*12*). One of the most incriminated culprits is pholcodine, an opioid cough suppressant containing two tertiary ammonium groups, that is now considered a risk factor for anaphylaxis to NMBA (*28*) and withdrawn from the European market in December 2022. These difficult to quantify exposures may have led to a diverse repertoire of memory B cells with cross-reactivity to rocuronium; if Patient#1 that demonstrated different V(D)J recombination 9 years apart is representative of rocuronium-allergics, one could hypothesize that their repertoires would not to be stable over time. Surprisingly, however, none of the mAbs corresponding to these V(D)J rearrangements demonstrated cross-reactivity for any other NMBA, including vecuronium

and pancuronium that differ only slightly from rocuronium. This result on monoclonals agrees with our previous data showing that polyclonal IgG from Patient#1 purified on a rocuronium-bound column showed exquisite specificity for rocuronium, with no binding to atracurium, pancuronium or vecuronium, although partial cross-reactivity with suxamethonium was detected (*16*). This preference may be the result of (i) a particular exposure of these patients to rocuronium-resembling molecules, (ii) the stringency of the cell sort using rocuronium-haptenized HSA, or (iii) the modification (functionalized linker) made to rocuronium to allow protein engraftment. As a comparison in the rocuronium-immunized mouse, from all hybridomas analyzed only 2 different V_H-V_L combinations could be identified (mAb m1B6, IGVH1-63*J4 x KV2-112*KJ2; mAb m2B1, IGVH1-81*J2 x KV2-112*KJ2), suggestive of a very restricted oligoclonal repertoire. These results agree with the affinity for rocuronium determined for these human or mouse antibodies: poor affinity when antibodies were isolated from polyclonal repertoires of cross-reactive BCRs to rocuronium (as none of the patients had been pre-exposed to rocuronium) and high affinity from oligoclonal repertoires of "antigen-trained" B cells.

The mAb 1F10 isolated from patient#1_2014 showed the best affinity towards rocuronium from all the antibodies identified from humans we studied herein, although this patient had been included after presenting with a grade 2 hypersensitivity reaction to atracurium (*16*), with no previous exposure to rocuronium. This mAb expressed as a human IgE gave positive results in a mast cell activation test, which has recently been proposed as an alternative for basophil activation tests (*62*), and enabled to induce severe hypothermia in a mouse model of rocuronium-induced anaphylaxis. Even though this mAb was isolated from an IgG-expressing B cell, it may represent an IgE expressed and/or secreted by a class-switched activated B cell as recently reported (*60, 61*) or plasmablast/plasma cell involved in hypersensitivity to rocuronium. Allergy-related IgE plasma cells have indeed recently been identified in the bone marrow of chronically exposed mice and allergic individuals (*63, 64*). From our study, it remains unclear, however, if such IgE plasma cells exist in patients exposed to a variety of compounds and not chronically to a given antigen, and will merit further investigation if bone marrow samples from NMBA-allergics become available.

The specificity for rocuronium of all the above-mentioned antibodies, with no crossreactivity for other NMBAs, can be explained for the antibodies raised from immunized mice by their co-crystal structures with rocuronium. These indicated a similar binding between the two pairs of V_H-V_L corresponding to mAbs 1B6 and 2B1, which possess different V-J rearrangements of the heavy chain but an identical V-J rearrangement of the light chain with only two amino acid differences). Both antibodies bound rocuronium through a hydrophobic pocket formed by residues from the V_H and V_L chains, that do directly interact with the ammonium group that had been hypothesized to be the main epitope involved in NMBA hypersensitivity (*22*). The quaternary ammonium group and the uncharged dihydrotestosterone counterpart were required for binding. The closely related NMBAs vecuronium and pancuronium were also unable to bind as their side chains differ and cannot fit into the tight hydrophobic binding cleft of these two antibodies. Indeed, the ring D substituent in vecuronium/pancuronium is a 6-atom piperidinium cycle instead of a 5-atom pyrrolidinium cycle in rocuronium (cf lack of space). In addition, the hydrogen bond between rocuronium and the serine residue at position 54 in the antibody heavy-chain (at least in the chair conformation) cannot be established with vecuronium or with pancuronium as the rocuronium morpholino heterocycle involved is replaced by a piperidin and piperidinium (no O3) in these compounds, respectively. One could speculate that these specificities are the result of high selective pressure in rocuronium-immunized mice and that these may not be present in antibodies generated in humans by exposure to various ammonium-containing compounds (*3*).

Ten years ago, almost 40%-60% of patients in post anesthesia care suffered from residual neuromuscular blockade (*5, 30, 65-68*). The increased use of neuromuscular monitoring in some countries allowed for this incidence to drop drastically e.g., to 3-5% in recent years in France and Portugal (*69, 70*). It remains an issue and even today it can have major adverse outcomes by prolonging postoperative recovery, affecting respiratory function, causing muscle weakness with sometimes fatal outcomes (*5, 71*). Similarly to the rocuronium-reversal agent sugammadex, both anti-rocuronium mAbs with high-affinity for rocuronium - identified from immunized mice - demonstrated ability to capture rocuronium in vivo dose-dependently in a prophylactic model of rocuronium-induced paralysis in mice. This rodent model, however, does not recapitulate the

state of deep neuromuscular blockade that is so difficult to reverse in patients. Currently, only rocuronium- and vecuronium-induced deep neuromuscular blockade can be, almost immediately, reversed by sugammadex, with no solution available for deep blockade induced by atracurium, the most used NMBA worldwide, nor pancuronium among many others. This possibility is of major importance for clinicians, especially for patients with unexpected impossible mechanical ventilation or tracheal intubation. Importantly, anti-rocuronium mAb m1B6 demonstrated efficiency at reversing deep neuromuscular blockade in cynomolgus macaques in this study, with similar kinetics at $8x10^{-8}$ M (15 mg/kg) as sugammadex at $4.5x10^{-7}$ M (1 mg/kg). The costs of production of sugammadex and a monoclonal antibody are incomparably in favor of sugammadex (*72*), but we believe this proof-of-concept study provides an alternative for reversal of deep neuromuscular blockade in patients with hypersensitivity to sugammadex (*12, 48*) or sugammadex-rocuronium inclusion complexes (*11*). Most importantly, it paves the way for the discovery of mAbs from patients or immunized animals to NMBAs lacking reversal agents i.e., atracurium and pancuronium.

In conclusion, this work reports on the underlying causes of anaphylactic reactions to NMBAs by identifying the first anti-rocuronium antibody repertoires from several patients, suggests novel diagnostic tools for rocuronium hypersensitivity, and provides a proof-of-concept for antibodies as drugs for the reversal of neuromuscular blockade.

MATERIALS AND METHODS

Clinical study design

Three clinical studies were approved for the recruitment of NMBA-allergic patients. The French multicentric NASA ("Neutrophil Activation in Systemic Anaphylaxis") study involved 11 Anaesthesia and Intensive Care departments in the Ile-de-France region in France. The study was approved for all centers by an Institutional Review Board (ethical committee "*Comité de Protection des Personnes Ile-de-France 1*", reference 2012-avril-12880), and registered before the first inclusion at ClinicalTrials.gov (Identifier: NCT0163722). The design of the study and detailed clinical characteristics of the patients are described elsewhere (*16, 73*), and its ancillary study NASAmAbs enabled the collection of 190 mL of blood from Patient#1_2014. The second French multicentric study was MEDIREP ("Repertoire and Properties of Anti-drug Antibodies Involved in Immediate Hypersensitivity in the Operating Room") was approved by an Institutional Review Board (ethical committee "*Comité de Protection des Personnes Ile-de-France IV*", reference 2022-A00709-34) on May 2022 and registered before the first inclusion at ClinicalTrials.gov (Identifier: NCT05420935), allowing for the inclusion of Patient#1_2023. The study "Anesthesia-associated allergy: from new pathogenic insights to reliable diagnoses" was approved by the Belgian ethical committee under #B300202042710 and is sponsored by the University of Antwerp, registered under #8300201316408 in Belgium, and enabled the collection of blood from Patient#2 and Patient#3. Written informed consent was obtained from the patients or their legal representative before study inclusion. Patient characteristics are described in Table 1.

Classical anaphylaxis parameters

As part of standard care procedures, the following circulating parameters were assessed as previously described (*55*): histamine (EIA, Immunotech, Beckman Coulter, Brea, California, USA) and tryptase (FEIA, ImmunoCAP 250 Phadia, Thermofisher®, Waltham, Massachusetts, USA) in plasma and anti-quaternary ammonium-specific IgE (FEIA, ImmunoCAP 250 Phadia, Thermofisher®, Waltham, Massachusetts, USA) in serum. A value less than 0.35 kU/L of specific

IgE was considered negative, as recommended (*55*). Tryptase concentrations two hours following acute hypersensitivity reaction (AHR) were considered elevated when greater than (1.2 x [baseline tryptase] + 2 µg/L) as recommended (*74*). A histamine concentration above 20 nmol/L 30 minutes following AHR was considered elevated. Data is summarized in Table 1.

In addition, specific IgE concentrations for rocuronium were assessed using the non-clinically-validated rocuronium ImmunoCAP (Phadia AB, Uppsala, Sweden; ImmunCAP#c202) (*75*) obtained as experimental prototypes made for research use, and with the LuLISA technique rocusing an anti-IgE nanobody-luciferase tandem (1:50) as previously described (*76*).

Mice

C57BL/6J mice were purchased from Charles River, and used for experiments after maintaining the mice for at least one week in SPF conditions after arrival in Institut Pasteur's animal facility. Human FcεRI^{tg} mouse FcεRI$^{-/-}$ mice on the C57BL/6 background were described previously (*77*). Mice were bred at Institut Pasteur and used for experiments at 7-12 weeks of age. All animal care and experimentation were conducted in compliance with the guidelines and specific approval of the Animal Ethics committee CETEA number 89 (Institut Pasteur, Paris, France) registered under #170043, #2013-0103 and #27465 and by the French Ministry of Research under agreement #00513.02.

Production and characterization of rocuronium bioconjugates

Hapten-protein couplings were performed using active ester derivatives of rocuronium and KLH or monomeric HSA as the carrier protein. A carboxylate function was first introduced by adding succinic anhydride to rocuronium bromide in the presence of 4-(dimethylamino)-pyridine in pyridine. After stirring overnight at room temperature under argon, the solvent was removed under vacuum. The crude compound was purified by reverse-phase flash chromatography, resulting in a rocuronium derivative with a carboxylic acid (Roc-COOH) at the 3-position of the steroid scaffold. The compound was characterized by mass spectrometry and by nuclear magnetic

resonance analysis. All quantities of products were calculated relative to the carrier protein. The functionalized rocuronium (300 equivalent) was dissolved in 0.05 M MES + 0.5 M NaCl buffer (pH 5.6) and combined with 1-ethyl-3-(3-dimethylaminopropyl) carbodiimide (1000 equivalent) in the presence of *N*-hydroxysulfosuccinimide (400 equivalent). After 5-min stirring at room temperature, pH was adjusted to 7.2 with 2 M NaOH. This solution was progressively added to the carrier protein dissolved in 100mM PBS (pH7.2). After 3 hours of gentle agitation at room temperature and buffer exchange in 20mM HEPES et 300mM NaCl with minitrap desalting columns. The exact measurement of the concentration of the bioconjugates was achieved by quantitative amino acid analysis. The average density of conjugated rocuronium derivatives was evaluated by matrix-assisted laser desorption/ionization time-of-flight mass spectrometry. The HSA-rocuronium conjugates used for all experiments were monomeric with a mean engraftment of 15 rocuronium molecules per HSA molecule, determined with the mean of the gaussian distribution of the m/z (mass-to-charge ratio) as previously described (*16*).

Human B cell single-cell culture

Culture supernatants from single-cell cultured memory B cells were generated according to the protocol previously described by Sokal et al.,[13]. After thawing, PBMCs were counted and stained with antibodies directed against surface markers (CD27-BV421^{+}, CD3/CD14^{-} Cy-7^{-} CD19-PE^{-}Texas Red^{+}, CD38-PercP-Cy5.5^{+}, IgD-PE^{-}, HSA-FITC^{-}, HSA-Roc-APC^{+}). HSA and HSA-rocuronium were conjugated to fluorescent probes using Alexa Fluor 488 and 647 microscale labeling kits (Invitrogen) following manufacturer's instructions. Conjugates with a mean of 15 rocuronium molecules grafted on a HSA carrier were used for the sort. Cells were then sorted using the ultra-purity mode (single cell) on Aria III in 96-well plates containing MS40Lo cells expressing CD40L (a kind gift from Pr Garnett Kelsoe)[14]. Cells were cultured for 25 days at 37°C with 5% CO2 in RPMI-1640 (Invitrogen) supplemented with 10% HyClone FBS (Thermo Scientific), 10 mM HEPES, 1 mM sodium pyruvate, 100 units/mL penicillin, 100 mg/mL streptomycin, and MEM non-essential amino acids (all Invitrogen) with the addition of recombinant human BAFF (10 ng/ml), IL-2 (50

ng/ml), IL-4 (10 ng/ml), and IL-21 (10 ng/ml; all Peprotech). The supernatant was removed and replaced every 3-4 days of the culture and harvested on day 18, 21 and 25 of cell culture.

Clones corresponding to supernatants with the highest ratio of optical density (OD) values from anti-rocuronium ELISA divided by OD value of the anti-IgG ELISA were considered to possess reactivity towards rocuronium (at least to HSA-rocuronium) and were selected to be recombinantly expressed as mAbs.

VH-VL sequencing from monoclonal cell cultures

Clones of interest were sequenced first by RNA extraction using NucleoSpin96 RNA extraction kit (Macherey-Nagel) according to the manufacturer's instruction. A reverse transcription step was then performed using the SuperScript IV enzyme (ThermoFisher) in a 14 ml final volume (42°C 10 min, 25°C 10 min, 50°C 60 min, 94°C 5 min) with 4 ml of RNA and random hexamers (Thermofisher scientific). A PCR was further performed based on the protocol established by Tiller et al (*78*). Briefly, 3.5 ml of cDNA was used as template and amplified in a total volume of 40 ml with a mix of primers and using the HotStar_Taq DNA polymerase (Qiagen) and 50 cycles of PCR (94°C 30 s, 58°C for VH and kappa/60°C for lambda 30 s, 72°C 60 s). Sanger sequencing was performed by Eurofins.

Gene synthesis, cloning and mAbs production

VH and VL synthesis in pUC19-Igγ1.N297A or pUC-kappachain/pUC-lambdachain-expressing vectors were performed by Synbio Technologies. Antibodies were produced by transient co-transfection of VH-CH and VL-CL expression plasmids into exponentially growing Freestyle™ HEK 293-F that were cultured in serum-free Freestyle™ 293 Expression Medium (Life Technologies) in suspension at 37°C in a humidified 8% CO_2 incubator on a shaker platform rotating at 110 rpm. Twenty-four hours before transfection, cells were harvested by centrifugation at 300 x g for 5 min and resuspended in expression medium at a density of 1 x 10^6 cells/ml, and cultured overnight in the same conditions as mentioned above. To produce mAbs, 40 µg of each VH and VL expressing

plasmids were diluted in 80 µl of FectoPRO reagent (Polyplus) at a final DNA concentration of 0.8 µg/ml, incubated for 10 minutes at RT before addition to the cells. Twenty-four hours post-transfection, cells were diluted 1:1 with expression medium. Cells were cultured for 6 days after transfection, supernatants were harvested, centrifuged at 1800 g for 40 min and filtered (0.2 µm). Antibodies were purified by affinity chromatography using an AKTA pure FPLC instrument (GE Healthcare) on a HiTrap Protein A Column (GE Healthcare) and desalted on a HiTrap Desalting Column (GE Healthcare).

Production of mouse anti-rocuronium hybridomas

Female C57Bl/6J were immunized subcutaneously with 10 µg KLH-Rocuronium combined with adjuvant alum 1:1 (v:v) and 20 ng pertussis toxin in physiological saline 0.9% NaCl for three times at 3-week intervals. Mice were boosted with 10 µg KLH-Rocuronium without adjuvant three weeks after the last immunization. Four days later the cervical lymph nodes were removed and fused with myeloma cells P3X63Ag8.653 for hybridoma generation using the ClonaCell™-HY Hybridoma kit (StemCell Technologies). After screening, the positive clones were expanded in T250cm^2 flasks, cells were introduced in 2L rollers and incubated in rotating rollers at 37°C for 10 days. The supernatant was filtered and purified with Protein A-affinity chromatography columns.

Anti-rocuronium ELISA

96-well plates (Costar) were coated with HSA-rocuronium (mean of 15 rocuronium molecules grafted on a HSA carrier molecule) or HSA at 1 µg/mL in PBS 1X (Gibco) overnight at 4°C overnight, washed 3 times with PBS Tween 20 0.5% (PBST), blocked with PBS-3% BSA for mAb detection or PBS + FBS low IgG to screen human serum, and washed three times with PBST. Mice serum (diluted 1:250,000-1:5,000-1:100) or pure cell culture supernatant or monoclonal antibodies were incubated for 2H at room temperature and bound antibodies were detected with HRP-conjugated goat anti mouse or human IgG (Bethyl Laboratories) at 1:10,000. The secondary was revealed using OPD substrate (Sigma-Aldrich) and the reaction stopped with 2M H_2SO_4 and

absorbance was subsequently recorded at 490 nm and corrected at 620 nm using a spectrophotometer (Biophotometer, Eppendorff). The final OD reported in all graphs/tables corresponds to the subtraction of the OD value of the HSA-rocuronium ELISA minus the OD value of the HSA ELISA: OD values were considered positive if at least three times higher than the OD value of the negative control.

Cross-reactivity with classical allergens (e.g., peanut extract, amoxicillin and ovalbumin) was assayed using 1 μg/mL of allergens for coating, and then the same protocol as for the HSA-rocuronium ELISA.

Competition ELISA

To ascertain antibody reactivity to rocuronium, and not towards the linker employed to attach rocuronium to HSA, or a neo-epitope formed between rocuronium, the linker and HSA, a competitive inhibition ELISA was developed. This inhibition ELISA also enabled to detect cross-binding of antibodies to a panel of different NMBAs. 96-well plates (Costar) were coated with 1μg/ml HSA-rocuronium at 4°C overnight, washed 3 times with PBST, blocked with PBST containing 3% BSA at room temperature for 2 hours.

- For inhibition ELISA of single B cell culture, supernatant was incubated with 3,000 μM of free rocuronium at RT for 20min. Note: HSA-rocuronium was coated at 1μg/mL, thus at 1.54x10-11 moles/mL (MW of HSA is 65 kD). An average of 15 rocuronium molecules per HSA molecule were present, thus 2.31x10-10 moles/mL (0.231 μM) of rocuronium. 3000 μM of rocuronium (3x10-3 M) thus corresponds to an excess to 13,000-fold.
- For purified antibodies, 300 ng/mL (for murine mAbs) or 1,500 ng/mL (for human mAbs) were pre-incubated with 5-fold serial dilution of free NMBA drug (rocuronium, vecuronium, pancuronium, suxamethonium), NMBA control devoid of the quaternary ammonium (5a-DHT or diisopentyl succinate) or pholcodine from 15,000 μM to 0.96μM.

The antibody-NMBA mixture was added to the ELISA plates and incubated at RT for 2 hours, washed 3 times and revealed with HRP-conjugated goat anti-mouse/human IgG (Bethyl Laboratories) at 1:10,000 dilution. Plates were revealed using an OPD substrate (Sigma-Aldrich). The reaction was stopped with 2M H2SO4 and absorbance was subsequently recorded at 490 nm and corrected at 620 nm using a spectrophotometer (Biophotometer, Eppendorff).

- Antibodies in the supernatant of B cell culture were considered rocuronium specific if more than 50% of the signal was inhibited in presence of free rocuronium.
- For purified mAbs, the IC50 was measured using a non-linear fit [Inhibitor] vs. response -- Variable slope (four parameters) with GraphPad Prism.

Affinity measurements using Bio-Layer Interferometry (BLI)

Affinity of mAbs for rocuronium was tested using Bio-layer interferometry with the OctetRED 384 system. Amine Reactive Second-Generation (AR2G) biosensors were covalently immobilized with HSA-rocuronium (mean of 15 rocuronium molecules grafted on a HSA carrier molecule), then inserted in wells containing different concentrations of antibodies for 1,800 s (association phase). The antigen-antibody complex was dissociated by introducing the biosensor in the reference buffer (PBS+BSA). Curves were retrieved as raw data from the Octet Data Analysis software and processed in the Scrubber2 software prior to analyses with the Biaevaluation software. IgG-free buffer was used as reference and for background subtraction. Fitting curves and KD values were obtained using the 1:1 Langmuir model.

Affinity measurements using Surface Plasmon Resonance (SPR)

CM5 chips were primed using PBS, washed 3 times with NaOH (50 mM) and SDS (0.1%) 180seconds each time (5uL/min). At least 5,000 RU of antibody was covalently bound to CM5 chip by activating using 1:1 NHS:EDC (6,000 s), injecting the antibody (900 s) in acetate buffer pH5.5 and quenching with EtNH2 (600 s). Free rocuronium was injected (30 μL/min) in PBS-BSA (1 mg/mL) at different concentrations. Signal was subtracted to reference canal bound with a non-

specific antibody. K_D was determined using a kinetic analysis (RI fixed to 0, model 1:1 binding) with Biaeval software.

Antibody repertoire analysis and representative mAb selection

Docker (https://www.docker.com) / Apptainer (https://apptainer.org), nextflow (https://www.nextflow.io) and git (https://about.gitlab.com) were used to better control reproducibility aspects (*79*). The Nextflow pipeline developed to analyze batches of nucleotide sequence fasta files, representing the raw single cell Sanger sequencing of the VH-VL IgG domains, is available at https://gitlab.pasteur.fr/gmillot/repertoire_profiler, and is detailed below. Most of the process is based on tools from the *immcantation portal* (https://immcantation.readthedocs.io/en/stable/), notably from the change-O toolset (*38*). VH and VL sequences, while single cell paired, could only be analyzed independently (VH sequences, then VL sequences), as no method taking this parameter into account currently exists. First, the *AssignGenes.py igblast* tool was run to detect and annotate the V, D, J, CDR and FWR domains in each sequence, using the *imgt* database (https://www.imgt.org/). Then, *MakeDb.py igblast* converted the result into a readable tsv file. The *ParseDb.py select* tool kept productive sequences, *i.e.*, those for which: (1) the coding region has an open reading frame, (2) no defect are present in the start codon, splicing sites or regulatory elements, (3) no internal stop codons were found, and (4) junction regions are in frame. The clustering of sequences into clonal groups was performed as follows: (1) grouping of the sequences according to same V and J genes (allelic variation not considered) and same length of the CDR3, (2) for each group, computation of the distance score D = (Hamming distance) / (CDR3 length) between each 2 x 2 sequences, (3) determination of the D threshold, that determine whether 2 sequences derive from the same germline cell sequence or not, using the *distToNearest()* function of the *shazam* R package, (4) clone assignment for each sequence, *i.e.*, same ID for sequences belonging to a same clonal group, using the *DefineClones.py* tool. Of note: a few sequences could be lost at that stage, as they did not fit the criteria required by this tool. Then, the putative germline sequence of each clonal group was inferred using the *CreateGermlines.py* tool. Finally, a single *all_passed_seq.tsv* file was obtained for each batch of VH or VL initial fasta files, containing notably, for each sequence, the V, D, J gene and allelic names returned by the *AssignGenes.py igblast* tool, the clone ID, the

putative germline sequence before somatic hypermutations, and the putative V, D, J gene and allelic names of the germline sequence returned by the *CreateGermlines.py* tool.

Donut plots in Fig. 1E, Supp. Fig. 5A and Supp. Fig. 6A were drawn after gathering the sequences of the all_passed_seq.tsv file according to the V and J gene and allelic names of their putative germline sequence. The tree plot in Supp. Fig. 6A was obtained with the formatClones() and getTrees() functions of the dowser R Package (*80*), and a homemade function wrapping functions of the ggtree R package (*81*), for clonal groups with at least 3 non-identical sequences. Amino acid sequence alignments and percentage identity calculations were performed with Jalview software using MUltiple Sequence Comparison by Log- Expectation (Muscle) and colored by percentage identity. Number of mutations were obtained with IMGT database by comparing sequences with germlines and plotted as histograms using GraphPad Prism

Human mast cell activation test

$CD34^+$ precursor cells were isolated from peripheral blood mononuclear cells of healthy donors (provided by the French Blood Bank EFS). $CD34^+$ cells were maintained for 1 week under serum-free conditions using StemSpan medium (9655 Stemcell Technologies) supplemented with recombinant human IL-6 (50 ng/ml; 200-06 Peprotech), human IL-3 (10 ng/ml; 200-03 Peprotech) 3% supernatant of CHO transfectants secreting murine SCF (a gift from Dr. P. Dubreuil, Marseille, France, 3% [corresponding to ~50 ng/ml SCF]) and ciprofloxacin (10 ng/mL; 17850-5G-F Sigma Aldrich). Thereafter, the cells were maintained in IMDM Glutamax I (31980048), 2-mercaptoethanol (31-350-010), insulin-transferrin selenium (2506865) (all from Gibco), sodium pyruvate (S8636 Sigma Aldrich), 0.5% BSA (A2153 Sigma Aldrich), Penicillin/Streptomycin (100 Units/mL / 100µg/mL; Life Technologies), IL-6 (50 ng/ml 200-06 Peprotech) and 3% supernatant of CHO transfectants secreting mouse SCF. Before their use in experiments, mast cells were tested for phenotype by flow cytometry ($CD117^+$, $Fc\varepsilon RI^+$). Cells were ready for experiments after ~10 weeks in culture (at which time >95% of all cells were $CD117^+$ $Fc\varepsilon RI^+$).

Human mast cells were sensitized overnight with the anti-rocuronium antibody h1F10 produced in a human IgE format at 1 µg/mL. Cells were then washed and stimulated with increasing doses

of HSA-rocuronium in Tyrode's buffer. Mast cell degranulation was measured by flow cytometry using fluorescent avidin (5 μg/mL; A2170 Invitrogen) which binds to heparin contained in mast cell granules. Data were acquired using a MACSQuant MQ10 flow cytometer (Miltenyi) and analyzed with FlowJo v10.8.1 software (TreeStar).

Passive Systemic anaphylaxis in mice

hFcεRI^{tg} mFcεRI$^{-/-}$ mice (*77*) were injected intravenously with 20 μg of anti-rocuronium human IgE h1F10 at 0h and 24h and challenged at 48h with 267 μg of HSA-roc. Control mice were injected with irrelevant human IgE and physiological serum. Central temperature was monitored using a digital thermometer with rectal probe (YSI), and time of death was recorded.

Prophylaxis of neuromuscular blockade in mice

C57BL/6 mice were pre-injected intravenously with roc-specific antibodies in a human IgG1 $N_{297}A$ format at different doses followed 10 minutes later by a lethal dose of free rocuronium (160 μg/kg). A vitally score was defined based on visual cues: 5= no symptom of neuromuscular blockade, 4= transient (<30s) symptoms of flattening, slowing down, difficulties to stand on legs, 3= longer symptoms (<1min) with respiratory distress, 2= inactivity, impossibility to stand on legs, severe respiratory difficulties, 1= death.

scFv production, purification and characterization

Rocuronium-specific VH and VL sequences were built into scFvs with a polyglycine-serine linker (GGGGS)4 between the VH and VL sequences. The VH-linker-VL sequences were synthesized at Genscript with codon optimization for expression in Drosophila S2 cells, cloned into pT-350 vector using BglII and BstBI restriction sites (the vector is a gift from Dr. Felix Rey, Institut Pasteur, Paris, France). For transfection, 5x10^6 Drosophila S2 cells were seeded in a T25 conical flask containing 5 ml Schneider's Drosophila medium (Gibco) complemented with 10% fetal bovine serum and

incubated at 28°C overnight. Twenty-four hours later, 2 µg of pMT-Roc-scFv-Strep plasmid were co-transfected with 0.1 µg (ratio 20:1) of selection plasmid pCoBlast carrying a gene that confers resistance to puromycin. Effectene transfection kit was used (Qiagen) according to the vendor's protocol. Forty-eight hours after transfection, the selection process was started by addition of puromycin (Invivogen) to the cells at a final concentration of 7 µg/ml. Transfected cells were collected every 4–5 days by centrifugation at 90g for 5 min, and cell pellets were resuspended in fresh medium containing 7 µg/ml puromycin. Cell propagation was initiated ~2 weeks after transfection. Puromycin-selected cells were adapted to serum-free HyClone Insect cell culture media (GE healthcare life science) and were amplified in large volume flasks as needed. Protein expression was induced with 0.5 mM CuSO4 when the cell density reached ~7.5x10^6 cells/ml. Seven days after induction, S2 cell suspension was centrifuged for 30 min at 15,000g to remove the cells and the supernatant was collected. Avidin was added at 15 mg/L to sequester any biotin present in the medium. The supernatant, cleared by centrifugation at 20,000g for 30 min and filtration, was loaded onto a Strep-Tactin Superflow high-capacity 5 mL column (IBA GmbH, Göttingen, Germany) using a peristaltic pump or Akta. The column was washed with 15 mL of 0.1 M Tris pH 8, 0.15 M NaCl, 1 mM EDTA, and the protein was eluted with 8 mL of the same buffer containing 2.5 mM desthiobiotin.

Fab preparation

Fab were prepared following Pierce™ Fab Preparation Kit (Thermo scientific) instructions by a 4h digestion with papain in the presence of 4 mM cysteine. After purification on protein A columns, a gel filtration was performed with Tris 50mM pH, 7.4; 100 mM NaCl.

Crystallization and X-ray data collection

Crystallization screening trials were carried out by the vapor diffusion method using a Mosquito TM nanodispensing system (STPLabtech, Melbourn, UK) following established protocols (*82*). Briefly, we set up crystallization sitting drops of 400 nL containing a 1:1 mixture of protein sample (Fab-m2B1 or scFv of Fabm1B6) in complex with 10 mM of rocuronium and crystallization

solutions (672 different commercially available conditions) equilibrated against 150 µl of reservoir solution in multiwell plates (Greiner Bio-One). The crystallization plates were stored at 18°C in a RockImager (Formulatrix) automated imaging system to monitor crystal growth. Manual optimization was performed in Linbro plates with the hanging-drop method by mixing 2 µl of protein samples with 2 µl of reservoir solution. The best crystals were obtained with the conditions shown in Supp. Table 3. The crystals were flash cooled in liquid nitrogen for data collection using the crystallization solution as cryoprotectant.

X-ray diffraction data were collected on beamlines PROXIMA-1 and PROXIMA-2A at the synchrotron SOLEIL (St Aubin, France). Diffraction images were integrated with autoPROC (*83*) and XDS (*84*) and crystallographic calculations were carried out with programs from the CCP4 program suite (*85*).

Structure determination and model refinement.

The structures of Fab-m2B1 and scFv-m1B6 in complex with rocuronium were solved by molecular replacement with Phaser (*86*) using the structures of the catalytic antibody Fab7A1 (pdb 2AJU) as search model. The final models of the complexes were obtained through interactive cycles of manual model building with Coot (*87*) and reciprocal space refinement with Refmac5 (*88*). X-ray data collection and model refinement statistics are summarized in Supp. Table 3. Figures showing the crystallographic models were generated with Pymol (Schrodinger, LLC).

Anesthesia and reversal of neuromuscular blockade in cynomolgus macaques

Adult cynomolgus macaques (Macaca fascicularis) were randomly assigned to this study. All animals were housed within IDMIT animal facilities at CEA, Fontenay-aux-Roses in Bio Safety Level (BSL)-2 facilities (Animal facility authorization #D92-032-02, Préfecture des Hauts de Seine, France) and in compliance with the European Directive 2010/63/EU, the French regulations and the Standards for Human Care and Use of Laboratory Animals of the Office for Laboratory Animal Welfare (OLAW, insurance number #A5826-01, US). Animals tested negative for Campylobacter, Yersinia, Shigella, and Salmonella before being used in the study. Experiments using macaques

were approved by the local ethical committee (CEtEA #44) and the French Research, Innovation, and Education Ministry under registration number APAFIS#36723-2022041910357437 v1. Anesthesia and monitoring of neuromuscular blockade in cynomolgus macaques was performed as described in (*46*). All animals were anaesthetized according to institutional guidelines. For all procedures, the animals were first sedated with ketamine (Imalgene 1000, 5 mg/kg) and medetomidine (Domitor, 0.5 mg/kg). An intravenous (IV) line was placed, followed by tracheal intubation allowing mechanical ventilation (Hallowell EMC Matrix 3002Pro veterinary ventilator), and anesthesia was maintained with isofluorane (Isoflu-vet 1,000 mg/g, 0.5-1.5%). Once complete anesthesia was assessed, macaques received rocuronium bromide (Esmeron®, MSD 50 mg/5mL) by IV bolus infusion. When indicated, animals also received sugammadex (Bridion®, MSD, 1 mg/kg) or antibody m1B6 (2.5-5-10-15 mg/kg) for rocuronium-induced neuromuscular blockade reversal. Animals were monitored using a Nihon Kohden® PVM-2703 monitor during all the anesthesia procedures. Physiological parameters (capnography, heart rate, respiratory rate, oxygen saturation, arterial blood pressure, and temperature) were followed in real-time and recorded in a chart every 10 minutes. Neuromuscular blockade monitoring devices (TOF-Watch® and ToFscan®) measuring the T4/T1 ratio were installed before NMBA infusion. Mechanical ventilation was maintained for the whole procedure until complete recovery of the neuromuscular function, assessed with a TOF ratio > 90%. All experiments were performed under the supervision of a trained anesthesiologist and a veterinarian. After the procedures, anesthesia was reversed with atipamezole (Antisedan, 0.5 mg/kg), and animals were resumed to their cage under supervision until complete recovery. Animals were clinically followed for three days post-infusion. Clinical examination, body weight, and rectal temperature were recorded at each bleeding time, including a complete blood count on each day and a blood biochemistry evaluation on days 0 and 1. Blood sampling did not exceed 7.5% of the total blood volume per week, following ethical recommendations.

Statistical analyses

The R environment v4.3.1 was used for all the analyses (R foundation, Vienna, Austria. https://www.r-project.org/). Data were neither averaged nor normalized prior to analyses.

Response variables were log2 converted when required for better adjustment to linear models. For Fig 1B-C and Fig 5A,C, data were fitted to a simple linear model. For Fig 2D and 3A, a mixed models using the lmer() function of the lme4 package was used in order to consider the repeated measures on each mouse. Resulting effects of interest of the linear model were two-by-two compared (contrast comparisons) using the emmeans() function of the emmeans package. Statistical significance was set to a P value of 0.05 or less. In each panel, type I error was controlled by correcting the P values according to the Benjamini & Hochberg method ("BH" option in the p.adjust() function of R).

FIGURES

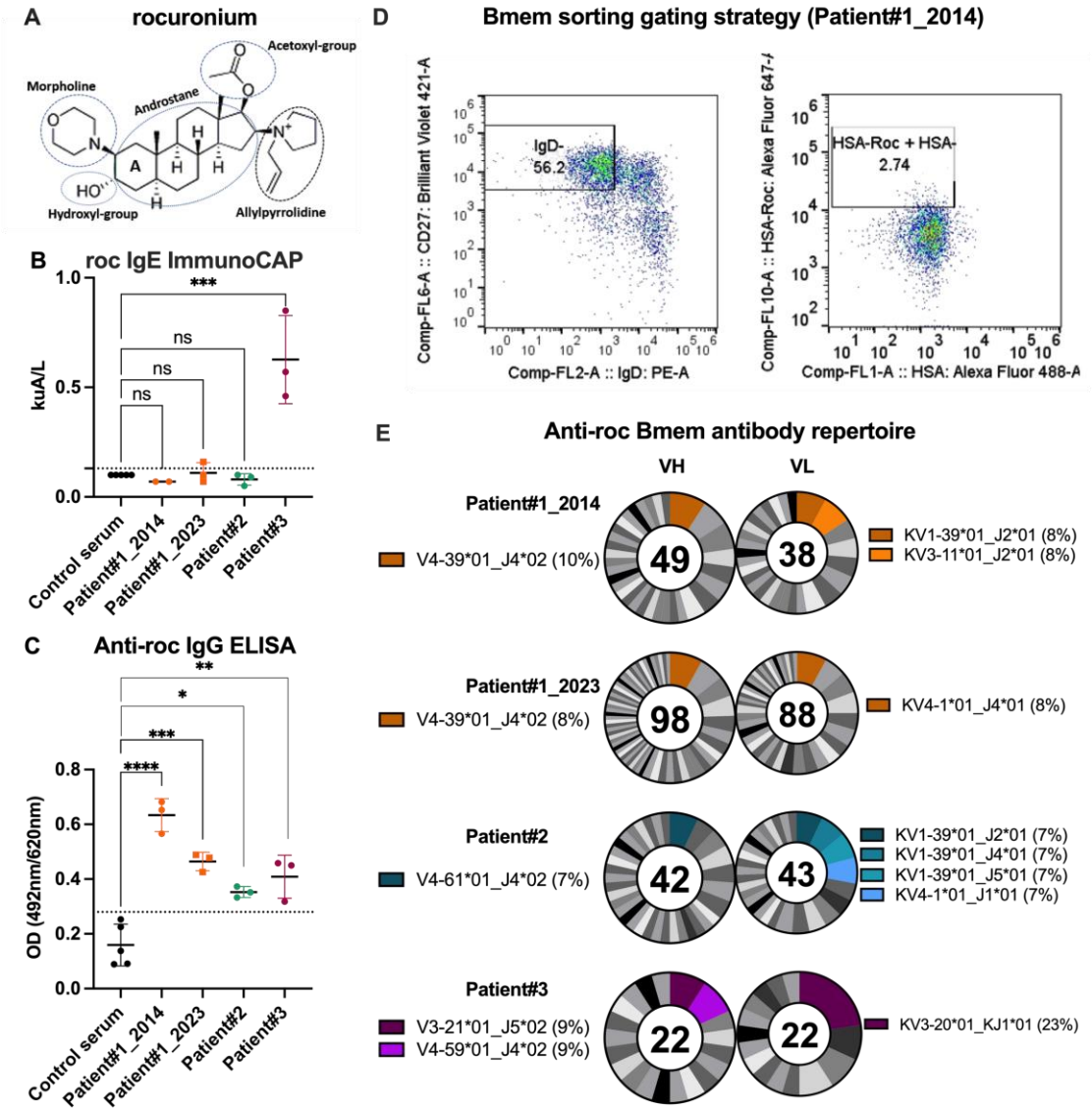

Figure 1. Identification of rocuronium-specific IgG repertoires from NMBA-allergic patients. (A) Schematic representation of Rocuronium with its major groups circled and named. (**B**) IgE anti-rocuronium ImmunoCAP results from the serum of indicated patients (each value is a replicate, n≥2), or serum from five blood bank donors (each value represents one donor). Cut-off set at 0.13 kUA/L. Means ± standard deviations are indicated. Statistical comparison were obtained using contrast analysis after simple linear modeling and multiple-testing P-value adjustment. .****, P ≤0.0001; ***, P ≤ 0.001; **, P ≤ 0.01; ns, not significant. (**C**) IgG anti-rocuronium ELISA results ($OD_{HSA\text{-}roc}$ minus OD_{HSA}) from the serum of indicated patients (each value is a replicate, n=3), or serum from five blood bank donors (each value represents one sample from one donor). Cut-off set at 0.28 OD. (**D**) Example of gating strategy for the single-cell sort of rocuronium-binding memory B cells ($CD3^-$ $CD14^-$ $CD19^+$ $CD38^-$ $CD27^+$ IgD^- HSA-roc^+ HSA^-) from the PBMCs of Patient#1_2014. Numbers in the panels indicate the percentage of cells gated among the represented cells in each panel. (**E**) Donut plot of VH and VL gene usage among the monoclonal B cell

cultures secreting anti-rocuronium IgG (total number of cells indicated in the center of the donut) from Patient#1_2014. The major V-J recombination and their frequency (in parentheses) are indicated in color.

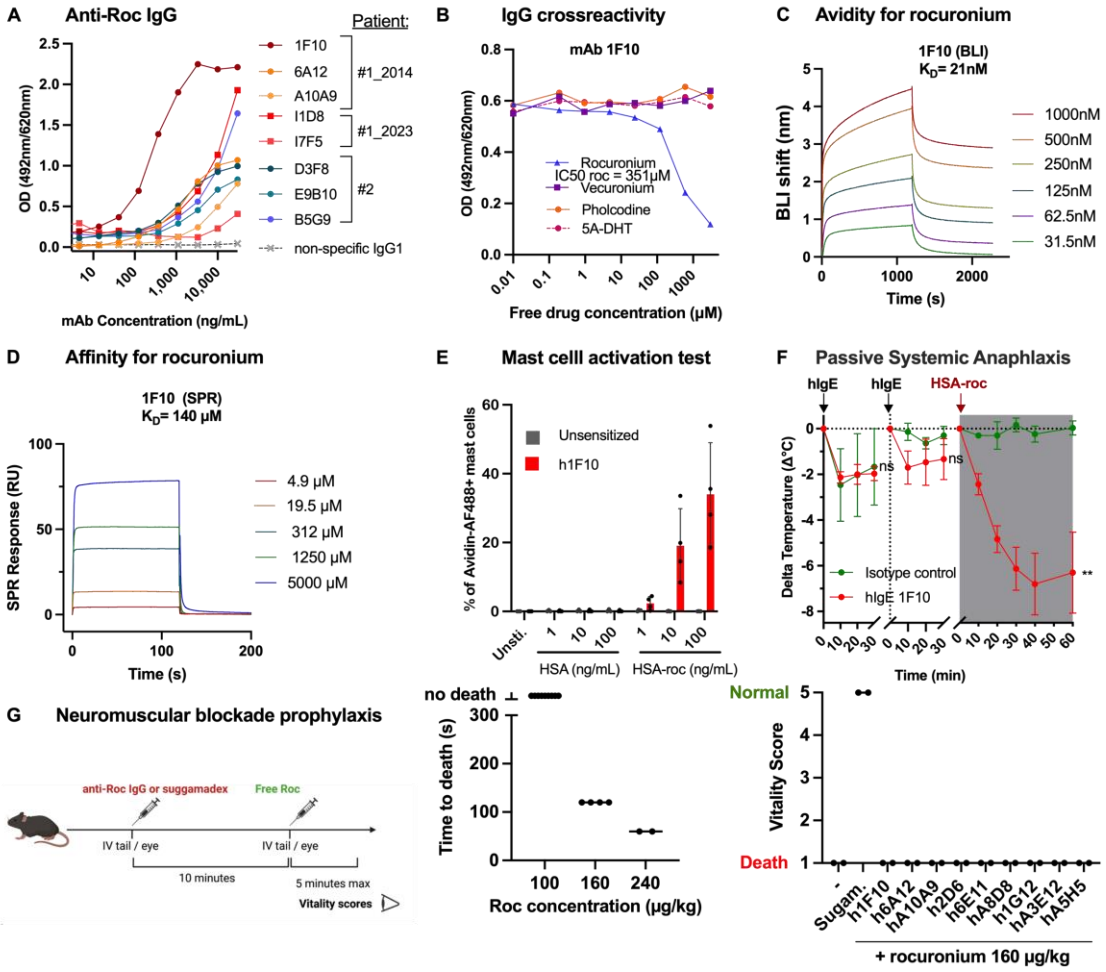

Figure 2: Characterization of recombinant roc-specific mAbs from patients. (**A**) IgG anti-rocuronium ELISA results from indicated human, and a non-specific human IgG1 as control. (**B**) "Competitive ELISA" of anti-IgG rocuronium ELISA at fixed mAb 1F10 concentration but increasing concentrations of indicated molecules free in solution. 5A-DHT, 5-alpha-Di-Hydro-Testosterone; IC50, half-maximal inhibitory concentration. (**C**) Bio-layer interferometry affinity measurement of the interaction between immobilized HSA-rocuronium and varying concentrations of mAb 1F10 in solution. (**D**) Surface Plasmon Resonance affinity measurement of the interaction between immobilized 1F10 and varying concentrations of free rocuronium in solution. (C-D) The KD was obtained by fitting the curves using a heterogenous ligand model. (**E**) Human mast cell activation test using mAb 1F10 in a human IgE format for sensitization, followed by challenge with HSA or HSA-roc, with degranulation measured using fluorescent avidin binding by flow cytometry (n=3). (**F)** Passive systemic anaphylaxis measured by changes in body temperature (Δ°C) in hFcεRI-transgenic mice sensitized twice with hIgE 1F10 and challenged with HSA-roc intravenously. Mean ± standard deviation of three mice per group are indicated. Each of the three post injection effects were analyzed separately, comparing the contrast between 1F10 and isotype control groups after mixed linear modeling and multiple-testing P-value adjustment. P values are indicated at the end of each time period analyzed with **, $P \leq 0.01$; ns, not significant. (**G**) Establishment of the lethal dose of rocuronium and time to death (bottom right; n≥2), and prophylaxis of neuromuscular blockade (left, n=2) in wt mice evaluated by vitality scores of mice injected first with sugammadex (sugam.) or 400µg/mouse of indicated

anti-rocuronium mAbs, followed by rocuronium injection. Vitality is scored as follows: 5 (no behavior changes), 4 (transient inactivity; ≤30 sec), 3 (respiratory distress and intermediate inactivity; >30 sec), 2 (flipping or inactivity; >1 min), 1 (death).

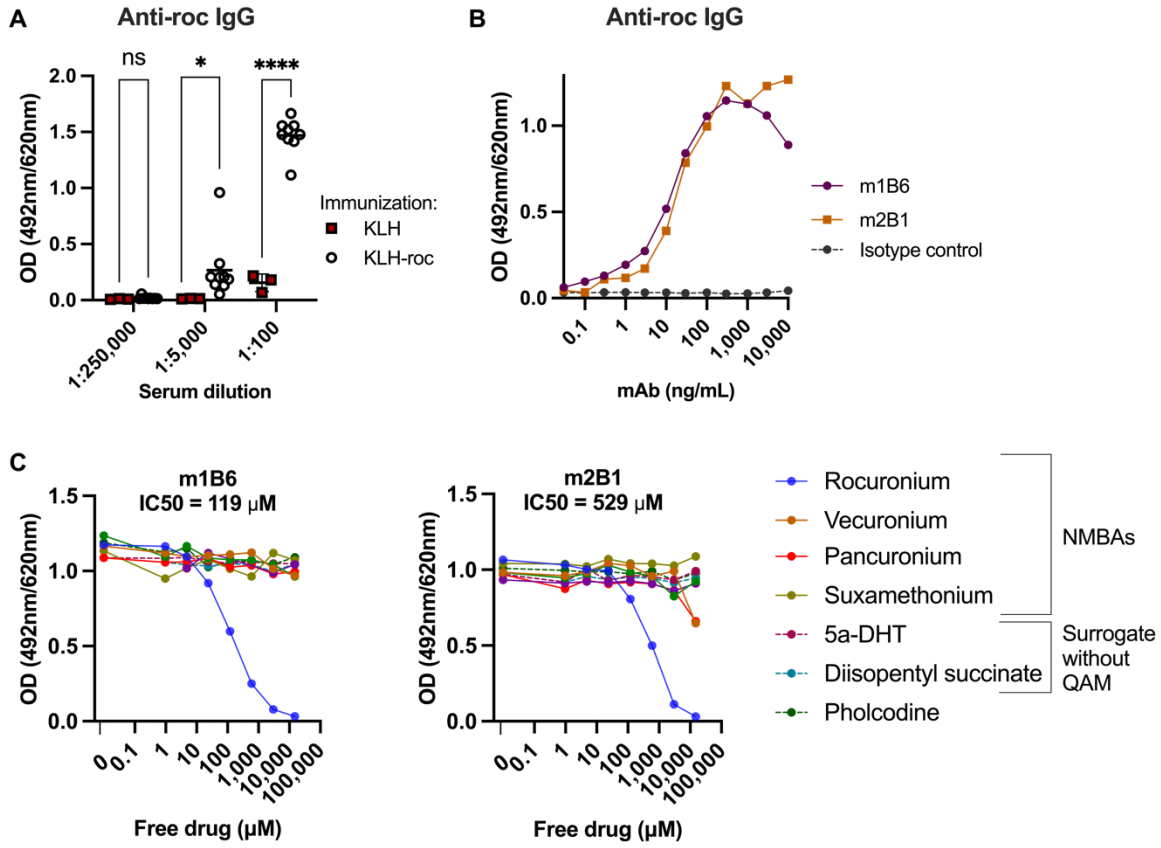

Figure 3. Exclusive rocuronium binding of mAbs isolated from immunized mice. (**A**) IgG anti-rocuronium ELISA results from sera of mice immunized with KLH or KLH-roc. Means are indicated by horizontal bars. Each dot represents a mouse. Statistical comparisons were obtained using contrast analysis after mixed linear modeling and multiple-testing P-value adjustment. ****, P ≤ 0.0001; *, P ≤ 0.05, using post hoc contrast analysis after mixed linear modeling and multiple-testing P-value adjustment. ns, not significant. (**B**) IgG anti-rocuronium ELISA results from indicated mouse mAbs or a non-specific mouse IgG as isotype control. (**C**) "Competitive ELISA" of anti-IgG rocuronium ELISA at fixed mouse mAbs concentration but increasing concentrations of indicated molecules free in solution. 5a-DHT: 5-alpha-Di-Hydro-Testosterone.

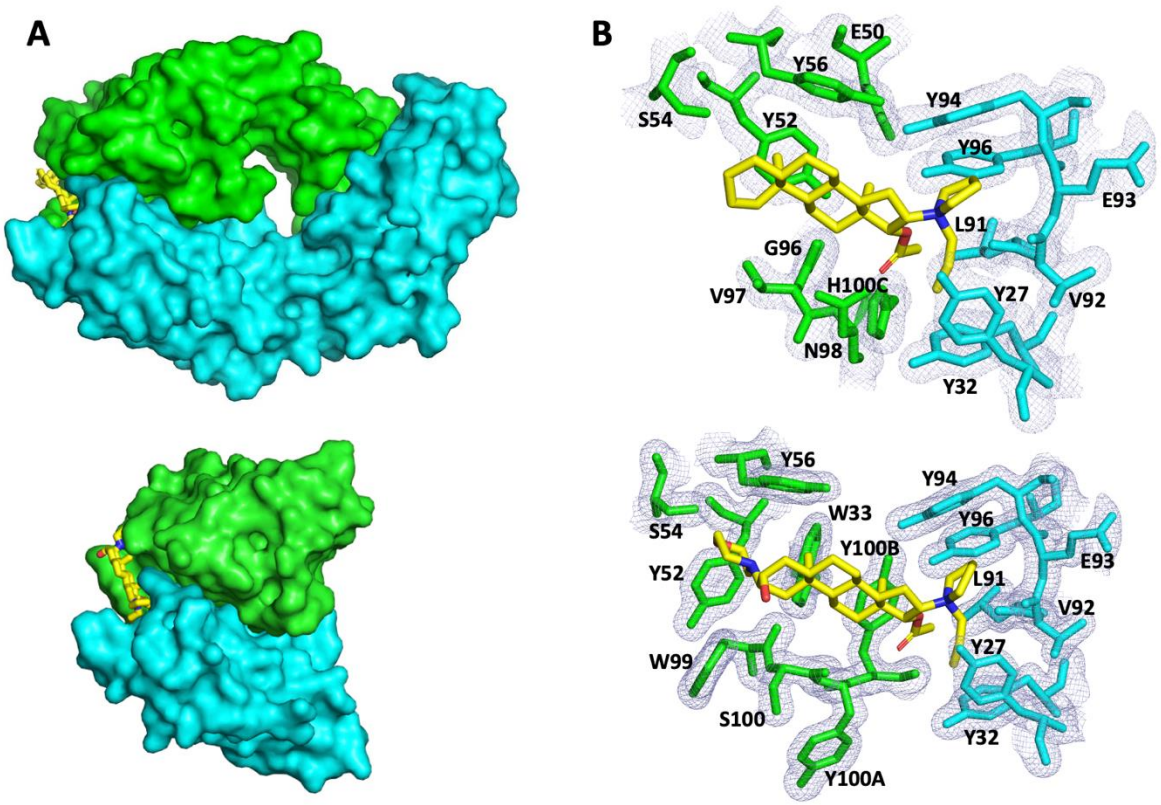

Figure 4: X-ray structures of mAbs in complex with rocuronium. (A) Surface representation of co-crystal structures of rocuronium-specific mouse Fab-m2B1 (top) and scFv-m1B6 (bottom) in complex with rocuronium. (B) Superposition of the rocuronium and key residues (indicated by the one-letter code of the amino acid, and their position in the chain) of the binding site for the Fab-m2B1-rocuronium complex (top) and scFv-m1B6-rocuronium (bottom). The antibody heavy chain is colored in green and light chain in cyan. The different atoms of the rocuronium molecule are colored: C atoms in yellow, O atoms in red and N atoms in dark blue.

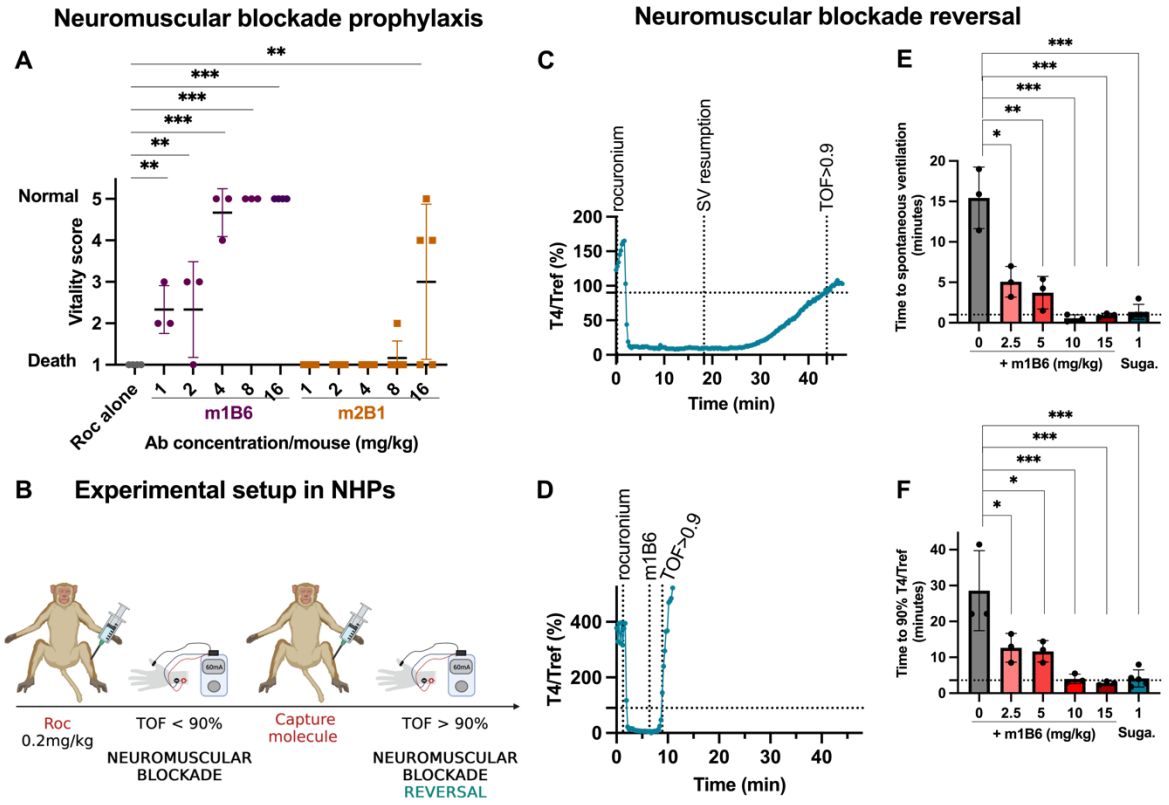

Figure 5: mAb m1B6 demonstrates therapeutic capacity to reverse neuromuscular blockade. (**A**) Prophylactic effect of indicated mAbs on rocuronium-induced neuromuscular blockade with vitality scores of wt mice (n≥3) as in Figure 2E. Mean (horizontal bar) and standard deviation are represented. Means ± standard deviations are indicated. Each dot represents a mouse. Statistical comparisons were obtained using contrast analysis after linear modeling and multiple-testing P-value adjustment. ***, P ≤ 0.001, **, P ≤ 0.01. Results for m2B1 1 to 8 mg/kg are not significant. (**B**) Scheme of the experimental protocol in macaques. (**C-D**) TOF measurement in one representative macaque following rocuronium injection to monitor neuromuscular reversal (**C**) without capture molecule or (**D**) following mAb m1B6 injection. The rocuronium injection time point and the time point of resumption of spontaneous ventilation (SV) and of TOF ratio T4/Tref > 0.9 are indicated. (**E-F**) Dose-dependent therapeutic effect of mAb m1B6 in macaques assessed by (**E**) time to spontaneous ventilation or (**F**) time for the TOF ratio T4/Tref to reach 90% (n=3 for all groups except n=4 for sugammadex (Suga. in mg/kg)). Statistical comparisons were obtained using contrast analysis after linear modeling and multiple-testing P-value adjustment. ***, P < 0.001; **, P < 0.01; *, P < 0.05.

TABLES

Table 1: Clinical signs and therapeutic interventions of the allergic patients included in the study. ICU, intensive care unit; IV, intravenous; N.A., not available; ACEI, Angiotensin-Converting-Enzyme Inhibitor; ARA, Angiotensin II Receptor Antagonist; BB, Beta-blocker; CI: Calcium channel inhibitor.

Variable	**Patient#1**	**Patient#2**	**Patient#3**
Gender	Female	Male	Female
Age (years)	43	47	69
Previous general anesthesia	Yes	No	*N.A.*
Medication (ACEI/ARA/BB/CI)	No	*N.A.*	*N.A.*
History of allergy			
Allergy*/Asthma/Atopy	No	No	No
Mastocytosis	*N.A.*	No	No
Type of surgery	Visceral	Neurosurgery	Orthopedic
Scheduled surgery	**Yes**	**Yes**	**Yes**
Surgery with a context of infection	No	No	No
NMBA used during surgery	Atracurium	**Rocuronium**	**Rocuronium**
Clinical signs			
Erythema	No	**Yes**	**Yes**
Tachycardia	**Yes**	No	**Yes**
Highest heart rate value (/min)	100	*N.A.*	115
Bradycardia	No	No	No
Arrhythmia	No	No	No
Arterial hypotension	**Yes**	**Yes**	**Yes**
Bronchospasm	No	**Yes**	**Yes**
Hypoxemia	No	No	No
Cardiac arrest	No	No	No
Ring and Messmer severity scale	**2**	**3**	**4**
Delay between anesthesia induction and first signs of the reaction (min)	**5**	**5**	**5**
Delay between first signs of the reaction and treatment initiation (min)	**15**	**10**	**10**
Therapeutic interventions			
Epinephrine IV alone	No	**Yes**	**Yes**
Phenylephrine IV alone	**Yes**	No	No
Glucocorticoids	No	**Yes**	No
Histamine receptor antagonists	No	**Yes**	No
Fluid resuscitation with crystalloids	No	**Yes**	**Yes**
Evolution			
Surgery cancelled	No	rescheduled	rescheduled
Admission to ICU	**Yes**	**Yes**	**Yes**
Delay between anaphylaxis and PBMC collection (months)	24	3.5	3
Allergy exploration			
QAM IgE ImmunoCAP (threshold 0.35)	0.1	**2.58**	0.28
Rocuronium Basophil Activation Test (BAT)	Negative	**Positive**	**Positive**
Rocuronium Skin Prick Test (SPT)	Negative	**Positive**	**Positive**
Allergen Exposure			
Pholcodine consumption in the past 12 months prior AHR	No	No	*N.A.*
Previous exposure to NMBA	**Yes(1993, 1996, 1999)**	*N.A.*	**Yes, once**
Occupational exposure to QAM (Patients reporting current or past cleaning profession or hairdressers)	No	*N.A.*	*N.A.*
Hair coloring frequency	**Regular**	No	*N.A.*

*includes: drugs, latex, food, Hymenoptera venom, pollen/moth, animals/mold

Table 2: Characteristics of anti-rocuronium antibodies with identical heavy chain rearrangements and CDR3 amino acid sequence. Antibodies produced recombinantly with demonstrated binding to rocuronium (roc) by ELISA are indicated in bold and their ELISA values indicated for a 1*µg/mL antibody concentration*. nd, not determined. Number of amino acid (AA) mutations compared to the imgt database are indicated.

Patient	Ab name	VH	CDR3 VH	AA mutation # in VH	VL	CDR3 VL	AA mutation # in VL	roc ELISA (OD)
#1_2023	I8F7	V3−7*01 J4*02	CARGYYGSGTYYASVFDYW	7	nd	nd	nd	nd
	I8D1				nd	nd	nd	nd
	5GI5				LV2-11*01 LJ3*02	CCSFAGTKTWMF	8	nd
	I2G11				KV4-1*02 KJ1*01	CQQYYNTPWTF	9	**0.16**
	I1G9	V4−59*01 J4*02	CARIWGSSGNYFDFW	7	IGLV2-11*01 LJ1*01	CCSYAGSFPYVF	6	nd
	I2H6				LV2-11*01 LJ1*01	CCSYAGSFPYVF	8	**0.21**
	I4D10							
	I7A2	V4-59*01 J4*02	CARGTGYSSDWHVEYW	5	LV3-1*01 LJ2*01	CQAWDSSTFVMF	20	nd
	I7C8				LV1-47*01 LJ1*01	CASWDDSLRGYVF	7	nd
	I1C10	V3-7*01 J6*02	CARTDYGYYYYYGVDVW	6	LV1-51*02 LJ3*02	CGTWDSSLSAEVF	6	**1.13**
	I1D8							
	I7B8							
	I2H10	V4-39*01 J4*02	CVAMVRGVPAYYW	6	LV2-8*01 LJ1*01	CSSYAGSNNPYVF	4	nd
	I5G8				KV3-20*01 KJ2*01	CQQYGSSPYTF	7	nd
	I7D10	V3-53*01 IGHJ3*01	CARAQTRNLYDGSGHYYKGAFDLW	11	KV1-5*03 F KJ1*01	CQQYNSYWTF	2	nd
	I7BI7							
	I7F5	HV4-61*02 J6*02	CARERRYSNGWGSYYYYGLDVW	15	LV2-18*02 LJ3*02	CSSYTNTKNWVF	10	**0.23**
	I2G10							

#2	G4E12	V4−38*02	AMYYCARAPCAGECRTLNIWFDPW	41	KV3-20*01	CQQYGTSPSTF	5	nd
	G5H9	J5*02			KJ2*02			nd
#3	**B1G2**	V3−21*01	CARGHSSFDDFWSGYSPNWFDPW	1	KV4-1*01	CQQYYSTPCSF	1	**0.96**
	B5G9	J5*02			KJ2*04			

Table 3: Characteristics of human anti-rocuronium antibodies. Antibodies were produced recombinantly and demonstrated binding to rocuronium by ELISA: they are ranked by their K_D value to HSA-rocuronium. roc, rocuronium; K_D, dissociation constant determined using biolayer interferometry for HSA-rocuronium and using surface plasmon resonance for free roc; nd, not determined; IC50, Half-maximal inhibitory concentration.

		Heavy chain			Light chain				
Patient	**human mAb**	**VH gene**	**DH gene**	**JH gene**	**VL gene**	**JL gene**	**K_D to HSA-roc (nM)**	**IC50 free roc (μM)**	**K_D to free roc (μM)**
#1_2014	**h1F10**	V3-48	D3-10	J4*02	KV2-30	KJ2*01	**21**	351	**140**
	A4E5	V4-61*07	D2-21*01	J6*02	KV3-11*01	KJ4*01	**22**	917	760
	h1G12	V4-61*02	D3-3*01	J3*02	LV2-8*01	LJ1*01	**28**	735	**>1,000**
	h6E11	V3-15*07	D3-22*01	J6*02	KV1-5*03	KJ2*01	**30**	nd	nd
	A6H7	V4-39*01	D2-15*01	J6*02	KV3-11*01	KJ4*01	**35**	917	**>2,000**
#2	**D3F8**	V4-39*08	D2-21*01	J6*03	KV3-15*01	J4*01	**40**	464	**>2,000**
#1_2014	**hA3E12**	V3-30*18	D6-13*01	J6*02	KV1-9*01	KJ2*01	**49**	539	nd
	h1B8	V4-39*01	D3-3*01	J3*02	KV4-1*01	KJ1*01	**50**	375	nd
	hA5H5	V4-61*02	D6-19*01	J3*02	GKV3-11*01	KJ1*01	**63**	684	nd
	h6A12	V1-2	D3-16	J4*02	KV1-5	KJ3*01	**74**	2,100	nd
	hA10A9	V1-18	D2-8	J1*01	LV2-14	LV2-14*03	**249**	2,718	nd
	hA8D8	V1-69*06	D3-22*01	J6*02	KV1-5*03	KJ2*01	**257**	473	nd
#2	**E9B10**	V4-34*01	D3-22*01	J3*01	KV1-39*01	KJ4*01	**275**	2105	nd
#1_2014	**h2D6**	V3-30-3	D2-15	J5*02	KV2-28	KJ2*01	**922**	612	nd
#2	**E11B8**	V4-30-4*09	D3-10*02	J6*03	KV3-20*01	KJ1*01	nd	2191	nd
	E11G7	V4-61*01	D6-6*01	J4*02	KV1-39*01	KJ4*01	nd	nd	nd

REFERENCES

1. S. R. Thilen, W. A. Weigel, M. M. Todd, R. P. Dutton, C. A. Lien, S. A. Grant, J. W. Szokol, L. I. Eriksson, M. Yaster, M. D. Grant, M. Agarkar, A. M. Marbella, J. F. Blanck, K. B. Domino, 2023 American Society of Anesthesiologists Practice Guidelines for Monitoring and Antagonism of Neuromuscular Blockade: A Report by the American Society of Anesthesiologists Task Force on Neuromuscular Blockade. *Anesthesiology* **138**, 13-41 (2023).
2. T. Fuchs-Buder, C. S. Romero, H. Lewald, M. Lamperti, A. Afshari, A. M. Hristovska, D. Schmartz, J. Hinkelbein, D. Longrois, M. Popp, H. D. de Boer, M. Sorbello, R. Jankovic, P. Kranke, Peri-operative management of neuromuscular blockade: A guideline from the European Society of Anaesthesiology and Intensive Care. *Eur J Anaesthesiol* **40**, 82-94 (2023).
3. P. M. Mertes, I. Aimone-Gastin, R. M. Gueant-Rodriguez, C. Mouton-Faivre, G. Audibert, J. O'Brien, D. Frendt, M. Brezeanu, H. Bouaziz, J. L. Gueant, Hypersensitivity reactions to neuromuscular blocking agents. *Curr Pharm Des* **14**, 2809-2825 (2008).
4. P. H. Sadleir, R. C. Clarke, D. L. Bunning, P. R. Platt, Anaphylaxis to neuromuscular blocking drugs: incidence and cross-reactivity in Western Australia from 2002 to 2011. *Br J Anaesth* **110**, 981-987 (2013).
5. G. Cammu, Residual Neuromuscular Blockade and Postoperative Pulmonary Complications: What Does the Recent Evidence Demonstrate? *Curr Anesthesiol Rep* **10**, 131-136 (2020).
6. C. Zaouter, S. Mion, A. Palomba, T. M. Hemmerling, A Short Update on Sugammadex with a Special Focus on Economic Assessment of its Use in North America. *J Anesth Clin Res* **8**, (2017).
7. W. Ji, X. Zhang, J. Liu, G. Sun, X. Wang, L. Bo, X. Deng, Efficacy and safety of neostigmine for neuromuscular blockade reversal in patients under general anesthesia: a systematic review and meta-analysis. *Ann Transl Med* **9**, 1691 (2021).
8. C. Rex, U. A. Bergner, F. K. Puhringer, Sugammadex: a selective relaxant-binding agent providing rapid reversal. *Curr Opin Anaesthesiol* **23**, 461-465 (2010).
9. L. Savic, S. Savic, P. M. Hopkins, Anaphylaxis to sugammadex. *Anaesth Intensive Care* **42**, 7-9 (2014).
10. B. A. Baldo, Anaphylaxis caused by sugammadex- rocuronium inclusion complex: What is the basis of the allergenic recognition? *J Clin Anesth* **54**, 48-49 (2019).
11. D. G. Ebo, B. A. Baldo, A. L. Van Gasse, C. Mertens, J. Elst, L. Sermeus, C. H. Bridts, M. M. Hagendorens, L. S. De Clerck, V. Sabato, Anaphylaxis to sugammadex-rocuronium inclusion complex: An IgE-mediated reaction due to allergenic changes at the sugammadex primary rim. *J Allergy Clin Immunol Pract* **8**, 1410-1415 e1413 (2020).
12. M. Orihara, T. Takazawa, T. Horiuchi, S. Sakamoto, K. Nagumo, Y. Tomita, A. Tomioka, N. Yoshida, A. Yokohama, S. Saito, Comparison of incidence of anaphylaxis between sugammadex and neostigmine: a retrospective multicentre observational study. *Br J Anaesth* **124**, 154-163 (2020).
13. L. Savic, S. Savic, P. M. Hopkins, Anaphylaxis to sugammadex: should we be concerned by the Japanese experience? *Br J Anaesth*, (2020).
14. P. M. Mertes, D. G. Ebo, T. Garcez, M. Rose, V. Sabato, T. Takazawa, P. J. Cooke, R. C. Clarke, P. Dewachter, L. H. Garvey, A. B. Guttormsen, D. L. Hepner, P. M. Hopkins, D. A. Khan, H. Kolawole, P. Kopac, M. Kroigaard, J. J. Laguna, S. D. Marshall, P. R. Platt, P. H. M. Sadleir, L. C. Savic, S. Savic, G. W. Volcheck, S. Voltolini, Comparative epidemiology of suspected perioperative hypersensitivity reactions. *Br J Anaesth* **123**, e16-e28 (2019).
15. P. Bruhns, S. Chollet-Martin, Mechanisms of human drug-induced anaphylaxis. *J Allergy Clin Immunol* **147**, 1133-1142 (2021).
16. F. Jonsson, L. de Chaisemartin, V. Granger, A. Gouel-Cheron, C. M. Gillis, Q. Zhu, F. Dib, P. Nicaise-Roland, C. Ganneau, M. Hurtado-Nedelec, C. Paugam-Burtz, S. Necib, H. Keita-Meyer, M. Le Dorze, B. Cholley, O. Langeron, L. Jacob, B. Plaud, M. Fischler, C. Sauvan, M. T. Guinnepain, P. Montravers, M. Aubier, S. Bay, C. Neukirch, F. Tubach, D. Longrois, S. Chollet-Martin, P. Bruhns, An IgG-induced neutrophil activation pathway contributes to human drug-induced anaphylaxis. *Sci Transl Med* **11**, (2019).
17. P. Vadas, M. Gold, B. Perelman, G. M. Liss, G. Lack, T. Blyth, F. E. Simons, K. J. Simons, D. Cass, J. Yeung, Platelet-activating factor, PAF acetylhydrolase, and severe anaphylaxis. *N Engl J Med* **358**, 28-35 (2008).
18. K. Arias, M. Baig, M. Colangelo, D. Chu, T. Walker, S. Goncharova, A. Coyle, P. Vadas, S. Waserman, M. Jordana, Concurrent blockade of platelet-activating factor and histamine prevents life-threatening peanut-induced anaphylactic reactions. *J Allergy Clin Immunol* **124**, 307-314, 314 e301-302 (2009).
19. M. M. van der Poorten, A. L. Van Gasse, M. M. Hagendorens, M. A. Faber, L. De Puysseleyr, J. Elst, C. M. Mertens, V. Sabato, D. G. Ebo, Serum specific IgE antibodies in immediate drug hypersensitivity. *Clin Chim Acta* **504**, 119-124 (2020).

20. Decuyper, II, D. G. Ebo, A. P. Uyttebroek, M. M. Hagendorens, M. A. Faber, C. H. Bridts, L. S. De Clerck, V. Sabato, Quantification of specific IgE antibodies in immediate drug hypersensitivity: More shortcomings than potentials? *Clin Chim Acta* **460**, 184-189 (2016).
21. A. P. Uyttebroek, V. Sabato, C. H. Bridts, L. S. De Clerck, D. G. Ebo, Immunoglobulin E antibodies to atracurium: a new diagnostic tool? *Clin Exp Allergy* **45**, 485-487 (2015).
22. B. A. Baldo, M. M. Fisher, Substituted ammonium ions as allergenic determinants in drug allergy. *Nature* **306**, 262-264 (1983).
23. W. J. Russell, C. Lee, D. Milne, Is allergy to rocuronium a high probability cross-reaction with suxamethonium? *Anaesth Intensive Care* **31**, 333 (2003).
24. M. A. Rose, J. Anderson, S. L. Green, J. Yun, S. L. Fernando, Morphine and pholcodine-specific IgE have limited utility in the diagnosis of anaphylaxis to benzylisoquinolines. *Acta Anaesthesiol Scand* **62**, 628-634 (2018).
25. B. A. Baldo, M. M. Fisher, N. H. Pham, On the origin and specificity of antibodies to neuromuscular blocking (muscle relaxant) drugs: an immunochemical perspective. *Clin Exp Allergy* **39**, 325-344 (2009).
26. M. Peyneau, L. de Chaisemartin, N. Gigant, S. Chollet-Martin, S. Kerdine-Romer, Quaternary ammonium compounds in hypersensitivity reactions. *Front Toxicol* **4**, 973680 (2022).
27. E. Florvaag, S. G. Johansson, The Pholcodine Case. Cough Medicines, IgE-Sensitization, and Anaphylaxis: A Devious Connection. *World Allergy Organ J* **5**, 73-78 (2012).
28. P. M. Mertes, N. Petitpain, C. Tacquard, M. Delpuech, C. Baumann, J. M. Malinovsky, D. Longrois, A. Gouel-Cheron, D. Le Quang, P. Demoly, J. L. Gueant, P. Gillet, A. S. Group, Pholcodine exposure increases the risk of perioperative anaphylaxis to neuromuscular blocking agents: the ALPHO case-control study. *Br J Anaesth*, (2023).
29. R. Jimenez-Saiz, Y. Ellenbogen, K. Bruton, P. Spill, D. D. Sommer, H. Lima, S. Waserman, S. U. Patil, W. G. Shreffler, M. Jordana, Human BCR analysis of single-sorted, putative IgE(+) memory B cells in food allergy. *J Allergy Clin Immunol* **144**, 336-339 e336 (2019).
30. J. M. Davies, T. A. Platts-Mills, R. C. Aalberse, The enigma of IgE+ B-cell memory in human subjects. *J Allergy Clin Immunol* **131**, 972-976 (2013).
31. B. Laffleur, S. Duchez, K. Tarte, N. Denis-Lagache, S. Peron, C. Carrion, Y. Denizot, M. Cogne, Self-Restrained B Cells Arise following Membrane IgE Expression. *Cell Rep*, (2015).
32. R. A. Hoh, S. A. Joshi, J. Y. Lee, B. A. Martin, S. Varma, S. Kwok, S. C. A. Nielsen, P. Nejad, E. Haraguchi, P. S. Dixit, S. V. Shutthanandan, K. M. Roskin, W. Zhang, D. Tupa, B. J. Bunning, M. Manohar, R. Tibshirani, N. Q. Fernandez-Becker, N. Kambham, R. B. West, R. G. Hamilton, M. Tsai, S. J. Galli, R. S. Chinthrajah, K. C. Nadeau, S. D. Boyd, Origins and clonal convergence of gastrointestinal IgE(+) B cells in human peanut allergy. *Sci Immunol* **5**, (2020).
33. K. Haniuda, S. Fukao, T. Kodama, H. Hasegawa, D. Kitamura, Autonomous membrane IgE signaling prevents IgE-memory formation. *Nat Immunol* **17**, 1109-1117 (2016).
34. I. Hoof, V. Schulten, J. A. Layhadi, T. Stranzl, L. H. Christensen, S. Herrera de la Mata, G. Seumois, P. Vijayanand, C. Lundegaard, K. Niss, A. Lund, J. Ahrenfeldt, J. Holm, E. Steveling, H. Sharif, S. R. Durham, B. Peters, M. H. Shamji, P. S. Andersen, Allergen-specific IgG(+) memory B cells are temporally linked to IgE memory responses. *J Allergy Clin Immunol* **146**, 180-191 (2020).
35. X. M. Luo, E. Maarschalk, R. M. O'Connell, P. Wang, L. Yang, D. Baltimore, Engineering human hematopoietic stem/progenitor cells to produce a broadly neutralizing anti-HIV antibody after in vitro maturation to human B lymphocytes. *Blood* **113**, 1422-1431 (2009).
36. A. Sokal, G. Barba-Spaeth, L. Hunault, I. Fernandez, M. Broketa, A. Meola, S. Fourati, I. Azzaoui, A. Vandenberghe, P. Lagouge-Roussey, M. Broutin, A. Roeser, M. Bouvier-Alias, E. Crickx, L. Languille, M. Fournier, M. Michel, B. Godeau, S. Gallien, G. Melica, Y. Nguyen, F. Canoui-Poitrine, F. Pirenne, J. Megret, J. M. Pawlotsky, S. Fillatreau, C. A. Reynaud, J. C. Weill, F. A. Rey, P. Bruhns, M. Mahevas, P. Chappert, SARS-CoV-2 Omicron BA.1 breakthrough infection drives late remodeling of the memory B cell repertoire in vaccinated individuals. *Immunity*, (2023).
37. D. R. Glass, A. G. Tsai, J. P. Oliveria, F. J. Hartmann, S. C. Kimmey, A. A. Calderon, L. Borges, M. C. Glass, L. E. Wagar, M. M. Davis, S. C. Bendall, An Integrated Multi-omic Single-Cell Atlas of Human B Cell Identity. *Immunity* **53**, 217-232 e215 (2020).
38. N. T. Gupta, J. A. Vander Heiden, M. Uduman, D. Gadala-Maria, G. Yaari, S. H. Kleinstein, Change-O: a toolkit for analyzing large-scale B cell immunoglobulin repertoire sequencing data. *Bioinformatics* **31**, 3356-3358 (2015).

39. J. Elst, V. Sabato, M. A. Faber, C. H. Bridts, C. Mertens, M. Van Houdt, A. L. Van Gasse, M. M. Hagendorens, V. Van Tendeloo, M. Maurer, D. Campillo-Davo, J. P. Timmermans, I. Pintelon, D. G. Ebo, MRGPRX2 and Immediate Drug Hypersensitivity: Insights From Cultured Human Mast Cells. *J Investig Allergol Clin Immunol* **31**, 489-499 (2021).
40. A. Gouel-Cheron, A. Dejoux, E. Lamanna, P. Bruhns, Animal Models of IgE Anaphylaxis. *Biology (Basel)* **12**, (2023).
41. L. Fielding, G. H. Grant, Conformational equilibria in amino steroids. 1. A proton and carbon-13 NMR spectroscopy and molecular mechanics study of 3.alpha.-hydroxy-2.beta.-(4-morpholinyl)-5.alpha.H-androstan-17-one. *J. Am. Chem. Soc.* **113**, 9785-9790 (1991).
42. B. A. Baldo, M. M. Fisher, Anaphylaxis to muscle relaxant drugs: cross-reactivity and molecular basis of binding of IgE antibodies detected by radioimmunoassay. *Mol Immunol* **20**, 1393-1400 (1983).
43. P. M. Jones, T. P. Turkstra, Mitigation of rocuronium-induced anaphylaxis by sugammadex: the great unknown. *Anaesthesia* **65**, 89-90; author reply 90 (2010).
44. A. E. Funnell, J. Griffiths, I. Hodzovic, A further case of rocuronium-induced anaphylaxis treated with sugammadex. *Br J Anaesth* **107**, 275-276 (2011).
45. B. Conte, L. Zoric, G. Bonada, B. Debaene, J. Ripart, Reversal of a rocuronium-induced grade IV anaphylaxis via early injection of a large dose of sugammadex. *Can J Anaesth* **61**, 558-562 (2014).
46. H. Letscher, J. Lemaitre, E. Burban, R. Le Grand, P. Bruhns, F. Relouzat, A. Gouel-Chéron, Optimization of neuromuscular blockade protocols in cynomolgus macaques: monitoring, doses and antagonism. *bioRxiv*, (2023).
47. J. I. Reddy, P. J. Cooke, J. M. van Schalkwyk, J. A. Hannam, P. Fitzharris, S. J. Mitchell, Anaphylaxis is more common with rocuronium and succinylcholine than with atracurium. *Anesthesiology* **122**, 39-45 (2015).
48. T. Takazawa, H. Mitsuhata, P. M. Mertes, Sugammadex and rocuronium-induced anaphylaxis. *J Anesth* **30**, 290-297 (2016).
49. C. Tacquard, O. Collange, P. Gomis, J. M. Malinovsky, N. Petitpain, P. Demoly, S. Nicoll, P. M. Mertes, Anaesthetic hypersensitivity reactions in France between 2011 and 2012: the 10th GERAP epidemiologic survey. *Acta Anaesthesiol Scand* **61**, 290-299 (2017).
50. J. M. Hunter, Rocuronium: the newest aminosteroid neuromuscular blocking drug. *Br J Anaesth* **76**, 481-483 (1996).
51. W. J. Pichler, Anaphylaxis to drugs: Overcoming mast cell unresponsiveness by fake antigens. *Allergy*, (2020).
52. R. C. Aalberse, I. Kleine Budde, M. Mulder, S. O. Stapel, W. Paulij, F. Leynadier, M. W. Hollmann, Differentiating the cellular and humoral components of neuromuscular blocking agent-induced anaphylactic reactions in patients undergoing anaesthesia. *Br J Anaesth* **106**, 665-674 (2011).
53. A. Dejoux, L. de Chaisemartin, P. Bruhns, D. Longrois, A. Gouel-Cheron, Neuromuscular blocking agent induced hypersensitivity reaction exploration: an update. *Eur J Anaesthesiol* **40**, 95-104 (2023).
54. M. M. Fisher, B. A. Baldo, Immunoassays in the diagnosis of anaphylaxis to neuromuscular blocking drugs: the value of morphine for the detection of IgE antibodies in allergic subjects. *Anaesth Intensive Care* **28**, 167-170 (2000).
55. D. Laroche, S. Chollet-Martin, P. Leturgie, L. Malzac, M. C. Vergnaud, C. Neukirch, L. Venemalm, J. L. Gueant, P. N. Roland, Evaluation of a new routine diagnostic test for immunoglobulin e sensitization to neuromuscular blocking agents. *Anesthesiology* **114**, 91-97 (2011).
56. J. Leysen, A. Uyttebroek, V. Sabato, C. H. Bridts, L. S. De Clerck, D. G. Ebo, Predictive value of allergy tests for neuromuscular blocking agents: tackling an unmet need. *Clin Exp Allergy* **44**, 1069-1075 (2014).
57. J. Anderson, S. Green, M. Capon, B. Krupowicz, J. Li, R. Fulton, S. L. Fernando, Measurement of pholcodine-specific IgE in addition to morphine-specific IgE improves investigation of neuromuscular blocking agent anaphylaxis. *Br J Anaesth* **125**, e450-e452 (2020).
58. K. L. Chow, K. Patchett, G. Reeves, T. de Malmanche, D. Gillies, M. Boyle, Morphine-specific IgE testing in the assessment of neuromuscular blocking agent allergy: a single centre experience. *Br J Anaesth*, (2023).
59. T. J. Looney, J. Y. Lee, K. M. Roskin, R. A. Hoh, J. King, J. Glanville, Y. Liu, T. D. Pham, C. L. Dekker, M. M. Davis, S. D. Boyd, Human B-cell isotype switching origins of IgE. *J Allergy Clin Immunol* **137**, 579-586 e577 (2016).
60. M. Ota, K. B. Hoehn, W. Fernandes-Braga, T. Ota, C. J. Aranda, S. Friedman, M. G. C. Miranda-Waldetario, J. Redes, M. Suprun, G. Grishina, H. A. Sampson, A. Malbari, S. H. Kleinstein, S. H. Sicherer, M. A. Curotto de Lafaille, CD23(+)IgG1(+) memory B cells are poised to switch to pathogenic IgE production in food allergy. *Sci Transl Med* **16**, eadi0673 (2024).

61. J. F. E. Koenig, N. P. H. Knudsen, A. Phelps, K. Bruton, I. Hoof, G. Lund, D. D. Libera, A. Lund, L. H. Christensen, D. R. Glass, T. D. Walker, A. Fang, S. Waserman, M. Jordana, P. S. Andersen, Type 2-polarized memory B cells hold allergen-specific IgE memory. *Sci Transl Med* **16**, eadi0944 (2024).
62. J. Elst, M. Van Houdt, M. M. van der Poorten, A. L. Van Gasse, C. Mertens, A. Toscano, M. Beyens, E. De Boeck, V. Sabato, D. G. Ebo, Comparison of the passive mast cell activation test with the basophil activation test for diagnosis of perioperative rocuronium hypersensitivity. *Br J Anaesth*, (2023).
63. S. Asrat, N. Kaur, X. Liu, L. H. Ben, D. Kajimura, A. J. Murphy, M. A. Sleeman, A. Limnander, J. M. Orengo, Chronic allergen exposure drives accumulation of long-lived IgE plasma cells in the bone marrow, giving rise to serological memory. *Sci Immunol* **5**, (2020).
64. S. Asrat, J. C. Devlin, A. Vecchione, B. Klotz, I. Setliff, D. Srivastava, A. Limnander, A. Rafique, C. Adler, S. Porter, A. J. Murphy, G. S. Atwal, M. A. Sleeman, W. K. Lim, J. M. Orengo, TRAPnSeq allows high-throughput profiling of antigen-specific antibody-secreting cells. *Cell Rep Methods* **3**, 100522 (2023).
65. N. Stawicki, P. Gessner, Residual Neuromuscular Blockade in the Critical Care Setting. *AACN Adv Crit Care* **29**, 15-24 (2018).
66. L. Saager, E. M. Maiese, L. D. Bash, T. A. Meyer, H. Minkowitz, S. Groudine, B. K. Philip, P. Tanaka, T. J. Gan, Y. Rodriguez-Blanco, R. Soto, O. Heisel, Incidence, risk factors, and consequences of residual neuromuscular block in the United States: The prospective, observational, multicenter RECITE-US study. *J Clin Anesth* **55**, 33-41 (2019).
67. P. Goncalves, A. V. Vieira, C. Silva, R. S. Gomez, Residual neuromuscular blockade and late neuromuscular blockade at the post-anesthetic recovery unit: prospective cohort study. *Braz J Anesthesiol* **71**, 38-43 (2021).
68. J. Ross, D. P. Ramsay, L. J. Sutton-Smith, R. D. Willink, J. E. Moore, Residual neuromuscular blockade in the ICU: a prospective observational study and national survey. *Anaesthesia* **77**, 991-998 (2022).
69. C. Baillard, C. Clec'h, J. Catineau, F. Salhi, G. Gehan, M. Cupa, C. M. Samama, Postoperative residual neuromuscular block: a survey of management. *Br J Anaesth* **95**, 622-626 (2005).
70. S. Esteves, F. Correia de Barros, C. S. Nunes, A. Puga, B. Gomes, F. Abelha, H. Machado, M. Ferreira, N. Fernandes, P. Vitor, S. Pereira, T. A. Lapa, V. Pinho-Oliveira, Incidence of postoperative residual neuromuscular blockade - A multicenter, observational study in Portugal (INSPIRE 2). *Porto Biomed J* **8**, e225 (2023).
71. A. D. Raval, V. R. Anupindi, C. P. Ferrufino, D. L. Arper, L. D. Bash, S. J. Brull, Epidemiology and outcomes of residual neuromuscular blockade: A systematic review of observational studies. *J Clin Anesth* **66**, 109962 (2020).
72. K. Suzuki, T. Takazawa, S. Saito, History of the development of antagonists for neuromuscular blocking agents. *J Anesth* **34**, 723-728 (2020).
73. A. Gouel-Cheron, L. de Chaisemartin, F. Jonsson, P. Nicaise-Roland, V. Granger, A. Sabahov, M. T. Guinnepain, S. Chollet-Martin, P. Bruhns, C. Neukirch, D. Longrois, N. s. group, Low end-tidal CO2 as a real-time severity marker of intra-anaesthetic acute hypersensitivity reactions. *Br J Anaesth* **119**, 908-917 (2017).
74. J. Sprung, T. N. Weingarten, L. B. Schwartz, Presence or absence of elevated acute total serum tryptase by itself is not a definitive marker for an allergic reaction. *Anesthesiology* **122**, 713-714 (2015).
75. D. G. Ebo, L. Venemalm, C. H. Bridts, F. Degerbeck, H. Hagberg, L. S. De Clerck, W. J. Stevens, Immunoglobulin E antibodies to rocuronium: a new diagnostic tool. *Anesthesiology* **107**, 253-259 (2007).
76. S. Goyard, B. Balbino, R. S. Chinthrajah, S. C. Lyu, Y. L. Janin, P. Bruhns, P. Poncet, S. J. Galli, K. C. Nadeau, L. L. Reber, T. Rose, A highly sensitive bioluminescent method for measuring allergen-specific IgE in microliter samples. *Allergy* **75**, 2952-2956 (2020).
77. D. A. Mancardi, B. Iannascoli, S. Hoos, P. England, M. Daeron, P. Bruhns, FcgammaRIV is a mouse IgE receptor that resembles macrophage FcepsilonRI in humans and promotes IgE-induced lung inflammation. *J Clin Invest* **118**, 3738-3750 (2008).
78. T. Tiller, E. Meffre, S. Yurasov, M. Tsuiji, M. C. Nussenzweig, H. Wardemann, Efficient generation of monoclonal antibodies from single human B cells by single cell RT-PCR and expression vector cloning. *J Immunol Methods* **329**, 112-124 (2008).
79. M. Djaffardjy, G. Marchment, C. Sebe, R. Blanchet, K. Bellajhame, A. Gaignard, F. Lemoine, S. Cohen-Boulakia, Developing and reusing bioinformatics data analysis pipelines using scientific workflow systems. *Comput Struct Biotechnol J* **21**, 2075-2085 (2023).
80. K. B. Hoehn, O. G. Pybus, S. H. Kleinstein, Phylogenetic analysis of migration, differentiation, and class switching in B cells. *PLoS Comput Biol* **18**, e1009885 (2022).
81. G. Yu, Using ggtree to Visualize Data on Tree-Like Structures. *Curr Protoc Bioinformatics* **69**, e96 (2020).

82. P. Weber, C. Pissis, R. Navaza, A. E. Mechaly, F. Saul, P. M. Alzari, A. Haouz, High-Throughput Crystallization Pipeline at the Crystallography Core Facility of the Institut Pasteur. *Molecules* **24**, (2019).
83. C. Vonrhein, C. Flensburg, P. Keller, A. Sharff, O. Smart, W. Paciorek, T. Womack, G. Bricogne, Data processing and analysis with the autoPROC toolbox. *Acta Crystallogr D Biol Crystallogr* **67**, 293-302 (2011).
84. W. Kabsch, Xds. *Acta Crystallogr D Biol Crystallogr* **66**, 125-132 (2010).
85. J. Agirre, M. Atanasova, H. Bagdonas, C. B. Ballard, A. Basle, J. Beilsten-Edmands, R. J. Borges, D. G. Brown, J. J. Burgos-Marmol, J. M. Berrisford, P. S. Bond, I. Caballero, L. Catapano, G. Chojnowski, A. G. Cook, K. D. Cowtan, T. I. Croll, J. E. Debreczeni, N. E. Devenish, E. J. Dodson, T. R. Drevon, P. Emsley, G. Evans, P. R. Evans, M. Fando, J. Foadi, L. Fuentes-Montero, E. F. Garman, M. Gerstel, R. J. Gildea, K. Hatti, M. L. Hekkelman, P. Heuser, S. W. Hoh, M. A. Hough, H. T. Jenkins, E. Jimenez, R. P. Joosten, R. M. Keegan, N. Keep, E. B. Krissinel, P. Kolenko, O. Kovalevskiy, V. S. Lamzin, D. M. Lawson, A. A. Lebedev, A. G. W. Leslie, B. Lohkamp, F. Long, M. Maly, A. J. McCoy, S. J. McNicholas, A. Medina, C. Millan, J. W. Murray, G. N. Murshudov, R. A. Nicholls, M. E. M. Noble, R. Oeffner, N. S. Pannu, J. M. Parkhurst, N. Pearce, J. Pereira, A. Perrakis, H. R. Powell, R. J. Read, D. J. Rigden, W. Rochira, M. Sammito, F. Sanchez Rodriguez, G. M. Sheldrick, K. L. Shelley, F. Simkovic, A. J. Simpkin, P. Skubak, E. Sobolev, R. A. Steiner, K. Stevenson, I. Tews, J. M. H. Thomas, A. Thorn, J. T. Valls, V. Uski, I. Uson, A. Vagin, S. Velankar, M. Vollmar, H. Walden, D. Waterman, K. S. Wilson, M. D. Winn, G. Winter, M. Wojdyr, K. Yamashita, The CCP4 suite: integrative software for macromolecular crystallography. *Acta Crystallogr D Struct Biol* **79**, 449-461 (2023).
86. A. J. McCoy, R. W. Grosse-Kunstleve, P. D. Adams, M. D. Winn, L. C. Storoni, R. J. Read, Phaser crystallographic software. *J Appl Crystallogr* **40**, 658-674 (2007).
87. P. Emsley, K. Cowtan, Coot: model-building tools for molecular graphics. *Acta Crystallogr D Biol Crystallogr* **60**, 2126-2132 (2004).
88. G. N. Murshudov, P. Skubak, A. A. Lebedev, N. S. Pannu, R. A. Steiner, R. A. Nicholls, M. D. Winn, F. Long, A. A. Vagin, REFMAC5 for the refinement of macromolecular crystal structures. *Acta Crystallogr D Biol Crystallogr* **67**, 355-367 (2011).

ACKNOWLEDGMENTS

We would like to thank our colleagues from the Institut Pasteur, Paris, France for their help and advice: Delphine Brun and Annalisa Meola (Structural virology unit) for ScFv generation and production; Bertrand Raynal, Sébastien Brulé and Sylviane Hoos for assistance with affinity measurements (Molecular Biophysics Core Facility), Fabrice Agou for access to the BLI instrument (Plateforme de Criblage Chémogénomique et Biologique; PF-CCB), the Cytometry and Biomarkers technological unit (UTechS CB); and Michel Perez for advice and support (Direction Des Applications De la Recherche et des Relations Industrielles; DARRI). We would like to thank Garnett Kelsoe (Duke University, Durham, NC, USA) for providing us with invaluable advice and the human B cell culture system; the team of the Pharmacoepidemiology, Center of the Assistance Publique-Hôpitaux de Paris (AP-HP) and, in particular, N. Yelles, K. Chandirakumaran, and I. Younes at the Bichat Hospital for help with the NASA clinical study logistics; G. Chabot and O. Kacimi at Hôpital Bichat, Paris, France for the MEDIREP study; J. Lehacaut and C. Da Costa Ribeiro Coutinho from the CIC at Hôpital Bichat, Paris, France; the staff of the crystallography platform at Institut Pasteur for crystallization screening, and acknowledge synchroton SOLEIL (Saint-Aubin, France) for granting access to their facility and the staff of Proxima1 and Proxima2A for helpful assistance.

NASA study group: Pierre Bruhns[1,2], Friederike Jönsson[1,2], Caitlin M. Gillis[1,2], David A. Mancardi[1,2], Pascale Nicaise-Roland[3], Luc de Chaisemartin[3,4], Sylvie Chollet-Martin[3,4], Vanessa Granger[3,4], Qianqian Zhu[1,2,4], Dan Longrois[3,5], Aurélie Gouel-Chéron[1,2,5], Philippe Montravers[5,19], Caroline Sauvan[17], Fadia Dib[6], Sylvie Bay[7,8], Christelle Ganneau[7,8], Catherine Paugam-Burtz[10], Skander Necib[10], Hawa Keita-Meyer[11], Valentina Faitot[11], Alexandre Mebazaa[12], Matthieu Le Dorze[12], Bernard Cholley[13], Jean Mantz[13] (deceased), Olivier Langeron[14], Sabrine Roche[14], Laurent Jacob[15], Benoit Plaud[15], Carole Chahine[15], Marc Fischler[16], Marie-Thérèse Guinnepain[18], Julie Bresson[15], Michel Aubier[17,19], Catherine Neukirch[17,19], Florence Tubach[20], Antoine Mignon[21].

[1]Institut Pasteur, Department of Immunology, Unit of Antibodies in Therapy and Pathology, Paris, France; [2]INSERM, U1222, Paris, France; [3]HUPNVS, INSERM 1148, Université Paris-Diderot, Paris, France; [4]Inflammation Chimiokines et Immunopathologie, INSERM UMRS996, Faculté de

Pharmacie, Université Paris-Sud, Université Paris-Saclay, Châtenay-Malabry, France; [5]APHP, Hôpital Bichat, Département d'Anesthésie-Réanimation, HUPNVS, Paris, France; [6]APHP, Hôpital Bichat, Department of Epidemiology and Clinical Research, INSERM, Paris, France; [7]Institut Pasteur, Département Biologie Structurale et Chimie, Unité de Chimie des Biomolécules, Paris , France; [8]CNRS UMR 3523, Paris, France; [10]Département d'Anesthésie-Réanimation, Hôpital Beaujon, AP-HP, Clichy, France, and Université Paris Diderot, Paris, France; [11]Service d'anesthésie, Hôpital Louis Mourier, AP-HP, Colombes, France and Université Paris Diderot, Sorbonne Paris Cité, EA Recherche Clinique coordonnée ville-hôpital, Méthodologies et Société (REMES), Paris, France; [12]Département d'Anesthésie-Réanimation, Hôpital Lariboisière, AP-HP, Paris, France; [13]Service d'Anesthésie-Réanimation, Hôpital Européen Georges Pompidou, UMR1140 INSERM, AP-HP, Paris, France and Université Paris Descartes, Sorbonne Paris Cité, Paris, France; [14]Department of Anesthesia and Critical Care, Hôpital Pitié Salpêtrière, AP-HP, Sorbonne Université, Paris, France and Infection and Epidemiology Department, Institut Pasteur Human Histopathology and Animal Models Unit, Paris, France; [15]Département d'Anesthésie-Réanimation, Hôpital Saint Louis, AP-HP, Paris, France; [16]Service d'Anesthésie, Hôpital Foch, Sureses, France; [17]APHP, Hôpital Bichat, Service de Pneumologie A, HUPNVS, Paris, France; [18]Hôpital Foch, Service de médecine interne, Suresnes, France; [19]INSERM 1152, DHU FIRE, Labex Inflamex, Université Paris Diderot Paris 7, Paris, France; [20]Sorbonne Université, INSERM, Institut Pierre Louis d'Epidémiologie et de Santé Publique, PEPITES, AP-HP, Hôpitaux Universitaires Pitié Salpêtrière - Charles Foix, Département Biostatistique Santé Publique et Information Médicale, Centre de Pharmacoépidémiologie (Cephepi), CIC-1421, F75013, Paris, France.; [21]Département d'anesthésie-réanimation, Hôpital Cochin, AP-HP, Paris, France.

FUNDING

Work in the Bruhns' lab was supported by the Institut Pasteur, Institut National de la Santé et de la Recherche Médicale (Inserm), Fondation pour la Recherche Médicale, Paris, France (Programme Equipe FRM grant EQU202203014631), Accélérateur de l'innovation de l'Institut Pasteur (grant rocuCEPT), Agence Nationale de la Recherche (ANR grant ANR-21-CE15-0027), European Research Council (ERC)–Seventh Framework Program (ERC-2013-CoG 616050). Data partially

results from the work performed in the *International Research Program* IRP “ALLERGYMINE” (Inserm grant call 2022-2026) to PB. AD and LH were doctoral fellows of Sorbonne Université. AD was partly supported by a fellowship from the Fondation pour la Recherche Médicale. QZ received a PhD scholarship from the Chinese Science Council. AGC was a recipient of a poste d’accueil 2017 Institut Pasteur – Assistance Publique des Hôpitaux de Paris (APHP) and from a grant provided by INSERM, SFAR (Société Française d’Anesthésie et de Réanimation), and SRLF (Société de Réanimation de Langue Française) through the “Bourse de Recherche du Comité d’interface INSERM-SFAR-SRLF 2012. CMG was supported partly by a stipend from the Pasteur-Paris University (PPU) International PhD program and by the Institut Carnot Pasteur Maladies Infectieuses. PB benefited from an additional support from AP-HP through a “Contrat Local d’Interface 2014” and the “Département Hospitalo-Universitaire” (DHU) FIRE. The sponsor of the NASA study was the Direction de la Recherche Clinique et de l’Innovation de l’AP-HP (France).

COMPETING INTERESTS

Unrelated to the submitted work, PB received consulting fees from Regeneron Pharmaceuticals. LdC (Luc de Chaisemartin) reports lecture fees from MSD France, without any relation to the content of this manuscript. The other authors declare no competing interests.

DATA AND MATERIALS AVAILABILITY

Coordinates and structure factors of crystallographic data have been deposited in the Protein Data Bank under the accession codes 8S4K (Fab2B1 in complex with rocuronium) and 8S4H (scFv-1B6 in complex with rocuronium). (PDB are available).

Article 2: Plasma cell repertoires identify high-affinity anti-rocuronium antibodies that recapitulate anaphylaxis *in vivo*.

In the second article under preparation, we depicted an in-depth rocuronium-specific plasma cell repertoire of two different mice.

First, using a bioinformatic analysis we could describe the rocuronium-specific antibody repertoires that were comprised of three major clonal families and displayed convergency. We performed a functional analysis by reproducing recombinantly the most representative antibodies of each clonal family to evaluate their specificity, avidity, affinity for rocuronium, and cross-reactivity with other NMBAs or QA-containing compounds. We observed subnanomolar affinities for rocuronium with antibodies specific for aminosteroid NMBAs. To understand the underlying mechanisms of anaphylaxis, we expressed the antibodies as human IgE and demonstrated that they could trigger human mast cell and basophils degranulation and anaphylaxis in mice humanized for human IgE and their receptor FcεRI. Under their IgG isotype, the antibodies could also activate neutrophils by forming immune complexes.

To tackle the commonly admitted hypothesis that the QA group contained in all NMBA represents the allergenic epitopes, we generated co-crystal structures of the antibodies with rocuronium. These co-crystal structures revealed different interaction modes but the QA was systematically involved in the binding interface.

All in all, this work allowed the identification of the allergenic epitope of rocuronium, gave insights into the underlying IgE-dependent and IgG-dependent pathways involved in NMBA-mediated AHR, and established the first mouse model of NMBA anaphylaxis.

Plasma cell repertoires identify high-affinity anti-rocuronium antibodies that recapitulate anaphylaxis *in vivo.*

Authors: Alice Dejoux[1,2,†], Qianqian Zhu[1,3,†], Adam Woolfe[4,5,‡], Ophélie Godon[1,‡], Sami Ellouze[4], Guillaume Mottet[1], Carlos Castrillon[1], Caitlin Gillis[1], Cyprien Pecalvel[6], Christelle Ganneau[7], Bruno Iannascoli[1], Frédéric Lemoine[8], Frederick Saul[9], Patrick England[10], Laurent L. Reber[6], Aurélie Gouel-Chéron[1,11,12], Luc de Chaisemartin[3,13], Ahmed Haouz[9], Gaël A. Millot[1,8], Sylvie Bay[7], Annabelle Gérard[4,5,§], Friederike Jönsson[1,14,§], Sylvie Chollet-Martin[3,13,§] and Pierre Bruhns[1,15,§,*].

Affiliations:

[1]Institut Pasteur, Université Paris Cité, INSERM UMR1222, Antibodies in Therapy and Pathology, 75015 Paris, France.

[2]Sorbonne Université, Collège Doctoral, 75005 Paris, France.

[3]Université Paris-Saclay, INSERM, Inflammation Microbiome Immunosurveillance, Orsay, France.

[4]HiFiBiO Therapeutics SAS, Paris, France.

[5]Present address: SABER BIO, Institut du Cerveau, iPEPS The HealthtechHub, 47 boulevard de l'Hôpital CS21414, 75646 Paris Cedex

[6]Toulouse Institute for Infectious and Inflammatory Diseases (Infinity), INSERM UMR1291, CNRS UMR5051, University Toulouse III; Toulouse, France.

[7]Institut Pasteur, Université Paris Cité, CNRS UMR3523, Chimie des Biomolécules, 75015 Paris, France.

[8]Institut Pasteur, Université Paris Cité, Bioinformatics and Biostatistics Hub, Paris, France.

[9]Institut Pasteur, Université Paris Cité, CNRS UMR3528, Plate-forme Cristallographie-C2RT, Paris, France.

[10]Institut Pasteur, Université Paris Cité, CNRS UMR3528, Molecular Biophysics Core Facility, Paris, France.

[11]Anaesthesiology and Critical Care Medicine Department, DMU Parabol, Bichat-Claude Bernard Hospital, AP-HP, 75018 Paris, France.

[12]Université Paris Cité, 75010 Paris, France.

[13]Service d'immunologie, Hôpital Bichat, APHP, Paris, France.

[14]CNRS, F-75015 Paris.

[15]INSERM 1152, DHU FIRE, Labex Inflamex, Université Paris Diderot Paris 7, Paris, France.

[†] or [‡]: Equal contribution.

[§]: Co-senior authorship.

ABSTRACT

Neuromuscular blocking agents (NMBA) are muscle relaxants used to assist mechanical ventilation but lead in 1/10,000 anesthesia to severe acute hypersensitivity reactions i.e., anaphylaxis. Incidences vary between types of NMBAs. Rocuronium, a widely used non-depolarizing aminosteroid NMBA, induces among the highest anaphylaxis rates. Rocuronium-induced anaphylaxis is proposed to rely on pre-existing rocuronium-binding antibodies, but no such antibodies have ever been identified. Ammonium groups present in all NMBAs, which allow them to compete with acetylcholine for the binding to acetylcholine receptor, is hypothesized to represent the main allergenic epitopes. Herein, we engrafted rocuronium onto carrier proteins allowing immunization of mice against rocuronium, screening for rocuronium-specific antibody responses, and sorting of rocuronium-specific plasma cells using droplet microfluidics coupled to single-cell antibody gene (VH and VL) sequencing. The two >500 VH-VL paired repertoires we characterized were oligoclonal, comprised of three major clonal families, and displayed convergence. Expressed as human IgG1, these antibodies demonstrated subnanomolar affinities for rocuronium with families either monospecific for rocuronium or cross-reactive only for closely-related NMBAs. Expressed as human IgE, they triggered human mast cell and basophil activation, and severe passive systemic anaphylaxis in mice humanized for the IgE receptor FcεRI. Co-crystal structures between rocuronium and antibody representatives of three different VH-VL families revealed distinct interaction modes with, however, the ammonium group involved systematically in the binding interface. This work identifies the epitopes of antibody reactivity to rocuronium, demonstrates anaphylactogenic potential of anti-rocuronium IgE and establishes the first mouse model of NMBA anaphylaxis.

INTRODUCTION

Neuromuscular Blocking agents (NMBAs) are used in the clinic to paralyze skeletal muscles during surgery conducted under general anesthesia[1, 2]. They help assist airway management in elective or urgent anesthesia by facilitating endotracheal intubation. NMBAs possess two tertiary and/or quaternary substituted ammonium groups at physiological pH that enable them to compete at the neuromuscular junction with the quaternary ammonium group of acetylcholine for binding to muscle-type nicotinic receptors[3].

The most dramatic adverse event following NMBA exposure is anaphylaxis, the severest form of allergic reactions that can lead to death[4, 5]. In some countries, half of perioperative anaphylaxis is caused by NMBAs with a global mortality rate of 4.1%[6]. The current dogma proposes that allergen-specific IgE antibodies, including anti-NMBA IgEs, lead to mast cell and basophil activation in allergen-sensitized patients[7]. We reported earlier that, indeed, circulating anti-NMBA IgE levels, but also anti-NMBA IgG levels, correlate with the severity of anaphylaxis[8]. In our view, two antibody-dependent pathways are involved in NMBA-induced anaphylaxis: the IgE pathway leading to mast cell and basophil activation with histamine release as a major mediator, and the IgG pathway leading to neutrophil and monocyte activation with Platelet-activating Factor (PAF) release as a main mediator[7]. Both histamine and PAF induce vasodilation, bronchoconstriction, cardiac and pulmonary failure, with probable cumulative or potentiating effects when both mediators are released. The current treatment relies on adrenaline administration to induce vasoconstriction and bronchodilation, and also antihistamines administered mainly as a safety measure as these are not efficient at controlling anaphylactic shock[9]. Intriguingly, the non-depolarizing aminosteroid NMBA rocuronium can be captured within minutes by the cyclodextrin Sugammadex to reverse neuromuscular blockade in patients, leading in a few cases to amelioration of anaphylactic severity[10, 11].

The tertiary and quaternary substituted ammonium groups present in NMBAs have been proposed to be part of the epitope recognized by anti-NMBA antibodies in patients, as patient sera reacting with one or several NMBAs[12] cross-react with unrelated molecules possessing a quaternary ammonium[13, 14]. Since anti-NMBA mAbs have never been reported, neither from

patients nor animals, molecular or structural evidence is lacking to confirm these hypotheses. Adding complications to the understanding of the allergenic epitope, different conformer species can coexist. Indeed, rocuronium ring A can adopt a chair or a twist-boat conformation[15], with the twist-boat conformation being favorable for the accommodation of rocuronium within the cyclodextrin sugammadex[16].

Importantly, anaphylaxis occurs at the first exposure to aminosteroid NMBAs in half of the patients[17], excluding NMBAs as primary sensitizing epitopes in these patients' history. In addition, NMBAs are small (Molecular Weight ≈ 300-1,000 Da) and non-immunogenic. Several families of compounds are however considered to sensitize towards NMBAs, including cough syrups containing pholcodine (morphine-based compound), cosmetics, cleaning and bleaching products[12, 18-20]. Routinely, anti-NMBA IgEs are quantified using a surrogate for NMBA in ImmunoCAP™ detection: a morphine group termed Quaternary Ammonium Molecule (QAM) that resembles core structures of aminosteroid NMBAs[21, 22]. Large variations in serum reactivity profiles to NMBAs are found between individuals, from a single NMBA to NMBAs belonging to the same chemical family, and even to all NMBAs in 4% of the cases[12]. This suggests B cell responses with one or multiple monospecificities each toward a particular compound, and/or cross-reactive B cell responses towards different NMBAs. Understanding the reason for mono-or cross-reactivity in patients would require analyzing their antibody repertoire and study representative antibodies to determine if cross-reactive mAbs do exist in patients, or rather a collection of monospecific mAbs targeting different NMBAs. The antibody repertoire is classically studied from circulating memory B cells[23, 24], but can also be defined from tissue-resident plasma cells that are proposed to harbor the highest affinity antibodies[25-28].

Rocuronium represents an advantageous study model of NMBA anaphylaxis as it has among the highest anaphylaxis incidences[5, 29-31] and is widely used. In addition, rocuronium advantageously possesses a hydroxyl group that can be targeted chemically to allow engraftment on larger molecules for immunization or assay development. In this study, we analyzed the rocuronium-specific antibody repertoires from plasma cells of rocuronium-immunized mice using single cell droplet-based microfluidic technologies[25]. Affinities for rocuronium were in the subnanomolar to nanomolar range with either monospecificity for rocuronium or crossreactivity

only to closely related aminosteroid NMBAs that could be explained by crystallographic structures. Anti-rocuronium antibodies were anaphylactogenic when expressed as human IgE *in vitro* and *in vivo* in mice. Identification of anti-rocuronium mAbs allowed to develop the first mouse model of rocuronium anaphylaxis.

RESULTS

Anti-rocuronium antibody repertoires in mice are oligoclonal.

To generate the first anti-rocuronium mAbs, we decided to immunize mice against rocuronium and to use rocuronium-specific plasma cells as a source of the highest affinity mAbs[32, 33]. Since rocuronium is non-immunogenic, we immunized mice with rocuronium coupled to keyhole limpet hemocyanin (KLH), as a large carrier protein that favors bystander activation. Cervical lymph nodes were collected from two mice displaying the highest anti-rocuronium titer (Fig. 1A), and their cells were encapsulated into microfluidic droplets with fluorescent bioassay reagents and magnetic beads coated with an anti-mouse kappa light chain (Igκ) nanobody (VHH) (Fig. 1B). Immediately after droplet generation, these were subjected to a magnetic field that induced magnetic beads within each droplet to form a line (beadline) (Fig. 1C) and serve as a physical surface for a double-fluorescent sandwich ELISA, revealing IgG secretion from the cell using Alexa Fluor 647-labeled Fc-specific anti-mouse IgG, and specificity of that IgG for rocuronium using Alexa Fluor 488-labeled rocuronium-coupled HSA (Sup. Fig.1-2). The spatial distribution of fluorescence in the droplets was analyzed by re-injecting them into a second microfluidic chip where each droplet was scanned with superimposed laser lines and epifluorescence was detected using photomultiplier tubes. Secreted IgG and antigen binding were determined from red and green fluorescence localization to the beadline, respectively, and droplets that contained a cell of interest were sorted by fluorescence-activated dielectrophoretic sorting: 2,000 and 1,000 droplets that contained secreted IgG with detectable binding to HSA-rocuronium were sorted from lymph node cells of Mouse1 and Mouse2, respectively. Single cell barcoded-RNA sequencing followed immediately after (Fig. 1D) to retrieve the sequences encoding the variable heavy (VH) and light (VL) chains of the IgG secreted by the sorted plasma cell, as we reported earlier[25]. Sequencing data were processed computationally to identify cell-specific barcodes and to identify cognate VH–VL pairs (one pair per barcode, selecting the most probable VH and VL pair) and were corrected for errors introduced by PCR or sequencing by creation of consensus sequences[25].

Using the *repertoire-profiler* bioinformatic pipeline (refer to the Methods section)[34], we established the anti-rocuronium antibody repertoire profile of the two immunized mice. We obtained a total of 628 VH and VL pairs from Mouse1 and 421 VH and VL pairs from Mouse2. Analyses of V(D)J gene usage demonstrated an oligoclonal antibody repertoire profile for both mice. Indeed, for Mouse1, two V_HJ_H-V_LJ_L rearrangements encoded >92% of all the VH-VL pairs, with VH1-7_J2/VK2-112_J2 representing 48% and VH1-55_J2/VK4-68_J5 representing 44% of all VH-VL pairs. Strikingly, the latter rearrangement also represented 26% of all VH-VL pairs for Mouse2 (Fig. 1E). Clonal groups were defined as at least three distinct VH-VL pairs with identical VJ gene rearrangement and identical CDR3 length, leading to two VH clonal groups and two VL clonal groups for Mouse1, and 4 VH clonal groups and 15 VL clonal groups for Mouse2. The V1-55_J2 rearrangement represented 33% and 74% of the VH clonal groups, and the V4-68_J5 rearrangement 65% and 51% of the VL clonal groups of Mouse1 and Mouse2, respectively (Fig. 1F). Circos plot representation of the VH-VL pairing highlights these clonal groups among the total repertoire, with a given V_HJ_H rearrangement pairing systematically with a given V_LJ_L rearrangement, with a few exceptions (Fig. 1G). For each VH clonal group, a phylogenic analysis of the VH amino acid sequence was performed, and 15 and 13 VH-VL pairs from the major clonotypes of Mouse1 and Mouse2, respectively, were selected (Supp. Fig. 3A-D) and expressed as chimeric human IgG1,κ for further characterization and validation as anti-rocuronium mAbs.

Anti-rocuronium mAbs interact with rocuronium at high affinity.

Using ELISA, we confirmed that 11 out of 15 (73%) and 7 out of 13 (54%) of mAbs selected from Mouse1 and Mouse2, respectively (Fig. 2A, Supp. Fig. 4, Table 1) bound HSA-rocuronium. No mAbs among IP6 (V1-75_J3), IP13 (V1-62-2/71_J2), IP14 (V1-85_J2), IP15 (V3-8/3_J3) from Mouse1, and IP28 and IP29 (V3-6_J3), IP30 and IP31 (HV1-18_J2), IP32 (HV1-26_J3) and IP33 (HV1-39_J1) from Mouse2 bound HSA-rocuronium, suggesting that these VH-VL pairs rather bound fluorophores used for cell sorting. To ensure that the other 18 mAbs bound rocuronium and not the linker used to engraft rocuronium onto HSA, we performed competition ELISA in the presence of free NMBA molecule. These demonstrated exquisite specificity for rocuronium of 9

of these mAbs (IP7, IP8, IP9, IP10, IP12, IP21, IP22, IP23). Indeed, only free rocuronium, but not free molecules with the same aminosteroid scaffold *i.e.*, the closely-related homologues vecuronium and pancuronium, NMBAs atracurium and cisatracurium, nor 5α-dihydrotestosterone and diisiopentyl succinate that lack quaternary ammonium groups, could inhibit their interaction with HSA-rocuronium. mAbs IP5, IP11, IP24 and IP25 cross-reacted to rocuronium and vecuronium, whereas mAbs IP1, IP2, IP3 and IP4 cross-reacted to rocuronium, vecuronium and pancuronium. Estimated IC50s of these cross-reactions indicated 100- to 1,000-fold better affinities for rocuronium than for vecuronium and pancuronium, respectively (Fig. 2B, Table 1 and Supp. Fig. 4). However, IP26 and IP27 (V3-6_J3) from Mouse2 neither bound free rocuronium not HSA itself, but rather the linker used to couple rocuronium to HSA, or a neoepitope created by this chemical modification. Thus, competitive inhibition ELISA confirmed that only 11 out of 15 (73%) and 5 out of 13 (38%) of mAbs selected initially from Mouse1 and Mouse2, respectively (Table 1), bound free rocuronium. Identification of these confirmed anti-rocuronium mAbs allowed us to reanalyze the antibody repertoires by only considering the clonal groups those VH or VL rearrangement corresponds to a V_HJ_H or V_LJ_L used in a mAb confirmed to bind free rocuronium. These "functional" repertoires were reduced to 3 VH and 2 VL rearrangements for Mouse1 and a single VH and VL rearrangement for Mouse2 (Supp. Fig. 6A-B), with a mutational load compared to germline showing gaussian distributions for Mouse1 and Mouse2 with an average of ~5-7 nucleotide mutations in the VH and ~3-5 in the VL (Supp. Fig. 6C). These functional repertoires highlight unequivocally the preferential pairing of HV1-55_J2 with KV4-68_J5, and of both HV1-7_J2 and HV1-81_J2 with KV2-112_J2, with only rare exceptions like IP11 i.e., HV1-81_J2 paired with KV4-68_J5. Even if both mice generated large numbers of HV1-55_J2 encoded sequences that almost exclusively paired to KV4-68_J5, suggestive of a public VH repertoire (identical rearrangements with similar/identical CDR3 size and sequence), CDR sequences diverged largely between the plasma cells from the two mice and clustered separately (Supp. Fig.3 E).

As a first exploration of the interaction of these 16 mAbs with rocuronium, we used Bio-layer interferometry (BLI) to measure their avidity towards rocuronium haptenized to HSA with

an average molar ratio of 15:1. The avidity of these mAbs were very high towards rocuronium-HSA and ranged from 10 pM to 1.5 nM, except for mAb IP12 at 220 nM. The very small size of rocuronium (530 Da) is incompatible with the relatively poor sensitivity of BLI but remains inside the lower limit of detection for Surface Plasmon Resonance (SPR). SPR thus allowed to measure the affinity (K_D) between immobilized mAbs and free rocuronium in solution ranging from 1.2 to 56 nM for all mAbs except mAb IP12 that exhibited a poor K_D of 1.9 mM, in a transitory mode with a very fast association and dissociation (Fig. 2C and Table 1 and Supp. Fig. 5).

Anti-rocuronium mAbs interact differently with rocuronium.

Rocuronium ring A exists in two different conformations, chair or twist-boat[15] (Fig. 3A), with the sterically less demanding twist-boat conformation being favorable for its accommodation within sugammadex[16]. We thus wondered (i) if anti-rocuronium mAbs would also bind preferentially to one of these conformations, (ii) if the ammonium groups of rocuronium would be essential for the binding as suggested earlier[13, 14], and (iii) if differences in binding modalities existed among the collection of mAbs we identified. We thus performed crystallographic studies with either Fab fragments or single-chain variable fragments (ScFv) of representative mAbs from different clonal groups: IP2 (V1-55_J2 KV4-68_KJ5), IP8 (V1-7_J2_KV2-112_KJ2) and IP11 (V1-81_J2 KV2-112_KJ2) representing the three clonal groups of Mouse1 and the clonal group of Mouse2, and mAbs cross-binding rocuronium and vecuronium (IP2, IP11) and a mAb with exclusive binding to rocuronium (IP8). These antibody fragments and rocuronium co-crystalized efficiently and we solved the structure of Fab-IP2, Fab-IP8, and ScFv-IP11 complexed with rocuronium, respectively, at 2.4Å, 1.7 Å, and 1.2 Å resolution. (Fig. 3B-D, Table 2).

In the co-crystal structure of Fab-IP8 (Fig. 3B), the antibody VH and VL form a pocket inside of which the androstane component of rocuronium binds flat, the hydroxyl group is exposed to the solvent, and the acetoxyl group is buried inside the binding pocket. The specificity for rocuronium and not vecuronium or pancuronium could be explained by the fact that no space remained in the hydrophobic pocket formed by the VH and the VL to accommodate the

methylpiperidinium substituent of vecuronium and pancuronium, and by hydrophobic contacts made by the allyl group of rocuronium.

In the Fab-IP2 complex, rocuronium interacts differently with VH and VL compared to Fab-IP8 *i.e.*, like an arrow in a target (Fig. 3C). The quaternary ammonium and allylpyrrolidinium groups are completely buried in the binding pocket, but the morpholino with the hydroxyl group is exposed to the solvent. This allows vecuronium and pancuronium to bind as their methylpiperidinium substituent is outside the binding pocket and exposed to the solvent.

ScFv-IP11 bound similarly to rocuronium as Fab-IP8, but the binding of rocuronium induced a rearrangement of the binding site. The androstane moiety is stacked between VH residues Trp98 and Tyr56, but unlike IP2 and IP8, the hydroxyl group makes a hydrogen bond with VH Ser54 (Fig. 3D). Interestingly, the stacking interaction with Trp98-H and hydrogen bond with Ser54-H appear to sequester rocuronium in the binding site (Fig. 3E).

Of note, the hydroxyl group, which served as the attachment point to the rocuronium-carrier proteins used herein for immunization and screening is not involved in the binding, whereas the acetoxyl group is buried inside the binding pocket of all three antibodies. Importantly these co-crystal structures revealed that the allylpyrrolidine substituent containing the quaternary ammonium is completely buried and makes numerous van der Waals contacts with the antibody light chain (Fig. 3B-D), emphasizing the important role of this group in the rocuronium binding mode, in agreement with hypotheses extrapolated from serum cross-reactivity in patients[12, 35]. These data demonstrate that IP2, IP8 and IP11 complexes with rocuronium display an essential role of the quaternary ammonium group for the interaction with antibodies, in a twist-boat conformation, with the hydroxyl group O-atom (rocuronium twist-boat) making a hydrogen bond with Ser54H if the VH of IP11. The rocuronium conformation observed in these structures may be due to induced fit, as described for rocuronium-cyclodextrin complexes[16].

Anti-rocuronium mAbs allow to model rocuronium anaphylaxis *in vivo*.

Next, we wondered if anti-rocuronium mAbs expressed as human IgEs could sensitize and promote human mast cell and basophil activation in the presence of rocuronium. Human mast

cells and basophils express the high-affinity IgE receptor FcεRI that allows them to be sensitized (pre-armed) with IgE *in vivo* for immediate cell activation following IgE engagement with allergens, leading to rapid anaphylactogenic mediator release. Human mast cells derived from PBMCs of healthy donors were used to develop a Mast cell Activation Test (MAT), and whole blood from healthy donors to develop a Basophil Activation Test (BAT) (Fig. 4A). Mast cells sensitized with IP2, IP8 or IP11 human IgEs degranulated in the presence of HSA-rocuronium but not in the presence of HSA alone. IP12 human IgE weakly degranulated mast cells and only at elevated doses of HSA-rocuronium, as expected from IP12's poor affinity for rocuronium (Fig. 4B). Similarly, basophils sensitized with IP2, IP8 or IP11, but not IP12, human IgEs became dose-dependently activated in the presence of HSA-rocuronium (Fig. 4C). Because we previously reported that NMBA anaphylaxis in humans can engage an IgE pathway but also an IgG pathway leading to neutrophil activation by IgG receptors (FcγR)[8], we investigated neutrophil activation by immune complexes made of anti-rocuronium human IgG mAbs and HSA-rocuronium. Neutrophils from healthy donors expressed higher levels of CD11b and lower levels of CD62L when stimulated with immune complexes made of anti-rocuronium human IgG1, but not their effector-less variants (N_{297}A mutation of the IgG1 heavy chain), and HSA-rocuronium (Fig. 4D).

To test the anaphylactogenic potential of IP2, IP8, IP11 and IP12 human IgEs *in vivo*, we used mice expressing human FcεRI, sensitized them with anti-rocuronium IgEs and challenged them with HSA-rocuronium in a classical model of passive systemic anaphylaxis. Mice sensitized with 5 μg of human IgE formats of IP2, IP8 or IP11, but not IP12 nor unsensitized mice, and challenged with 2 μg HSA-rocuronium displayed a pronounced drop in central body temperature (Fig. 5A-C), a hallmark of anaphylaxis in mice[36]. Thus, although identified from IgG-secreting plasma cells or plasmablasts, the IP2, IP8 and IP11 VH-VL rearrangements generate rocuronium-specific antibodies of high affinity that demonstrate potential as human IgE for human mast cell and basophil activation *in vitro* and induction of anaphylaxis *in vivo* in mice humanized for FcεRI. To induce passive systemic anaphylaxis with the low-affinity anti-rocuronium IP12 human IgE, it was necessary to increase sensitization 8-fold (40 μg IP12 hIgE) in two separate injections to favor hIgE biodistribution [37] and antigen dose 70-fold (140 μg) (Fig. 5D).

DISCUSSION

In this work, we selected rocuronium, one of the most widely used NMBA, to investigate the rocuronium-specific antibody response in immunized mice and devise the first mouse model of rocuronium anaphylaxis. A cutting-edge high-throughput microfluidic droplet sorting system[25] allowed for the identification of hundreds of rocuronium-specific antibodies from immunized mice. These antibodies were derived from limited V(D)J-VJ rearrangements and showed convergence between the two immunized mice. The representative antibodies from different rearrangements show high avidity and affinity for rocuronium, and for some examples also crossreactivity to rocuronium chemical family members vecuronium and pancuronium, but not any other NMBA. Co-crystal structures revealed different binding modes of rocuronium by these mAbs, with the ammonium group of rocuronium always involved in the binding. Expressed as human IgE or IgG1 antibodies and aggregated by rocuronium, these antibodies demonstrated *in vitro* efficacy to activate human mast cells, basophils and neutrophils, respectively. Passively transferred to mice expressing human IgE receptors FcεRI, high- and low-affinity anti-rocuronium IgE antibodies sensitized mice that developed systemic anaphylaxis upon injection of rocuronium coupled to HSA.

NMBA are small molecules of less than 1 kDa (rocuronium: 530 Da). The antibody repertoire against low molecular weight drugs (<1 kDa) has never been investigated which may be due to the technical difficulty in identifying the scarce drug-specific B cells elicited by poorly or non-immunogenic small compounds. The classical method for generating antibody repertoires relies on the sorting of antigen-specific memory B cells from PBMCs that bound enough fluorescently labeled antigen monomers or multimers through their surface BCR. Low molecular weight compounds may not be ideal antigens for this “bait” approach and may require high levels of BCR to be sufficiently bound to enable flow cytometric detection. Here we used for B cell screening and sorting plasma cells and plasmablasts from draining lymph nodes that secrete high amounts of IgG, and a bioassay setup and duration that allows accumulation of these IgG onto a physical surface before detection and sorting. Even if we obtained several hundred VH-VL pairs of potential anti-rocuronium mAbs using this approach, we cannot compare it to standard methods

for this type of small drug as no other repertoire is currently available. However, by expressing representative VH-VL pairs from the clonal families of these repertoires and considering only those families with confirmed members binding to free rocuronium, we predict that this method allowed to obtain ~700 potential anti-rocuronium mAbs from two immunized mice (Supp. Fig. 6). The same method applied to large, highly immunogenic, protein antigens demonstrated earlier that from 150 to 530 mAbs could be identified from a single immunized mouse[25].

Bioinformatic analyses of the initial VH-VL repertoires identified only two major VH-VL rearrangements from both mice, with one (VH1-55_J2/KV4-68_J5) shared between the two mice. Further analyses on representative VH-VL pairs expressed as IgG mAbs and extrapolations thereof demonstrated that only these two clonal families (VH1-7_J2 and VH1-55_J2) and the VH1-81_J2 family represented the functional anti-rocuronium repertoire from these immunized mice. These three families represented >90% of the VH-VL sequences of Mouse1 but only 25% of the VH-VL sequences of Mouse2. This might be a consequence of the low cell number sorted from Mouse2 that may have led to higher "noise" in the Illumina sequencing. In both cases, however, the functional repertoires were oligoclonal and monoclonal, respectively, which might be a consequence of (i) the small size of rocuronium, (ii) the restricted number of mouse germline VH-VL sequence able to bind this drug, and/or (iii) the effect of the linker attached to the hydroxyl group of rocuronium that may restrict even more the number of these germline sequences. The mono/oligoclonal nature of the repertoire is not due to the cell population (plasma cells and plasmablasts) chosen or to the droplet microfluidic method used, as we previously reported several highly diverse repertoires of IgG-secreting plasma cells against tetanus toxoid, glucose-6-phosphate isomerase or Tetraspanin-8 covering multiple V-gene families[25]. The mono/oligoclonal nature of the anti-rocuronium repertoires is thus due to the antigen size and nature rather than to the method used to identify these repertoires.

A strong rearrangement convergence was observed between the two mouse repertoires in this study. Convergent (or public) clonotypes (identical rearrangements with similar/identical CDR3 size and sequence) in unrelated individuals with viral infection or vaccination has been reported in particular for IGK and IGL due to the lack of combination diversity and junction diversity during light chain rearrangement[38, 39], but less so for IGH[40, 41]. These public VLs were able to pair with diverse VHs in multiple donors[42]. In our work, two V_LJ_L rearrangements (KV2-112_J2 and KV4-68_J5) paired with over 90% of VH sequences in the two mice analyzed. With

only a few exceptions, HV1-55_J2 paired with KV4-68_J5 and HV1-7_J2 paired with KV2-112_J2 (Fig.1G). For the HV1-81_J2 clonal group, we expressed two mAbs that shared the same VH rearrangement with identical CDRH1 and CDRH3, and only 2 amino acid mutations in the CDRH2, one mAb with light chain KV2-112_J2 (IP11) and one mAb with light chain KV4-68_J5 (IP12): these demonstrated a ~35,000-fold difference in affinity for rocuronium in favor of IP11. Due to the barcoding method used (split-and-pool synthesis) in the single cell sequencing method and the probabilistic pairing of the most abundant VH and VL associated to a given barcode, we wondered if IP12 was not the consequence of a VH-VL mispairing that led to the recombinant expression of this antibody, whereas it should have been paired with a more "favorable" light chain for this heavy chain rearrangement i.e., KV2-112_J2. Indeed, when we expressed the VH of IP11 with the VL of IP12, the avidity for HSA-rocuronium was equivalent to that of IP12 and when we expressed the VH of IP12 with the VL of IP11 the avidity was equivalent to that of IP11 (data not shown). The less common VL pairings to VH found in these repertoires may therefore mostly/all result in lower affinity antibodies, and one could propose to choose in the probability ranking the first "favorable VL i.e., a KV4-68_J5 VL for a V1-55_J2 or a V1-7_J2 VH and a KV2-112_J2 VL for a V1-81_J2 VH. This method may result in ameliorating affinity for rocuronium, but would reduce the diversity in these repertoires by excluding other light chain rearrangements. A previous study indicated that nitrophenyl (NP), a commonly used hapten of less than half the size of rocuronium, induced convergent and oligoclonal antibody responses in different mice centered on one heavy chain V(D)J rearrangement[43, 44]. The fact that the proportion of public clonotypes in mice has been reported to be much higher compared to humans[45, 46] may explain these observations for the hapten NP and our observations for rocuronium.

All the randomly selected VH-VL pairs representative of each clonal family demonstrated high avidity (0.01 nM to 1.2 nM) towards rocuronium coupled to HSA, except IP12 (220 nM; refer to previous paragraph). These results are in agreement with the values we obtained for mouse antibodies against tetanus toxoid or glucose-6-phosphate isomerase we described using the same technological approach and focusing on plasma cells and plasmablasts[25]; thus, the selectivity towards high affinity antibodies can be a consequence of the cell population chosen or the stringency of the bioassay and detection/sorting thereof. However, the same droplet bioassay was used to describe – without sorting – affinity repertoires of circulating plasmablasts after SARS-CoV-2 vaccination in humans[47], or tissue plasma cells and circulating plasmablasts in chronic

immune thrombocytopenia patients[27] or in mice immunized with tetanus toxoid[48], and revealed that low-affinity antibody secreting cells represented >90% of plasma cells and plasmablasts. The high-affinity repertoires we identified herein are thus most probably due to the stringency of the microfluidic sorting used. These high-affinity avidities translated into nanomolar affinities for free rocuronium (1-56 nM) with monospecific anti-rocuronium mAbs IP8, IP11 and IP24 at 1 nM, 56 nM and 12 nM, respectively, and cross-reactive anti-rocuronium/vecuronium/pancuronium mAb IP2 at 3.9 nM. Cross-reactivity among these aminosteroid NMBAs thus does not imply lower affinity.

The ability of mAbs either to bind specifically rocuronium or to cross-bind vecuronium and pancuronium was explained by the three co-crystal structures of antibody fragments of IP2, IP8 and IP11 in complex with rocuronium that we reported herein. These three different structures represent the binding mode of one representative of each VH family V1-55_J2, V1-7_J2 and V1-81_J2 and all reveal that both VH and VL of each mAb are involved in the binding and that the allylpyrrolidinium substituent containing the quaternary ammonium of rocuronium is completely buried in the binding cleft of the antibodies. These first co-crystal structures of mAbs with rocuronium, even if these mAbs were raised in mice immunized with rocuronium, are thus in agreement with hypotheses extrapolated from serum cross-reactivity in patients suggesting that the ammonium group is part of the binding interaction with antibodies[12, 35]. In the same manner as in rocuronium-sugammadex complexes, rocuronium bound IP2, IP8 and IP11 in a twist-boat conformation which might be due to induced fit, as reported for rocuronium-sugammadex complexes[16] or by the selection among the two rocuronium conformers. Crossreactivity with vecuronium and pancuronium required that their extra side chains (compared to rocuronium) would remain outside the binding pocket and be exposed to the solvent. Cross-binding had already been reported decades ago for IgE antibodies in the serum of patients with NMBA hypersensitivity to alcuronium: their binding to alcuronium was inhibited strongly by tubocurarine, modestly by pancuronium and weakly by decamethonium and gallamine, and even less by succinylcholine[17]. If these types of cross-binding represent the property of a single mAb in each patient sera or that of different populations of antibodies within each serum that each recognize a different NMBA with little or no cross-reactivity with other NMBA remains unknown. Surprisingly however, the three co-crystal structures we report herein highlighted three different binding modalities for such a small antigen and such restricted repertoire with only 3 VHs and 2 VLs, with the two mAbs using the

same VL rearrangement KV2-112_J2 (IP2 and IP11) not binding in the same manner rocuronium. Whether our results are predictive of antibodies involved in NMBA hypersensitivity in humans remains to be clarified and human anti-rocuronium antibody repertoire to be explored.

This first description of anti-rocuronium mAbs allowed us to demonstrate their ability to induce cell activation when aggregated by rocuronium. As we reported earlier for NMBA hypersensitivity in humans, at least two activation pathways co-exist that lead to severe anaphylactic reaction to NMBAs, the IgE pathway leading to mast cell and basophil activation and the IgG pathway leading to neutrophil and platelet activation[49]. All the high-affinity anti-rocuronium mAbs expressed as human IgEs activated human mast cells and basophils *in vitro*, and expressed as human IgG1s activated neutrophils *in vitro*. Importantly, once passively transferred into mice expressing human IgE receptors, both high- and low-affinity anti-rocuronium IgE mAbs led to severe anaphylactic reactions *in vivo* upon exposure to haptenized rocuronium. Rocuronium is indeed devoid of neuromuscular blocking properties once haptenized onto a larger protein that cannot freely diffuse into the neuromuscular junction. This strategy allowed us to generate for the first time a model of rocuronium-induced anaphylaxis in mice and to follow anaphylaxis by central body temperature. More complex setups including anesthesia, intubation and artificial ventilation could be envisioned to model anaphylaxis, but these would require using other parameters than body temperature - that is uncontrolled during anesthesia - to monitor anaphylaxis. Free rocuronium could also be used instead of haptenized rocuronium, or larger animals like non-human primates to increase the relevance to human physiopathology.

This work could not have been performed without chemically modifying rocuronium which represents a limitation of this study. We used rocuronium derivatives by extending the OH group with a functionalized linker for grafting on carrier proteins KLH and HSA that were used for B cell sorting, ELISA, avidity measurements, and functional assays. This strategy allowed for identification of anti-rocuronium antibodies with no crossreactivity for NMBAs from other families outside aminosteroids, not even to dihydrotestosterone, the rocuronium mimetic devoid of ammonium groups. Validated by other groups, these anti-rocuronium IgE or IgG mAbs could be used as internal standards and references in routine assays like skin prick tests, basophil activation tests, or the more recently developed mast cell activation tests[50]. Another limitations is the use of rocuronium to immunize mice, whereas patients become sensitized in the vast majority without any exposure to rocuronium but to other ammonium-containing compounds present in cough syrup,

cosmetics, hair dyes, household cleaning products or drugs at the probable initiation of the immune reaction towards rocuronium[51].

In conclusion, this work reports on the underlying mechanisms of anaphylactic reactions to NMBAs by identifying the first anti-rocuronium antibody repertoires from immunized mice, suggests novel diagnostic tools for rocuronium hypersensitivity, and provides a proof-of-concept for modeling NMBA hypersensitivity *in vivo* in mice.

FIGURES

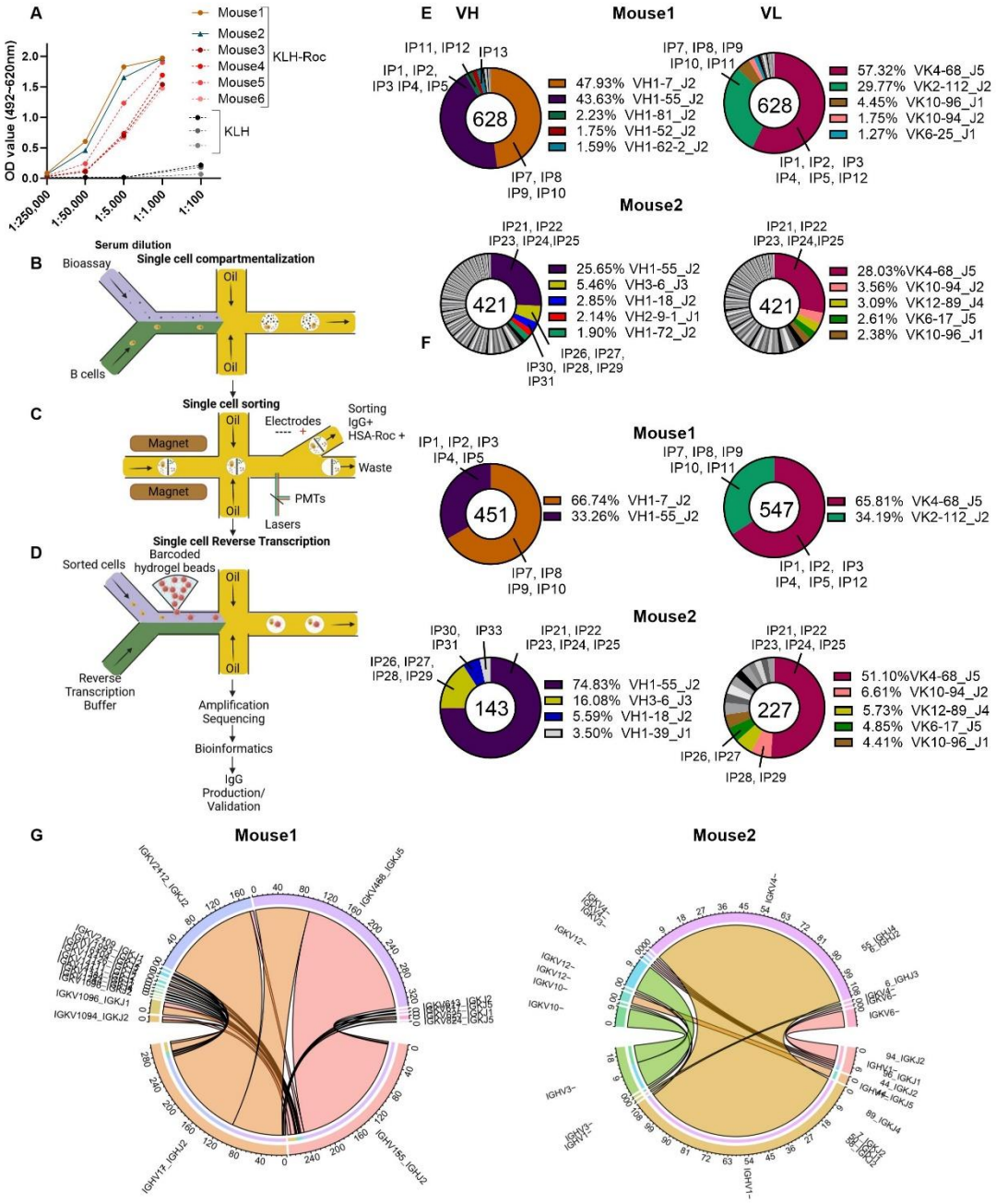

Figure 1. Generation of rocuronium-specific antibody repertoires from immunized mice. (**A**) IgG anti-rocuronium ELISA results from sera of mice immunized with KLH or KLH-rocuronium. (**B-D**) Schematic representation of droplet microfluidic steps: (**B**) droplet generation, (**C**) droplet sorting, (**D**) in-droplet single cell reverse transcription and barcoding. (**E**) Donut plots of the VJ gene usage among all the VH and VL identified from Mouse1 and Mouse2. VH-VL pairs corresponding to mAbs further characterized in this work are indicated (IP1-IP12 for Mouse1 and IP21-IP33 for Mouse2). The 5 most representative families are colored and labeled, the others are in shades of grey. (**F**) Donut plots representing only the clonal groups (identical VJ genes and CDR3 length) coding for the VH and VL of each mouse. (**G**) Circos plots of the pairing of VH clonal groups with their VL rearrangement.

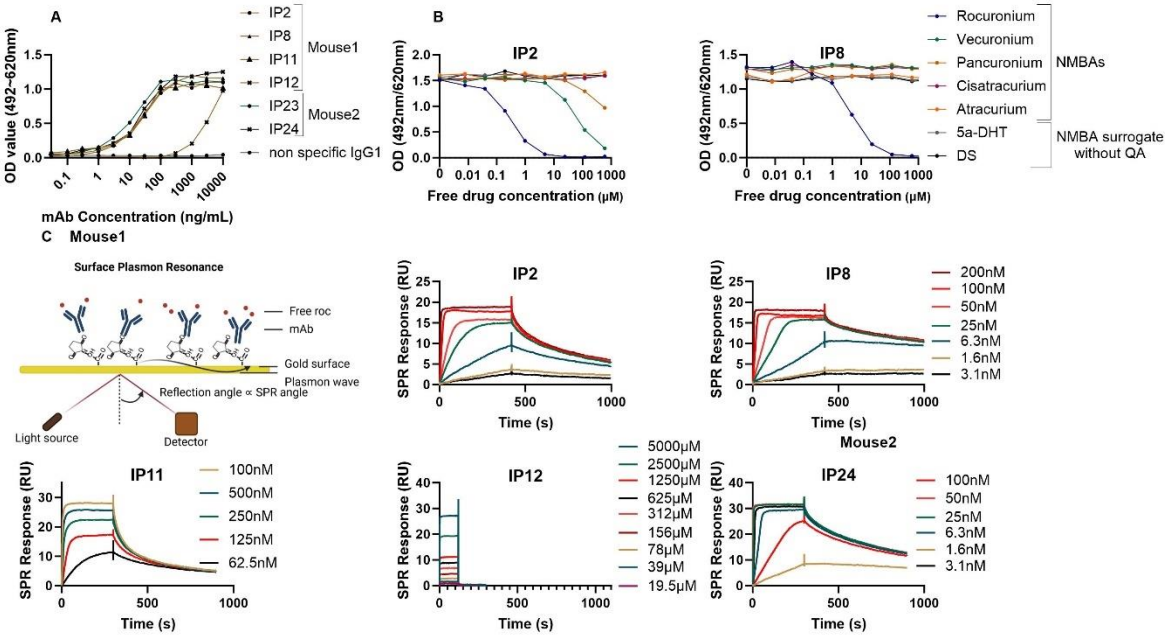

Figure 2: Characterization of roc-specific mAbs from immunized mice. (**A**) Roc-specific ELISA of representative mAbs from indicated mice. (**B**) "Competition ELISA" of anti-IgG rocuronium ELISA at fixed mouse mAbs concentration but increasing concentrations of indicated molecules free in solution. 5a-DHT: 5-alpha-Di-Hydro-Testosterone. DS: Diisiopentyl succinate. QA: Quaternary Ammonium. (**C**) Scheme of Surface Plasmon Resonance affinity measurements and results thereof for the interaction between immobilized mAbs and varying concentrations of free rocuronium in solution. The K_D was obtained by fitting the curves using a heterogenous ligand model.

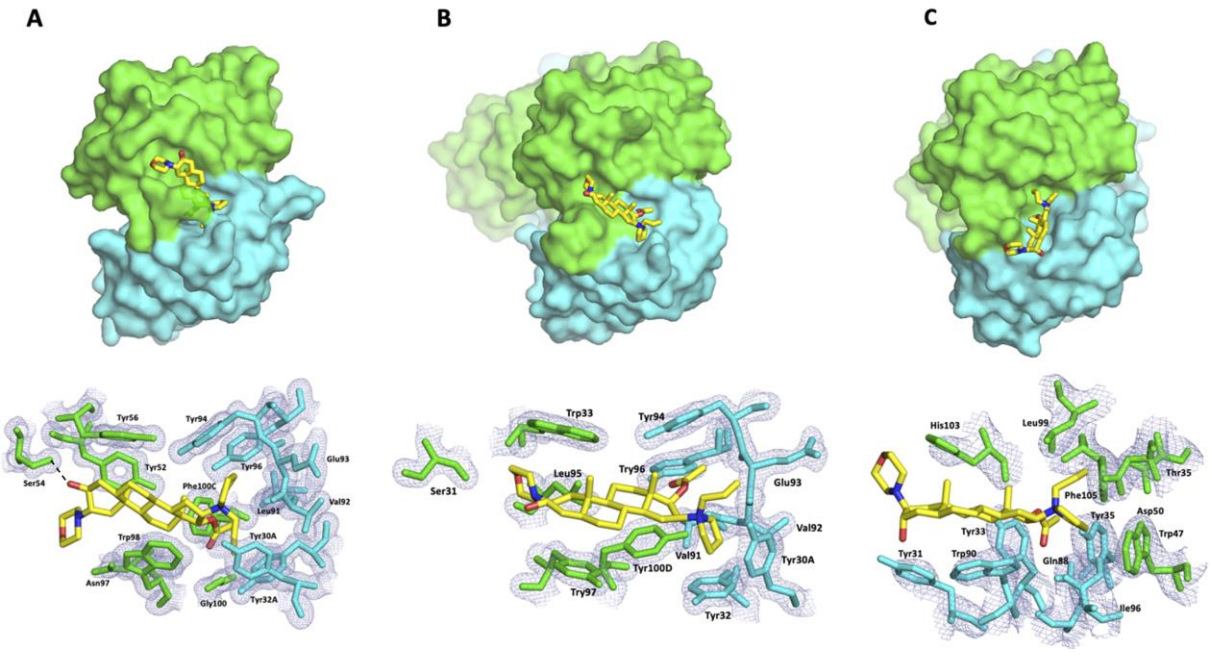

Figure 3: Crystal structures of mAbs in complex with rocuronium. Top: surface representation of co-crystal structures of rocuronium-specific scFv IP11 (A), Fab-IP8 (B) and Fab-IP2 (C). Bottom: superposition of the rocuronium and key residues of the binding site. The rocuronium molecule is shown in yellow and the antibody heavy chain and light chain are colored in green and cyan, respectively.

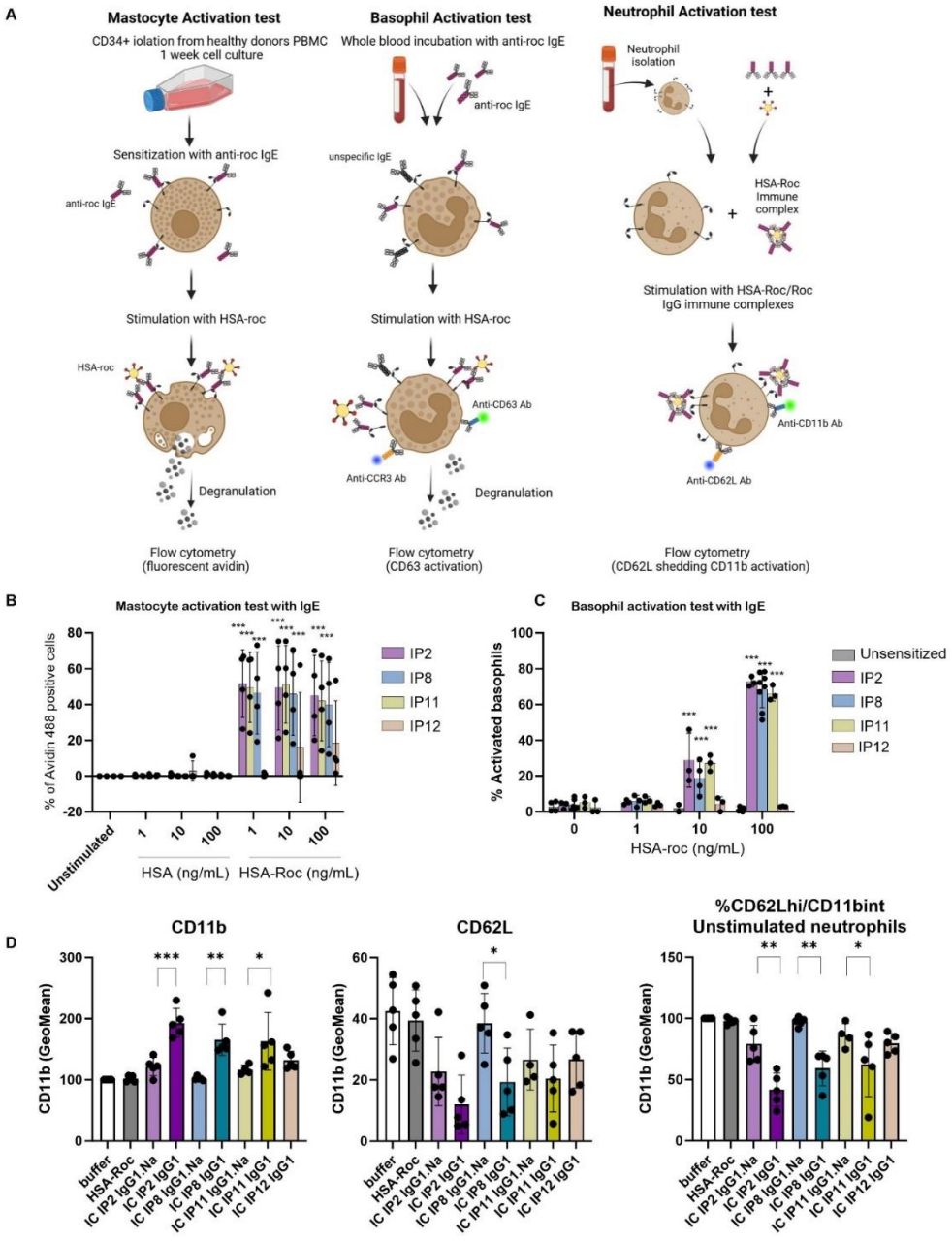

Figure 4: Anti-rocuronium mAbs activate human mast cells, basophils and neutrophils following aggregation by rocuronium. (**A**) Schematic representation of mastocyte and basophil activation tests. Briefly, chimeric IgE are pre-incubated either with *in vitro* cultured human mast cells or human basophils in whole blood, and incubated with HSA-rocuronium. Degranulation is assessed by flow cytometry. (**B**) Human mast cell and (**C**) human basophil activation test using hIgE for sensitization, followed by challenge with HSA or HSA-rocuronium, with degranulation measured using fluorescent avidin or anti-CD63 staining, respectively, (n≥3). Mean ± standard deviation of results from different donors are indicated. Each antibody was analyzed separately, comparing the contrast between HSA and HSA-rocuronium after mixed linear modeling and multiple-testing P-value adjustment. ***, P < 0.001; ns, not significant. (**D**) Human neutrophil activation test using preformed immune complexes (IC) made of anti-rocuronium hIgG and HSA-rocuronium, with activation measured using anti-CD11b or anti-CD62L staining (n≥4). Effector-less (heavy-chain $N_{297}A$ mutation) IgG antibodies were used as negative controls. Buffer condition is normalized to 100.

(n=5). Mean ± standard deviation of different human sampless are indicated. IgG1.Na was copared to IgG1 for each antibody, after 2-way anova modeling and multiple-testing P-value adjustment. ***, P < 0.001; ns, not significant. ***, P < 0.001; **, P < 0.01; *, P < 0.05.

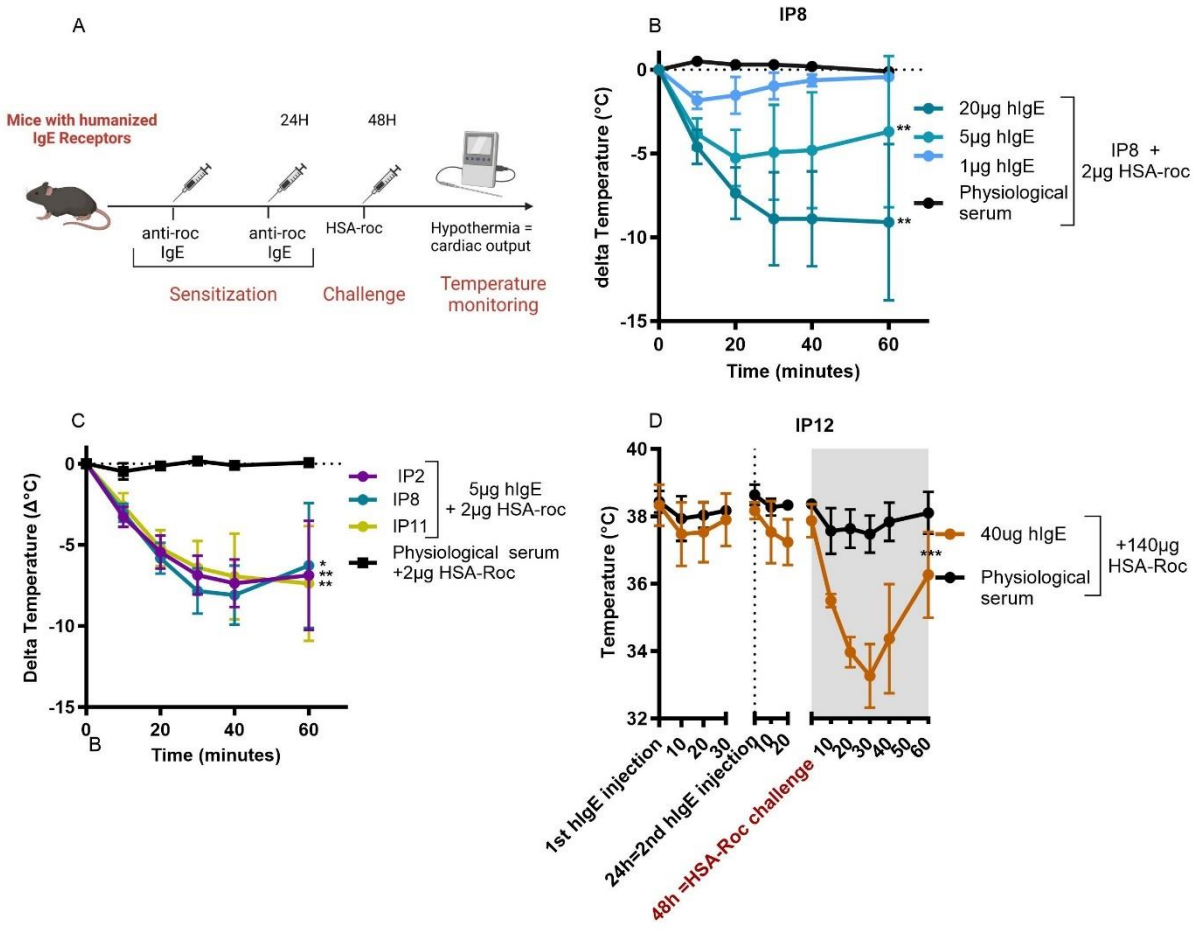

Figure 5: **Passive systemic anaphylaxis in mice using hIgE antibodies**. (**A**) Scheme of induction of passive systemic anaphylaxis in mice. (**B-D**) Passive systemic anaphylaxis measured by changes in body temperature (Δ°C) in hFcεRI-transgenic mice sensitized (**B**) once with hIgE IP8 at indicated doses (n=3), (**C**) once with hIgE IP2, IP8 or IP11 (n=6), (**D**) twice with hIgE IP12 at 24h interval (n=3), and challenged with HSA-roc intravenously 24h later. Mean ± standard deviation are indicated. Each of the three post injection effects were analyzed separately, comparing the contrast between hIgE IP12 and the control group after mixed linear modeling and multiple-testing P-value adjustment. P values are indicated at the end of each time period analyzed with **, P ≤ 0.01; ns, not significant. . ***, P < 0.001; **, P < 0.01; *, P < 0.05.

TABLES

Table 1: Characteristics of the mAbs expressed from repertoires of Mouse1 and Mouse2. Antibodies produced recombinantly were tested for binding to HSA-rocuronium by BLI (avidity), to free rocuronium by SPR (affinity), and to rocuronium (R), vecuronium (V) and pancuronium (P) by inhibition ELISA (specificity and IC50 values). Number of amino acid (aa) mutations (≠) compared to the germline sequence are indicated. nd, not determined; NB, not binding; nt, not tested; IC50, Half-maximal inhibitory concentration.

	mAb	VH gene	JH gene	VL gene	JL gene	KD to HSA-roc (nM)	KD to free roc (nM)	Spec.	IC50 Roc (µM)	IC50 Vec (µM)	IC50 Panc (µM)	VH aa ≠	VL aa ≠
Mouse1	**IP1**	V1-55	J2	KV4-68	KJ5	**0.9**	nd	R-V-P	**0.3**	**177**	**6,995**	3	5
	IP2	V1-55	J2	KV4-68	KJ5	**0.6**	**3.9**	R-V-P	**3.8**	**20**	**787**	3	4
	IP3	V1-55	J2	KV4-68	KJ5	**1.2**	nd	R-V-P	**1.3**	**110**	**737**	3	4
	IP4	V1-55	J2	KV4-68	KJ5	**0.9**	nd	R-V-P	**3.1**	**240**	**3,635**	7	3
	IP5	V1-55	J2	KV4-68	KJ5	**0.4**	nd	R-V	**289**	**615**	nt	6	3
	IP6	*V1-75*	*J3*	*KV6-25*	*KJ1*	*NB*	*nt*	*nt*	*nt*	*nt*	*nt*	*6*	*7*
	IP7	V1-7	J2	KV2-112	KJ2	**0.82**	nd	R	**4.4**	nt	nt	9	3
	IP8	V1-7	J2	KV2-112	KJ2	**0.46**	**1.0**	R	**3.3**	nt	nt	3	3
	IP9	V1-7	J2	KV2-112	KJ2	**0.8**	nd	R	**3.5**	nt	nt	4	2
	IP10	V1-7	J2	KV2-112	KJ2	**0.86**	nd	R-V	**5.0**	**442**	nt	8	5
	IP11	V1-81	J2	KV2-112	KJ2	**0.53**	**56**	R-V	**5.0**	**548**	nt	5	1
	IP12	V1-81	J2	KV4-68	KJ5	**220**	**1,990,000**	R	**2,572**	nt	nt	4	4
	IP13	*V1-62-2/71*	*J2*	*KV19-93*	*KJ2*	*NB*	*nt*	*nt*	*nt*	*nt*	*nt*	*5*	*7*
	IP14	*V1-85*	*J2*	*KV6-13*	*KJ2*	*NB*	*nt*	*nt*	*nt*	*nt*	*nt*	*9*	*7*
	IP15	*V3-8/3*	*J1*	*KV14-111*	*KJ1*	*NB*	*nt*	*nt*	*nt*	*nt*	*nt*	*5*	*8*
Mouse2	**IP21**	V1-55	J2	KV4-68	KJ5	**0.13**	nd	R	**26**	nt	nt	10	6
	IP22	V1-55	J2	KV4-68	KJ5	**0.2**	nd	R	**14**	nt	nt	6	1
	IP23	V1-55	J2	KV4-68	KJ5	nd	nd	R	**109**	nt	nt	9	8

	IP24	V1-55	J2	KV4-68	KJ5	**0.01**	**12**	R	**18**	nt	nt	6	1
	IP25	V1-55	J2	KV4-68	KJ5	nd	nd	R-V	**20**	**682**	nt	2	1
	IP26	*V3-6*	*J3*	*KV12-89*	*GKJ4*	*Binding linker (neoepitope)*						*3*	*0*
	IP27	*V3-6*	*J3*	*KV12-89*	*GKJ4*	*Binding linker (neoepitope)*						*7*	*1*
	IP28	*V3-6*	*J3*	*KV10-94*	*KJ2*	*NB*	*nt*	*nt*	*nt*	*nt*	*nt*	*3*	*4*
	IP29	*V3-6*	*J3*	*KV10-94*	*KJ2*	*NB*	*nt*	*nt*	*nt*	*nt*	*nt*	*6*	*4*
	IP30	*HV1-18*	*J2*	*KV6-17*	*KJ5*	*NB*	*nt*	*nt*	*nt*	*nt*	*nt*	*1*	*7*
	IP31	*HV1-18*	*J2*	*KV6-17*	*KJ5*	*NB*	*nt*	*nt*	*nt*	*nt*	*nt*	*4*	*10*
	IP32	*HV1-26*	*J3*	*KV12-46*	*J2*	*NB*	*nt*	*nt*	*nt*	*nt*	*nt*	*12*	*4*
	IP33	*HV1-39*	*J1*	*KV12-44*	*KJ2*	*NB*	*nt*	*nt*	*nt*	*nt*	*nt*	*5*	*3*

Table 2: Crystallization conditions, data collection and refinement statistics. Values in parentheses are for the highest resolution shell.

Crystal	Fab IP8 + Rocuronium	Fab IP2 + Rocuronium	ScFv IP11 + Rocuronium
Reservoir solution	60 % (w/v) MPD 0.01 M $CaCl_2$ 0.1 M Na Acetate pH 4.6	10 % (w/v) PEG 4K 5 %w/v 2-PropOH 0.1 M HEPES pH7.5	20 % (w/v) PEG 4K 10 % (v/v) 2-PropOH 0.1 M HEPES pH 7.5 pH
Protein concentration, mg/ml	5	12	10
Data collection			
Synchrotron beamline	PROXIMA 1	PROXIMA 2	PROXIMA 2
Space group	P21	P31211	P212121
Unit cell dimensions,			
a,b,c (Å)	56.5, 55.17, 76.89	131.56, 131.56, 95.16	50.89, 63.69, 80.61
a,b,c (°)	90, 104.87, 90	90, 90, 90	90, 90, 90
Resolution, Å	44.3-1.72 (1.76-1.72)	113.9-2.41 (2.78-2.43)	50.8-1.20 (1.22-1.20)
Rmerge	0.078 (1.202)	0.233 (0.977)	0.069 (0.864)
Rpim	0.029 (0.440)	0.087 (0.409)	0.029 (0.430)
Unique reflections	48808 (3369)	17378 (871)	81866 (3978)
<I/sigma(I)>	13.9 (1.5)	7.7 (2.0)	12.1 (1.8)
Mn(I) half-set correlation	0.999 (0.706)	0.994 (0.725)	0.998 (0.668)
Completeness, %	99.3 (94.1)	47.1 (6.9)	99.2 (97.8)
Multiplicity	8.5 (8.0)	8.1 (6.6)	7.2 (5.8)
Refinement			
Resolution, Å	39.4-1.72 (1.74-1.72)	113.9-2.41 (2.65-2.41)	50.0-1.20 (1.22-1.20)
No. of reflections	48623 (1756)	17 376 (395)	80214 (2945)
Rvalue, working set	0.163 (0.304)	0.211 (0.280)	0.183 (0.281)
Rfree	0.205 (0.310)	0.261 (0.488)	0.201 (0.285)
Non-hydrogen protein atoms	3782	3242	2123
No. of Waters	354	6	288
RMS deviations from ideal			
bond length, Å	0.010	0.009	0.007
bond angles, °	1.654	1.14	1.45
Ramachandran plot, %			
preferred regions	97.49	94.59	98.22
allowed regions	2.05	4.47	1.33
outliers	0.46	0.94	0.44

MATERIALS AND METHODS

Mice

C57BL/6J mice were purchased from Charles River, and used for experiments after maintaining the mice for at least one week in SPF conditions after arrival in Institut Pasteur's animal facility. Human FcεRI^{tg} mouse FcεRI$^{-/-}$ mice on the C57BL/6 background were described previously[52]. Mice were bred at Institut Pasteur and used for experiments at 7-12 weeks of age. All animal care and experimentation were conducted in compliance with the guidelines and specific approval of the Animal Ethics committee CETEA number 89 (Institut Pasteur, Paris, France) registered under #170043, #2013-0103 and #27465 and by the French Ministry of Research under agreement #00513.02.

Production and characterization of rocuronium bioconjugates

Hapten coupling to HSA or KLH were performed as reported earlier [8] using a rocuronium derivative with a carboxylic acid (Roc-COOH) at the 3-position of the steroid scaffold. The exact measurement of the concentration of the bioconjugates was achieved by quantitative amino acid analysis. The average density of conjugated rocuronium derivatives was evaluated by matrix-assisted laser desorption/ionization time-of-flight mass spectrometry. Rocuronium derivatives with different densities (1:10 and 1:32) were produced and for distinct reasons (Supp. Fig1). Conjugates with higher density were used for sorting experiments and conjugates with lower densities for characterization (ELISA and BLI).

Immunization of mice against rocuronium

Female C57Bl/6J were immunized subcutaneously with 10 μg KLH-rocuronium (or KLH only as control) combined with adjuvant alum 1:1 (v:v) and 20 ng pertussis toxin in physiological saline 0.9% NaCl for three times at 3-week intervals. Mice were boosted with 10 μg KLH-rocuronium without adjuvant three weeks after the last immunization. Four days later, the superficial cervical

lymph nodes were removed, and cells resuspended as single cells for immediate sorting using droplet microfluidics.

Plasma cell sorting using droplet microfluidics

Plasma cells and plasmablasts were sorted based on their secretion of IgG antibodies binding to HSA-rocuronium using methods and instruments as we reported earlier[25]. In brief, single cells from lymph nodes of immunized mice were encapsulated into microfluidic droplets with paramagnetic nanoparticles (Strep Plus, 300 nm, Ademtech) coated with biotinylated anti-mouse IgGκ V_HH, 75 nM rabbit $F(ab')_2$ anti-mouse IgG Fc-specific (AlexaFluor647-labeled, Jackson ImmunoResearch) and 50 nM HSA-rocuronium (purified monomer, AlexaFluor488-labeled). Under the influence of a magnetic field, the nanoparticles align into a beadline within each droplet[48] and are flown through a droplet sorting chip placed under a high-speed camera, lasers and PMTs. Relocation of both AlexaFluor647 and FITC fluorescence onto the beadline of one drop triggered sorting of these droplets by dielectrophoresis into a collection tube, followed by cell recovery, re-compartmentalized in droplets with single barcoded hydrogel beads and lysis and reverse transcription reagents using a microfluidic device for subsequent cell lysis and cDNA synthesis. The sequencing library was generated by two-step nested PCR with the barcoded cDNA. Final products were sequenced on an Illumina MiSeq (2x300 bp paired-end reads), which allowed sequencing of the entire VH and VL domain as well as the barcode sequence, as described[25]. A bioinformatics pipeline was developed to allow sequence read trimming, merging, barcode extraction and clustering, and antibody sequence characterization and filtering. Importantly, for all barcode clusters that contained productive VH and VL made up of at least 20 reads each, the most abundant VH and VL regions were considered to be paired.

Antibody repertoire analysis and representative mAb selection

Docker (https://www.docker.com) / Apptainer (https://apptainer.org), nextflow (https://www.nextflow.io) and git (https://about.gitlab.com) were used to better control

reproducibility aspects[53]. The Nextflow pipeline developed to analyze batches of nucleotide sequence fasta files, representing the raw single cell Sanger sequencing of the VH-VL IgG domains, is available at https://gitlab.pasteur.fr/gmillot/repertoire_profiler, and is detailed below. Most of the process is based on tools from the *immcantation portal* (https://immcantation.readthedocs.io/en/stable/), notably from the change-O toolset[34]. VH and VL sequences, while single cell paired, could only be analyzed independently (VH sequences, then VL sequences), as no method taking this parameter into account currently exists. First, the *AssignGenes.py igblast* tool was run to detect and annotate the V, D, J, CDR and FWR domains in each sequence, using the *imgt* database (https://www.imgt.org/). Then, *MakeDb.py igblast* converted the result into a readable tsv file. The *ParseDb.py select* tool kept productive sequences, *i.e.*, those for which: (1) the coding region has an open reading frame, (2) no defect are present in the start codon, splicing sites or regulatory elements, (3) no internal stop codons were found, and (4) junction regions are in frame. The clustering of sequences into clonal groups was performed as follows: (1) grouping of the sequences according to same V and J genes (allelic variation not considered) and same length of the CDR3, (2) for each group, computation of the distance score D = (Hamming distance) / (CDR3 length) between each 2 x 2 sequences, (3) determination of the D threshold, that determine whether 2 sequences derive from the same germline cell sequence or not, using the *distToNearest()* function of the *shazam* R package, (4) clone assignment for each sequence, *i.e.*, same ID for sequences belonging to a same clonal group, using the *DefineClones.py* tool. Of note: a few sequences could be lost at that stage, as they did not fit the criteria required by this tool. Then, the putative germline sequence of each clonal group was inferred using the *CreateGermlines.py* tool. Finally, a single *all_passed_seq.tsv* file was obtained for each batch of VH or VL initial fasta files, containing notably, for each sequence, the V, D, J gene and allelic names returned by the *AssignGenes.py igblast* tool, the clone ID, the putative germline sequence before somatic hypermutations, and the putative V, D, J gene and allelic names of the germline sequence returned by the *CreateGermlines.py* tool.

Donut plots were drawn after gathering the sequences of the all_passed_seq.tsv file according to the V and J gene and allelic names of their putative germline sequence. Amino acid sequence alignments and percentage identity calculations were performed with Jalview software using

MUltiple Sequence Comparison by Log- Expectation (Muscle) and colored by percentage identity. Number of mutations were obtained with IMGT database by comparing sequences with germlines and plotted as histograms using GraphPad Prism. The circos plot from Fig. 1G, has been obtained using the R package circlize (ref: https://academic.oup.com/bioinformatics/article/30/19/2811/2422259) and an input file merging the VH and VL all_passed_seq.tsv files from the repertoire_profiler pipeline.

Gene synthesis, cloning and mAbs production

VH and VL synthesis were performed by Synbio Technologies. VHs were cloned into pUC19 vectors containing the sequence encoding the constant regions of human IgG1 heavy-chain (CH), effector-less human IgG1 heavy-chain mutated $N_{297}A$, human IgE heavy-chain. VLs were cloned into pUC19 vectors containing the sequence encoding the constant regions (CL) of human kappa light-chain. Antibodies were produced by transient co-transfection of VH-CH and VL-CL expression plasmids into exponentially growing Freestyle™ HEK 293-F that were cultured in serum-free Freestyle™ 293 Expression Medium (Life Technologies) in suspension at 37°C in a humidified 8% CO_2 incubator on a shaker platform rotating at 110 rpm. Twenty-four hours before transfection, cells were harvested by centrifugation at 300 x g for 5 min and resuspended in expression medium at a density of 1 x 10^6 cells/ml, and cultured overnight in the same conditions as mentioned above. To produce mAbs, 40 µg of each VH and VL expressing plasmids were diluted in 80 µl of FectoPRO reagent (Polyplus) at a final DNA concentration of 0.8 µg/ml, incubated for 10 minutes at RT before addition to the cells. Twenty-four hours post-transfection, cells were diluted 1:1 with expression medium. Cells were cultured for 6 days after transfection, supernatants were harvested, centrifuged at 1800 g for 40 min and filtered (0.2 µm). Antibodies were purified by affinity chromatography using an AKTA pure FPLC instrument (GE Healthcare) on a HiTrap Protein A Column (GE Healthcare) for human IgG1 and human $IgG1_{N297A}$, and on a anti-human IgE omalizumab-bound affinity column for human IgE, and desalted on a HiTrap Desalting Column (GE Healthcare).

Anti-rocuronium ELISA

96-well plates (Costar) were coated with HSA-rocuronium or HSA at 1 μg/mL in PBS 1X (Gibco) overnight at 4°C overnight, washed 3 times with PBS Tween 20 0.5% (PBST), blocked with PBS-3% BSA, and washed three times with PBST. Mouse serum (diluted 1:250,000-1:5,000-1:100) or monoclonal antibodies were incubated for 2H at room temperature and bound antibodies were detected with HRP-conjugated goat anti-mouse or -human IgG (Bethyl Laboratories) at 1:10,000 dilution. The secondary antibody was revealed using OPD substrate (Sigma-Aldrich) and the reaction stopped with 2M H_2SO_4, and absorbance subsequently recorded at 490 nm and corrected at 620 nm using a spectrophotometer (Biophotometer, Eppendorff). The final OD reported in all graphs/tables corresponds to the subtraction of the OD value of the HSA-rocuronium ELISA minus the OD value of the HSA ELISA. A signal was considered positive if the OD value was at least three times higher than the background signal of the negative control.

Inhibition ELISA

To ascertain antibody reactivity to rocuronium, and not towards the linker employed to attach rocuronium to HSA, or a neo-epitope formed between rocuronium, the linker and HSA, a competitive inhibition ELISA was developed. This inhibition ELISA also enabled to detect cross-binding of antibodies to a panel of different NMBAs. 96-well plates (Costar) were coated with 1μg/ml HSA-rocuronium at 4°C overnight, washed 3 times with PBST, blocked with PBST containing 3% BSA at room temperature for 2 hours. 300 ng/mL mAbs were pre-incubated with 5-fold serial dilution of free NMBA drug (rocuronium, vecuronium, pancuronium, cisatracurium, atracurium), or NMBA surrogates devoid of quaternary ammoniums (5a-DHT or diisopentyl succinate) from 15,000 μM to 0.96μM. The antibody-NMBA mixture was added to the ELISA plates and incubated at RT for 2 hours, washed 3 times and revealed with HRP-conjugated goat anti-mouse/human IgG (Bethyl Laboratories) at 1:10,000 dilution. Plates were revealed using an OPD substrate (Sigma-Aldrich). The reaction was stopped with 2M H2SO4 and absorbance was subsequently recorded at 490 nm and corrected at 620 nm using a spectrophotometer

(Biophotometer, Eppendorff). For purified mAbs, the IC50 was measured using a non-linear fit [Inhibitor] vs. response -- Variable slope (four parameters) with GraphPad Prism.

Affinity measurements using Bio-Layer Interferometry (BLI)

Affinity of IgG mAbs for rocuronium was tested using Bio-layer interferometry with the OctetRED 384 system. Amine Reactive Second-Generation (AR2G) biosensors were covalently immobilized with HSA-rocuronium, then inserted in wells containing different concentrations of antibodies for 1,800 s (association phase). The antigen-antibody complex was dissociated by introducing the biosensor in the reference buffer (PBS+BSA). Curves were retrieved as raw data from the Octet Data Analysis software and processed in the Scrubber2 software prior to analyses with the Biaevaluation software. IgG-free buffer was used as reference and for background subtraction. Fitting curves and KD values were obtained using the 1:1 Langmuir model.

Affinity measurements using Surface Plasmon Resonance (SPR)

CM5 chips were primed using PBS, washed 3 times with NaOH (50 mM) and SDS (0.1%) 180 seconds each time (5uL/min). At least 5,000 RU of IgG antibody was covalently bound to CM5 chip by activating using 1:1 NHS:EDC (6,000 s), injecting the antibody (900 s) in acetate buffer pH5.5 and quenching with EtNH2 (600 s). Free rocuronium was injected (30 µL/min) in PBS-BSA (1 mg/mL) at different concentrations. Signal was subtracted to reference canal bound with a non-specific antibody. K_D was determined using a kinetic analysis (RI fixed to 0, model 1:1 binding) with Biaeval software.

Fab preparation

Fab were prepared following Pierce™ Fab Preparation Kit (Thermo scientific) instructions by a 4h digestion with papain in the presence of 4 mM cysteine. After purification on protein A columns, a gel filtration was performed with Tris 50mM pH, 7.4; 100 mM NaCl.

scFv production, purification and characterization

Rocuronium-specific VH and VL sequences were built into scFvs with a polyglycine-serine linker (GGGGS)4 between the VH and VL sequences. The VH-linker-VL sequences were synthesized at Genscript with codon optimization for expression in Drosophila S2 cells, cloned into pT-350 vector using BglII and BstBI restriction sites (the vector is a gift from Dr. Felix Rey, Institut Pasteur, Paris, France). For transfection, $5x10^6$ Drosophila S2 cells were seeded in a T25 conical flask containing 5 ml Schneider's Drosophila medium (Gibco) complemented with 10% fetal bovine serum and incubated at 28°C overnight. Twenty-four hours later, 2 µg of pMT-Roc-scFv-Strep plasmid were co-transfected with 0.1 µg (ratio 20:1) of selection plasmid pCoBlast carrying a gene that confers resistance to puromycin. Effectene transfection kit was used (Qiagen) according to the vendor's protocol. Forty-eight hours after transfection, the selection process was started by addition of puromycin (Invivogen) to the cells at a final concentration of 7 µg/ml. Transfected cells were collected every 4–5 days by centrifugation at 90g for 5 min, and cell pellets were resuspended in fresh medium containing 7 µg/ml puromycin. Cell propagation was initiated ~2 weeks after transfection. Puromycin-selected cells were adapted to serum-free HyClone Insect cell culture media (GE healthcare life science) and were amplified in large volume flasks as needed. Protein expression was induced with 0.5 mM CuSO4 when the cell density reached ~$7.5x10^6$ cells/ml. Seven days after induction, S2 cell suspension was centrifuged for 30 min at 15,000g to remove the cells and the supernatant was collected. Avidin was added at 15 mg/L to sequester any biotin present in the medium. The supernatant, cleared by centrifugation at 20,000g for 30 min and filtration, was loaded onto a Strep-Tactin Superflow high-capacity 5 mL column (IBA GmbH, Göttingen, Germany) using a peristaltic pump or AKTA. The column was washed with 15 mL of 0.1 M Tris pH 8, 0.15 M NaCl, 1 mM EDTA, and the protein was eluted with 8 mL of the same buffer containing 2.5 mM desthiobiotin.

Crystallization and X-ray data collection

Crystallization screening trials were carried out by the vapor diffusion method using a Mosquito TM nanodispensing system (STPLabtech, Melbourn, UK) following established protocols [54]. Briefly, we set up crystallization sitting drops of 400 nL containing a 1:1 mixture of protein sample (Fab or scFv) in complex with 10 mM of rocuronium and crystallization solutions (672 different commercially available conditions) equilibrated against 150 µl of reservoir solution in multiwell plates (Greiner Bio-One). The crystallization plates were stored at 18°C in a RockImager (Formulatrix) automated imaging system to monitor crystal growth. Manual optimization was performed in Linbro plates with the hanging-drop method by mixing 2 µl of protein samples with 2 µl of reservoir solution. The best crystals were obtained with the conditions shown in Table 2. The crystals were flash cooled in liquid nitrogen for data collection using the crystallization solution as cryoprotectant.

X-ray diffraction data were collected on beamlines PROXIMA-1 and PROXIMA-2A at the synchrotron SOLEIL (St Aubin, France). Diffraction images were integrated with autoPROC[55] and XDS[56] and crystallographic calculations were carried out with programs from the CCP4 program suite[57].

Structure determination and model refinement.

The structures of anti-rocuronium Fab and scFv in complex with rocuronium were solved by molecular replacement with Phaser[58] using the structures of the catalytic antibody Fab7A1 (pdb 2AJU) as search model. The final models of the complexes were obtained through interactive cycles of manual model building with Coot [59] and reciprocal space refinement with Refmac5[60]. X-ray data collection and model refinement statistics are summarized in Supp. Table 2. Figures showing the crystallographic models were generated with Pymol (Schrodinger, LLC).

Human mast cell activation test

$CD34^+$ precursor cells were isolated from peripheral blood mononuclear cells of healthy donors (provided by the French Blood Bank EFS). $CD34^+$ cells were maintained for 1 week under serum-

free conditions using StemSpan medium (9655 Stemcell Technologies) supplemented with recombinant human IL-6 (50 ng/ml; 200-06 Peprotech), human IL-3 (10 ng/ml; 200-03 Peprotech) 3% supernatant of CHO transfectants secreting mouse SCF (a gift from Dr. P. Dubreuil, Marseille, France, 3% [corresponding to ~50 ng/ml SCF]) and ciprofloxacin (10 ng/mL; 17850-5G-F Sigma Aldrich). Thereafter, the cells were maintained in IMDM Glutamax I (31980048), 2-mercaptoethanol (31-350-010), insulin-transferrin selenium (2506865) (all from Gibco), sodium pyruvate (S8636 Sigma Aldrich), 0.5% BSA (A2153 Sigma Aldrich), Penicillin/Streptomycin (100 Units/mL / 100µg/mL; Life Technologies), IL-6 (50 ng/ml 200-06 Peprotech) and 3% supernatant of CHO transfectants secreting mouse SCF. Before their use in experiments, mast cells were tested for phenotype by flow cytometry ($CD117^+$, $Fc\varepsilon RI^+$). Cells were ready for experiments after ~10 weeks in culture (at which time >95% of all cells were $CD117^+$ $Fc\varepsilon RI^+$).

Human mast cells were sensitized overnight with anti-rocuronium human IgE antibodies at 1 µg/mL. Cells were then washed and stimulated with increasing doses of HSA-rocuronium in Tyrode's buffer. Mast cell degranulation was measured by flow cytometry using fluorescent avidin (5 µg/mL; A2170 Invitrogen) which binds to heparin contained in mast cell granules. Data were acquired using a MACSQuant MQ10 flow cytometer (Miltenyi) and analyzed with FlowJo v10.8.1 software (TreeStar).

Basophil activation test

Human whole blood was pre-incubated for 3 hours at room temperature with anti-rocuronium IgE at 10 µg/mL. According to manufacturers' instructions (Flow CAST®, FK-CCR, Buhlmann) 50µL of blood was incubated with HSA or HSA-rocuronium for 15 minutes at 37°C with staining reagents. Basophils were stained using anti-CCR3-PE for specificity and using anti-CD63-FITC to determine activation status. Red blood cells were lysed and the percentage of CD63 activation was determined by flow cytometry.

Neutrophil activation

Neutrophils were isolated from fresh human EDTA-drawn blood using the MACSxpress Neutrophil Isolation kit (Miltenyi). Immune complexes were formed for 30 mins at 37°C in HBSS/2%FCS. $1x10^5$ neutrophils were stimulated with ICs at a final concentration of 30 μg/mL HSA-Roc and 100 μg/mL anti-Roc IgG in 200μl in HBSS/2% FCS for 30 mins at 37°C, washed and stained with anti-CD62L (clone DREG-56) and anti-CD11b (clone M1/70) (both BD Bioscences) for 15 mins at 4°C, washed and analyzed by flow cytometry on MACSquant16 (Miltenyi).

Passive systemic anaphylaxis in mice

hFcεRI^{tg} mFcεRI$^{-/-}$ mice[52] were injected intravenously with 5 μg of anti-rocuronium human IgE mAbs at 0h and challenged 24h later with 2 μg of HSA-roc. Specifically for anti-rocuronoium low-affinity mAb IP12, 20 μg of human IgE mAb IP12 was injected intravenously twice at 0h and 24h, and mice were challenged 24h later with 100μg of HSA-roc. Control mice were injected with irrelevant human IgE and physiological serum. Central temperature was monitored using a digital thermometer with rectal probe (YSI), and time of death was recorded.

Statistical analyses

The R environment v4.3.1 was used for all the analyses (R foundation, Vienna, Austria. https://www.r-project.org/). Data were neither averaged nor normalized prior to analyses. Response variables were log2 converted when required for better adjustment to linear models. For Fig 4B-C, a mixed models using the lmer() function of the lme4 package was used in order to consider the repeated measures on each mouse. Resulting effects of interest of the linear model were two-by-two compared (contrast comparisons) using the emmeans() function of the emmeans package. Statistical significance was set to a P value of 0.05 or less. In each panel, type I error was controlled by correcting the P values according to the Benjamini & Hochberg method ("BH" option in the p.adjust() function of R).

REFERENCES

1. Thilen SR, Weigel WA, Todd MM, Dutton RP, Lien CA, Grant SA, et al. 2023 American Society of Anesthesiologists Practice Guidelines for Monitoring and Antagonism of Neuromuscular Blockade: A Report by the American Society of Anesthesiologists Task Force on Neuromuscular Blockade. Anesthesiology 2023; 138:13-41.
2. Fuchs-Buder T, Romero CS, Lewald H, Lamperti M, Afshari A, Hristovska AM, et al. Peri-operative management of neuromuscular blockade: A guideline from the European Society of Anaesthesiology and Intensive Care. Eur J Anaesthesiol 2023; 40:82-94.
3. Lien CA, Eikermann M. Neuromuscular Blockers and Reversal Drugs. Pharmacology and Physiology for Anesthesia (Second Edition) 2019:428-54.
4. Mertes PM, Aimone-Gastin I, Gueant-Rodriguez RM, Mouton-Faivre C, Audibert G, O'Brien J, et al. Hypersensitivity reactions to neuromuscular blocking agents. Curr Pharm Des 2008; 14:2809-25.
5. Sadleir PH, Clarke RC, Bunning DL, Platt PR. Anaphylaxis to neuromuscular blocking drugs: incidence and cross-reactivity in Western Australia from 2002 to 2011. Br J Anaesth 2013; 110:981-7.
6. Mertes PM, Ebo DG, Garcez T, Rose M, Sabato V, Takazawa T, et al. Comparative epidemiology of suspected perioperative hypersensitivity reactions. Br J Anaesth 2019; 123:e16-e28.
7. Bruhns P, Chollet-Martin S. Mechanisms of human drug-induced anaphylaxis. J Allergy Clin Immunol 2021; 147:1133-42.
8. Jonsson F, de Chaisemartin L, Granger V, Gouel-Cheron A, Gillis CM, Zhu Q, et al. An IgG-induced neutrophil activation pathway contributes to human drug-induced anaphylaxis. Sci Transl Med 2019; 11.
9. Winbery SL, Lieberman PL. Histamine and antihistamines in anaphylaxis. Clin Allergy Immunol 2002; 17:287-317.
10. Conte B, Zoric L, Bonada G, Debaene B, Ripart J. Reversal of a rocuronium-induced grade IV anaphylaxis via early injection of a large dose of sugammadex. Can J Anaesth 2014; 61:558-62.
11. Kim SM, Oh SH, Ryu SA. Treatment of rocuronium-induced anaphylaxis using sugammadex - A case report. Anesth Pain Med (Seoul) 2021; 16:56-9.
12. Baldo BA, Fisher MM. Substituted ammonium ions as allergenic determinants in drug allergy. Nature 1983; 306:262-4.
13. Russell WJ, Lee C, Milne D. Is allergy to rocuronium a high probability cross-reaction with suxamethonium? Anaesth Intensive Care 2003; 31:333.
14. Rose MA, Anderson J, Green SL, Yun J, Fernando SL. Morphine and pholcodine-specific IgE have limited utility in the diagnosis of anaphylaxis to benzylisoquinolines. Acta Anaesthesiol Scand 2018; 62:628-34.
15. Fielding L, Grant GH. Conformational equilibria in amino steroids. 1. A proton and carbon-13 NMR spectroscopy and molecular mechanics study of 3.alpha.-hydroxy-2.beta.-(4-morpholinyl)-5.alpha.H-androstan-17-one. J. Am. Chem. Soc. 1991; 113:9785-90.
16. Cooper A, Nutley M, MacLean EJ, Cameron K, Fielding L, Mestres J, et al. Mutual induced fit in cyclodextrin-rocuronium complexes. Org Biomol Chem 2005; 3:1863-71.
17. Baldo BA, Fisher MM, Pham NH. On the origin and specificity of antibodies to neuromuscular blocking (muscle relaxant) drugs: an immunochemical perspective. Clin Exp Allergy 2009; 39:325-44.
18. Peyneau M, de Chaisemartin L, Gigant N, Chollet-Martin S, Kerdine-Romer S. Quaternary ammonium compounds in hypersensitivity reactions. Front Toxicol 2022; 4:973680.
19. Florvaag E, Johansson SG. The Pholcodine Case. Cough Medicines, IgE-Sensitization, and Anaphylaxis: A Devious Connection. World Allergy Organ J 2012; 5:73-8.
20. Mertes PM, Petitpain N, Tacquard C, Delpuech M, Baumann C, Malinovsky JM, et al. Pholcodine exposure increases the risk of perioperative anaphylaxis to neuromuscular blocking agents: the ALPHO case-control study. Br J Anaesth 2023.
21. van der Poorten MM, Van Gasse AL, Hagendorens MM, Faber MA, De Puysseleyr L, Elst J, et al. Serum specific IgE antibodies in immediate drug hypersensitivity. Clin Chim Acta 2020; 504:119-24.
22. Decuyper, II, Ebo DG, Uyttebroek AP, Hagendorens MM, Faber MA, Bridts CH, et al. Quantification of specific IgE antibodies in immediate drug hypersensitivity: More shortcomings than potentials? Clin Chim Acta 2016; 460:184-9.
23. Wardemann H, Busse CE. Novel Approaches to Analyze Immunoglobulin Repertoires. Trends Immunol 2017; 38:471-82.
24. Victora GD, Nussenzweig MC. Germinal Centers. Annu Rev Immunol 2022; 40:413-42.

25. Gerard A, Woolfe A, Mottet G, Reichen M, Castrillon C, Menrath V, et al. High-throughput single-cell activity-based screening and sequencing of antibodies using droplet microfluidics. Nat Biotechnol 2020; 38:715-21.
26. Lindeman I, Zhou C, Eggesbo LM, Miao Z, Polak J, Lundin KEA, et al. Longevity, clonal relationship, and transcriptional program of celiac disease-specific plasma cells. J Exp Med 2021; 218.
27. Canales-Herrerias P, Crickx E, Broketa M, Sokal A, Chenon G, Azzaoui I, et al. High-affinity autoreactive plasma cells disseminate through multiple organs in patients with immune thrombocytopenic purpura. J Clin Invest 2022; 132.
28. Ehling RA, Weber CR, Mason DM, Friedensohn S, Wagner B, Bieberich F, et al. SARS-CoV-2 reactive and neutralizing antibodies discovered by single-cell sequencing of plasma cells and mammalian display. Cell Rep 2022; 38:110242.
29. Reddy JI, Cooke PJ, van Schalkwyk JM, Hannam JA, Fitzharris P, Mitchell SJ. Anaphylaxis is more common with rocuronium and succinylcholine than with atracurium. Anesthesiology 2015; 122:39-45.
30. Takazawa T, Mitsuhata H, Mertes PM. Sugammadex and rocuronium-induced anaphylaxis. J Anesth 2016; 30:290-7.
31. Tacquard C, Collange O, Gomis P, Malinovsky JM, Petitpain N, Demoly P, et al. Anaesthetic hypersensitivity reactions in France between 2011 and 2012: the 10th GERAP epidemiologic survey. Acta Anaesthesiol Scand 2017; 61:290-9.
32. Ise W, Kurosaki T. Plasma cell differentiation during the germinal center reaction. Immunol Rev 2019; 288:64-74.
33. Suan D, Sundling C, Brink R. Plasma cell and memory B cell differentiation from the germinal center. Curr Opin Immunol 2017; 45:97-102.
34. Gupta NT, Vander Heiden JA, Uduman M, Gadala-Maria D, Yaari G, Kleinstein SH. Change-O: a toolkit for analyzing large-scale B cell immunoglobulin repertoire sequencing data. Bioinformatics 2015; 31:3356-8.
35. Baldo BA, Fisher MM. Anaphylaxis to muscle relaxant drugs: cross-reactivity and molecular basis of binding of IgE antibodies detected by radioimmunoassay. Mol Immunol 1983; 20:1393-400.
36. Gouel-Cheron A, Dejoux A, Lamanna E, Bruhns P. Animal Models of IgE Anaphylaxis. Biology (Basel) 2023; 12.
37. Dombrowicz D, Brini AT, Flamand V, Hicks E, Snouwaert JN, Kinet JP, et al. Anaphylaxis mediated through a humanized high affinity IgE receptor. J Immunol 1996; 157:1645-51.
38. Hoi KH, Ippolito GC. Intrinsic bias and public rearrangements in the human immunoglobulin Vlambda light chain repertoire. Genes Immun 2013; 14:271-6.
39. Jackson KJ, Wang Y, Gaeta BA, Pomat W, Siba P, Rimmer J, et al. Divergent human populations show extensive shared IGK rearrangements in peripheral blood B cells. Immunogenetics 2012; 64:3-14.
40. Parameswaran P, Liu Y, Roskin KM, Jackson KK, Dixit VP, Lee JY, et al. Convergent antibody signatures in human dengue. Cell Host Microbe 2013; 13:691-700.
41. Jackson KJ, Liu Y, Roskin KM, Glanville J, Hoh RA, Seo K, et al. Human responses to influenza vaccination show seroconversion signatures and convergent antibody rearrangements. Cell Host Microbe 2014; 16:105-14.
42. DeKosky BJ, Kojima T, Rodin A, Charab W, Ippolito GC, Ellington AD, et al. In-depth determination and analysis of the human paired heavy- and light-chain antibody repertoire. Nat Med 2015; 21:86-91.
43. Cumano A, Rajewsky K. Structure of primary anti-(4-hydroxy-3-nitrophenyl)acetyl (NP) antibodies in normal and idiotypically suppressed C57BL/6 mice. Eur J Immunol 1985; 15:512-20.
44. Siekevitz M, Huang SY, Gefter ML. The genetic basis of antibody production: a single heavy chain variable region gene encodes all molecules bearing the dominant anti-arsonate idiotype in the strain A mouse. Eur J Immunol 1983; 13:123-32.
45. Collins AM, Jackson KJL. On being the right size: antibody repertoire formation in the mouse and human. Immunogenetics 2018; 70:143-58.
46. Hershberg U, Luning Prak ET. The analysis of clonal expansions in normal and autoimmune B cell repertoires. Philos Trans R Soc Lond B Biol Sci 2015; 370.
47. Broketa M, Sokal A, Mor M, Canales-Herrerias P, Perima A, Meola A, et al. Qualitative monitoring of SARS-CoV-2 mRNA vaccination in humans using droplet microfluidics. JCI Insight 2023; 8.
48. Eyer K, Doineau RCL, Castrillon CE, Briseno-Roa L, Menrath V, Mottet G, et al. Single-cell deep phenotyping of IgG-secreting cells for high-resolution immune monitoring. Nat Biotechnol 2017; 35:977-82.
49. Beutier H, Hechler B, Godon O, Wang Y, Gillis CM, de Chaisemartin L, et al. Platelets expressing IgG receptor FcgammaRIIA/CD32A determine the severity of experimental anaphylaxis. Sci Immunol 2018; 3.

50. Elst J, Van Houdt M, van der Poorten MM, Van Gasse AL, Mertens C, Toscano A, et al. Comparison of the passive mast cell activation test with the basophil activation test for diagnosis of perioperative rocuronium hypersensitivity. Br J Anaesth 2023.
51. Orihara M, Takazawa T, Horiuchi T, Sakamoto S, Nagumo K, Tomita Y, et al. Comparison of incidence of anaphylaxis between sugammadex and neostigmine: a retrospective multicentre observational study. Br J Anaesth 2020; 124:154-63.
52. Mancardi DA, Iannascoli B, Hoos S, England P, Daeron M, Bruhns P. FcgammaRIV is a mouse IgE receptor that resembles macrophage FcepsilonRI in humans and promotes IgE-induced lung inflammation. J Clin Invest 2008; 118:3738-50.
53. Djaffardjy M, Marchment G, Sebe C, Blanchet R, Bellajhame K, Gaignard A, et al. Developing and reusing bioinformatics data analysis pipelines using scientific workflow systems. Comput Struct Biotechnol J 2023; 21:2075-85.
54. Weber P, Pissis C, Navaza R, Mechaly AE, Saul F, Alzari PM, et al. High-Throughput Crystallization Pipeline at the Crystallography Core Facility of the Institut Pasteur. Molecules 2019; 24.
55. Vonrhein C, Flensburg C, Keller P, Sharff A, Smart O, Paciorek W, et al. Data processing and analysis with the autoPROC toolbox. Acta Crystallogr D Biol Crystallogr 2011; 67:293-302.
56. Kabsch W. Xds. Acta Crystallogr D Biol Crystallogr 2010; 66:125-32.
57. Agirre J, Atanasova M, Bagdonas H, Ballard CB, Basle A, Beilsten-Edmands J, et al. The CCP4 suite: integrative software for macromolecular crystallography. Acta Crystallogr D Struct Biol 2023; 79:449-61.
58. McCoy AJ, Grosse-Kunstleve RW, Adams PD, Winn MD, Storoni LC, Read RJ. Phaser crystallographic software. J Appl Crystallogr 2007; 40:658-74.
59. Emsley P, Cowtan K. Coot: model-building tools for molecular graphics. Acta Crystallogr D Biol Crystallogr 2004; 60:2126-32.
60. Murshudov GN, Skubak P, Lebedev AA, Pannu NS, Steiner RA, Nicholls RA, et al. REFMAC5 for the refinement of macromolecular crystal structures. Acta Crystallogr D Biol Crystallogr 2011; 67:355-67.

ACKNOWLEDGMENTS

We would like to thank our colleagues from the Institut Pasteur, Paris, France for their help and advice: Delphine Brun and Annalisa Meola (Structural virology unit) for ScFv generation and production; Bertrand Raynal, Sébastien Brulé and Sylviane Hoos for assistance with affinity measurements (Molecular Biophysics Core Facility), Fabrice Agou for access to the BLI instrument (Plateforme de Criblage Chémogénomique et Biologique; PF-CCB), Michel Perez for advice and support (Direction Des Applications De la Recherche et des Relations Industrielles; DARRI), Odile Richard-Le Goff for training and Henna Maulaboksh for administrative help. We would like to thank the staff of the crystallography platform at Institut Pasteur for crystallization screening, and acknowledge synchroton SOLEIL (Saint-Aubin, France) for granting access to their facility and the staff of Proxima1 and Proxima2A for helpful assistance.

No AI-based solution has been used to write this manuscript.

FUNDING

Work in the Bruhns' lab was supported by the Institut Pasteur, Institut National de la Santé et de la Recherche Médicale (Inserm), Fondation pour la Recherche Médicale, Paris, France (Programme Equipe FRM grant EQU202203014631), Accélérateur de l'innovation de l'Institut Pasteur (grant rocuCEPT), Agence Nationale de la Recherche (grants ANR-14-CE16-0011, ANR-16-CARN-0023-01 and ANR-21-CE15-0027), European Research Council (ERC)–Seventh Framework Program (ERC-2013-CoG 616050) and Inserm *International Research Program* (IRP grant ALLERGYMINE) to PB. AD was supported by a doctoral fellowship from Sorbonne Université, followed by by a fellowship from the Fondation pour la Recherche Médicale. QZ received a PhD scholarship from the Chinese Science Council. AGC was a recipient of a poste d'accueil 2017 Institut Pasteur – Assistance Publique des Hôpitaux de Paris (APHP), and was supported by a grant provided by INSERM, SFAR (Société Française d'Anesthésie et de Réanimation), and SRLF (Société de Réanimation de Langue Française) through the "Bourse de Recherche du Comité d'interface INSERM-SFAR-SRLF 2012. CMG was supported partly by a stipend from the Pasteur-Paris University (PPU) International PhD program and by the Institut Carnot Pasteur Maladies Infectieuses. CC acknowledges financial support from CONCYTEC, Peru. PB benefited from an

additional support from AP-HP through a “Contrat Local d’Interface 2014” and the “Département Hospitalo-Universitaire” (DHU) FIRE.

DATA AND MATERIALS AVAILABILITY

Coordinates and structure factors of crystallographic data have been deposited in the Protein Data Bank under the accession codes XXX (FabIP2 in complex with rocuronium), XXX (FabIP8 in complex with rocuronium), XXX (ScFvIP8 in complex with rocuronium), and YYY (scFv-IP11 in complex with rocuronium). (process ongoing)

Further information and requests for resources, reagents and material should be directed to and will be fulfilled by the Lead Contact, Pierre Bruhns bruhns@pasteur.fr

This work reports for the first time anti-rocuronium antibody repertoires from NMBA-allergic patients and immunized mice and allows an in-depth characterization of isolated rocuronium-specific mAbs generated with different models.

The antibodies isolated were sequenced to gain insight into the repertoire generation and clonality of the rocuronium-specific B cells using various bioinformatic tools such as sequence alignment and phylogenic analysis. The originality of the work lies in the functional analysis of the antibody repertoires by further characterizing representative mAbs through recombinant expression. To bypass a potential overestimation of the dissociation constant (K_D), two distinct methods were employed to determine the affinities of the mAbs for rocuronium. The use of HSA-rocuronium probes grafted on biolayer interferometry biosensors provided information on the avidities of the mAbs whilst surface plasmon resonance technology allowed the assessment of affinities with free NMBAs. An in-house inhibition ELISA was established to ascertain the mAbs specificity for rocuronium and cross-reactivities for other NMBAs or chemical structures devoid of a QA. The binding modalities of the mAbs with rocuronium were deciphered for the first time at the atomic level by determining their co-crystal structures which allowed the identification of the probable allergenic epitopes.

The underlying pathways were explored using various approaches. First, the IgG-dependent pathway was investigated by activating neutrophils with immune complexes, and then the IgE-dependent one was studied by degranulating effector cells (mast cells and basophils) in the presence of HSA-rocuronium. A very sensitive model of passive systemic anaphylaxis with transgenic mice expressing a humanized FcεRI was established with various antibody-antigen concentrations to determine the sensibility threshold of the model and to validate the role of the mAbs in the induction of hypersensitive reactions.

An unprecedented proof of concept taking advantage of the high specificity and affinity of the mAbs to capture small drugs *in vivo* and to block their effect was validated. First, a prophylactic model of prevention of rocuronium-induced neuromuscular blockade was established in mice, and then the reversal potency of the therapeutic mAb was confirmed in non-human primates.

This work provides meaningful knowledge on the mechanisms of NMBA-mediated AHR and paves the way for novel immunotherapies.

5 Note on the differences in generating mAbs from immunized mice and allergic patients

In this project, a parallel was drawn between the differences in generating rocuronium-specific mAbs from immunized mice and allergic patients which generates a lot of questions concerning, the methods used, the results obtained, and the interpretation of the underlying mechanisms (Fig 9).

To isolate rocuronium-specific IgG antibodies from mice and patients, different techniques were employed. Mice were exposed to a synthetic KLH-rocuronium conjugate composed of multimeric antigen molecules, co-administered with an adjuvant (alum and pertussis toxin). The antibody-secreting plasma cells were isolated from the lymph nodes of these mice using two distinct methods: hybridoma generation and microfluidic sorting. Then, the rocuronium-positive ASC were isolated using HSA-rocuronium probes either conjugated to a fluorochrome or directly used in ELISA. Alternatively, patients were selected according to two criteria: 1) they had a medium to severe grade of NMBA-mediated AHR, and 2) they possessed positive levels of rocuronium-specific IgG antibodies in their serum. Their Bmem-expressing rocuronium-specific IgM or IgG antibodies were isolated using HSA-rocuronium fluorescent probes by single-cell sorting and were artificially differentiated in ASC *in vitro* using cytokines and CD40L-expressing feeder cells. Then, positive cells were identified using inhibition ELISA from the supernatant on the cell culture. The variable regions of the BCRs of the positive clones were sequenced and a bioinformatic analysis allowed the rocuronium-specific antibody repertoire comparison between patients by identifying VJ genes, CDR3s, and mutation load. The methods were clearly distinct since in the two models the individual patients and mice were exposed to different allergens (different in nature, valency, presence of adjuvants, frequency of exposition), different cell subsets were isolated (plasma cells from lymph nodes of mice versus Bmem from blood of allergic donors) and distinct sequencing strategies (bar-coded single cells for the microfluidic sort versus RNA extraction for hybridoma generation and single-cell sequencing of identical clones in cell culture). The screening methods via HSA-rocuronium ELISA, inhibition ELISA, or biolayer interferometry, and surface plasmon resonance were identical and the sequencing analysis (IMGT tool, pipeline to align the sequences and to draw the phylogenic trees) was also performed using a similar method (Fig 9).

The results obtained were also divergent with high-affinity and monospecific antibodies generated with the mouse animal model. The isolated antibodies were confirmed to play a role in anaphylaxis via the

activation of the IgG and IgE-mediated pathways. Indeed, IgG-immune complexes could activate neutrophils, and mAbs expressed as human IgE antibodies could trigger mast cell, and basophil degranulation and induce passive systemic anaphylaxis with very low doses of antibody and antigen. The IgG antibody repertoires were oligoclonal with a predominant VJ pair (V1-55_J2 for the VH and V4-68_J5 for the VL) coding for the variable regions of the mouse mAbs even in the repertoire of distinct mice with antibodies generated using different methods. In contrast, anti-rocuronium IgG antibody repertoires of AHR patients were polyclonal, with a high diversity among V(D)J genes and the absence of clonal families (identical VJ genes and CDR3 length for the VH). The human rocuronium-specific IgG antibodies had medium- to low affinities and avidities, none of them in their IgE format could activate basophils and only the one with the highest affinity could degranulate mast cells and induce passive systemic anaphylaxis in mice with high antigen and antibody doses. Ultimately, only the work on mice allowed the generation of a sufficiently high-affinity antibody able to reverse rocuronium-induced deep neuromuscular blockade in non-human primates in a competitive time frame compared to the current standard of care, sugammadex (Fig 9).

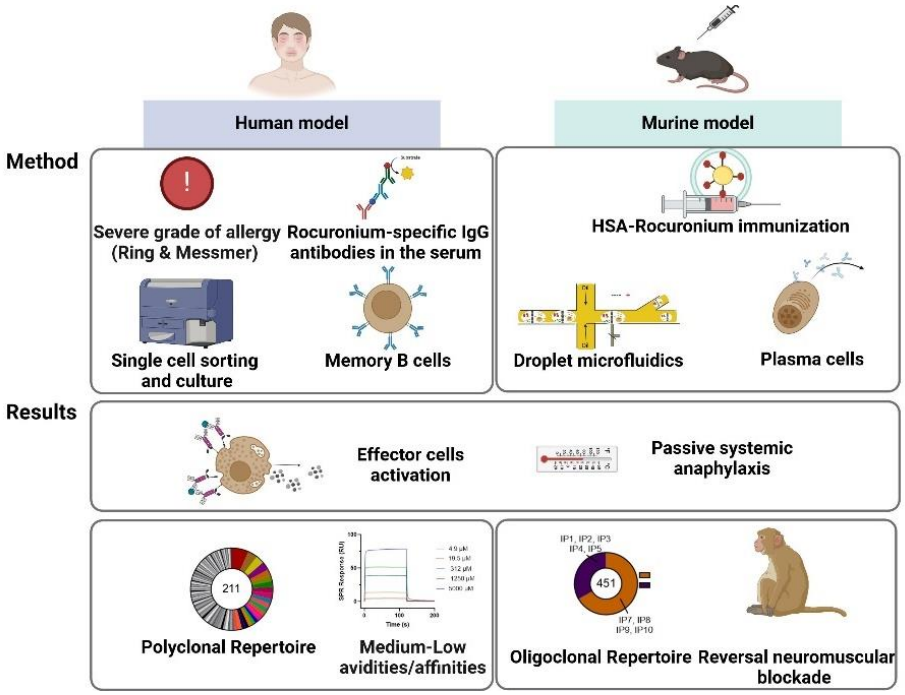

Figure 9: Comparison of the models used to generate rocuronium-specific mAbs.
The main methods and results obtained to generate rocuronium-specific mAbs from allergic patients or immunized mice are summarized.

Therefore, these results raise some questions concerning the limitations of the models used and the interpretation of the results that will be discussed in the following sections. We will first try to understand how these results can provide insights into the underlying mechanisms of the sensitization and activation phases in allergic patients by mirroring the data obtained with the two models. Then, we will provide lines of thought that could explain antigen presentation and activation of immune cells in the context of a small, non-immunogenic drug, lacking chemically reactive groups. The consensual haptenization hypothesis will be defended and then questioned. Finally, therapeutic applications of this work will be approached by demonstrating the clinal implications in the context of AHR diagnostic and neuromuscular blockade reversal.

6 What are the potential mechanisms behind NMBA-mediated AHR?

6.1 The hypothetical origins of the sensitization phase explained by cross-reactivity

The comparison between the human and murine rocuronium antibody repertoires casts light on the origin of the allergen sensitization. Indeed, mice immunized with a multitude of rocuronium molecules grafted on a carrier protein (KLH) possess an oligoclonal antibody repertoire with similar VJ genes coding for the variable regions of the mAbs generated from different mice. Even more surprising, mAbs isolated with distinct methods (IP8 and IP11 from droplet microfluidics from sort#1 and mAb 2B1 and 1B6 from hybridoma generation) shared identical VL chains. This redundancy across individual mice and methods suggests that this type of immunization process forces the affinity maturation process to generate a restricted variety of specific antibodies. This could be partially explained by the fact that anti-hapten BCRs are prone to bind antigens with a smaller number of amino acid residues in their antibody binding sites compared to anti-protein or anti-peptide mAbs[185]. The variation in the length of BCRs has been shown to impact the topography of the binding sites (usually deep pockets for haptens versus flat binding sites for bigger proteins)[185] but does not influence the diversity of the antibody repertoires. Therefore, the origin of the differences in the diversity of the clonal groups between the human and mouse models should be explained by the dynamic of clonal selection in the GC driven by antigenic exposure rather than BCR length.

Previous findings on mice immunization with the hapten (4-hydroxy-3-nitrophenyl)acetyl (NP) bound to a chicken gamma globulin carrier protein report the generation of GC B cells with a reduced clonal diversity[186]. These results hint that GC populations elicited by haptens are driven by intraclonal competition mediated by an antigen-mediated selection for a preferred epitope. The density of haptens on the carrier also plays a role in the antibody repertoire generation, as it has been shown in the context of tumor-associated antigen (referred to as Tn antigen) that higher haptens density generates a broader

spectrum of reactive antibodies in rabbits[187]. Li, Q et al., also showed in their model, that the vaccination with tumor-associated antigens elicited multiple subpopulations of antibodies that bind a small subset of antigens rather than a single population of polyspecific antibodies, which is in line with our results obtained from the mice plasma cell repertoires which are composed of diverse monospecific mAbs that predominantly bind to aminosteroid NMBAs. Nonetheless, in the study described by Li, Q et al., experiments were performed on polyclonal animal serum with inhibition ELISA, and antibodies were not sequences nor characterized. A more recent study also evaluated the BCR repertoire evolution following repeated immunization (6 immunizations with a 1-month interval) against haptens in rabbits, this time providing sequencing results. The data showed that repeated immunization reduced the diversity of the BCR repertoire and increased antibody affinities[188]. All these results in animal models immunized with haptens bound to an immunogenic carrier protein led to similar observations: restricted antibody repertoire diversity and generation of high-affinity antibodies for small antigens.

Based on the rocuronium-specific B cell repertoires from immunized mice and the small nature of the antigen, we would have also expected that most sequences would derive from a few VH-VL germline sequences in the human antibody repertoires if the sensitization routes were identical. Our results contradict these expectations with polyclonal human repertoires that can be partially explained by the fact that murine antibody repertoires have been shown to be less diverse than the human ones because of the higher number of residues in the CDR3 loops of human mAbs (mean length of 15.2 residues) than the murine ones (mean length of 11.5 residues)[189]. This striking difference in repertoire diversity and the low-affinity of the human mAbs isolated support the commonly admitted hypothesis that humans are sensitized in the environment by chemically similar but distinct molecules to NMBAs. This would also explain why a majority of patients who undergo an NMBA-mediated AHR have never been exposed to the culprit molecule before[190]. The remaining part of this subsection will delve into details of the potential sensitizing molecules found in the environment.

Several potential culprit agents have been described in the literature, all of them possessing a QA, which supports the original hypothesis demonstrated by Baldo et al in 1983[100]. Using an inhibition ELISA with QA-containing compounds (such as morphine, choline, and tetraalkylammonium bromides) on the serum of patients who did an AHR to NMBAs, the authors claimed that the QA is the allergenic epitope in NMBA-mediated AHR[100] (Fig 10.A). Our data of co-crystal structures of the mAbs in complex with rocuronium confirmed for the first time that the hydrophobic pocket formed by the mAbs VH and VL chains make strong Van der Waals bonds with the QA of the rocuronium which goes in line with this hypothesis.

Nonetheless, so far, the crystal structures were generated only with the murine mAbs identified in this work, a future perspective would be to crystallize human mAbs.

A major limitation in our model to be fully confident that the QA is the allergenic epitope is caused by the way the rocuronium derivatives were designed. Indeed, we designed the rocuronium derivative relying on the hypothesis that the QA was the immunogenic epitope. Therefore, we intentionally activated the hydroxyl group (which happened to be the only chemically modifiable one) that was located on the opposite side of the QA. The introduction of the linker also brought flexibility to the conjugate which favored the accessibility of the QA. Undoubtedly, the structure of the carrier:rocuronium conjugates biased the generation of BCR binding to the QA since this epitope possessed the lowest steric hindrance, hence chances were higher that the antibodies generated targeted the QA. The selection of the positive antibody candidates either by ELISA or flow cytometry also utilized the carrier:rocuronium conjugates, hence forcing the selection for antibodies that recognized the QA. Were the antibodies isolated recognizing the QA because we biased the mAbs generation and selection process? Or were we fortuitous that the only chemically modifiable group on rocuronium was the hydroxyl one, therefore making our model optimal since the antibodies naturally bind to the QA? We do not have enough evidence to answer this question today. The natural haptenization route in humans will be discussed in §6.3 but it is also possible that the *in vivo* chemical modification faces a similar bias since the hydroxyl group is the only reactive one on rocuronium and is positioned at the opposite side of the QA atom.

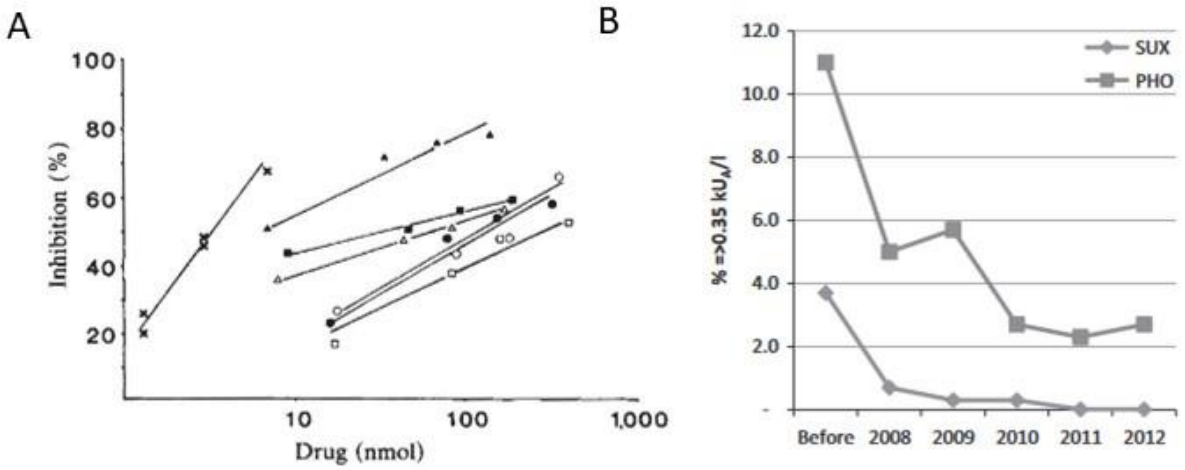

Figure 10: Cross-sensitization to QA-containing compounds in NMBA-allergic patients.
(**A**) Inhibition of the binding of IgE antibodies in serum of alcuronium-sensitive patients by QA-containing compounds demonstrated by Baldo et al., to show the cross-reactivity of alcuronium-reactive antibodies with other muscle relaxants and unrelated QA-containing drugs. ●chlorpromazine-HCl; ○Promethazine-HCl; ■ pentolineum tartrate; □ neostigmine bromide; ▲ morphine-HCl, x alcuronium, △ trimethaphan camphorsulphonate. Extracted from Baldo et al.,[100]. (**B**) Prevalence of IgE sensitization to pholcodine (PHO) and suxamethonium (SUX) in sera from patients suspected to be allergic measured when PHO was on the market (before) and yearly up to 5 years after its withdrawal in 2007. Prevalence (%) on the vertical axis was estimated from 300 consecutive, anonymized sera sampled each year from the 1st of April onward from sera submitted for routine allergy diagnostics. Extracted from G. H. de Pater et al., [106]. HCl: Hydrochloric acid; PHO, pholcodine; SUX, suxamethonium.

The most blamed QA-containing agent potentially responsible for sensitization to NMBAs is pholcodine, a molecule found in anti-tussive syrups. Several studies support this evidence, the first one originates from 2005 in which it was shown that the incidence of anaphylaxis to NMBAs was six times higher in Norway than in a country where pholcodine was never on the market such as Sweden. Six years after the withdrawal of pholcodine from the Norwegian market, the incidence of suxamethonium and rocuronium-specific IgEs decreased in the Norwegian population compared to the level observed in Sweden, and the reporting of perioperative allergy in which NMBA was used drastically dropped to a single case per 1-2 years[106] (Fig 10.B). The results of this study must be nuanced since a real cause-consequence effect has never been demonstrated and it is the **reporting** of perioperative allergy **in which NMBA was used** that fell (and not the incidence of NMBA-mediated allergy). This reduction could also be related to a reporting fatigue during these six years study, reduction of antibiotic allergy due to changes in prophylaxis guidelines or other factors. In France, the ALPHO study was undertaken, in which pholcodine exposure was evaluated within a year before NMBA-mediated AHR compared to control patients with uneventful anesthesia. The

authors showed that patients exposed to pholcodine had a higher risk of NMBA-mediated AHR[107]. Populations more frequently exposed to QA-containing compounds such as hairdressers (compounds in hair products)[109], cleaners and healthcare workers (exposed to detergents, disinfectants), and women (more exposed to detergents, cosmetics, and household chemicals)[36] were also more prone to undergo NMBA-mediated AHR and possessed a higher prevalence of QA sIgE. Nonetheless, the sex factor must be discussed here since it is still unclear if this difference in allergy was influenced by environmental and/or genetic factors. Indeed, it was demonstrated that allergies are driven by sex hormones such as estrogen and progesterone that have been described to exacerbate the development of a Th2-mediated response and autoimmune diseases[191-192]. Another trend that questions both environmental and hormonal factors is the fact that children were less sensitive to NMBAs than adults and for instance more allergic to latex than to NMBAs which is the contrary for adults[36]. Is it because children were less exposed to QA-containing compounds during their early life and/or because of hormonal factors? It is still unclear.

We also tried to undertake a study during this project to test the cross-sensitization hypothesis by exposing mice to pholcodine and by evaluating the generation of cross-reactive IgG antibodies that were specific to rocuronium. This experiment faced several challenges: the prohibition of pholcodine in the European market since September 2022 and the absence of pholcodine-carrier protein conjugates. By immunizing mice intraperitoneally and subcutaneously with pure pholcodine, we were unsuccessful at identifying cross-reactive anti-rocuronium IgG antibodies in the serum of the mice immunized with pholcodine. These findings were limited by the fact that we could not verify the generation of pholcodine-specific mAbs due to the absence of pholcodine-carrier conjugates. These conjugates are necessary to quantify pholcodine-specific IgG antibodies by ELISA since pholcodine does not possess any chemically reactive group (similarly to rocuronium), hence it does not bind to the bottom of the ELISA plates by adsorption without being grafted to a carrier molecule. Nonetheless, we are aiming to continue this experiment by improving the sensitization procedure (through gavage or with an immunogenic carrier protein), which could potentially demonstrate mechanistically this sensitization route that probably requires an adjuvant to play the role of an irritant and sensitizer. Indeed, QA compounds found in disinfectants, antiseptics, or detergents because of their antimicrobial properties are large amphiphilic molecules with a hydrophilic (positively charged QA molecule) region that can adhere to the negatively charged virus/bacteria and a hydrophobic (alkyl chain) region that can enter the lipid membrane to cause cellular leakage[193]. The allergenic properties of those compounds are suspected to be potentiated by their irritant, sensitizer, or adjuvant effects even though the mechanisms underlying the sensitization effects are still under investigation[193].

The fact that patients allergic to one NMBA can undergo an AHR to other NMBAs, even originating from a distinct chemical family (cross-reactivity), supports the indirect route of sensitization through structurally similar but distinct molecules. Cross-reactivity was first demonstrated by Baldo et al., using inhibition ELISA on sera of allergic donors with other NMBAs being more potent at inhibiting the signal than the one responsible for anaphylaxis in 50% of patients[98]. The incidence of cross-reactivity was estimated to be 80% by sIgE measurements and 65% by skin tests[194]. We also observed in Article1, that Patient#1 had rocuronium-specific mAbs even though that individual was exposed to atracurium and never to our knowledge to rocuronium. Another parameter for cross-reactivity is the flexibility of the carbon chain linking the QAs. More flexible NMBAs such as suxamethonium have been shown to trigger more mediator release thus being more cross-reactive than rigid backbone NMBAs such as pancuronium[195]. Our work opens a lot of questions concerning the origin of cross-reactivity. It is still unclear if the cross-reactivity of human sera originates from several sIgE antibodies recognizing each a different NMBA and/or the existence of cross-reactive sIgE binding to the conserved epitope across the NMBAs. From the data of the crystallized murine mAbs, we would speculate that antibodies were mostly monospecific at least for the same chemical family since 1B6, 2B1, and IP2 could only bind rocuronium and IP8 and IP11 rocuronium and vecuronium, both members of the aminosteroid chemical family, thus sharing similar chemical backbones. By pursuing screening for the specificity of the antibodies of other NMBAs such as pancuronium or vecuronium and by working on samples from other patients, we might be able to show a pattern of cross-reactivity. Did the patient studied in this work develop an AHR to atracurium by mounting an immune response towards rocuronium and by possessing some cross-reactive antibodies? Or did the patient mount an immune response capable of cross-recognizing atracurium separately from mounting an immune response capable of cross-recognizing rocuronium? Why do some patients cross-react to various NMBAs and not others? There are a lot of open questions by studying different profiles of patients, we might better understand the origin of the cross-reactivity, or at least anticipate it better.

So far, the most probable route of sensitization to NMBAs remains a cross-sensitization to QA-containing compounds present in the environment such as the molecule pholcodine found in anti-tussive syrup, detergents, or cosmetics. This hypothesis would explain NMBA-mediated AHR in naive patients, the cross-reactivity and it is supported by our crystal structure results. Following the exposition phase to NMBA mimicking molecules, the activation phase leading to anaphylaxis remains to be elucidated. In the following section we will discuss the underlying potential mechanisms: which cell subsets could be involved, how are the antibodies generated to recognize such a small molecule and what isotype of antibodies are potentially responsible for NMBA-mediated AHR?

6.2 The activation phase of anaphylaxis: who is responsible?

6.2.1 From Bmem to antibody-secreting cells

The fact that the antibodies found in the human repertoires possess a medium to low-affinity for rocuronium was not the result we anticipated: given the severity and the rapidity of the anaphylactic reaction, we would have presumed antibodies to require high-affinity to rocuronium. Additionally, the fact that the human antibodies isolated could not activate basophils and that only one mAb could degranulate mast cells raises questions concerning the biological relevance of our findings.

A potential explanation for the medium to low-affinity antibodies identified in human blood could be related to the experimental setting. Are our results biased by where we are looking at? For instance, we searched for Bmems since they express antibodies at their surface, thus making their isolation easier than plasma cells but Bmems tend to possess lower affinity BCRs than long-lived plasma cells[196]. Indeed, in a mouse model with an adoptive transfer, Weisel et al., showed that Bmem formation precedes long-lived plasma cell generation[196]. In this work, the authors also demonstrate that a fraction of long-lived Bmem expressing IgM antibodies is formed before GC reaction, hence producing poorly mutated and lower affinity antibodies. In the method we used in this work to sort Bmem (protocol originating from Kuei-Ying Su et al.,[197] and optimized from Sokal et al.,[198]) Bmem were transformed *in vitro* in ASCs using a cocktail of cytokines and feeder cells expressing CD40L (Fig 11). A negative selection (IgD dump) was performed and not a positive selection for IgG antibodies since we observed that adding a fluorochrome-labeled anti-IgG antibody in the sort decreased the yield of IgG-producing ASC at the end of the cell culture, which could be explained with anti-IgG mAbs interfering with IgG production. Indeed, antibody binding to the BCRs could cross-link the IgG BCRs and engage their signalization pathways, thus interfering with the proliferation or differentiation of these B cells. Therefore, 30% of B cell cultures positive for IgG antibodies were also positive for IgM. After sequencing, both heavy and light chains had identical variable regions which hints that these cells originate from an IgM-expressing Bmem that underwent a class switch recombination IgM → IgG *in vitro* in the cell culture since it is compatible with the half-life of IgM antibodies (5-6 days). From the original protocol, Kuei-Ying Su et al., observed this class-switch recombination on day 8 of cultures with 5 – 20% of cultured naïve mature B cells expressing membrane IgG and increasing gradually to peak at 30% – 40% of B cells by day 14[197]. It is unclear if this unintentional bias in the system might have favored the selection of lower affinity IgG antibodies *in fine* and if it necessarily reflects biological reality. On the one hand, the IgM+ B cells are less affinity matured and tend to be of lower affinity due to their pentavalent binding mode, on the other hand, some very high-affinity

IgM+ B cells undergo GC reactions and have been described[199]. Regardless, we later optimized the protocol by removing IgM-expressing B cells, using an IgM dump staining. So far, the preliminary results of this protocol modification do not seem to increase the affinity of the selected antibodies but this optimization step will be further investigated. Due to practical reasons as well, we searched for Bmems circulating in peripheral blood but we might have been overlooking the major Bmem reservoir: the spleen[200].

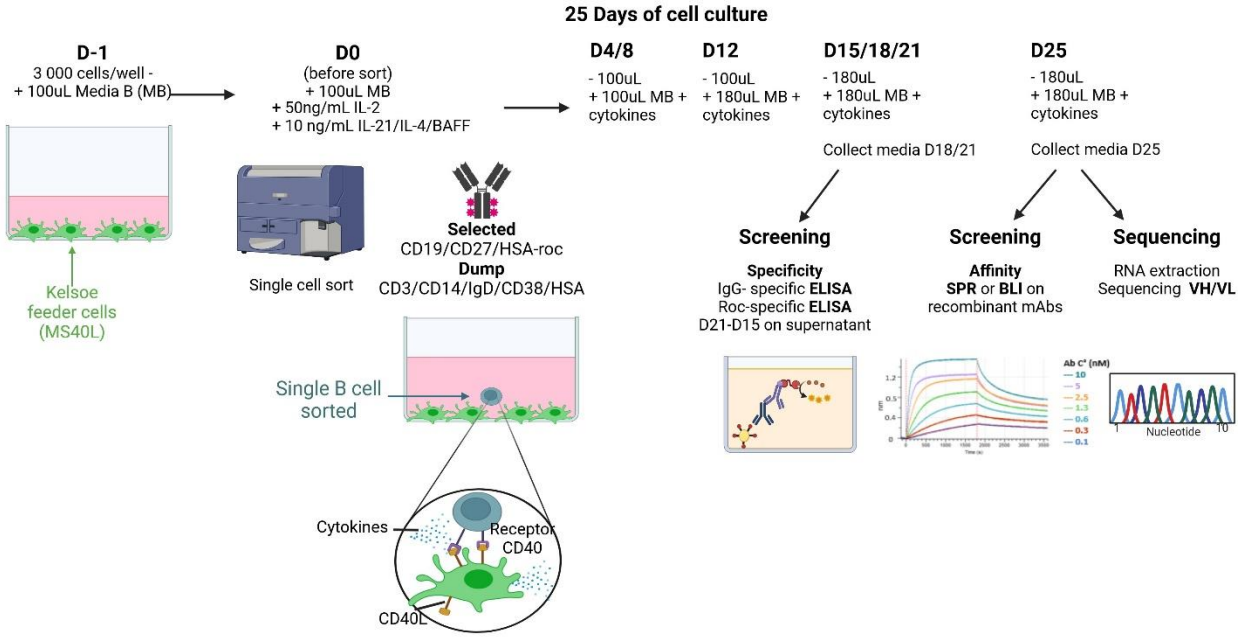

Figure 11: Pipeline to sort and culture antigen-specific IgG from Bmem cells into antibody-secreting cells.

Bmem cells from PBMC of allergic patients were sorted in 96 well plates in the presence of CD40L-expressing cell lines. Cytokines (hIL-2, hIL-21, hIL-4, and BAFF) were added to the media. Once at D18-21 and once at D25 in cell culture, the supernatant is collected and tested by ELISA or BLI for antigen-specific binding of the IgG present in the supernatant. At day 25 cells are collected, their RNA extracted, and their antibody genes sequenced for repertoire analyses and future expression as recombinant IgG. The protocol originated from Kuei-Ying Su et al.,[197] and was optimized from Sokal et al.,[198]. BAFF, B cell activating factor; BLI, Biolayer Interferometry; CD40L, Cluster of Differentiation 40 Ligand; D, Day; HSA, Human Serum Albumin; IL-, Interleukin-; SPR, Surface Plasmon Resonance; VH, Variable Heavy chain; VL, Variable Light chain. (Biorender).

Another bias that could explain the selection of low-medium affinities IgG antibodies is the use of carrier:rocuronium conjugates to select the rocuronium-specific BCRs during the single cell sorting. To increase the yield of this experiment, we used carrier:rocuronium complexes with a high ratio of haptens grafted on a carrier protein. Therefore, IgG antibodies were selected for their avidity and not affinity since the BCRs could bind several molecules of rocuronium. The subsequent selection process with HSA-rocuronium-specific ELISA also favors the selection of high avidity antibodies since this step uses as bait the haptenized complex. We tried to solve this caveat by generating rocuronium-peg-biotin streptavidin

complexes with monomeric streptavidin to generate rocuronium conjugates bound to a protein with a 1:1 ratio. These tools were used only for affinity measurement but not the sorting of B cells and gave inconclusive results since the detection threshold of biolayer interferometry was too low to detect any binding mAb. A potential perspective could be to sort a double rocuronium-positive population, with one fluorochrome bound to a rocuronium complex with a lower ratio of rocuronium molecules or even a single rocuronium and to compare the affinity of the isolated antibodies.

It is difficult to decipher if the differences in affinities obtained in the repertoire of immunized mice and exposed patients reflect biological reality or if it is biased by the model used. To complement this work, an interesting perspective would be to investigate the anti-rocuronium IgE plasma cells repertoires of long-lived IgE+ plasma cells that niche in the bone marrow of allergic individuals or immunized mice to compare the repertoires and affinities of the rocuronium-specific IgG and IgE antibodies. This supplementary information would allow us to better speculate on the origin and evolution of the antibody isotypes. After having investigated the different B cell subsets that could be involved in antibody production, we will now investigate what this work can teach us about the dynamic of antibody production and maturation in the GCs.

6.2.2 GC considerations: disputable involvement and the kinetic evolution

The current dogma would presume that the generation of haptens-specific mAb would require a GC-dependent mechanism. The murine antibody repertoires possessed few clonal groups which hint at multiple rounds of clonal selection, and accumulation of hypermutation driven by an intraconal selection in the GCs. Nonetheless, this hypothesis is disputable since among the 30 mAbs expressed recombinantly, we did not find a correlation between affinity and the number of amino acid mutations. Additionally, we never identified germline sequences that bound rocuronium and few mutations (up to 3) were sufficient to reach sub-nanomolar affinity, with no increase with added mutations. Therefore, in the mice model, it seems likely that some B cells undergo affinity maturation but that this mechanism is not a requisite for high-affinity for rocuronium.

Concerning the antibodies isolated from the allergic patients, the mutational loads were also diverse with the best binder (1F10) being poorly mutated and other binding mAbs highly mutated. To confirm the necessity of a GC-based affinity maturation process, we would need to retrieve the germline sequences of diverse mAbs and test their binding for rocuronium. Nonetheless, in the human model, the methodology used biased the selection of GC-derived B cells since we selected $CD27^+$ cells. Indeed, we excluded atypical

Tbet$^+$ B cells that are primarily extrafollicularly derived B cells[201]. Therefore, in this work, we can only draw conclusions concerning the GC-dependent mechanism which does not imply that an extrafollicular response is not possible, which has been shown in several studies for instance about SARS-Cov-2 vaccination[202].

Sampling the same patient with a nine-year interval gave us insights into the evolution kinetics of the Bmem repertoires and opened a lot of questions. GC are transient and evolving structures in which B cells proliferate rapidly, within 4-6 hours after antigen exposure. It was shown with a slow delivery immunization approach in rhesus macaques that the lifespan of GC can be extended up to 6 months with evidence of continuous activity and selection in the absence of further antigen exposure[203]. Bmem can persist for a lifetime which justifies vaccination strategies for example with individuals vaccinated 40 years ago against smallpox who still possessed persistent Bmem clones over such a long period[204]. Nonetheless, it is still unclear if nine years later, the Bmem isolated originate from identical GCs to the original ones or if *de novo* GCs were formed. The study of the evolution of repertoire within nine years also hints that this maturation process is dynamic and evolving. The decrease in mutation load for Patient#1 between 2014 and 2023 suggests that the Bmems isolated nine years later did not undergo subsequent GC-based affinity maturation processes. To our knowledge Patient#1 was not exposed to NMBAs during these nine years. Whether this evolution can be explained by the absence (or not) of exposure to QA-containing compounds during this period remains unclear since we did not gather information on the patient's exposure to QA-containing compounds during these 9 years. In this work, the majority of the mAbs characterized came from the PBMC sort of Patient#1 in 2014, whereas the ones from the same patient sampled in 2023 are in the process of being produced as recombinant mAbs. It would be interesting to compare the affinity of the antibodies isolated in 2014 and 2023 to decipher if this affinity maturation process correlates with increasing, decreasing, or stable antibody affinities. Nonetheless, the panel of characterized mAb would need to be elevated to draw firm conclusions in order not to bias the results with aleatory factors. On the contrary, the fact that we identified the identical most predominant VJ recombination in the antibody repertoires of the same patient with 9 years interval hints at a conserved BCR selection with time, hence the recall of pre-existing GCs years later.

It is possible that both cell subsets (B cells generated by either pre-existing or *de novo* GCs) were generated and involved in the immune response such as for viral vaccination. Indeed, it has been shown during seasonal influenza that immediate plasma cell response relies on pre-existing Bmem but also on naïve B cells novel response that can target new epitopes[205]. Garnett Kelsoe and his team studied the role and

evolution of a GC in the generation of long-lived antibody-secreting cells in the bone marrow of mice immunized with NP-OVA[206]. Their work confirmed that GCs are necessary to generate high-affinity antibody-producing cells but that they are not the only sites for affinity-driven clonal selection. They also showed that affinity-based selection in the bone marrow occurred long after the end of the GC reaction. Nonetheless in this mode, the localization and mechanism of clonal selection post GC environment remains unanswered. One possible explanation is that affinity maturation continues to take place after GC disappearance in the bone marrow, but it is also possible that high affinity plasma cells proliferate more after getting out of the GC than those with lower affinity, so the overall affinity of the plasma cell compartment in the bone marrow increases which increases the overall antibody affinity. The fact that subsequent selection for higher affinity antibody-producing cells does not necessarily require GCs could explain why Patient#1 still possesses NMBA-specific Bmem long after antigen exposure. The remaining questions are: how does clonal selection take place in the post-GC environment and how are Bmem cells maintained with time?

The evolution of Bmem GCs is thought to be tightly driven by antigen exposure by follicular dendritic cells even though it is still unclear whether memory necessitates a persistent antigen exposure or if Bmem can be re-activated years later by a punctual stimulation. It was first shown by adoptive transfer experiments that antigen presence is necessary for the persistence of Bmem[175], then experiments on mice lacking follicular dendritic cells and GCs disputed these results and demonstrated that the antigen-specific Bmem cells were resting and can persist in the absence of antigen persistence[177]. The second hypothesis was further supported with a model of mice possessing a genetic switch mediated by Cre recombinase[178]. Mitsuo Maruyama et al., generated an irreversible switch in the VH locus to equip mice with a Bmem specificity that did not recognize the inducing antigen. They showed that Bmem persistence did not require persisting immunizing antigen and that Bmem switching their antibody specificity away from the immunizing antigen was indeed maintained in the animal over long periods of time[178].

Immune memory is also thought to be influenced by the first cohort of B cells that encountered the original antigen, which is referred to as the theory of the antigenic sin[207]. At a close time point to the first antigen exposure, the antigenic sin phenomenon is highly predominant, and the existing antibody response prevents the emergence of novel antibodies due to the boost of primarily established GC. But this tendency decreases as time increases between the priming and the boost[208]. This theory initially exposed in the 1950s[207] is nowadays supported by molecular fate-mapping tools established by D. Victora[208] which permit the tracking of antibody generation by distinguishing old antibodies from new ones in mice serum

following antigen exposure. In the case of NMBAs, it is highly probable that patients were continuously exposed to similar antigens in their environment but that this antigen was not unique, hence generating cross-reactive BCRs. An elegant bioinformatics model studied the evolution of cross-reactive GC. This work tried to explain the evolution of affinity maturation after immunization either by a "chimera" (heterotrimer) or a cocktail of three homotrimer epitopes. Previous *in vivo* work demonstrated that immunization with the chimera elicits better neutralizing antibodies. They showed that the valency and diversity of the antigens were two important factors in engaging cross-reactive B cells[209]. In the context of our work, the immunized mice would have a closer mechanism to the chimera antigen whereas patients would be exposed to a cocktail of antigens, which could explain the difference in diversity and affinity of both repertoires.

Since the original antigen triggering the immune response remains speculative in NMBA-mediated AHR cases, it is very difficult to understand the dynamic of antibody generation and maturation. Our results hint at a GC-dependent response given the high mutation load of the BCRs. Since patients are likely exposed to distinct antigens over time with related epitopes, it is highly probable that pre-existing GC centers generating antibodies against the conserved motif can be recalled to improve affinity maturation against the culprit NMBA. This affinity maturation process and the generation of antigen-specific BCRs allows B cells to be involved in the humoral response by secreting antibodies following exposure to antigen-presenting cells and T cells. The potential mechanisms for B cell activation, including non-canonical pathways will be discussed in the following sub-sections.

6.2.3 The effector phase of AHR and the role of T cells

In rocuronium-immunized mice, we can anticipate that the generation of NMBA-specific B cells is T-cell-dependent with a bystander activation effect. This bystander effect occurs when an antigen-induced T cell is activated in an antigen-independent manner (TCR independent) due to the presence of a cytotoxic context and inflammatory cytokines (Fig 12). Indeed, KLH is an immunostimulant carrier protein that drives T-cell mediated immune responses, which has been extensively studied in mice and humans since it is often used as an adjuvant in cancer vaccine[210]. Concerning the generation of NMBA-specific mAbs in humans, it still remains unclear if the pathway is T-dependent or independent. One could speculate that the generation of specific IgE and IgG antibodies would require NMBA-specific T cells to trigger the humoral response by activating B cells and inducing a class switch. Indeed, the existence of NMBA-specific memory T cells has been demonstrated in human PBMC[211], and the consensual pathway to generate sIgE requires T helper cells (CD4+ cells) or cytotoxic T cells (CD8+) to generate B cell producing IgE antibodies.

Studies in mice have shown that in the absence of T cells, sIgE generation requires additional stimuli than IL-4[212], such as Toll-like receptors ligands[213] or BAFF stimulation[214].

Interestingly, Marine Peyneau showed in her thesis[215] that QA-containing compounds and pholcodine induced activation and maturation of dendritic cells and T cell proliferation whilst rocuronium and suxamethonium did not. Indeed, pholcodine activated opioid receptors on monocyte-derived dendritic cells and induced T cell activation and proliferation. These results are an additional argument in favor of NMBA sensitization by pholcodine or QA-containing compounds in the context of NMBA-mediated AHR since the activation phase of the immune response by pholcodine has been elucidated[215] (Fig 12). Allergic reactions triggered by cross-sensitization have, indeed, been previously described in the context of anaphylaxis against the anti-cancer mAb cetuximab or allergies to non-primate red meat (referred to as the Alpha-gal syndrome) in non-exposed patients. For instance, tick bites were shown to induce IgE pre-sensitization to galactose-alpha-1,3-galactose (an oligosaccharide found in mammalian cell membranes) which concomitantly triggered cross-reactive IgE antibodies involved in allergies to red meat or cetuximuab[216]. In the context of NMBA-mediated AHR, the activation of antigen-presenting cells and T cell proliferation via QA-containing compounds such as pholcodine could explain NMBA-mediated AHR via this cross-sensitization pathway.

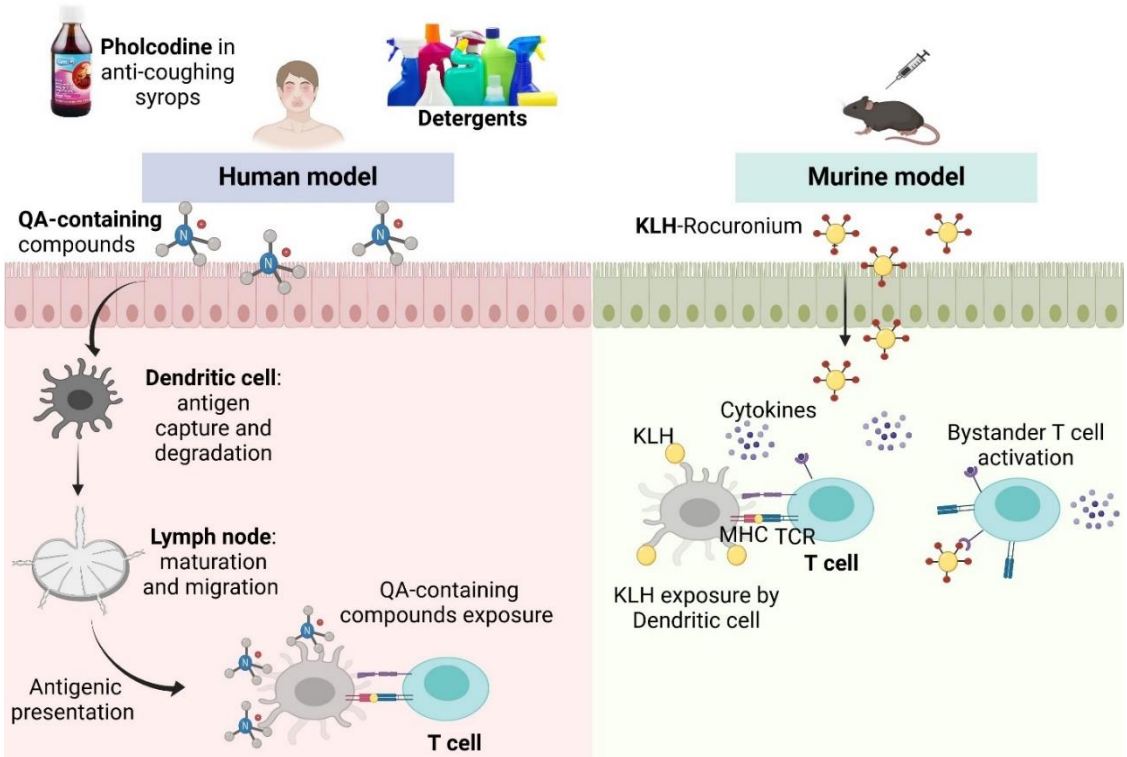

Figure 12: Comparison of the potential sensitization routes at the origins of rocuronium-specific mAbs in the different models.
Allergic patients are probably exposed to QA-containing compounds present in the environment. Mice are immunized with KLH-rocuronium, hence potentially initiating a bystander T cell activation effect. KLH, Keyhole Limpet Hemocyanin*;* MHC, Major histocompatibility Complex; QA, Quaternary Ammonium. (Biorender).

Even though it is less probable, we cannot eliminate the possibility of a T cell-independent mechanism. Indeed, T-independent mechanisms can be of type I (activation mostly by bacterial polysaccharides which causes B cell proliferation independently of BCR specificity but via Toll-like receptors) or type II (antigens with a repetitive structure which leads to the cross-linking and activation of BCRs). It was shown in mice that T-independent type II immune responses can generate Bmems lasting for months after immunization elicited by liposaccharide and bacterial antigen[217]. In the case of haptens, it is highly probable that the underlying mechanism requires T cell activation but since the hapten can be presented in the form of a repetitive structure carried by a protein, a T-independent type II immune response cannot be 100% excluded.

Regardless of the involvement of T cells, B cells are necessarily activated to explain antibody production, hence the activation of effector cells and the symptoms of an AHR. The following subsection will discuss on the different antibody isotypes potentially involved in NMBA-mediated AHR.

6.2.4 The role of antibodies: the close (or not) relation between IgG and IgE antibodies

My lab has previously demonstrated that two pathways can be involved separately or concomitantly to mediate an NMBA AHR. The canonical type 1 AHR involves sIgE leading to mast cell and basophil activation with histamine mediator release whereas the non-canonical type 2 pathway involves IgG antibody immune complexes leading to neutrophil and monocyte activation and subsequent PAF release. Both mediators are responsible for the clinical symptoms inducing vasodilation, bronchoconstriction, and cardiac and pulmonary failure[93]. Therefore, we decided to isolate IgG-expressing B cells in the first place, as they might be precursors of class-switched activated B cells expressing later IgE antibodies. A main challenge remains the understanding of the origin of IgE antibodies. Would the specific IgE antibodies necessarily originate from IgG antibodies or could they come from a direct switch from an IgM antibody? Looney et al., demonstrated that in humans, most IgE originate from mutated IgG1-expressing B cells and to a lesser extent from IgM or IgD[167].

The existence of IgE Bmem remains controversial. On one hand, it was shown in a reporter mouse expressing green fluorescent protein associated with membrane IgE transcripts, that serum IgE can be

produced by IgE^+ Bmem that later differentiate in plasma cells[218]. On the other hand, even if IgE Bmem would exist, their life span is limited by several factors: 1) IgE switched B cells are programmed to rapidly differentiate into PC, 2) IgE bearing cells in GC are transient and rapidly undergo apoptosis[219], 3) the generation of IgE-B cells is less favored (genetic mechanism that induces inefficient processing of mRNA of the membrane-bound form of IgE in the murine and human epsilon heavy chains)[220].

The existence of IgE-secreting plasma cells in chronically exposed mice to house dust mites and in the bone marrow of human allergic patients was described by Asrat et al.,[221]. These results in humans were supported by two recent studies in which Ota et al. and Koenig et al. demonstrated the existence of a type 2 Bmem population characterized by the expression of IgG antibodies, CD23 (the low-affinity IgE receptor, FcεRII), IL- 4 receptor (IL- 4R), and germline IGHE in peanut-allergic children[222] or birch pollen/house dust mites allergic individuals[223]. Koenig et al., further demonstrated that this type 2 B cell phenotype with the presence of Th2 cells required IL-4 but that circulating IgE and GCs were not essential. Their results also demonstrated that somatic hypermutation and the production of high-affinity allergen-specific IgE were driven by IL-13 and IL-4 produced by follicular Th cells. These two papers draw the conclusion that "it takes two" to make IgE in allergy: 1) a type 2 phenotype mediated by the presence of IL-4 and 2) high-affinity BCR specific for the allergen[224].

Interestingly, in my PhD work, not all the human IgG anti-rocuronium mAbs isolated could activate mast cells, and basophils and induce passive systemic anaphylaxis when switched to an IgE isotype, only the ones with the highest affinity. The question remains if there is an affinity threshold for antibodies to switch from an IgG to an IgE or for these IgE antibodies to activate effector cells. Similar results were obtained in short-term exposed mice to house dust mites that resulted in the production of IgE from plasma cells that could not degranulate mast cells using a passive cutaneous anaphylaxis model and serum transfer[221]. Nonetheless, with chronic allergen exposure, the mice could generate long-lived IgE PC niched in the bone marrow and the IgE antibodies were capable of inducing anaphylaxis. In the context of our work, patients were exposed to a variety of compounds and it is difficult to track if their exposure was chronic or not since their route of sensitization can be punctual and diverse: oral (syrop), cutaneous (detergents, cosmetics, disinfectants) or respiratory (hair products, aerosolized droplets from cleaning sprays). In most cases, excluding professional allergies (hairdressers or employees frequently exposed to cleaning products), we could speculate that the exposure would be punctual which could partially explain the low-affinity of the human mAbs isolated. Since the existence of long-lived IgE+ PC has been demonstrated in allergic donors, a perspective of the project would be to isolate IgE+ plasma cells in the bone marrow of

the allergic patients and to compare the repertoires with the ones obtained from IgG+ Bmem. If the existence of IgE+ Bmem were to be true, and if this cell subset would originate from IgG+ Bmem, then the two repertoires obtained would have similar clonal families and predominant V(D)J genes.

Whether the incapacity of the human IgE antibodies to trigger anaphylaxis reflects the biological reality or if it could be explained by experimental limitations, remains an open question. Indeed, our models show some limitations since the lower sensitivity of the basophil activation test compared to the mast cells activation test could be explained by experimental factors. First, the basophil test is undertaken on whole blood whilst the mast cell test is performed on mast cell cultures derived from isolated $CD34^+$ cells that were cultured for one week in serum-free conditions. Therefore, mast cells have their FcεRI free from any IgE, whereas IgE antibodies were pre-bound to the basophil. In addition, serum proteins present in the basophil activation test could interfere with the binding of IgE so this test could be optimized by pre-washing the cells. For the passive systemic anaphylaxis model, with very high-affinity mAb generated from immunized mice (IP2, IP11, and IP8), anaphylaxis was triggered with mAb concentrations as low as 1µg of IgE and allergen concentrations as low as 2µg of HSA-rocuronium. Whereas for lower affinity mAbs such as murine IP12 and human 1F10, doses of 20 µg of specific IgE antibodies were injected twice within 24H and challenged with 267µg of HSA-rocuronium. This protocol forces the overexpression of FcεRI on the surface of effector cells (that upregulate their receptor expression in the presence of monomeric IgE)[225] but certainly does not reflect reality due to the scarcity of circulating IgE antibodies in humans.

Whilst this project did not directly focus on the antibody-independent pathway mediated by MRGPRX2, our results showed that HSA-rocuronium alone on unsensitized isolated mast cells could not trigger their degranulation. These results are in line with the findings of Elst et al., demonstrating that atracurium could induce mast cell degranulation via the activation of MRGPRX2 but not rocuronium[226]. It is still unclear why not all the NMBAs tend to activate MRGPRX2 as intensively as others. Indeed, suxamethonium and cisatracurium have been shown to possess the lowest potency for mast cell activation and atracurium the highest in human volunteers using intradermal insertion of microdialysis capillaries[96]. Can the higher incidence of anaphylactoid reactions mediated by atracurium be explained only by an isomer-specific effect or also by the higher potency of cisatracurium, thus lower dose injected than atracurium since this study also demonstrated that atracurium and cisatracurium had similar ED50 value for mast cell activation?[96] Nonetheless, the possible activation of human mast cells via the binding of NMBAs to MRGPRX2 receptor is mitigated by the fact that the NMBA doses tested in the previous studies are supra-therapeutic, even sometimes toxic. Most of the research has been performed on the ortholog murine

receptor (Mrgprb2)[95] which was shown to be more sensitive to NMBAs than the human receptor which questions the reliability of the results *in vivo*.

A lot of questions remain unanswered concerning the underlying mechanism of rocuronium-mediated AHR. The canonical pathway would require a GC and T cell-dependent generation of specific B cells that can produce IgG antibodies able to switch in the IgE isotype with both antibody classes involved in the activation of effector cells. Nonetheless, the incapacity of most human mAbs we isolated in this work and expressed as IgE antibodies, to activate basophils and mast cells suggests the involvement of IgG-mediated or antibody-independent potential additional pathways. Another unanswered question resides: how is the allergenic epitope presentation possible for such as small drug in the context of a GC-reaction and T cell help?

6.3 NMBAs' partner in crime: do they have one, who is it and do they need one?

6.3.1 The concept of haptenization to explain the effector phase

In the mouse immunization model, we artificially haptenized NMBAs on carrier proteins to elicit an immune response and to perform the downstream experiments. In humans, it is still unclear if a similar haptenization process occurs naturally with NMBAs. The first part of section §6.3 will defend the hypothesis of a natural haptenization phenomenon to induce NMBA-mediated AHR and the last part will propose alternative mechanisms.

At first sight, it seems necessary that NMBAs would naturally bind to a bigger carrier molecule to activate cells responsible for immune response. Given size considerations (rocuronium being equivalent to 2-3 amino acids, the CDR3s of mAbs between 10-20 amino acids, and the length of presented peptides by MHC molecules being typically between 8-11 amino acids[227]), we would presume that a multivalent drug-carrier complex would be required for rocuronium be presented by an MHC molecule (on follicular dendritic cells in particular) for T cell activation, to induce the cross-linking of IgE-FcεRI complexes on mast cells and basophils or to be bound as an immune complex by activating FcγRs. In our work, the 10-100 fold difference in affinity measured from the isolated mAb when rocuronium is grafted on the carrier HSA (using biolayer interferometry) or when it is a free molecule (using surface plasmon resonance), also suggests that rocuronium needs to be haptenized to bind antibodies with high avidity.

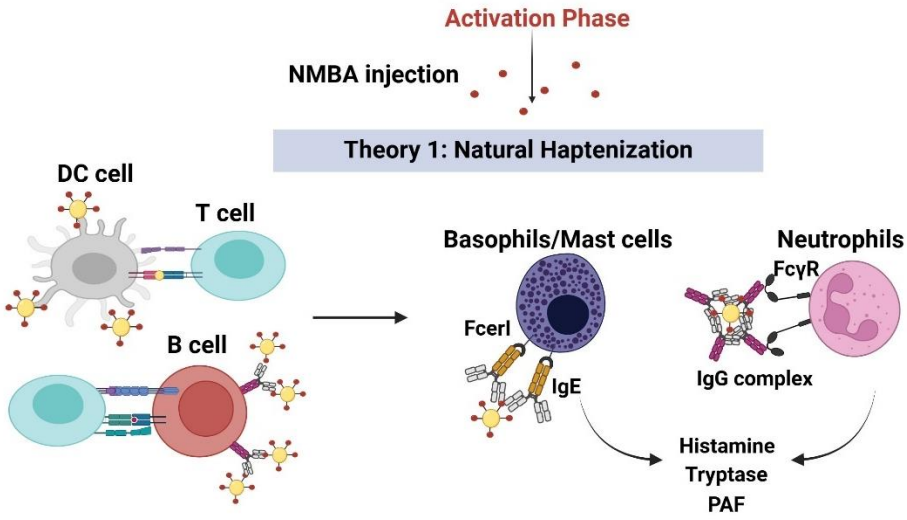

Figure 13: Underlying mechanisms to explain an NMBA-mediated AHR with the cross-sensitization and self-haptenization theories.
In this theory, patients are sensitized by QA-containing compounds found in the environment (such as pholcodine in anti-coughing syrop or detergents) for which T cell activation has been demonstrated[215]. Then, natural haptenization with a carrier molecule would occur to explain the activation phase. A carrier:rocuronium complex would allow the rocuronium to be presented by an MHC molecule (on dendritic cells or B cells) for T cell activation, to induce the cross-linking of IgE-FcεRI complexes bound as an immune complex by activating FcγRs on neutrophils. DC, Dendritic Cells; NMBA, Neuromuscular-Blocking Agent; PAF, Platelet Activating Factor; QA, quaternary-ammonium. (Biorender)

To prove if the carrier molecule is present in human serum, we could passively immunize mice with human serum of allergic patients and challenge them with free rocuronium. So far, our experiments lack to show evidence for this natural haptenization process. Indeed, mast cells and basophils pre-sensitized with sIgE could degranulate in the presence of HSA-rocuronium but failed to do so with rocuronium alone, even when pre-incubated with bovine serum albumin (BSA), HSA and human serum. The fact that even by preincubating rocuronium with human serum we never succeeded in reproducing natural haptenization might be due to chemical modifications of either rocuronium or the carrier with pH or temperature changes that remain unknown, potentially performed via intracellular enzymatic reactions. Indeed, since NMBAs lack chemically reactive groups it is highly probable that they would need to be metabolized to become chemically reactive to be able to bind to a carrier molecule.

Natural haptenization or chemical modification of haptens has been identified in several small allergens. For example, β-lactam antibiotic piperacillin (~500Da) has been shown to naturally form irreversible covalent bonds with the HSA in the serum, forming a protein abduct processed by antigen-presenting cells that exposed peptides associated with MHC molecules to activate T cells. Using quantitative mass spectrometry on the human plasma of drug-tolerant and hypersensitive patients, hydrolyzed haptens

were identified on lysine residues of HSA of both groups[228-229-230]. This natural haptenization process is thought to occur via chemical modifications on the lysine residues of HSA to generate antigenic HSA-derived peptides. Direct chemical modifications on the haptens enabling their immunogenicity can also occur. This phenomenon has previously been described in allergies against the antibiotic sulfamethoxazole (~253Da) that gained antigenicity by intracellular mechanisms occurring in the liver leading to its oxidation[231]. Haptens chemical modifications have also been described in the context of chemicals in skin allergies, in which electrophilic haptens interact with nucleophilic skin sensitizers or proteins[232]. In the case of non-electrophilic haptens, it has been hypothesized that disulfide linkages were formed which allows the binding to enzymes or cysteine residues[232]. Concerning rocuronium, we could have hinted at a potential *in vivo* chemical pathway by inspiring ourselves from the structure of rocuronium metabolites but it is excreted unchanged in urine (10–25%) and bile (>70%)[233]. Even though we are facing difficulties in understanding the chemical modifications occurring to rocuronium, can we provide more tangible leads to identify the potential carrier molecule?

6.3.2 Potential leads to identify a carrier molecule

In the context of allergic patients to NMBAs, it is highly probable that the carrier molecule would be a self-molecule already present in the body such as a protein. It is also possible (but less likely) that the carrier molecule would be a foreign molecule administered during surgery, such as an additive found with the administration of other drugs like hypnotics, sedatives, antibiotics, diuretics, or local anesthetics co-administered. So far, such an additive is not found in commercial rocuronium since it is conserved with classical salts (acetate and sodium chloride)[234]. Jönsson et al., tried to understand the haptenization chemistry as it may occur *in vivo* by looking at the interaction of NMBAs with HSA, orosomucoid (a carrier of acidic and neutral compounds), transferrin, and human IgG1 using microscale thermophoresis. Their conclusions lead to the observation of interactions in the millimolar range at NMBA concentrations 100 times higher than the standard intubation doses[93].

Presuming that the carrier molecule would be present in the body, how could we show evidence of its existence? We could try to first deprive antibodies from the blood, serum, or skin tissue of allergic donor using a protein G (for IgG) or omalizumab (for IgE) high-affinity columns, then pre-incubate a high-affinity rocuronium-specific human mAb with the “clean” human samples and free rocuronium. Admitting that the mAb would possess a very high-affinity with the carrier:rocuronium, the mAb:carrier:rocuronium would stay as a complex and we could purify again this complex using a protein G column (for IgG) or omalizumab (for IgE). Another idea would be to perform this technique the other way around by binding

rocuronium-specific mAb to an affinity column, eluting serum of allergic patients, and pulling down the mAbs theoretically bound to the carrier:rocuronium complex. Using size exclusion chromatography, western blot, mass spectrometry, or mass photometry, we could compare the sizes of the mAb alone and the mAb in complex with the potential carrier to prove the existence of the carrier molecule (if it exists).

Another caveat that we are facing in identifying the carrier molecule is that we are not certain where this haptenization process would occur, would it be in circulation in the blood or at the skin level? Depending on the localization of the potential haptenization process, then the cell subsets involved, the environment (pH), and the proteins (enzymes?) would be different. It is more probable that haptenization would happen at the skin level than in the blood since the elevation of total IgG1 and IgE in blood from exposure to a small drug has not been reported in humans, only in mouse models[235] and elevated IgE concentrations in humans has only been shown on bigger proteins such as house dust mite and pollen. Most models on allergies to haptens are indeed studied at the skin level where it has been shown that haptens alone can sensitize mice and cause skin inflammation with an increase of plasma IgE and IgG1 and gene expression of IL4 and IFNγ[236]. This study was in line with the one of Dhingra et al showing that hapten allergens induce both Th2 and Th1-type responses on patch-tested human skin samples.

Despite the lack of evidence of the carrier molecule for NMBAs, it is difficult to conceive the effector phase of NMBA-mediated AHR without its existence. Could this natural haptenization process occur at a different stage as well?

6.3.1 A case scenario: haptenization during the sensitization phase explained by a break of self-tolerance

In this subsection, we will imagine that haptenization occurs during the sensitization phase to look at the impact on the cells that could be involved. Haptenization could occur during allergen exposure in two scenarios:

1) Patients sensitized by exposure to NMBAs. This includes patients who were exposed to an NMBA, did not do a shock for years and one day did a shock to the same NMBA or another one. This is possible given the profile of Patient#1 who did a shock to atracurium but possesses rocuronium-specific antibodies.

2) Patients never exposed to NMBAs but potentially cross-sensitized by QA-containing compounds for which the sensitization mechanism has not been elucidated and that are also haptens that would

necessitate binding to a bigger molecule to activate cells during the sensitization phase (pesticides, disinfectants, detergents, sanitizers, and cosmetics).

Since NMBAs are non-immunogenic and the carrier molecule is very likely to be a self-molecule already present in the body, the immune response could be explained only if self-tolerance would be broken. This context would explain the low-affinity of the antibodies identified and would open a door to the theory of poly-reactive cell subsets involved in the mechanism.

To understand the potential underlying mechanism we need to travel back to the 1970s when vaccination against the hapten 2,4-dinitrophenyl (DNP) bound to BSA was performed in rabbits rendered immunologically tolerant to BSA. The authors rendered rabbits immunologically tolerant to BSA, vaccinated them with DNP-BSA, and investigated the binding mode of the antibodies using inhibition ELISA. This study revealed three main results: 1) rabbits tolerant to BSA and immunized to DNP-BSA produced antibodies with a greater avidity for DNP-BSA than BSA, (they bound little or not to BSA), 2) immune tolerance against the carrier protein led to the production of better avidity antibodies against the hapten-BSA than “normal” rabbits not rendered tolerant to the carrier, 3) the cross-reactive antibodies produced in tolerant rabbits had no specificity for the DNP group alone, and were probably binding to BSA via modifications of the BSA molecule resulting from the presence and/or coupling of DNP group. This work argues in favor of tolerant immune cells that could play a role in immunization against hapten-self-carrier proteins. In this context, an antibody recognizing a self-antigen would break tolerance when the antigen would be slightly modified (e.g.: coupling to haptens).

In the context of self-haptenization, the antigen would need to bind to a self-molecule already present in the body. This molecule would be non-immunogenic under its natural form (if we consider that the patient is not autoimmune), but tolerance would be broken when haptenized to rocuronium/QA-sensitizing compounds by potential conformational/structure modifications. Tolerant immune cells such as Th could be involved by predominantly recognizing the self-protein carrier protein to which the body is tolerant. By sorting CD27+ cells, we inadvertently excluded a subset of Bmem, referred to as T-bet+ B cells that are protective, GC-derived, and could be involved in this tolerant mechanism. A perspective of the project would be to use a more appropriate Bmem marker that would identify the early memory population, referred to as the CD45RB to include this subset of protective Bmem[201]. This hypothesis would also explain why it was difficult to identify real negative controls in the general population. Indeed, when screening for NMBA-specific IgG in the serum of human samples, the “negative” controls used as a reference often possessed high levels of IgG NMBA-specific antibodies. It is also possible that self-reactive cells like

regulatory T cells (T_{regs}) might be involved, which would dampen the immune responses since the carrier is not immunogenic. It is probable that what we observe is part of the adaptive immune response and that the majority of the population possesses weak antibodies against QA-containing molecules (and/or NMBAs if they have been exposed to them).

As mentioned previously, work on AHR to small drug β-lactam antibiotic piperacillin could give us more insights into the mechanism underlying natural covalent modification of self-proteins that induce self-tolerance disruption since this antigen has been demonstrated to covalently bind to HSA molecules[228-229-230]. It has been shown that levels of piperacillin-HSA modifications that activated T cells were equivalent in tolerant and sensitive groups but that the CD4+ clones expressed a more restricted Vβ repertoire in hypersensitive patient[230]. Thus in this context, the propensity to develop an AHR depends on the T cell repertoire and/or an imbalanced immune regulation rather than antigen concentration or conformation[230]. A similar conclusion was drawn concerning nickel-mediated AHR (metal of 44Da) in which allergy severities were correlated with the content of TCR repertoire. It was shown that specific amino acids in the CDR3α of the VB17+ of CD4+ TCRs were crucial for antigen recognition[237 -238].

This concept of NMBA natural haptenization to sensitize patients is counterintuitive since in immune system is trained not to elicit an immune response against self-proteins. In this context, haptenization to a self-protein would require breaking immune tolerance to sensitize the patients either by the generation of a neo-epitope due to conformational changes during the haptenization process or by generating reactive T cells possessing restricted TCR repertoire specific for the antigen. The sensitization phase is therefore very likely envisioned without the haptenization theory with the concept of cross-sensitization by QA-containing compounds that do not require self-haptenization. Given the difficulty in identifying a carrier protein and the absence of chemically reactive groups of rocuronium, would it be possible that NMBAs are not haptenized in the body? In the following subsection, we will question the haptenization theory and provide thoughts for alternative mechanisms.

6.3.3 Proposition of alternative mechanisms bypassing haptenization to a carrier molecule

First of all, kinetic considerations favor a carrier-independent mechanism. Indeed, when considering the rapidity of the symptoms of anaphylaxis that can appear within a few minutes after injection of the NMBA, it seems incompatible with the timeframe of natural haptenization that has been demonstrated to take hours (up to 24H)[230] in the context of natural haptenization of beta-lactam antibiotics to HSA[229]. Self-haptenization kinetic has only been studied in this context, therefore it is impossible to state whether this

time frame can be generalized. Additionally, NMBA grafted on a carrier protein would not be able to extravasate the cutaneous blood vessels to activate mast cells in the skin due to their high molecular weight if conditions would not enable vasodilatation and barrier opening. Only free rocuronium molecules which are hydrophobic and small enough could diffuse, enter the extracellular matrix, and activate basophils in a competitive timeframe that could explain the rapidity of the symptoms. Therefore, either the carrier molecule that induces effector activation would be located also in tissues (nearby mast cells) or non-covalent binding with rocuronium and a serum protein could activate basophils in the blood and mast cells in tissues. One can also imagine that basophil activation would lead to systemic inflammation and could allow NMBA-molecule complexes to extravasate towards tissue mast cells.

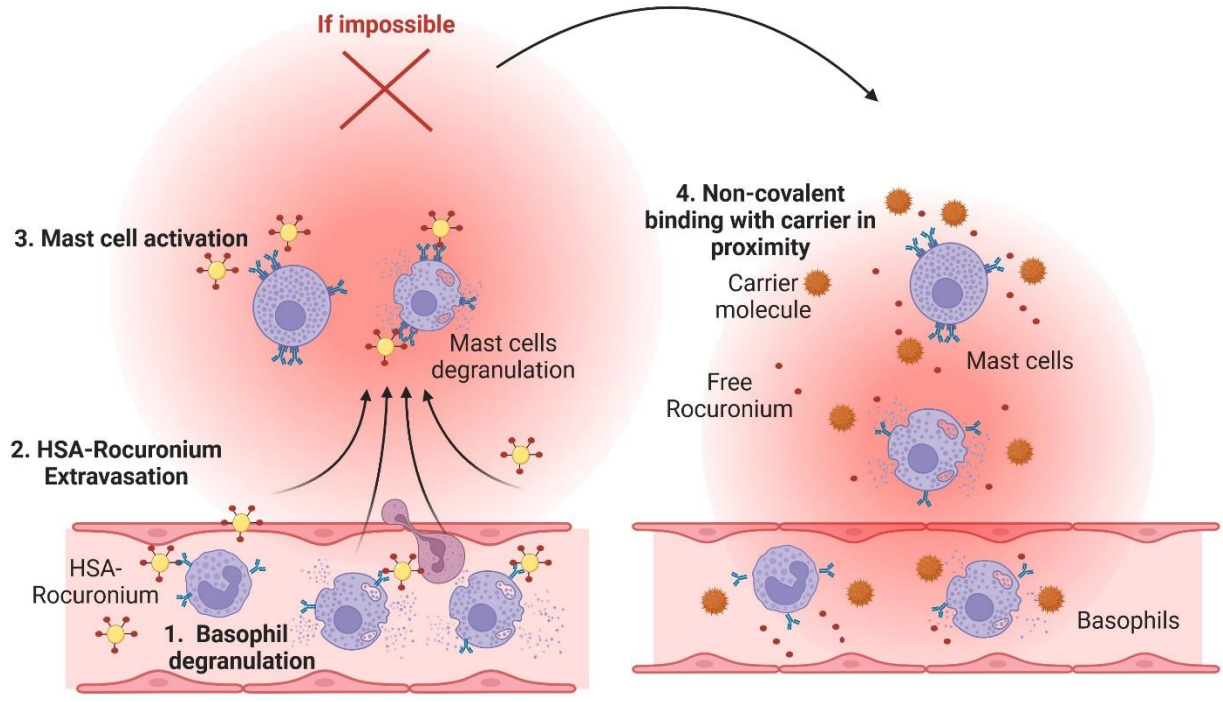

Figure 14: Mechanism to explain mast cell activation if the theory of self-haptenization were to be true or not.
Since mast cells are mostly located under the skin, their activation would require the extravasation of rocuronium outside blood vessels. Supposing that the haptenization theory was to be true, then we would difficulty understand how the carrier:rocuronium complex would extravasate cutaneous blood vessels given the high molecular weight. Therefore, the first hypothesis is the activation of basophil (1) that would lead to a systemic inflammation that would allow the rocuronium:complex extravasation (2) and the

activation of mast cells (3). If the self-haptenization theory were to be false, then the activation of effector cells would require non-covalent binding with a serum protein present in the nearby environment (4).

An alternative hypothesis to the carrier:hapten dogma would be that dendritic cells and/or T cells can be activated via direct binding to TCRs or MHC molecules (Fig 15). For instance, concerning allergies to metal, it has been shown for nickel allergies that the metal-protein bounds are not strong enough to survive antigen processing by antigen-presenting cells. It was proposed that nickel links TCRs and MHC in a carrier-protein independent manner by forming non-covalent coordination complexes in which Ni^{+}ions can interact with MHC-embedded peptides to form a hapten-like epitope for nickel-reactive T cells[237-238]. Additionally, Pichler et al., introduced the pi-concept which consists of the direct activation of T cells via non-covalent binding of the TCR with haptens through Van der Waals forces/hydrogen bonds. This mechanism has been described in allergies against small drugs such as lidocaine (234Da) and p-phenylenediamine (108Da)[239].

Other mechanisms that could explain the humoral response in the absence of haptenization would be through bystander T and B cell activation. Through this mechanism, non-antigen-specific lymphocytes can be activated in the presence of signals that favor an inflammatory environment: cytokines, chemokines, pathogen-associated molecular patterns, etc (Fig 15). This mechanism is well studied to understand autoimmune diseases that are characterized by a loss of immunological tolerance to self-antigen[240]. The concept of T cell activation independent of TCR signaling has been studied since the 1980s in the context of viral infection[241] and several cytokines (type I interferon, IL-2, IL-6...) have been shown to mediate this activation. Bystander B cell activation has been demonstrated *in vitro* and *in vivo* in mice by using B cell mitogen (lipopolysaccharide), which leads to the transfer of antigen-specific BCR. Since B cells have been demonstrated to activate T cells by capturing and processing a specific antigen for presentation on HMC class II molecules[242], the authors addressed the question of whether bystander B cells could also play this role. They showed that bystander B cells also gained their ability to activate $CD4^{+}$ T cells which could increase the antigen-presenting pool[243].

Alternatively, the antibody-independent pathway through MRGPRX2 activation is another potential lead that could explain symptoms of AHR without activation of lymphocytes or dendritic cells (Fig 15). Concerning rocuronium it is very unlikely given the receptor's low-affinity for rocuronium in humans, but for other NMBAs, it remains speculative.

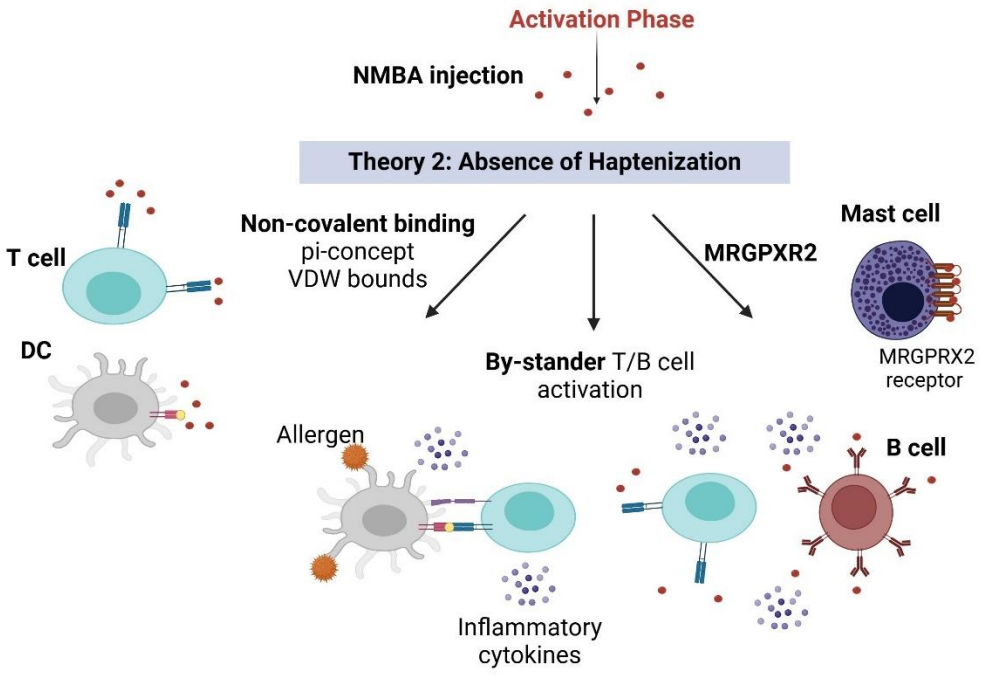

Figure 15: Potential mechanisms to explain the effector phase in the absence of the haptenization theory.
In this theory, T cells, B cells, and DC could be activated either by non-covalent binding or bystander activation. The MRGPRX2 pathway could also explain mast cell activation with free rocuronium. DC, dendritic cells; MRGPRX2, Mas-related G-protein coupled receptor member X2; NMBA, neuromuscular blocking agent; VDW, Van Der Waals. (Biorender).

To summarize, we are uncertain about the underlying mechanism that can explain the activation of antigen-presenting cells, T cells, B cells, and effector cells (basophil/mast cells) by NMBAs. The haptenization hypothesis remains the most plausible one but the nature of the carrier protein and the chemical pathway are unresolved. Alternative activation pathways relying on non-covalent binding or bystander effects could provide some answers.

All in all, it remains highly probable that patients are cross-sensitized by QA-containing compounds that can activate DC, leading to T cell proliferation. Following an intravenous injection, the high NMBA concentration rapidly activates effector cells due to the presence of cross-reactive antibodies that can recognize the common epitope between the sensitizing antigen and the culprit NMBA.

6.4 What do we learn from the binding of antibodies to rocuronium?

Insightful information could be drawn from the crystallographic structures of the complexes of rocuronium with the scFv or Fab antibodies. The data generated showed that both the VH and VL chains of the antibodies were involved in the binding of rocuronium by forming non-covalent Van der Waals bonds and

hydrogen bonds. The rocuronium molecule was buried in the chains, even locked with a conformational change for the mAb IP11. This binding mode of the antibodies forming a deep pocket that grooved rocuronium is in agreement with the previously described binding mode with hapten binders forming a concave interface[185]. This study also demonstrated that antibodies that recognized haptens tended to have shorter CDR3-H loops to favor the formation of a pocket or grooves. The grooving of rocuronium inside the antibody chains is one more argument in favor of the haptenization of rocuronium to activate BCRs since the cross-linking of two antibodies onto the rocuronium molecule seems incompatible with the binding mode revealed by the crystal structure. The crystallographic data also confirmed the QA atom to be the allergenic epitope since it forms strong bonds with the mAbs in all crystal structures. One may wonder if it is a consequence of the immunization strategy we chose that biases QA presentation to immune cells by grafting the rocuronium molecule to the carrier via the hydroxyl group on the opposite side of the QA.

Our data also pointed out the importance of the light chain in the binding which was unexpected since the VH CDR3 is often considered as solely responsible for antibody specificity[244]. Indeed, the VL chains are generated after the VH and the CDR-L3 loop is less diverse than the CDR-H3 loop of the VH chain one due to the absence of the D gene. Surprisingly, our data showed that in the murine antibody repertoires we generated, the VL played a crucial role since two mAbs (IP11 and IP12) sharing identical VH but distinct VL chains have a 400-fold difference in affinities. This observation was in line with the fact that in the crystallographic structures, the VL chains played a major role and were the ones involved in the binding with the QA.

Moreover, the crystallographic data highlighted the importance of the 3D conformation of the NMBAs. Indeed, rocuronium has been reported to exist in two different conformations, the twist-boat, and the chair conformation, depending on the polarity of the solvent (Fig 16). In a hydrophobic medium (e.g: Deuterated chloroform: CDCl3), rocuronium was in a twist-boat conformation, whereas in a polar solvent (e.g: Dimethyl sulfoxide: DMSO) the chair conformation was favored. This conformational change may help rocuronium to cross membranes. The different spatial rearrangements of its substituents are another argument in favor of its capacity to be chemically modified to bind to a carrier protein or to form neoepitopes[245]. In the structure of the scFv-m1B6-rocuronium complex, the rocuronium ring adopted the chair conformation, whereas in the Fab-IP11, IP8, and IP2-rocuronium were found in its twist-boat conformation. One must mitigate these results since the crystal structure is a snapshot of the complex, therefore it might depict the favored conformation which does not imply that the mAbs do not bind the

other conformation. A recent crystal structure of rocuronium binding to the nicotinic receptors revealed that its binding mode occurred in two different states: one with rocuronium blocking the channel in a resting-like state and another one in which rocuronium is bound in the pore[246]. In the two states, rocuronium bound the receptor[246], but unfortunately, the electron density was too poorly defined to determine if rocuronium bound to the receptors in the chair or twist-boat conformation. Literature also lacks evidence concerning the presence of either conformations of rocuronium in the commercial mixture or in the body which are aqueous polar environments, that can potentially favor the twist-boat conformation. Rocuronium probably exists in both conformations, which would orient our therapeutic strategy by administrating a cocktail of therapeutic antibodies that can capture both isomers and/or a bispecific capture antibody if our mAbs do not bind both conformations. Further investigations are necessary to address this question.

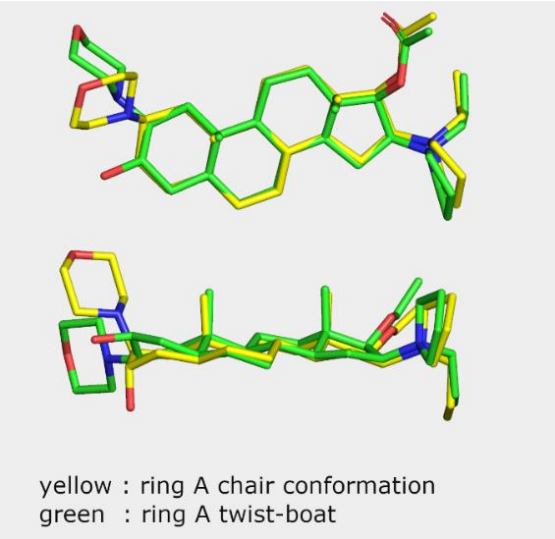

Figure 16: Rocuronium conformers observed in anti-rocuronium scFv-1B6-rocuronium complexes in the chair conformation (yellow) or twist boat conformation (green).

7 How can this work improve the diagnosis or treatment of NMBA-mediated AHR?

7.1 Ideas for novel tools to improve AHR diagnostic work-up

Following a perioperative AHR, the anaesthesiologists seek to identify the underlying mechanism (IgE or non-IgE-mediated) to identify the culprit allergen, and therefore decide a strategy for subsequent anesthetic procedures. However, current tools lead to inconclusive diagnostic work-up in up to 30% of AHRs, partially because they rely exclusively on the detection of the IgE-dependent pathway (drug-specific IgE, histamine, tryptase levels, skin test, and basophil activation test), thus overlooking other pathways.

This work might help to improve future diagnostic tools after an NMBA-mediated allergy. First, the anti-rocuronium antibodies isolated in this project will be useful positive controls for the screening methods (ImmunoCap, ELISA, Basophil Activation Tests), to establish a threshold or determine a concentration of polyclonal anti-rocuronium antibodies in the serum of patients.

Currently, the detection of NMBA-sIgE in the clinic relies on the detection of mAbs to morphine conjugates grafted on a solid phase which faces several limitations. First, we detect rocuronium-specific antibodies with a chemically distinct molecule: the backbones of the two molecules are different (not the same number and type of aromatic rings) and the morphine molecule possesses a tertiary ammonium that becomes QUATERNARY at physiological pH, therefore not a "real" QA. The detection of rocuronium-specific antibodies could be improved by using our rocuronium derivative on which a linker and a reactive carboxylic acid group would be grafted on the hydroxyl group. This chemical modification allows rocuronium to easily bind to a solid phase or a carrier protein possessing amines. Nonetheless, it remains uncertain if drugs bound on a solid phase retain their antibody binding capacity after coupling. Indeed, can the poor correlation mentioned previously (§6.1) in the study of Baldo et al., between the allergenic drug and the most potent inhibiting drug be explained entirely by the cross-reactivity of the sera of the patients or also by the limitations of the diagnostic tools?

In the clinics, it remains very difficult to assess or anticipate anti-NMBA antibody cross-reactivity. The gold standard remains *in vivo* skin tests, nonetheless, it is argued that it might not reflect sIgE-mediated anaphylaxis but the activation of MRGPRX2 on mast cells[247]. However, the outcome of the tests did not always correlate according to the techniques used. For instance, a study demonstrated only 15% of matching results between the assessment of cross-reactivity by skin tests and the Basophil Activation Test[248]. Some claim that drug-provocation tests should be the gold standard to anticipate cross-reactivity, but the potentially dangerous outcomes of this method remain under debate. Understanding and

anticipating cross-reactivity in NMBA-mediated AHR is of the utmost importance if a patient needs to undergo another subsequent anesthesia, especially in case of an emergency. As it remains too costly to test the sensitivity of every patient to each NMBA before each anesthesia, it would be beneficial to establish a trend or a decision tree for the "typical" allergic profiles but so far, our study is not broad enough to do so. If the patient was already exposed to an NMBA before, should he/she be re-exposed to the same one if he was not allergic years ago? The case of Patient#1 is complicated for instance since we would recommend avoiding exposure to atracurium and rocuronium, but would cisatracurium be a safer alternative than suxamethonium?

The protein-NMBA derivatives we developed could be used as an alternative to drug provocation tests. Indeed, those diagnostic tools sometimes remain the most conclusive method to decipher an allergy, but anaesthesiologists are often reluctant due to one of the dangers associated with symptoms of neuromuscular blockade resulting even if 1/10 of the therapeutic dose is used. To circumvent this aftermath, we could use NMBA bound to carrier proteins to test the sensitivity: the carrier-NMBA complex being too big to enter the neuromuscular junction, we could test the specificity without inducing neuromuscular blockade in patients. However, the detection would largely favor the binding of anti-NMBA-IgG immune complexes due to the big size of the carrier-rocuronium complex.

Current diagnostic tools are limited not only by experimental factors but also by biological reality that can cause false negative results which can severely undermine correct secondary prevention. Indeed, circulating sIgE are very scarce (low concentration, short half-life) and their non-detection does not implicate their non-existence. It can mean that they are already bound to FcεRI on effector cells (mast cells/basophils), ready to activate them and trigger mediator release (histamine, PAF). An identical reasoning is applied for basophil activation tests that would be falsely negative if the receptors are unavailable due to pre-bound culprit sIgEs. This shows the importance of the timing of sampling. If sampling is performed too early after the AHR, we will end up in the previously described situation. Overall, it is better to sample the patient 4-6 weeks after the event[194] and it is recommended to rely on different tests before drawing conclusions on negative results. After having depicted the limitations to diagnose NMBA-mediated AHR, are there potential solutions to treat these allergies?

7.2 Could desensitization be a potential solution?

In chronic allergies, the only available long-term disease-modifying treatment is allergen immunotherapy. This therapy consists of continuously administrating the allergen either sublingually or subcutaneously. Mechanistically, the immune tolerance induced by antigen-immunotherapy is explained by a shift towards the immune phenotype Th1 and T_{reg} cells with a downregulation of the Th2 response, which drives the production of allergen-specific IgG antibodies[249]. These antibodies diminish the effect of IgE by blocking IgE-dependent mediator release on histamine/mast cells by binding to the inhibitory receptor FcgRIIb[250-251]. IgG antibodies also neutralize allergens which decreases T cell responses by preventing IgE-allergen complexes from binding to antigen-presenting cells[252]. Among the antibodies produced, the isotype IgG4 was identified as playing the biggest role as a blocking antibody[253]. Other key players are T_{regs} that secrete the inhibitory cytokine IL-10 which suppressed antigen-presenting cells and innate lymphoid cells[254] and favors B cells class-switch to produce IgG4.

In the context of NMBA-mediated allergies, it is difficult to envision the use of antigen immunotherapy as a routine, first due to economic costs and second given that the risk to re-expose a patient to the culprit NMBA is very high. Additionally, allergens must be available in a safe format for allergen immunotherapy to be considered, so NMBAs might never be used unless grafted to a carrier large enough to block its diffusion and therefore prevent neuromuscular blockade. Nonetheless, in the rare case of a cross-reactive patient who is sensitive to all the NMBAs (who did a shock to one or more NMBAs and possesses cross-reactive mAbs to all the NMBAs in his serum), then one potential solution (except not exposing him/her to NMNBAs which is not always feasible) could be allergen immunotherapy.

Despite the potential improvement of allergen immunotherapy in the future, the hopes to use this method in the context of NMBA-mediated AHR are slim, what are the other perspectives of immunotherapy, this time by valorizing the potential of anti-NMBA mAbs?

8 Perspectives for rocuronium-specific antibody-based immunotherapy

8.1 How could a therapeutic antibody reverse neuromuscular blockade?

Antibodies can be used as therapeutics due to their high-affinity and specificity for their target. We hypothesized that antibodies with high-affinity for free rocuronium could capture NMBAs, hence inhibiting their binding to nicotinic receptors and therefore reversing neuromuscular blockade. We selected the rocuronium-specific antibody with the highest affinity, validated a prophylactic model in mice, and succeeded in reversing neuromuscular blockade in 1-2 minutes in cynomolgus macaque. Nonetheless, antibody engineering and optimization can be anticipated as a future perspective of this work.

First, the format of the therapeutic antibody would need further improvement to decrease the chances of antibody-dependent cell cytotoxicity since mouse IgG antibodies were injected in cynomolgus macaques. Indeed, we had to produce almost a gram of antibodies (up to 15mg/kg in cynomolgus macaques weighing between 3-10kg with three replicates) so we produced antibodies from hybridoma technology that permits high production yields (up to 50mg of antibody in 1L of cell culture) at low cost.

To use the antibody as a therapeutic tool, optimization of the antibody format would be necessary by modifying the full IgG (~180 kDa) into an effector-less IgG (N297A[255] or LALA[256] mutation) that inhibits the activation of effector cells, preventing side-effect allergic reactions (Fig 17). We would also need to shorten the antibody half-life if the patient would require a prompt NMBA re-administration which could be performed by mutating the antibody to alter binding to the FcRn[257] but it would increase the cost of production. To circumvent those two limitations, we could also design single domain antibodies (VHH, scFvs) or Fabs that lack heavy chain constant regions and that also diffuse better in the tissues and can extravasate from the bloodstream due to their small size (Fig 17). VHH are camelid-derived single-chain antibodies consisting of a heavy-chain variable domain, scFvs are composed of the VH and VL chains joined together by a flexible peptide linker and Fabs are composed of VH/VL chains, and one constant domain of each chain connected by disulfide bonds. In mice, scFv fragments have a terminal half-life of approximately 10–30 minutes and Fabs of 4-6 Hours[258]. Even though no adverse events were observed after administering the therapeutic mAb to macaques, we would need to mitigate the risks of immunogenicity and antidrug antibody development in humans, by humanizing (using human frameworks) the final drug candidate (Fig 17).

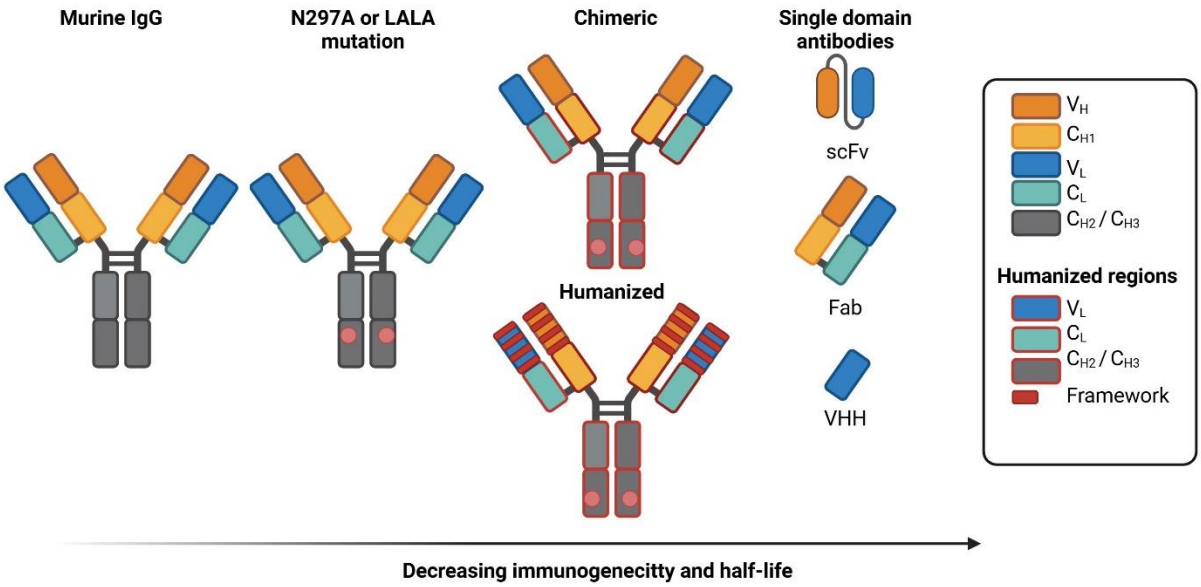

Figure 17: Transition from mouse mAb to less immunogenic and shorter half-life potential therapeutic antibodies format.
C_H, Constant Heavy; C_L, constant Light; Fab, Fragment antigen binding; scFv, Single-Chain Fragment Variable; V_H, variable Heavy; VHH, variable heavy chain; V_L, variable light. (Biorender).

The antigen binding affinity and specificity can also be optimized using site mutagenesis and computer-aided design. A lot of progress has been made in this field with *in silico* approaches that can perform affinity maturation models. The affinity can be improved more than 100-fold by combining *in silico* affinity maturation and mutagenesis, such as anti-lysozyme mAb that reached a 140-fold affinity improvement[259]. The co-crystal structures of the rocuronium:mAb complexes give us insights into the critical amino acids involved in the binding of rocuronium allowing performing mutagenesis around these residues to verify their importance and improve the binding efficiency. We would also probably need to target residues not in direct contact with the antigen since it has been shown that during affinity maturation, somatic mutations in residues in direct contact with the antigen are less frequent than in residues adjacent to the residues in contact[260]. Modeling will greatly help in this regard, or antibody library generation based on our best anti-rocuronium VHH, ScFv, or Fab.

A lot of improvement can be achieved in the design of a therapeutic antibody, but would this tool still be competitive with the already existing capture molecule, sugammadex?

8.2 Is a therapeutic antibody competitive with sugammadex?

The only commercially available drug that can reverse deep rocuronium-induced neuromuscular blockade is sugammadex, a modified gamma-cyclodextrin (Fig 18.A). It is administered intravenously to encapsulate aminosteroid NMBAs (rocuronium and vecuronium) in the plasma. After rocuronium infusion, a concentration gradient of free rocuronium between the neuromuscular junction and blood plasma is created with an accumulation of free rocuronium at the neuromuscular junction. With the administration of sugammadex, there is a reduction of rocuronium concentration in the blood plasma where rocuronium is encapsulated which reduces the amount of rocuronium in the neuromuscular junction that can bind to the nicotinic receptor (Fig 18.B). The elimination half-life of sugammadex is 2 hours with 90% excreted within 24 hours via the kidneys without being metabolized[261]. Cyclodextrins are rigid rings of sugar molecules with a lipophilic cavity that allows sugammadex to bind to the lipophilic steroids of rocuronium. During the design of this cyclodextrin, a negatively charged end group was added to hold the positively charged QA of rocuronium in a fixed position.

To compare the efficacy of the therapeutic antibodies with sugammadex to reverse neuromuscular blockade, we performed *in vitro* and *in vivo* experiments. The theoretical KD of sugammadex is 10^{-7}M, which was measured using isothermal titration microcalorimetry[262]. We were not able to confirm these results experimentally with free rocuronium since it would require to chemically modify sugammadex to bind it to a surface plasmon resonance chip. Nonetheless, the anti-rocuronium mAb avidities/affinities for free rocuronium and HSA-rocuronium were measured: avidities ~10pm-5nM and affinities with free rocuronium ~5-10nM for the best antibodies. We also evaluated the efficacy of the mAbs to prevent rocuronium-induced neuromuscular blockade *in vivo* using a prophylactic model. Since the molecular weights of sugammadex (2 178Da), of a full IgG (180kDa), and a scFv (25KDa) are widely different, it was necessary to compare the effective doses using molar weight considerations. In the prophylactic model of prevention of neuromuscular blockade in mice, full protection (no lethality) was obtained with ratios of rocuronium:drug as low as 1:7 for sugammadex, 1:0.05 for m1B6 as an IgG1 and 1:1.4 in its scFv format (Fig 18). The bivalent binding capacity of a full IgG antibody compared to sugammadex or a scFv needs to be taken into consideration in these results. The scFv format protected mice from a lethal dose of free rocuronium with a dose 2 times higher than the full IgG1 but 2-3 times lower than sugammadex in molar ratio which validated the model (Fig 18.C)

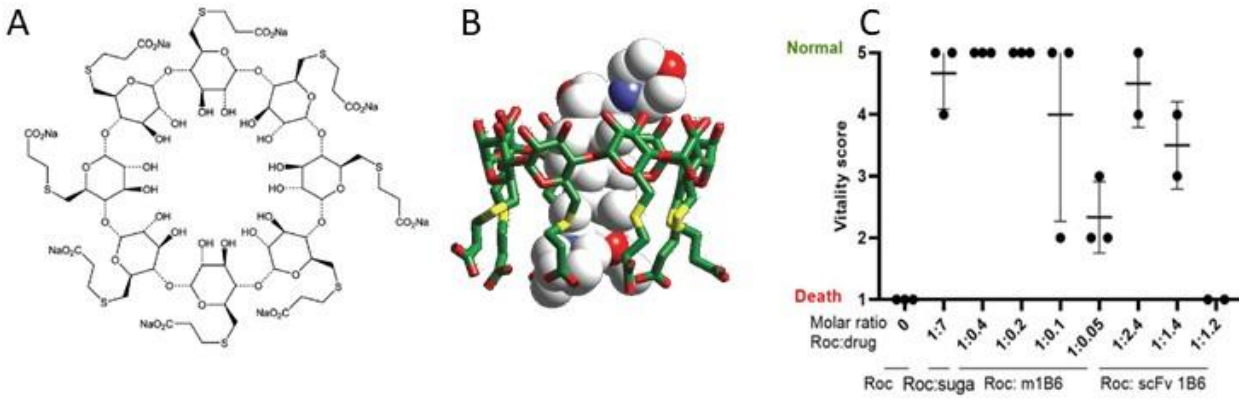

Figure 18: Reversal of rocuronium-induced neuromuscular blockade using sugammadex or immunotherapy.
(**A**) Structure of sugammadex sodium[145]. (**B**) Complex formation of sugammadex and rocuronium as obtained by X-ray diffraction. The rocuronium molecule (model with spheres) is completely encapsulated by sugammadex (model with sticks in green)[146]. (**C**) Prophylaxis of rocuronium-induced neuromuscular blockade in mice. Suggamadex and rocuronium-specific murine antibody m1B6 were injected as full IgG1 or scFv followed by rocuronium injection at a lethal dose of 2µg/kg. Vitality was scored as follows: 5 (no behavior changes), 4 (transient inactivity; ≤30 seconds), 3 (respiratory distress and intermediate inactivity; >30 seconds), 2 (flipping or inactivity; >1 minute), and 1 (death).

Next, in a curative strategy, the potency to reverse neuromuscular blockade was tested in non-human primates by first inducing deep-neuromuscular blockade and injecting the capture molecule (either the mAb or the positive control sugammadex). The neuromuscular blockade was monitored similarly to patients in care units by measuring the TOF ratio on the ulnar nerves of the cynomolgus macaques. Spontaneous ventilation recovery and TOF ratio superior to 90% was achieved with 1mg/kg of sugammadex versus 10mg/kg of mAb m1B6. This antibody dose is not financially competitive with sugammadex. When considering molar concentrations, given that sugammadex has a molar weight ~90 times lower than a full IgG1, the molar mass required to reverse neuromuscular blockade is 9 times lower for m1B6 than sugammadex (1mg/kg sugammadex with molar weight: 2 178 Da → 0.5µmol/kg versus 10mg/kg m1B6 with molar weight: 180 000 Da→ 0.055µmol/kg). Once again, if we consider that one mAb can capture two rocuronium molecules, as justified by the crystal structures, then the mAb is 4-5 times more competitive than sugammadex when considering the molar perspective. If we were to design a single domain mAb with one binding site and a size approximatively 10 times higher than sugammadex (molar weight: 25 000Da), then with the same molar calculations, by injecting an identical mass of antidote, 10 times fewer moles of therapeutic mAbs would be administered, making this approach competitive in terms of dose, but probably not economically in regards of scFv/Fab production costs, since in January 2026, commercial sugammadex will not be protected from generic competition anymore[263].

These results validate the capture potency of single-domain antibodies in a prophylactic model of rocuronium-based neuromuscular blockade, but the production costs are in favor of sugammadex even though its use is restricted in some countries due to existing side effects. Indeed, AHR can arise by the creation of a neoepitope during the complex formation of rocuronium:sugammadex[141]. Moreover, sugammadex is specific only to aminosteroid NMBAs rocuronium and vecuronium. To improve the efficacy of the rocuronium-capture antibody we could mutate mAb residues, modify the immunization strategy, generate a bi-specific mAb or generate a cocktail of mAbs each specific for a different conformation of rocuronium.

8.3 Could a capture molecule mitigate NMBA-induced AHR?

So far, mAbs commercially available to mitigate allergies either directly target IgE antibodies (e.g. omalizumab), FcεRI, cytokine receptors (dupilumab that targets IL-4Ra), or inhibitory receptors on mast cells (anti-Siglec mAb)[264], but rarely the culprit molecule. One recent study targeted the antigen Arah 2 involved in peanut allergy but this treatment was effective as a prophylactic to protect for the allergy and not as a therapy[265].

Administration of sugammadex following a rocuronium-mediated AHR has been shown and reported to successfully treat anaphylaxis in a few several clinical cases, without pre-injection of adrenaline which is the commonly used drug to treat the symptoms of anaphylaxis[266]. These results are surprising since it seems complicated that a capture molecule can cease an already initiated allergic reaction with pre-bound IgE antibodies on effector cells. In our case, the IgEs are also pre-bound to their receptors on effector cells so the reduction of mediator release would be mediated by hindering the cross-linking of the IgE by removal of the allergen rather than the classical FcεRI down-regulation due to the decreasing concentration of specific IgE antibodies. Experiments performed on basophils *in vitro* confirmed that encapsulating rocuronium by sugammadex can prevent, but not stop, basophil activation by the NMBAs since pre-incubation of sugammadex with rocuronium could prevent basophil activation but not after 3 minutes exposure to rocuronium[267].

Nonetheless, even without stopping the activation of effector cells, reducing the allergen concentration by capture can only decrease the severity of the AHR and be proposed as an additional treatment to NMBA-mediated AHR complementary to adrenaline. When designing the therapeutic mAb two criteria will need to be taken into consideration: first, the affinity of the antidote for rocuronium will need to be higher than the affinity of rocuronium for the endogenous antibodies of the patient at the origin of the allergy. Therefore, isolating antibodies from human patients might not be sufficient, the therapeutic might

need to be optimized by mutagenesis. Second, if the allergenic epitope of rocuronium is unique (supposedly the QA), then ideally the therapeutic mAb would need to bind this allergenic epitope to mask it to the allergenic IgE paratope.

All in all, in the context of perioperative NMBA administration, immunotherapy seems like a promising strategy either to reverse neuromuscular blockade or to attenuate the symptoms of an already triggered NMBA-mediated AHR.

This work proved for the first time the existence of rocuronium-specific IgG+ B cell antibodies in immunized mice and allergic patients. The B cells (Bmem and plasma cells) isolation allowed the characterization of their antibodies in terms of specificity, affinity, structure, involvement in anaphylaxis, and therapeutic efficacy. This work helps to elucidate the underlying causes and mechanisms of NMBA-mediated AHR, it could improve diagnostic tools and it paves the way for therapeutic solutions using antibody immunotherapy. A lot of questions remain following the results obtained concerning the sensitization phase in allergic patients, the activation phase, the nature of the allergen during these two phases, the involvement of antibodies and their isotype. A wide range of future perspectives for the project was mentioned in the discussion and will be quickly summarized in the following section.

Firstly, the sorting strategy of human Bmem could be improved in terms of capture probes, markers, and culture systems. As mentioned previously, we could sort a double positive population binding rocuronium labeled with 2 different dies to optimize the yield of specific B cell clones to eliminate the BCRs that bind to the fluorochromes. We could also replace the marker CD27 that excludes Tbet+ B cells with the marker of early Bmem CD45RB and we should add an IgM dump in the sort. Moreover, it would be interesting to obtain crystal structures of human mAbs that are monospecific and cross-reactive to different NMBAs to compare their binding modes.

Concerning the mouse models, we could improve the sensitization phase to mimic more closely the natural route of human sensitization by environmental factors. Sensitizing the mice with QA-containing compounds such as pholcodine or detergents and identifying NMBA-specific mAbs would validate the cross-sensitization theory. Work can also be undertaken to identify the carrier molecule (if it exists) with passive sensitization, mAb:rocuronium:protein pull-downs as mentioned in §6.3.2. Extending the work on human models could greatly benefit the diagnostic work-up following an NMBA-mediated AHR in the clinics to better anticipate the (cross)-reactivity to NMBAs by establishing a trend for the “typical” allergic profiles.

Regarding the therapeutic applications and the reversal of neuromuscular, a lot of improvement can be done in terms of therapeutic potency by optimizing antibody engineering, generating single domain mAbs,

bi-specific mAbs, or using a cocktail of mAbs each targeting a distinct NMBA. Targeted mutagenesis could be performed based on the crystal structures.

Finally, the major perspective of the project would be to identify anti-rocuronium IgE plasma cells and their repertoires. We would need to access the long-lived IgE+ plasma cells that niche in allergic individuals in the bone marrow and to sort antigen-specific plasma cells. For instance, we could use the technology implemented in my lab that relies on the relocation of fluorescence onto a cluster of magnetic particles inside a 40pL microfluidic droplets. It allows sorting based on the class of antibodies that is secreted by a cell within a droplet (IgG, IgE) and if that antibody binds a given antigen[184]. Patients are currently being selected according to their IgE levels in the serum (ImmunoCAP or ELISA) and positive skin test to generate a bone marrow aspirate biobank.

Hopefully, this work has cast light on the mechanisms and therapeutic applications of rocuronium-mediated AHR and opens a lot of doors to unravel the mysteries behind these life-threatening and unpredictable allergies.

REFERENCES

1. Li, J., Murphy-Lavoie, H., Bugas, C., Martinez, J. & Preston, C. Complications of emergency intubation with and without paralysis. *Am. J. Emerg. Med.* **17**, 141–143 (1999).
2. Ma, O. J. *et al.* Intubation success rates improve for an air medical program after implementing the use of neuromuscular blocking agents. *Am. J. Emerg. Med.* **16**, 125–127 (1998).
3. Mosier, J. M. *et al.* Neuromuscular blockade improves first-attempt success for intubation in the intensive care unit. A propensity matched analysis. *Ann. Am. Thorac. Soc.* **12**, 734–741 (2015).
4. Jain, A., Wermuth, H. R., Dua, A., Singh, K. & Maani, C. V. Rocuronium. in *StatPearls* (StatPearls Publishing, Treasure Island (FL), 2023).
5. R. L. STILLER, D. RYAN COOK AND S. CHAKRAVORTI. IN VITRO DEGRADATION OF ATRACURIUM IN HUMAN PLASMA. *Br.J. Anaesth* **57**, (1985).
6. REGINALD E. PLEASANC. CURARE, Presidential Address to the Society of Sheffield Anaesthetists January 15th, 1948. *British Journal of Anaesthesia* (1948).
7. Hill, S. A., Scott, R. P. F. & Savarese, J. J. Structure-activity relationships: from tubocurarine to the present day. *Baillières Clin. Anaesthesiol.* **8**, 317–348 (1994).
8. Raghavendra, T. Neuromuscular blocking drugs: discovery and development. *J. R. Soc. Med.* **95**, 363–367 (2002).
9. WHO Model Lists of Essential Medicines. https://www.who.int/groups/expert-committee-on-selection-and-use-of-essential-medicines/essential-medicines-lists.
10. Donati, F. *et al.* Pharmacokinetics and pharmacodynamics of atracurium with and without previous suxamethonium administration. *Br. J. Anaesth.* **66**, 557–561 (1991).
11. Unwin, N. Refined structure of the nicotinic acetylcholine receptor at 4A resolution. *J. Mol. Biol.* **346**, 967–989 (2005).
12. Gharpure, A., Noviello, C. M. & Hibbs, R. E. Progress in nicotinic receptor structural biology. *Neuropharmacology* **171**, 108086 (2020).
13. Ahring, P. K. *et al.* Engineered α4β2 nicotinic acetylcholine receptors as models for measuring agonist binding and effect at the orthosteric low-affinity α4–α4 interface. *Neuropharmacology* **92**, 135–145 (2015).
14. Nachmansohn, D., Coates, C. W. & Cox, R. T. ELECTRIC POTENTIAL AND ACTIVITY OF CHOLINE ESTERASE IN THE ELECTRIC ORGAN OF ELECTROPHORUS ELECTRICUS (LINNAEUS). *J. Gen. Physiol.* **25**, 75–88 (1941).
15. Cartaud, J., Benedetti, E. L., Cohen, J. B., Meunier, J. C. & Changeux, J. P. Presence of a lattice structure in membrane fragments rich in nicotinic receptor protein from the electric organ of Torpedo marmorata. *FEBS Lett.* **33**, 109–113 (1973).
16. Unwin, N. Refined structure of the nicotinic acetylcholine receptor at 4A resolution. *J. Mol. Biol.* **346**, 967–989 (2005).
17. Horenstein, N. A., Leonik, F. M. & Papke, R. L. Multiple pharmacophores for the selective activation of nicotinic alpha7-type acetylcholine receptors. *Mol. Pharmacol.* **74**, 1496–1511 (2008).
18. Gulenay, M. & Mathai, J. K. Depolarizing Neuromuscular Blocking Drugs. in *StatPearls* (StatPearls Publishing, Treasure Island (FL), 2023).
19. Ahmad, M., Khan, N. A. & Furqan, A. Comparing The Functional Outcome Of Different Dose Regimes Of Succinylcholine When Used For Rapid Induction And Intubation. *J. Ayub Med. Coll. Abbottabad JAMC* **30**, 401–404 (2018).
20. Bohringer, C., Moua, H. & Liu, H. Is There Still a Role for Succinylcholine in Contemporary Clinical Practice? *Transl. Perioper. Pain Med.* **6**, 129–135 (2019).
21. Mayer, M., Doenicke, A., Hofmann, A. & Peter, K. ONSET AND RECOVERY OF ROCURONIUM (ORG 9426) AND VECURONIUM UNDER ENFLURANE ANAESTHESIA. *Br. J. Anaesth.* **69**, 511–512 (1992).

22. Fisher, D. M. *et al.* Elimination of atracurium in humans: contribution of Hofmann elimination and ester hydrolysis versus organ-based elimination. *Anesthesiology* **65**, 6–12 (1986).
23. Weindlmayr-Goettel, M., Kress, H. G., Hammerschmidt, F. & Nigrovic, V. In vitro degradation of atracurium and cisatracurium at pH 7.4 and 37 degrees C depends on the composition of the incubating solutions. *Br. J. Anaesth.* **81**, 409–414 (1998).
24. Cavallito, C. J. & Foldes, F. F. Molecular Modifications and Modulation of Adverse Actions of Muscle Relaxants in Anesthesiology. *Drug Metab. Rev.* **15**, 591–618 (1984).
25. Keith Hillier. *xPharm: The Comprehensive Pharmacology Reference*. vol. Succinylcholine (2008).
26. Dollery, C. & Boobis, A. R. *Therapeutic Drugs*. (Churchill Livingstone, Edinburgh, 1999).
27. Wastila, W. B., Maehr, R. B., Turner, G. L., Hill, D. A. & Savarese, J. J. Comparative pharmacology of cisatracurium (51W89), atracurium, and five isomers in cats. *Anesthesiology* **85**, 169–177 (1996).
28. Kandasamy, J. & Carlo, W. Pharmacologic Therapies IV: Other Medications. in *Assisted Ventilation of the Neonate: An Evidence-Based Approach to Newborn Respiratory Care: Sixth Edition* 366-379.e5 (2016). doi:10.1016/B978-0-323-39006-4.00034-X.
29. Levitt, R. C. & Ewart, S. L. Genetic susceptibility to atracurium-induced bronchoconstriction. *Am. J. Respir. Crit. Care Med.* **151**, 1537–1542 (1995).
30. Cohen, S. G. & Zelaya-Quesada, M. Portier, Richet, and the discovery of anaphylaxis: a centennial. *J. Allergy Clin. Immunol.* **110**, 331–336 (2002).
31. Turner, P. J. *et al.* Time to revisit the definition and clinical criteria for anaphylaxis? *World Allergy Organ. J.* **12**, 100066 (2019).
32. Yao, T.-C., Wu, A. C., Huang, Y.-W., Wang, J.-Y. & Tsai, H.-J. Increasing trends of anaphylaxis-related events: an analysis of anaphylaxis using nationwide data in Taiwan, 2001-2013. *World Allergy Organ. J.* **11**, 23 (2018).
33. Motosue, M. S., Bellolio, M. F., Van Houten, H. K., Shah, N. D. & Campbell, R. L. National trends in emergency department visits and hospitalizations for food-induced anaphylaxis in US children. *Pediatr. Allergy Immunol. Off. Publ. Eur. Soc. Pediatr. Allergy Immunol.* **29**, 538–544 (2018).
34. Gibbison, B., Sheikh, A., McShane, P., Haddow, C. & Soar, J. Anaphylaxis admissions to UK critical care units between 2005 and 2009. *Anaesthesia* **67**, 833–839 (2012).
35. Fisher, M. M. & More, D. G. The epidemiology and clinical features of anaphylactic reactions in anaesthesia. *Anaesth. Intensive Care* **9**, 226–234 (1981).
36. Mertes, P. M. *et al.* Anaphylaxis during anesthesia in France: an 8-year national survey. *J. Allergy Clin. Immunol.* **128**, 366–373 (2011).
37. Harper, N. J. N. *et al.* Anaesthesia, surgery, and life-threatening allergic reactions: epidemiology and clinical features of perioperative anaphylaxis in the 6th National Audit Project (NAP6). *Br. J. Anaesth.* **121**, 159–171 (2018).
38. Reitter, M. *et al.* Fatal anaphylaxis with neuromuscular blocking agents: a risk factor and management analysis. *Allergy* **69**, 954–959 (2014).
39. Berroa, F. *et al.* The incidence of perioperative hypersensitivity reactions: a single-center, prospective, cohort study. *Anesth. Analg.* **121**, 117–123 (2015).
40. Misbah, S. A. & Krishna, M. T. Peri-Operative Anaphylaxis—An Investigational Challenge. *Front. Immunol.* **10**, 1117 (2019).
41. Regateiro, F. S., Marques, M. L. & Gomes, E. R. Drug-Induced Anaphylaxis: An Update on Epidemiology and Risk Factors. *Int. Arch. Allergy Immunol.* **181**, 481–487 (2020).
42. Management of Latex-allergic Patients - Australasian Society of Clinical Immunology and Allergy (ASCIA). https://www.allergy.org.au/hp/papers/management-of-latex-allergic-patients.
43. Chabanne, R., Colomb, S., Gonzalez, D. & Perbet, S. [Use of neuromuscular blocking agents in prehospital medicine: practice survey in Emergency Mobile Services of the South-East of France]. *Ann. Fr. Anesth. Reanim.* **30**, 636–640 (2011).

44. Admin, B. Communiqué concernant la modification du RCP de la célocurine - La SFAR. *Société Française d'Anesthésie et de Réanimation* https://sfar.org/communique-concernant-modification-rcp-de-celocurine/ (2018).
45. Orihara, M. *et al.* Comparison of incidence of anaphylaxis between sugammadex and neostigmine: a retrospective multicentre observational study. *Br. J. Anaesth.* **124**, 154–163 (2020).
46. Horiuchi, T. *et al.* Drug-induced anaphylaxis during general anesthesia in 14 tertiary hospitals in Japan: a retrospective, multicenter, observational study. *J. Anesth.* **35**, 154–160 (2021).
47. Sadleir, P. H. M., Clarke, R. C., Bunning, D. L. & Platt, P. R. Anaphylaxis to neuromuscular blocking drugs: incidence and cross-reactivity in Western Australia from 2002 to 2011. *Br. J. Anaesth.* **110**, 981–987 (2013).
48. Sampson, H. A. *et al.* Second symposium on the definition and management of anaphylaxis: summary report--Second National Institute of Allergy and Infectious Disease/Food Allergy and Anaphylaxis Network symposium. *J. Allergy Clin. Immunol.* **117**, 391–397 (2006).
49. Ring, J. & Messmer, K. Incidence and severity of anaphylactoid reactions to colloid volume substitutes. *Lancet Lond. Engl.* **1**, 466–469 (1977).
50. Dewachter, P. & Savic, L. Perioperative anaphylaxis: pathophysiology, clinical presentation and management. *BJA Educ.* **19**, 313–320 (2019).
51. Gouel-Chéron, A. *et al.* Low end-tidal CO2 as a real-time severity marker of intra-anaesthetic acute hypersensitivity reactions. *Br. J. Anaesth.* **119**, 908–917 (2017).
52. Dejoux, A., de Chaisemartin, L., Bruhns, P., Longrois, D. & Gouel-Chéron, A. Neuromuscular blocking agent induced hypersensitivity reaction exploration: an update. *Eur. J. Anaesthesiol.* **40**, 95–104 (2023).
53. Cha, L. M.-J., Lee, W. S., Han, M. Y. & Lee, K. S. The Timely Administration of Epinephrine and Related Factors in Children with Anaphylaxis. *J. Clin. Med.* **11**, 5494 (2022).
54. Ring, J. *et al.* Guideline for acute therapy and management of anaphylaxis. *Allergo J. Int.* **23**, 96–112 (2014).
55. Simons, F. E. R. *et al.* 2015 update of the evidence base: World Allergy Organization anaphylaxis guidelines. *World Allergy Organ. J.* **8**, 32 (2015).
56. Lin, R. Y. *et al.* Histamine and tryptase levels in patients with acute allergic reactions: An emergency department-based study. *J. Allergy Clin. Immunol.* **106**, 65–71 (2000).
57. Mertes, P. M. *et al.* Reducing the risk of anaphylaxis during anesthesia: 2011 updated guidelines for clinical practice. *J. Investig. Allergol. Clin. Immunol.* **21**, 442–453 (2011).
58. Harle, D. G., Baldo, B. A. & Fisher, M. M. Immunoassays employing substituted ammonium compounds other than neuromuscular blocking drugs to increase the detection of IgE antibodies to these drugs. *Mol. Immunol.* **27**, 1039–1045 (1990).
59. Rose, M. A., Anderson, J., Green, S. L., Yun, J. & Fernando, S. L. Morphine and pholcodine-specific IgE have limited utility in the diagnosis of anaphylaxis to benzylisoquinolines. *Acta Anaesthesiol. Scand.* **62**, 628–634 (2018).
60. Singh, S. K., Bohara, A. & Rai, T. Comparison of Sensitivities of Skin Prick and Intradermal Tests with Oral Rechallenge Test: A Prospective Interventional Hospital-Based Study. *Indian J. Dermatol.* **66**, 55–59 (2021).
61. Carr, T. F. & Saltoun, C. A. Chapter 2: Skin testing in allergy. *Allergy Asthma Proc.* **33 Suppl 1**, 6–8 (2012).
62. Li, J. *et al.* Integrating basophil activation tests into evaluation of perioperative anaphylaxis to neuromuscular blocking agents. *Br. J. Anaesth.* **123**, e135–e143 (2019).
63. Uyttebroek, A. P. *et al.* Flowcytometric diagnosis of atracurium-induced anaphylaxis. *Allergy* **69**, 1324–1332 (2014).

64. Lawrence, M. G. *et al.* Half-life of IgE in serum and skin: Consequences for anti-IgE therapy in patients with allergic disease. *J. Allergy Clin. Immunol.* **139**, 422-428.e4 (2017).
65. Kalinski, P. & Moser, M. Consensual immunity: success-driven development of T-helper-1 and T-helper-2 responses. *Nat. Rev. Immunol.* **5**, 251–260 (2005).
66. Hasegawa, S. *et al.* Functional expression of the high affinity receptor for IgE (FcepsilonRI) in human platelets and its' intracellular expression in human megakaryocytes. *Blood* **93**, 2543–2551 (1999).
67. Gounni, A. S. *et al.* Human neutrophils express the high-affinity receptor for immunoglobulin E (Fc epsilon RI): role in asthma. *FASEB J. Off. Publ. Fed. Am. Soc. Exp. Biol.* **15**, 940–949 (2001).
68. Ishizaka, K., Ishizaka, T. & Hornbrook, M. M. Physicochemical properties of reaginic antibody. V. Correlation of reaginic activity wth gamma-E-globulin antibody. *J. Immunol. Baltim. Md 1950* **97**, 840–853 (1966).
69. Walker, S. A. *et al.* Total and allergen-specific IgE in relation to allergic response pattern following bone marrow transplantation. *Clin. Exp. Immunol.* **66**, 633–639 (1986).
70. Dombrowicz, D., Flamand, V., Brigman, K. K., Koller, B. H. & Kinet, J. P. Abolition of anaphylaxis by targeted disruption of the high affinity immunoglobulin E receptor alpha chain gene. *Cell* **75**, 969–976 (1993).
71. Wershil, B. K., Mekori, Y. A., Murakami, T. & Galli, S. J. 125I-fibrin deposition in IgE-dependent immediate hypersensitivity reactions in mouse skin. Demonstration of the role of mast cells using genetically mast cell-deficient mice locally reconstituted with cultured mast cells. *J. Immunol. Baltim. Md 1950* **139**, 2605–2614 (1987).
72. Wood, R. A. *et al.* A randomized, double-blind, placebo-controlled study of omalizumab combined with oral immunotherapy for the treatment of cow's milk allergy. *J. Allergy Clin. Immunol.* **137**, 1103-1110.e11 (2016).
73. Ricciardi, L. Omalizumab: A useful tool for inducing tolerance to bee venom immunotherapy. *Int. J. Immunopathol. Pharmacol.* **29**, 726–728 (2016).
74. Carter, M. C. *et al.* Omalizumab for the treatment of unprovoked anaphylaxis in patients with systemic mastocytosis. *J. Allergy Clin. Immunol.* **119**, 1550–1551 (2007).
75. Gouel-Chéron, A., Dejoux, A., Lamanna, E. & Bruhns, P. Animal Models of IgE Anaphylaxis. *Biology* **12**, 931 (2023).
76. Leysen, J. *et al.* Predictive value of allergy tests for neuromuscular blocking agents: tackling an unmet need. *Clin. Exp. Allergy J. Br. Soc. Allergy Clin. Immunol.* **44**, 1069–1075 (2014).
77. Laroche, D. *et al.* Evaluation of a new routine diagnostic test for immunoglobulin E sensitization to neuromuscular blocking agents. *Anesthesiology* **114**, 91–97 (2011).
78. Romantowski, J. *et al.* A Challenge for Allergologist: Application of Allergy Diagnostic Methods in Mast Cell Disorders. *Int. J. Mol. Sci.* **22**, 1454 (2021).
79. Oppenheimer, J. & Nelson, H. S. Skin testing: a survey of allergists. *Ann. Allergy Asthma Immunol. Off. Publ. Am. Coll. Allergy Asthma Immunol.* **96**, 19–23 (2006).
80. Oettgen, H. C. *et al.* Active anaphylaxis in IgE-deficient mice. *Nature* **370**, 367–370 (1994).
81. Dombrowicz, D. *et al.* Absence of Fc epsilonRI alpha chain results in upregulation of Fc gammaRIII-dependent mast cell degranulation and anaphylaxis. Evidence of competition between Fc epsilonRI and Fc gammaRIII for limiting amounts of FcR beta and gamma chains. *J. Clin. Invest.* **99**, 915–925 (1997).
82. Vadas, P. *et al.* Platelet-activating factor, PAF acetylhydrolase, and severe anaphylaxis. *N. Engl. J. Med.* **358**, 28–35 (2008).
83. Hamilton, R. G. Human IgG subclass measurements in the clinical laboratory. *Clin. Chem.* **33**, 1707–1725 (1987).

84. Gillis, C., Gouel-Chéron, A., Jönsson, F. & Bruhns, P. Contribution of Human FcγRs to Disease with Evidence from Human Polymorphisms and Transgenic Animal Studies. *Front. Immunol.* **5**, 254 (2014).
85. James, L. K. *et al.* Long-term tolerance after allergen immunotherapy is accompanied by selective persistence of blocking antibodies. *J. Allergy Clin. Immunol.* **127**, 509-516.e1–5 (2011).
86. Cooke, R. A., Barnard, J. H., Hebald, S. & Stull, A. SEROLOGICAL EVIDENCE OF IMMUNITY WITH COEXISTING SENSITIZATION IN A TYPE OF HUMAN ALLERGY (HAY FEVER). *J. Exp. Med.* **62**, 733–750 (1935).
87. Zinkhan, S., Thoms, F., Augusto, G., Vogel, M. & Bachmann, M. F. On the role of allergen-specific IgG subclasses for blocking human basophil activation. *Front. Immunol.* **13**, 892631 (2022).
88. Beutier, H. *et al.* IgG subclasses determine pathways of anaphylaxis in mice. *J. Allergy Clin. Immunol.* **139**, 269-280.e7 (2017).
89. Million, M., Fioramonti, J., Zajac, J. M. & Buéno, L. Effects of neuropeptide FF on intestinal motility and temperature changes induced by endotoxin and platelet-activating factor. *Eur. J. Pharmacol.* **334**, 67–73 (1997).
90. Jönsson, F. *et al.* Mouse and human neutrophils induce anaphylaxis. *J. Clin. Invest.* **121**, 1484–1496 (2011).
91. Finkelman, F. D., Rothenberg, M. E., Brandt, E. B., Morris, S. C. & Strait, R. T. Molecular mechanisms of anaphylaxis: lessons from studies with murine models. *J. Allergy Clin. Immunol.* **115**, 449–457; quiz 458 (2005).
92. Gillis, C. M. *et al.* Mechanisms of anaphylaxis in human low-affinity IgG receptor locus knock-in mice. *J. Allergy Clin. Immunol.* **139**, 1253-1265.e14 (2017).
93. Jönsson, F. *et al.* An IgG-induced neutrophil activation pathway contributes to human drug-induced anaphylaxis. *Sci. Transl. Med.* **11**, eaat1479 (2019).
94. Tatemoto, K. *et al.* Immunoglobulin E-independent activation of mast cell is mediated by Mrg receptors. *Biochem. Biophys. Res. Commun.* **349**, 1322–1328 (2006).
95. McNeil, B. D. *et al.* Identification of a mast-cell-specific receptor crucial for pseudo-allergic drug reactions. *Nature* **519**, 237–241 (2015).
96. Koppert, W. *et al.* Different patterns of mast cell activation by muscle relaxants in human skin. *Anesthesiology* **95**, 659–667 (2001).
97. Elst, J. *et al.* Novel Insights on MRGPRX2-Mediated Hypersensitivity to Neuromuscular Blocking Agents And Fluoroquinolones. *Front. Immunol.* (2021) doi:10.3389/fimmu.2021.668962.
98. Baldo, B. A., Fisher, M. M. & Pham, N. H. On the origin and specificity of antibodies to neuromuscular blocking (muscle relaxant) drugs: an immunochemical perspective. *Clin. Exp. Allergy J. Br. Soc. Allergy Clin. Immunol.* **39**, 325–344 (2009).
99. Mertes, P.-M. & Laxenaire, M.-C. Épidémiologie des réactions anaphylactiques et anaphylactoïdes peranesthésiques en France. Septième enquête multicentrique (Janvier 2001–Décembre 2002). *Ann. Fr. Anesth. Réanimation* **23**, 1133–1143 (2004).
100. Baldo, B. A. & Fisher, M. M. Substituted ammonium ions as allergenic determinants in drug allergy. *Nature* **306**, 262–264 (1983).
101. Mertes, P. M., Laxenaire, M.-C., Alla, F., & Groupe d'Etudes des Réactions Anaphylactoïdes Peranesthésiques. Anaphylactic and anaphylactoid reactions occurring during anesthesia in France in 1999-2000. *Anesthesiology* **99**, 536–545 (2003).
102. Tacquard, C. *et al.* Anaesthetic hypersensitivity reactions in France between 2011 and 2012: the 10th GERAP epidemiologic survey. *Acta Anaesthesiol. Scand.* **61**, 290–299 (2017).
103. Petitpain, N. *et al.* Neuromuscular blocking agents induced anaphylaxis: Results and trends of a French pharmacovigilance survey from 2000 to 2012. *Allergy* **73**, 2224–2233 (2018).

104. Florvaag, E. *et al.* Prevalence of IgE antibodies to morphine. Relation to the high and low incidences of NMBA anaphylaxis in Norway and Sweden, respectively. *Acta Anaesthesiol. Scand.* **49**, 437–444 (2005).
105. Harboe, T., Johansson, S. G. O., Florvaag, E. & Oman, H. Pholcodine exposure raises serum IgE in patients with previous anaphylaxis to neuromuscular blocking agents. *Allergy* **62**, 1445–1450 (2007).
106. de Pater, G. H. *et al.* Six years without pholcodine; Norwegians are significantly less IgE-sensitized and clinically more tolerant to neuromuscular blocking agents. *Allergy* **72**, 813–819 (2017).
107. Mertes, P. M. *et al.* Pholcodine exposure increases the risk of perioperative anaphylaxis to neuromuscular blocking agents: the ALPHO case-control study. *Br. J. Anaesth.* **131**, 150–158 (2023).
108. Information de sécurité - Pholcodine : Suspension des autorisat. *ANSM* https://ansm.sante.fr/informations-de-securite/pholcodine-suspension-des-autorisations-de-mise-sur-le-marche-et-retrait-de-toutes-les-boites-de-sirop-contenant-de-la-pholcodine-en-raison-dun-risque-dallergie-croisee-avec-les-curares.
109. Dong, S. *et al.* Prevalence of IgE against neuromuscular blocking agents in hairdressers and bakers. *Clin. Exp. Allergy J. Br. Soc. Allergy Clin. Immunol.* **43**, 1256–1262 (2013).
110. Beecher, H. K. & Todd, D. P. A study of the deaths associated with anesthesia and surgery: based on a study of 599, 548 anesthesias in ten institutions 1948-1952, inclusive. *Ann. Surg.* **140**, 2–35 (1954).
111. Murphy, G. S. & Brull, S. J. Residual neuromuscular block: lessons unlearned. Part I: definitions, incidence, and adverse physiologic effects of residual neuromuscular block. *Anesth. Analg.* **111**, 120–128 (2010).
112. Maybauer, D. M. *et al.* Incidence and duration of residual paralysis at the end of surgery after multiple administrations of cisatracurium and rocuronium. *Anaesthesia* **62**, 12–17 (2007).
113. Berg, H. *et al.* Residual neuromuscular block is a risk factor for postoperative pulmonary complications. A prospective, randomised, and blinded study of postoperative pulmonary complications after atracurium, vecuronium and pancuronium. *Acta Anaesthesiol. Scand.* **41**, 1095–1103 (1997).
114. Edwards, L.-A., Ly, N., Shinefeld, J. & Morewood, G. Universal quantitative neuromuscular blockade monitoring at an academic medical center—A multimodal analysis of the potential impact on clinical outcomes and total cost of care. *Perioper. Care Oper. Room Manag.* **24**, 100184 (2021).
115. Jiang, Y., Bash, L. D. & Saager, L. A Clinical and Budgetary Impact Analysis of Introducing Sugammadex for Routine Reversal of Neuromuscular Blockade in a Hypothetical Cohort in the US. *Adv. Ther.* **38**, 2689–2708 (2021).
116. Murphy, G. S. & Brull, S. J. Quantitative Neuromuscular Monitoring and Postoperative Outcomes: A Narrative Review. *Anesthesiology* **136**, 345–361 (2022).
117. Ross, P. A., Lerman, J. & Coté, C. J. 52 - Pediatric Equipment. in *A Practice of Anesthesia for Infants and Children (Sixth Edition)* (eds. Coté, C. J., Lerman, J. & Anderson, B. J.) 1175-1203.e8 (Elsevier, Philadelphia, 2019). doi:10.1016/B978-0-323-42974-0.00052-5.
118. Duţu, M. *et al.* Neuromuscular monitoring: an update. *Romanian J. Anaesth. Intensive Care* **25**, 55–60 (2018).
119. Evaluation of Residual Neuromuscular Block Using Train-of-Four and Double Burst Stimulation at the Index Finger: Retraction Notice. *Anesth. Analg.* **128**, e16 (2019).
120. Plaud, B. *et al.* Guidelines on muscle relaxants and reversal in anaesthesia. *Anaesth. Crit. Care Pain Med.* **39**, 125–142 (2020).
121. Klein, A. A. *et al.* Recommendations for standards of monitoring during anaesthesia and recovery 2021: Guideline from the Association of Anaesthetists. *Anaesthesia* **76**, 1212–1223 (2021).

122. Carlos l. erraNDo, Ignacio garUtti, Guido MaZZiNari, Óscar DÍaZ-caMBroNero, John F. BeBaWY. Residual neuromuscular blockade in the postanesthesia care unit: observational cross-sectional study of a multicenter cohort. *Minerva anestesiologica* **82(12):1267–77**, (2016).
123. Adembesa, I., Mung'ayi, V., Premji, Z. & Kamya, D. A randomized control trial comparing train of four ratio > 0.9 to clinical assessment of return of neuromuscular function before endotracheal extubation on critical respiratory events in adult patients undergoing elective surgery at a tertiary hospital in Nairobi. *Afr. Health Sci.* **18**, 807–816 (2018).
124. Murphy, G. S. *et al.* Intraoperative Acceleromyography Monitoring Reduces Symptoms of Muscle Weakness and Improves Quality of Recovery in the Early Postoperative Period. *Anesthesiology* **115**, 946–954 (2011).
125. Jones, R. K., Caldwell, J. E., Brull, S. J. & Soto, R. G. Reversal of profound rocuronium-induced blockade with sugammadex: a randomized comparison with neostigmine. *Anesthesiology* **109**, 816–824 (2008).
126. Magorian, T. T., Lynam, D. P., Caldwell, J. E. & Miller, R. D. Can early administration of neostigmine, in single or repeated doses, alter the course of neuromuscular recovery from a vecuronium-induced neuromuscular blockade? *Anesthesiology* **73**, 410–414 (1990).
127. Kirkegaard-Nielsen, H. *et al.* Optimum time for neostigmine reversal of atracurium-induced neuromuscular blockade. *Can. J. Anaesth. J. Can. Anesth.* **43**, 932–938 (1996).
128. Bevan, J. C. *et al.* Early and late reversal of rocuronium and vecuronium with neostigmine in adults and children. *Anesth. Analg.* **89**, 333–339 (1999).
129. Brull, S. J. & Kopman, A. F. Current Status of Neuromuscular Reversal and Monitoring: Challenges and Opportunities. *Anesthesiology* **126**, 173–190 (2017).
130. Thilen, S. R. *et al.* 2023 American Society of Anesthesiologists Practice Guidelines for Monitoring and Antagonism of Neuromuscular Blockade: A Report by the American Society of Anesthesiologists Task Force on Neuromuscular Blockade. *Anesthesiology* **138**, 13–41 (2023).
131. Li, G. *et al.* Postoperative Pulmonary Complications' Association with Sugammadex versus Neostigmine: A Retrospective Registry Analysis. *Anesthesiology* **134**, 862–873 (2021).
132. de Boer, H. D., van Egmond, J., van de Pol, F., Bom, A. & Booij, L. H. D. J. Reversal of profound rocuronium neuromuscular blockade by sugammadex in anesthetized rhesus monkeys. *Anesthesiology* **104**, 718–723 (2006).
133. Nag, K. *et al.* Sugammadex: A revolutionary drug in neuromuscular pharmacology. *Anesth. Essays Res.* **7**, 302–306 (2013).
134. Kloosterstraat 6, 5349 AB Oss. SUMMARY OF PRODUCT CHARACTERISTICS. *Nertherlands NV Organon* (2008).
135. Hung, S.-K., Yeh, C.-C., Ting, P.-C., Chen, C.-H. & Kao, M.-C. Successful management of rocuronium-induced anaphylaxis with sugammadex: A case report. *J. Int. Med. Res.* **50**, 03000605221113913 (2022).
136. Kim, S.-M., Oh, S. & Ryu, S.-A. Treatment of rocuronium-induced anaphylaxis using sugammadex - A case report -. *Anesth. Pain Med.* **16**, 56–59 (2020).
137. Zecic, F., Smart, M. H., Abbey, T. C., Pazhempallil, A. & Korban, C. Sugammadex-induced anaphylactic reaction: A systematic review. *J. Anaesthesiol. Clin. Pharmacol.* **38**, 360–370 (2022).
138. Tomoronori Takazawa, H. I. Current Status of Sugammadex Usage and the Occurrence of Sugammadex-Induced Anaphylaxis in Japan. *Apsf Newsl.* **Circulation 122,210 • Volume 33, No. 1 • June 2018**,.
139. Min, K. C. *et al.* Hypersensitivity incidence after sugammadex administration in healthy subjects: a randomised controlled trial. *Br. J. Anaesth.* **121**, 749–757 (2018).
140. de Kam, P.-J. *et al.* Sugammadex hypersensitivity and underlying mechanisms: a randomised study of healthy non-anaesthetised volunteers. *Br. J. Anaesth.* **121**, 758–767 (2018).

141. Ebo, D. G. *et al.* Anaphylaxis to sugammadex-rocuronium inclusion complex: An IgE-mediated reaction due to allergenic changes at the sugammadex primary rim. *J. Allergy Clin. Immunol. Pract.* **8**, 1410-1415.e3 (2020).
142. Midtvedt, K. *et al.* Individualized T cell monitored administration of ATG versus OKT3 in steroid-resistant kidney graft rejection. *Clin. Transplant.* **17**, 69–74 (2003).
143. Sáez-Llorens, X. *et al.* Safety and pharmacokinetics of an intramuscular humanized monoclonal antibody to respiratory syncytial virus in premature infants and infants with bronchopulmonary dysplasia. The MEDI-493 Study Group. *Pediatr. Infect. Dis. J.* **17**, 787–791 (1998).
144. Ye, W. *et al.* Improving antibody affinity through in vitro mutagenesis in complementarity determining regions. *J. Biomed. Res.* **36**, 155 (2022).
145. V, A. C., Bbv, S. & A, P. K. METHOD DEVELOPMENT AND VALIDATION OF UV-VISIBLE SPECTROSCOPIC METHOD FOR THE ESTIMATION OF ASSAY OF SUGAMMADEX SODIUM, APREMILAST, RIOCIGUAT AND VORAPAXAR SULFATE DRUGS IN API FORM. *Asian J. Pharm. Clin. Res.* 241–250 (2017) doi:10.22159/ajpcr.2017.v10i2.15502.
146. de Boer, H. D., van Egmond, J., van de Pol, F., Bom, A. & Booij, L. H. D. J. Sugammadex, a new reversal agent for neuromuscular block induced by rocuronium in the anaesthetized Rhesus monkey†. *Br. J. Anaesth.* **96**, 473–479 (2006).
147. Popov, A. V., Zou, X., Xian, J., Nicholson, I. C. & Brüggemann, M. A Human Immunoglobulin λ Locus Is Similarly Well Expressed in Mice and Humans. *J. Exp. Med.* **189**, 1611–1620 (1999).
148. Keyt, B. A., Baliga, R., Sinclair, A. M., Carroll, S. F. & Peterson, M. S. Structure, Function, and Therapeutic Use of IgM Antibodies. *Antibodies Basel Switz.* **9**, 53 (2020).
149. Vidarsson, G., Dekkers, G. & Rispens, T. IgG Subclasses and Allotypes: From Structure to Effector Functions. *Front. Immunol.* **5**, 520 (2014).
150. Ortiz, D. F. *et al.* Elucidating the interplay between IgG-Fc valency and FcγR activation for the design of immune complex inhibitors. *Sci. Transl. Med.* **8**, 365ra158-365ra158 (2016).
151. Tomasi, T. B., Tan, E. M., Solomon, A. & Prendergast, R. A. CHARACTERISTICS OF AN IMMUNE SYSTEM COMMON TO CERTAIN EXTERNAL SECRETIONS. *J. Exp. Med.* **121**, 101–124 (1965).
152. Gutzeit, C., Chen, K. & Cerutti, A. The enigmatic function of IgD: some answers at last. *Eur. J. Immunol.* **48**, 1101–1113 (2018).
153. Tonegawa, S. Somatic generation of antibody diversity. *Nature* **302**, 575–581 (1983).
154. McBride, O. W. *et al.* Localization of human variable and constant region immunoglobulin heavy chain genes on subtelomeric band q32 of chromosome 14. *Nucleic Acids Res.* **10**, 8155–8170 (1982).
155. Alt, F. W. & Baltimore, D. Joining of immunoglobulin heavy chain gene segments: implications from a chromosome with evidence of three D-JH fusions. *Proc. Natl. Acad. Sci. U. S. A.* **79**, 4118–4122 (1982).
156. Cook, G. P. *et al.* A map of the human immunoglobulin VH locus completed by analysis of the telomeric region of chromosome 14q. *Nat. Genet.* **7**, 162–168 (1994).
157. Oettinger, M. A., Schatz, D. G., Gorka, C. & Baltimore, D. RAG-1 and RAG-2, adjacent genes that synergistically activate V(D)J recombination. *Science* **248**, 1517–1523 (1990).
158. Muramatsu, M. *et al.* Specific Expression of Activation-induced Cytidine Deaminase (AID), a Novel Member of the RNA-editing Deaminase Family in Germinal Center B Cells*. *J. Biol. Chem.* **274**, 18470–18476 (1999).
159. XU, Z. *et al.* DNA Lesions and Repair in Immunoglobulin Class Switch Recombination and Somatic Hypermutation. *Ann. N. Y. Acad. Sci.* **1050**, 146–162 (2005).
160. Rogozin, I. B. & Diaz, M. Cutting edge: DGYW/WRCH is a better predictor of mutability at G:C bases in Ig hypermutation than the widely accepted RGYW/WRCY motif and probably reflects a two-step activation-induced cytidine deaminase-triggered process. *J. Immunol. Baltim. Md 1950* **172**, 3382–3384 (2004).

161. Hood, L., Gray, W. R., Sanders, B. G. & Dreyer, W. J. Light Chain Evolution. *Cold Spring Harb. Symp. Quant. Biol.* **32**, 133–146 (1967).
162. Sajadi, M. M. *et al.* λ Light Chain Bias Associated With Enhanced Binding and Function of Anti-HIV Env Glycoprotein Antibodies. *J. Infect. Dis.* **213**, 156–164 (2016).
163. Briney, B., Inderbitzin, A., Joyce, C. & Burton, D. R. Commonality despite exceptional diversity in the baseline human antibody repertoire. *Nature* **566**, 393–397 (2019).
164. Ta, V.-T. *et al.* AID mutant analyses indicate requirement for class-switch-specific cofactors. *Nat. Immunol.* **4**, 843–848 (2003).
165. de Vries, J. E. & Yssel, H. Modulation of the human IgE response. *Eur. Respir. J. Suppl.* **22**, 58s–62s (1996).
166. Shang, X. Z. *et al.* IgE isotype switch and IgE production are enhanced in IL-21-deficient but not IFN-gamma-deficient mice in a Th2-biased response. *Cell. Immunol.* **241**, 66–74 (2006).
167. Davies, J. M., Platts-Mills, T. A. & Aalberse, R. C. The enigma of IgE+ B-cell memory in human subjects. *J. Allergy Clin. Immunol.* **131**, 972–976 (2013).
168. Liu, X., Shen, S. & Manser, T. Influence of B Cell Antigen Receptor Expression Level on Pathways of B Cell Tolerance Induction. *J. Immunol. Baltim. Md 1950* **182**, 398–407 (2009).
169. Roco, J. A. *et al.* Class-Switch Recombination Occurs Infrequently in Germinal Centers. *Immunity* **51**, 337-350.e7 (2019).
170. Akkaya, M., Kwak, K. & Pierce, S. K. B cell memory: building two walls of protection against pathogens. *Nat. Rev. Immunol.* **20**, 229–238 (2020).
171. Taylor, J. J., Pape, K. A. & Jenkins, M. K. A germinal center-independent pathway generates unswitched memory B cells early in the primary response. *J. Exp. Med.* **209**, 597–606 (2012).
172. Elsner, R. A. & Shlomchik, M. J. Germinal Center and Extrafollicular B Cell Responses in Vaccination, Immunity, and Autoimmunity. *Immunity* **53**, 1136–1150 (2020).
173. De Silva, N. S. & Klein, U. Dynamics of B cells in germinal centres. *Nat. Rev. Immunol.* **15**, 137–148 (2015).
174. Fooksman, D. R., Jing, Z. & Park, R. New insights into the ontogeny, diversity, maturation and survival of long-lived plasma cells. *Nat. Rev. Immunol.* 1–10 (2024) doi:10.1038/s41577-024-00991-0.
175. Celada, F. Quantitative studies of the adoptive immunological memory in mice. II. Linear transmission of cellular memory. *J. Exp. Med.* **125**, 199–211 (1967).
176. Oehen, S., Waldner, H., Kündig, T. M., Hengartner, H. & Zinkernagel, R. M. Antivirally protective cytotoxic T cell memory to lymphocytic choriomeningitis virus is governed by persisting antigen. *J. Exp. Med.* **176**, 1273–1281 (1992).
177. Karrer, U. *et al.* Antiviral B Cell Memory in the Absence of Mature Follicular Dendritic Cell Networks and Classical Germinal Centers in TNFR1−/− Mice1. *J. Immunol.* **164**, 768–778 (2000).
178. Maruyama, M., Lam, K.-P. & Rajewsky, K. Memory B-cell persistence is independent of persisting immunizing antigen. *Nature* **407**, 636–642 (2000).
179. Radbruch, A. *et al.* Competence and competition: the challenge of becoming a long-lived plasma cell. *Nat. Rev. Immunol.* **6**, 741–750 (2006).
180. Eyer, K. *et al.* Single-cell deep phenotyping of IgG-secreting cells for high-resolution immune monitoring. *Nat. Biotechnol.* **35**, 977–982 (2017).
181. Snapkov, I. *et al.* Progress and challenges in mass spectrometry-based analysis of antibody repertoires. *Trends Biotechnol.* **40**, 463–481 (2022).
182. Waltari, E., Nafees, S., McCutcheon, K. M., Wong, J. & Pak, J. E. AIRRscape: An interactive tool for exploring B-cell receptor repertoires and antibody responses. *PLoS Comput. Biol.* **18**, e1010052 (2022).
183. Rubelt, F. *et al.* Adaptive Immune Receptor Repertoire Community recommendations for sharing immune-repertoire sequencing data. *Nat. Immunol.* **18**, 1274–1278 (2017).

184. Gérard, A. *et al.* High-throughput single-cell activity-based screening and sequencing of antibodies using droplet microfluidics. *Nat. Biotechnol.* **38**, 715–721 (2020).
185. Collis, A. V. J., Brouwer, A. P. & Martin, A. C. R. Analysis of the antigen combining site: correlations between length and sequence composition of the hypervariable loops and the nature of the antigen. *J. Mol. Biol.* **325**, 337–354 (2003).
186. Jacob, J., Przylepa, J., Miller, C. & Kelsoe, G. In situ studies of the primary immune response to (4-hydroxy-3-nitrophenyl)acetyl. III. The kinetics of V region mutation and selection in germinal center B cells. *J. Exp. Med.* **178**, 1293–1307 (1993).
187. Li, Q., Rodriguez, L. G., Farnsworth, D. F. & Gildersleeve, J. C. Effects of Hapten Density on the Induced Antibody Repertoire. *Chembiochem Eur. J. Chem. Biol.* **11**, 1686–1691 (2010).
188. Li, Y. *et al.* Characteristics of rabbit hapten-specific and germline-based BCR repertoires following repeated immunization. *One Health Adv.* **1**, 17 (2023).
189. Zemlin, M. *et al.* Expressed murine and human CDR-H3 intervals of equal length exhibit distinct repertoires that differ in their amino acid composition and predicted range of structures. *J. Mol. Biol.* **334**, 733–749 (2003).
190. Fisher, M. M. & Munro, I. Life-threatening anaphylactoid reactions to muscle relaxants. *Anesth. Analg.* **62**, 559–564 (1983).
191. Lang, T. J. Estrogen as an immunomodulator. *Clin. Immunol. Orlando Fla* **113**, 224–230 (2004).
192. Mitchell, V. L. & Gershwin, L. J. Progesterone and environmental tobacco smoke act synergistically to exacerbate the development of allergic asthma in a mouse model. *Clin. Exp. Allergy J. Br. Soc. Allergy Clin. Immunol.* **37**, 276–286 (2007).
193. Peyneau, M., de Chaisemartin, L., Gigant, N., Chollet-Martin, S. & Kerdine-Römer, S. Quaternary ammonium compounds in hypersensitivity reactions. *Front. Toxicol.* **4**, 973680 (2022).
194. Ebo, D. G., Fisher, M. M., Hagendorens, M. M., Bridts, C. H. & Stevens, W. J. Anaphylaxis during anaesthesia: diagnostic approach. *Allergy* **62**, 471–487 (2007).
195. Didier, A. *et al.* Role of the quaternary ammonium ion determinants in allergy to muscle relaxants. *J. Allergy Clin. Immunol.* **79**, 578–584 (1987).
196. Weisel, F. J., Zuccarino-Catania, G. V., Chikina, M. & Shlomchik, M. J. A Temporal Switch in the Germinal Center Determines Differential Output of Memory B and Plasma Cells. *Immunity* **44**, 116–130 (2016).
197. Su, K.-Y., Watanabe, A., Yeh, C.-H., Kelsoe, G. & Kuraoka, M. Efficient Culture of Human Naive and Memory B Cells for Use as APCs. *J. Immunol. Baltim. Md 1950* **197**, 4163–4176 (2016).
198. Sokal, A. *et al.* mRNA vaccination of naive and COVID-19-recovered individuals elicits potent memory B cells that recognize SARS-CoV-2 variants. *Immunity* **54**, 2893-2907.e5 (2021).
199. Hara, Y. *et al.* High affinity IgM+ memory B cells are generated through a germinal center-dependent pathway. *Mol. Immunol.* **68**, 617–627 (2015).
200. Giesecke, C. *et al.* Tissue Distribution and Dependence of Responsiveness of Human Antigen-Specific Memory B Cells. *J. Immunol.* **192**, 3091–3100 (2014).
201. Glass, D. R. *et al.* An Integrated Multi-omic Single-Cell Atlas of Human B Cell Identity. *Immunity* **53**, 217-232.e5 (2020).
202. Sokal, A. *et al.* Maturation and persistence of the anti-SARS-CoV-2 memory B cell response. *Cell* **184**, 1201-1213.e14 (2021).
203. Lee, J. H. *et al.* Long-primed germinal centres with enduring affinity maturation and clonal migration. *Nature* **609**, 998–1004 (2022).
204. Chappert, P. *et al.* Human anti-smallpox long-lived memory B cells are defined by dynamic interactions in the splenic niche and long-lasting germinal center imprinting. *Immunity* **55**, 1872-1890.e9 (2022).

205. Turner, J. S. *et al.* Human germinal centres engage memory and naive B cells after influenza vaccination. *Nature* **586**, 127–132 (2020).
206. Takahashi, Y., Dutta, P. R., Cerasoli, D. M. & Kelsoe, G. In Situ Studies of the Primary Immune Response to (4-Hydroxy-3-Nitrophenyl)Acetyl. V. Affinity Maturation Develops in Two Stages of Clonal Selection. *J. Exp. Med.* **187**, 885–895 (1998).
207. Francis, T. On the Doctrine of Original Antigenic Sin. *Proc. Am. Philos. Soc.* **104**, 572–578 (1960).
208. Schiepers, A. *et al.* Molecular fate-mapping of serum antibody responses to repeat immunization. *Nature* **615**, 482–489 (2023).
209. Yang, L., Caradonna, T. M., Schmidt, A. G. & Chakraborty, A. K. Mechanisms that promote the evolution of cross-reactive antibodies upon vaccination with designed influenza immunogens. *Cell Rep.* **42**, 112160 (2023).
210. Wimmers, F. *et al.* Monitoring of dynamic changes in Keyhole Limpet Hemocyanin (KLH)-specific B cells in KLH-vaccinated cancer patients. *Sci. Rep.* **7**, 43486 (2017).
211. Baillard, S. *et al.* NMBA-specific memory T cell quantification by CD154 expression in anaphylaxis diagnosis. *World Allergy Organ. J.* **13**, (2020).
212. Nüsslein, H. G., Träg, T., Winter, M., Dietz, A. & Kalden, J. R. The role of T cells and the effect of hydrocortisone on interleukin-4-induced IgE synthesis by non-T cells. *Clin. Exp. Immunol.* **90**, 286–292 (1992).
213. Snapper, S. B. *et al.* Lysogeny and transformation in mycobacteria: stable expression of foreign genes. *Proc. Natl. Acad. Sci. U. S. A.* **85**, 6987–6991 (1988).
214. Litinskiy, M. B. *et al.* DCs induce CD40-independent immunoglobulin class switching through BLyS and APRIL. *Nat. Immunol.* **3**, 822–829 (2002).
215. Peyneau, M. Mécanismes de la sensibilisation aux curares dans le cadre de l'anaphylaxie per-anesthésique : Effet des ammoniums quaternaires et de la pholcodine sur les cellules dendritiques et la réponse lymphocytaire T in vitro. Tjhèse de doctorat sous la direction de Luc, de Chaisemartin, Saadia Kerdine-Römer et de Sylvie Chollet-Martin. (université Paris-Saclay, 2022).
216. Chung, C. H. *et al.* Cetuximab-induced anaphylaxis and IgE specific for galactose-alpha-1,3-galactose. *N. Engl. J. Med.* **358**, 1109–1117 (2008).
217. Obukhanych, T. V. & Nussenzweig, M. C. T-independent type II immune responses generate memory B cells. *J. Exp. Med.* **203**, 305–310 (2006).
218. Talay, O. *et al.* IgE^+ memory B cells and plasma cells generated through a germinal-center pathway. *Nat. Immunol.* **13**, 396–404 (2012).
219. He, J.-S. *et al.* Biology of IgE production: IgE cell differentiation and the memory of IgE responses. *Curr. Top. Microbiol. Immunol.* **388**, 1–19 (2015).
220. Karnowski, A., Achatz-Straussberger, G., Klockenbusch, C., Achatz, G. & Lamers, M. C. Inefficient processing of mRNA for the membrane form of IgE is a genetic mechanism to limit recruitment of IgE-secreting cells. *Eur. J. Immunol.* **36**, 1917–1925 (2006).
221. Asrat, S. *et al.* Chronic allergen exposure drives accumulation of long-lived IgE plasma cells in the bone marrow, giving rise to serological memory. *Sci. Immunol.* **5**, eaav8402 (2020).
222. Ota, M. *et al.* CD23+IgG1+ memory B cells are poised to switch to pathogenic IgE production in food allergy. *Sci. Transl. Med.* **16**, eadi0673 (2024).
223. Koenig, J. F. E. *et al.* Type 2–polarized memory B cells hold allergen-specific IgE memory. *Sci. Transl. Med.* **16**, eadi0944 (2024).
224. von Borstel, A., O'Hehir, R. E. & van Zelm, M. C. IgE in allergy: It takes two. *Sci. Transl. Med.* **16**, eadl1202 (2024).
225. MacGlashan, D. *et al.* In vitro regulation of FcepsilonRIalpha expression on human basophils by IgE antibody. *Blood* **91**, 1633–1643 (1998).

226. Elst, J. *et al.* MRGPRX2 and Immediate Drug Hypersensitivity: Insights From Cultured Human Mast Cells. *J. Investig. Allergol. Clin. Immunol.* **31**, 489–499 (2021).
227. Zajonc, D. M. Unconventional Peptide Presentation by Classical MHC Class I and Implications for T and NK Cell Activation. *Int. J. Mol. Sci.* **21**, 7561 (2020).
228. Schneider, C. H. & De Weck, A. L. A new chemical spect of penicillin allergy: the direct reaction of penicillin with epsilon-amino-groups. *Nature* **208**, 57–59 (1965).
229. Bechara, R., Maillere, B., Joseph, D., Weaver, R. J. & Pallardy, M. Identification and characterization of a naïve CD8+ T cell repertoire for benzylpenicillin. *Clin. Exp. Allergy J. Br. Soc. Allergy Clin. Immunol.* **49**, 636–643 (2019).
230. Meng, X. *et al.* Definition of the nature and hapten threshold of the β-lactam antigen required for T cell activation in vitro and in patients. *J. Immunol. Baltim. Md 1950* **198**, 4217–4227 (2017).
231. Jp, S. *et al.* Sulfamethoxazole and its metabolite nitroso sulfamethoxazole stimulate dendritic cell costimulatory signaling. *J. Immunol. Baltim. Md 1950* **178**, (2007).
232. Chipinda, I., Hettick, J. M. & Siegel, P. D. Haptenation: Chemical Reactivity and Protein Binding. *J. Allergy* **2011**, 839682 (2011).
233. Ahlström, S. *et al.* First genome-wide association study on rocuronium dose requirements shows association with SLCO1A2. *BJA Br. J. Anaesth.* **126**, 949–957 (2021).
234. Résumé des caractéristiques du produit - ESMERON 10 mg/mL, solution injectable - Base de données publique des médicaments. https://base-donnees-publique.medicaments.gouv.fr/affichageDoc.php?specid=68986795&typedoc=R.
235. Dhingra, N. *et al.* Molecular profiling of contact dermatitis skin identifies allergen-dependent differences in immune response. *J. Allergy Clin. Immunol.* **134**, 362–372 (2014).
236. Kamata, R. *et al.* Observation of hapten-induced sensitization responses for the development of a mouse skin sensitization test, including the elicitation phase. *Sci. Rep.* **12**, 19898 (2022).
237. Vollmer, J., Weltzien, H. U. & Moulon, C. TCR reactivity in human nickel allergy indicates contacts with complementarity-determining region 3 but excludes superantigen-like recognition. *J. Immunol. Baltim. Md 1950* **163**, 2723–2731 (1999).
238. Gamerdinger, K. *et al.* A new type of metal recognition by human T cells: contact residues for peptide-independent bridging of T cell receptor and major histocompatibility complex by nickel. *J. Exp. Med.* **197**, 1345–1353 (2003).
239. Adam, J., Pichler, W. J. & Yerly, D. Delayed drug hypersensitivity: models of T-cell stimulation. *Br. J. Clin. Pharmacol.* **71**, 701 (2011).
240. Pacheco, Y. *et al.* Bystander activation and autoimmunity. *J. Autoimmun.* **103**, 102301 (2019).
241. Shim, C.-H., Cho, S., Shin, Y.-M. & Choi, J.-M. Emerging role of bystander T cell activation in autoimmune diseases. *BMB Rep.* **55**, 57–64 (2022).
242. Clark, M. R., Massenburg, D., Zhang, M. & Siemasko, K. Molecular mechanisms of B cell antigen receptor trafficking. *Ann. N. Y. Acad. Sci.* **987**, 26–37 (2003).
243. Quah, B. J. C. *et al.* Bystander B cells rapidly acquire antigen receptors from activated B cells by membrane transfer. *Proc. Natl. Acad. Sci.* **105**, 4259–4264 (2008).
244. Townsend, C. L. *et al.* Significant Differences in Physicochemical Properties of Human Immunoglobulin Kappa and Lambda CDR3 Regions. *Front. Immunol.* **7**, (2016).
245. Fielding, L. & Grant, G. H. Conformational equilibria in amino steroids. 1. A proton and carbon-13 NMR spectroscopy and molecular mechanics study of 3.alpha.-hydroxy-2.beta.-(4-morpholinyl)-5.alpha.H-androstan-17-one. *J. Am. Chem. Soc.* **113**, 9785–9790 (1991).
246. Goswami, U., Rahman, M. M., Teng, J. & Hibbs, R. E. Structural interplay of anesthetics and paralytics on muscle nicotinic receptors. *Nat. Commun.* **14**, 3169 (2023).
247. Navinés-Ferrer, A. *et al.* MRGPRX2-mediated mast cell response to drugs used in perioperative procedures and anaesthesia. *Sci. Rep.* **8**, 11628 (2018).

248. Li, J. *et al.* Assessing cross-reactivity to neuromuscular blocking agents by skin and basophil activation tests in patients with neuromuscular blocking agent anaphylaxis. *Br. J. Anaesth.* **123**, e144–e150 (2019).
249. van Zelm, M. C., McKenzie, C. I., Varese, N., Rolland, J. M. & O'Hehir, R. E. Advances in allergen-specific immune cell measurements for improved detection of allergic sensitization and immunotherapy responses. *Allergy* **76**, 3374–3382 (2021).
250. Bruhns, P. *et al.* Specificity and affinity of human Fcgamma receptors and their polymorphic variants for human IgG subclasses. *Blood* **113**, 3716–3725 (2009).
251. Stone, K. D., Prussin, C. & Metcalfe, D. D. IgE, mast cells, basophils, and eosinophils. *J. Allergy Clin. Immunol.* **125**, S73-80 (2010).
252. Till, S. J., Francis, J. N., Nouri-Aria, K. & Durham, S. R. Mechanisms of immunotherapy. *J. Allergy Clin. Immunol.* **113**, 1025–1034 (2004).
253. García, B. E., Sanz, M. L., Gato, J. J., Fernández, J. & Oehling, A. IgG4 blocking effect on the release of antigen-specific histamine. *J. Investig. Allergol. Clin. Immunol.* **3**, 26–33 (1993).
254. Celebi Sözener, Z. *et al.* Tolerance mechanisms in allergen immunotherapy. *Curr. Opin. Allergy Clin. Immunol.* **20**, 591–601 (2020).
255. Wang, X., Mathieu, M. & Brezski, R. J. IgG Fc engineering to modulate antibody effector functions. *Protein Cell* **9**, 63–73 (2018).
256. Wilkinson, I. *et al.* Fc-engineered antibodies with immune effector functions completely abolished. *PLoS ONE* **16**, e0260954 (2021).
257. Grevys, A. *et al.* Fc Engineering of Human IgG1 for Altered Binding to the Neonatal Fc Receptor Affects Fc Effector Functions. *J. Immunol. Baltim. Md 1950* **194**, 5497–5508 (2015).
258. Kontermann, R. E. Strategies to extend plasma half-lives of recombinant antibodies. *BioDrugs Clin. Immunother. Biopharm. Gene Ther.* **23**, 93–109 (2009).
259. Wang, B., Gallolu Kankanamalage, S., Dong, J. & Liu, Y. Optimization of therapeutic antibodies. *Antib. Ther.* **4**, 45–54 (2021).
260. Ramirez-Benitez, M. C. & Almagro, J. C. Analysis of antibodies of known structure suggests a lack of correspondence between the residues in contact with the antigen and those modified by somatic hypermutation. *Proteins* **45**, 199–206 (2001).
261. Bom, A., Hope, F., Rutherford, S. & Thomson, K. Preclinical pharmacology of sugammadex. *J. Crit. Care* **24**, 29–35 (2009).
262. Cameron, K. S. *et al.* Modified gamma-cyclodextrins and their rocuronium complexes. *Org. Lett.* **4**, 3403–3406 (2002).
263. Merck Secures Bridion Patent Protection Through January 2026. *BioSpace* https://www.biospace.com/article/merck-secures-bridion-patent-protection-through-january-2026/.
264. Tontini, C. & Bulfone-Paus, S. Novel Approaches in the Inhibition of IgE-Induced Mast Cell Reactivity in Food Allergy. *Front. Immunol.* **12**, (2021).
265. Paolucci, M. *et al.* Targeting Ara h 2 with human-derived monoclonal antibodies prevents peanut-induced anaphylaxis in mice. *Allergy* **78**, 1605–1614 (2023).
266. De La Cruz, I., Errando, C. & Calaforra, S. Treatment of Anaphylaxis to Rocuronium with Sugammadex: A Case Report with Bronchospasm as the Only Symptom. *Turk. J. Anaesthesiol. Reanim.* **47**, 69–72 (2019).
267. Leysen, J., Bridts, C. H., De Clerck, L. S. & Ebo, D. G. Rocuronium-induced anaphylaxis is probably not mitigated by sugammadex: evidence from an in vitro experiment. *Anaesthesia* **66**, 526–527 (2011).

APPENDIX 1. Supplementary material from Article 1

LIST OF SUPPLEMENTARY DATA

Supp. Table 1: Summary of sorting data, monoclonal culture data rocuronium-binding human $CD27^+$ memory B cell sorting and monoclonal cultures

Supp. Table 2: ELISA results of all monoclonal cell cultures

Supp. Table 3: Crystallization conditions, data collection and refinement statistics of the m1B6-rocuronium and m2B1-rocuronium co-crystal structures

Supp. Fig. 1: Screening for anti-rocuronium IgG in patient's sera

Supp. Fig. 2: Gating strategy for the sorting of rocuronium-binding human memory B cells from human PBMCs.

Supp. Fig. 3: Analysis of single-cell sorts of rocuronium-binding atypical and typical memory B cells.

Supp. Fig. 4: Analysis of single-cell sorts of rocuronium-binding typical and atypical memory B cells from Patient#1_2023 and a healthy donor (HD).

Supp. Fig. 5: Anti-rocuronium human VH and VL nucleotidic mutation frequency

Supp. Fig. 6: Antibody repertoire analysis of the different patients

Supp. Fig. 7: Characteristics of the VL clonal group encoded by KV3-20*01_J1*01 from Patient#3

Supp. Fig. 8: Anti-rocuronium antibody repertoire comparison between Patient#1_2014 and Patient#1_2023

Supp. Fig. 9: Characterization of human anti-rocuronium mAbs

Supp. Fig. 10: Affinity of human anti-rocuronium mAbs for haptenized or free rocuronium

Supp. Fig. 11: Affinity of mouse anti-rocuronium mAbs for haptenized or free rocuronium

Supp. Fig. 12: Density map of rocuronium within the binding cleft of mAb m2B1 and mAb m1B6

Supp. Fig. 13: TOF measurement in the non-human primate cohort

Supp. Fig. 14: Follow-up of physiological parameters in macaques

	Sorting data			Monoclonal cultures				
Patient	**Sort**	**IgD- among CD27+ Bmem and among total cells %**	**HSA-roc+ HSA- among IgD- Bmem %**	**(A) cultured cells #**	**(B) Positive HSA-roc ELISA # (% among A)**	**(C) Not inhibited by free rocuronium # (% among B)**	**Total rocuronium-binding cultures # (% among A)**	**Total of sequenced and paired VH + VL (#)**
#1_2014	1	56.2 – 2.7	2.7	576	49 (8.5%)	10 (20%)	**57 (3.9%)**	25
	2	46.7 – 1	6.5	864	19 (2.1%)	1 (5%)		
#1_2023	1	31.3 – 1	1	768	142 (18%)	14 (10%)	**128 (16.7%)**	76
#2	1	42.7 – 1	1.5	576	23 (4%)	1 (4%)	**45 (2.6%)**	32
	2	25.8 – 1	2.2	576	20 (3,5%)	5 (25%)		
	3	34.9 – 1.2	2.2	576	3 (0.5%)	0 (0%)		
#3	1	29 – 0.7	3.7	576	5 (0.8%)	0 (0%)	**23 (1.3%)**	19
	2	20.5 – 0.9	3.9	576	16 (2.8%)	2 (13%)		
	3	45.3 – 1.1	3.1	576	4 (0.7%)	0 (0%)		

Supp. Table 1: Summary of sorting data, monoclonal culture data rocuronium-binding human CD27$^+$ memory B cell sorting and monoclonal cultures. (Left) For each sort of each patient, the percentage of memory B cells sorted (IgD$^-$) is indicated. IgD$^-$ memory B cells stained with HSA-roc but not with HSA (HSA-roc$^+$ HSA$^-$) are considered rocuronium-specific. (Right) The number of rocuronium-specific monoclonal B cell cultures (identified by positive anti-rocuronium ELISA and at least 50% signal inhibition using competitive ELISA with free rocuronium) are shown, as well as the number of paired VH/VL sequences retrieved.

	Clonal culture name	HSA-roc ELISA (OD)	Competition ELISA (OD)	Inhibition (%)
Patient#1_2014	1B3	0,235	0,067	71,5
	1B8	0,462	0,039	91,6
	1C3	0,208	0,12	42,3
	1D5	0,341	0,087	74,5
	1E9	0,568	0,08	85,9
	1F10	1,599	0,104	93,5
	1F12	0,558	0,107	80,8
	1G12	0,275	0,323	-17,5
	2A1	0,434	0,061	85,9
	2A9	0,583	0,043	92,6
	2B9	0,497	0,15	69,8
	2B10	0,676	0,101	85,1
	2D1	0,391	0,066	83,1
	2D6	1,159	0,055	95,3
	2D8	0,569	0,148	74,0
	2E2	0,319	0,203	36,4
	2E7	0,519	0,24	53,8
	2G4	0,285	0,131	54,0
	2G11	0,263	0,357	-35,7
	2H11	0,325	0,172	47,1
	3B3	0,709	0,598	15,7
	3C8	0,795	0,301	62,1
	3D7	0,596	0,068	88,6
	3E12	0,533	0,119	77,7
	3F3	0,338	0,069	79,6
	3F4	0,315	0,075	76,2
	3G6	0,578	0,058	90,0
	4E9	0,227	0,029	87,2
	4F4	0,38	0,176	53,7
	4G4	0,793	0,17	78,6
	4H8	0,282	0,096	66,0
	5A4	0,232	0,092	60,3
	5A10	0,349	0,326	6,6
	5B7	0,481	0,042	91,3
	5B12	0,686	0,249	63,7
	5C2	1,122	0,244	78,3
	5C12	0,357	0,097	72,8
	5D6	0,408	0,037	90,9
	5E8	0,735	0,057	92,2
	5G3	0,762	0,248	67,5
	6A1	0,286	0,28	2,1
	6A12	1,382	0,382	72,4
	6C2	0,747	0,517	30,8
	6C6	0,405	0,094	76,8
	6D9	1,392	0,38	72,7
	6E11	0,566	0,051	91,0
	6F7	0,814	0,064	92,1
	6F9	0,21	0,173	17,6
	6G6	0,679	0,077	88,7
	A2C1	0,273	0,042	84,6
	A2F11	0,211	0,051	75,8
	A2B4	0,657	0,067	89,8
	A2F12	0,452	0,046	89,8
	A3G4	0,595	0,136	77,1
	A3E12	1,102	0,124	88,7
	A3F3	0,331	0,04	87,9
	A3C5	0,241	0,037	84,6
	A4D1	0,27	0,042	84,4
	A4G4	0,204	0,047	77,0
	A4E5	0,398	0,036	91,0
	A10A9	0,783	0,038	95,1
	A6H7	0,638	0,039	93,9
	A5D4	0,415	0,041	90,1
	A7A6	0,676	0,063	90,7
	A7H12	0,997	0,082	91,8
	A7A3	1,164	0,679	41,7
	A8D8	0,334	0,045	86,5
	A5H5	0,699	0,061	91,3

	Clonal culture name	HSA-roc ELISA (OD)	Competition ELISA (OD)	Inhibition (%)
Patient#1_2023	I5C1	0,448	0,057	87,3
	I5C7	0,202	0,039	80,7
	I5D7	0,355	0,044	87,6
	I5D8	0,735	0,045	93,9
	I5E7	0,236	0,042	82,2
	I5E8	0,251	0,047	81,3
	I5F8	0,4	0,065	83,8
	I5F9	0,288	0,05	82,6
	I5Gi5	0,513	0,068	86,7
	I5G8	0,857	0,05	94,2
	I5G9	1,348	0,113	91,6
	I5H1	0,843	0,14	83,4
	I5H8	0,233	0,045	80,7
	I7A2	0,624	0,1	84,0
	I7Ai6	0,958	0,491	48,7
	I7Ai7	0,965	0,224	76,8
	I7A11	1,153	0,142	87,7
	I7A12	0,47	0,111	76,4
	I7B4	0,848	0,233	72,5
	I7Bi6	1,017	0,751	26,2
	I7Bi7	0,878	0,117	86,7
	I7B8	0,808	0,132	83,7
	I7B11	0,433	0,096	77,8
	I7C1	0,745	0,404	45,8
	I7C4	0,267	0,099	62,9
	I7C8	0,329	0,117	64,4
	I7D7	0,928	0,182	80,4
	I7D8	0,703	0,107	84,8
	I7D10	0,27	0,101	62,6
	I7Ei6	0,822	0,146	82,2
	I7Ei7	0,995	0,441	55,7
	I7E8	0,612	0,172	71,9
	I7E9	1,094	0,271	75,2
	I7F1	1,071	0,211	80,3
	I7F5	0,216	0,105	51,4
	I7Fi7	0,944	0,142	85,0
	I7F8	0,613	0,107	82,5
	I7F9	1,104	0,169	84,7
	I7F10	0,676	0,111	83,6
	I7G5	0,642	0,12	81,3
	I7Gi6	1,039	0,298	71,3
	I7Gi7	0,489	0,109	77,7
	I7G9	0,597	0,103	82,7
	I7H2	0,898	0,116	87,1
	I7H4	1,191	0,124	89,6
	I7H5	0,207	0,142	31,4
	I7Hi7	0,943	0,24	74,5
	I7H9	0,895	0,17	81,0
	I8A1	0,468	0,097	79,3
	I8A3	1,024	0,665	35,1
	I8A10	1,048	0,47	55,2
	I8B4	0,608	0,104	82,9
	I8Bi8	0,288	0,096	66,7
	I8C2	0,979	0,902	7,9
	I8C3	1,008	0,175	82,6
	I8Ci8	0,206	0,089	56,8
	I8C12	1,004	0,446	55,6
	I8D2	0,759	0,147	80,6
	I8D1	0,828	0,134	83,8
	II8D5	0,45	0,106	76,4
	I8E1	0,695	0,11	84,2
	I8E3	1,115	0,254	77,2
	I8E4	0,83	0,306	63,1
	I8E5	0,907	0,129	85,8
	I8EI8	0,982	0,763	22,3
	I8E9	0,426	0,264	38,0
	I8E11	0,9	0,436	51,6
	I8F1	0,734	0,139	81,1
	I8F3	0,753	0,119	84,2
	I8F7	0,511	0,104	79,6
	II8F10	0,226	0,093	58,8
	I8G2	0,49	0,102	79,2
	I8G10	0,595	0,111	81,3
	I8H3	0,344	0,117	66,0

	Clonal culture name	HSA-roc ELISA (OD)	Competition ELISA (OD)	Inhibition (%)
Patient#1_2023	I1A3	1,191	0,088	92,6
	I1A8	0,872	0,064	92,7
	I1Ai10	0,879	0,061	93,1
	I1B8	0,895	0,147	83,6
	I1C5	0,967	0,373	61,4
	IC10	0,225	0,053	76,4
	I1D2	0,945	0,503	46,8
	I1D3	0,605	0,537	11,2
	I1D8	0,243	0,052	78,6
	I1E2	0,8	0,097	87,9
	I1E5	0,872	0,443	49,2
	I1Ei12	0,557	0,054	90,3
	I1Fi1i1	0,921	0,332	64,0
	I1Gi1	0,956	0,104	89,1
	I1G4	0,31	0,047	84,8
	I1G5	0,615	0,036	94,1
	I1Gi6	0,526	0,05	90,5
	I1G9	0,509	0,059	88,4
	I2Ai2	0,452	0,05	88,9
	I2A7	0,522	0,417	20,1
	I2B1	0,873	0,565	35,3
	I2B3	0,922	0,362	60,7
	I2B5	0,436	0,039	91,1
	I2C3	0,79	0,077	90,3
	I2C5	0,985	0,183	81,4
	I2C9	0,472	0,049	89,6
	I2C10	0,803	0,055	93,2
	I2C11	0,458	0,041	91,0
	I2D1	0,908	0,085	90,6
	I2D4	1,095	0,065	94,1
	I2D5	0,425	0,044	89,6
	I2Di6	1,004	0,293	70,8
	I2D9	0,512	0,044	91,4
	I2E3	0,78	0,146	81,3
	I2E9	0,696	0,052	92,5
	I2E10	0,786	0,085	89,2
	I2F3	0,409	0,044	89,2
	I2F8	0,334	0,046	86,2
	I2G1	0,805	0,085	89,4
	I2G4	0,452	0,042	90,7
	I2G10	0,842	0,066	92,2
	I2G11	0,923	0,385	58,3
	I2H6	0,561	0,054	90,4
	I2H8	0,504	0,036	92,9
	I2H10	1,004	0,168	83,3
	I2H1i2	0,688	0,067	90,3
	I3A10	0,551	0,04	92,7
	I3A12	0,359	0,048	86,6
	I3C11	0,531	0,051	90,4
	I3G9	0,619	0,049	92,1
	I4Ai4	0,31	0,055	82,3
	I4B12	0,293	0,045	84,6
	I4D9	0,241	0,043	82,2
	I4D10	0,652	0,111	83,0
	I4E1	0,568	0,047	91,7
	I4E5	0,694	0,063	90,9
	I4E10	0,213	0,044	79,3
	I4G12	0,994	0,273	72,5
	I4H1	0,945	0,979	-3,6
	I4H8	0,235	0,079	66,4
	I5A2	0,549	0,061	88,9
	I5A7	0,73	0,239	67,3
	I5A8	0,613	0,096	84,3
	I5A11	0,216	0,035	83,8
	I5B1	0,755	0,071	90,6
	I5B2	0,249	0,048	80,7
	I5Bi6	0,237	0,062	73,8
	I5B12	0,24	0,05	79,2

	Clonal culture name	HSA-roc ELISA (OD)	Competition ELISA (OD)	Inhibition (%)
Patient#2	D1A9	0,846	0,021	97,5
	D1A11	0,33	0,028	91,5
	D1B3	1,033	0,032	96,9
	D1C8	0,313	0,04	87,2
	D1D10	0,569	0,024	95,8
	D1F11	0,519	0,068	86,9
	D1H10	1,107	0,064	94,2
	D2E2	1,343	0,156	88,4
	D3F7	0,233	0,05	78,5
	D3F8	1,459	0,246	83,1
	D3H12	0,218	0,053	75,7
	D4G11	1,083	0,233	78,5
	D4H7	0,293	0,041	86,0
	D5B8	0,353	0,033	90,7
	D5D5	0,235	0,034	85,5
	D5E4	1,213	0,092	92,4
	D5E10	0,872	0,581	33,4
	D6B9	0,247	0,043	82,6
	D6C5	0,46	0,029	93,7
	D6F2	0,994	0,075	92,5
	D6F11	1,153	0,067	94,2
	D6G1	0,832	0,039	95,3
	D6H8	0,228	0,037	83,8
	G3E1	1,943	0,419	78,4
	G3H9	1,05	0,303	71,1
	G4E12	0,993	0,353	64,5
	G4G12	1,419	0,865	39,0
	G5A4	0,872	0,129	85,2
	G5D1	0,432	0,284	34,3
	G2G4	0,845	0,147	82,6
	G3A7	0,457	0,195	57,3
	G3F2	0,313	0,049	84,3
	G3G8	0,365	0,055	84,9
	G3F11	1,319	0,398	69,8
	G3H10	1,415	0,206	85,4
	G4F12	1,404	0,944	32,8
	G4E12	1,453	0,465	68,0
	G5H4	1,018	0,283	72,2
	G5H9	0,904	0,28	69,0
	G6B3	0,786	0,788	-0,3
	G6D6	0,756	0,276	63,5
	G6G5	1,298	0,82	36,8
	G6B12	1,245	0,189	84,8
	E7B8	1,479	0,345	76,7
	E11G7	0,278	0,073	73,7
	E11B8	1,401	0,391	72,1

	Clonal culture name	HSA-roc ELISA (OD)	Competition ELISA (OD)	Inhibition (%)
Patient#3	B1A12	1,416	0,115	91,9
	B1C9	0,497	0,041	91,8
	B1G2	0,669	0,098	85,4
	B2B9	0,971	0,055	94,3
	B2G12	0,653	0,039	94,0
	B2H2	0,766	0,032	95,8
	B3A9	0,441	0,046	89,6
	B3F11	1,115	0,06	94,6
	B4D8	1,402	0,465	66,8
	B4G4	1,346	0,046	96,6
	B4G8	0,379	0,029	92,3
	B5F3	0,549	0,029	94,7
	B5F5	0,26	0,036	86,2
	B5G9	1,271	0,208	83,6
	B6C3	1,268	0,041	96,8
	B6E3	0,35	0,042	88,0
	H3A4	0,536	0,139	74,1
	H3C3	0,402	0,286	28,9
	H2A12	0,859	0,157	81,7
	H6C2	1,328	0,814	38,7
	F3A6	1,539	0,117	92,4
	F1D3	1,394	0,12	91,4
	F2F6	1,422	0,154	89,2
	F3H5	1,485	0,289	80,5
	F5E.1	1,722	0,341	80,2

Supp. Table 2: ELISA results of all monoclonal cell cultures. Supernatant of monoclonal cultures with an ELISA signal of HSA_{15}-rocuronium minus the ELISA signal of HSA (HSA-roc ELISA) superior to 3 times the background (i.e., OD>0.2) are shown. Competition was performed with 3,000 μM of free rocuronium. A monoclonal culture with a percentage of inhibition ≥ 50% was considered specific. Grey, non-specific cultures. Blue, cultures from which mAbs were recombinantly produced.

Crystal	Fab m2B1+rocuronium	ScFv m1B6+rocuronium
Reservoir solution	70% (v/v) MPD 0.1M HEPES pH7.5	30%(v/v) PEG400 0.1M MES pH6.5 0.1 M Na Acetate
Protein concentration, mg/m	7.1	15
Data collection		
Synchrotron beamline	PROXIMA 1	PROXIMA 2
Space group	C2	C2221
Unit cell dimensions		
a,b,c (Å)	161.57, 40.52, 69.78	135.47, 165.34, 127.52
a,b,g (°)	90, 100.40, 90	90, 90, 90
Resolution, Å	47.8-1.65 (1.68-1.65)	128-1.70 (1.73-1.70)
Rmerge	0.092 (1.372)	0.079 (1.707)
Rpim	0.038 (0.561)	0.027 (0.594)
Unique reflections	53958 (2663)	93815 (4304)
<I/sigma(I)>	10.7 (1.4)	16.4 (1.4)
Mn(I) half-set correlation	0.998 (0.603)	0.999 (0.567)
Completeness, %	100.0 (100.0)	100.0 (100.0)
Multiplicity	6.9 (6.9)	9.6 (9.2)
Refinement		
Resolution, Å	37.5-1.65 (1.67-1.65)	50.0-1.70 (1.72-1.70)
No. of reflections	52843 (1948)	153886 (5647)
Rvalue, working set	0.173 (0.200)	0.167 (0.299)
Rfree	0.301 (0.344)	0.189 (0.288)
Non-hydrogen protein	3644	6409
atoms	340	818
No. of Waters		
RMS deviations from ideal	0.012	0.015
bond length, Å	1.86	1.99
bond angles, °		
Ramachandran plot, %	98.07	96.15
preferred regions	1.45	3.11
allowed regions	0.48	0.74
outliers		

Supp. Table 3: Crystallization conditions, data collection and refinement statistics of the m1B6-rocuronium and m2B1-rocuronium co-crystal structures. Crystallization conditions, data collection and refinement statistics. Values in parentheses are for the highest resolution shell.

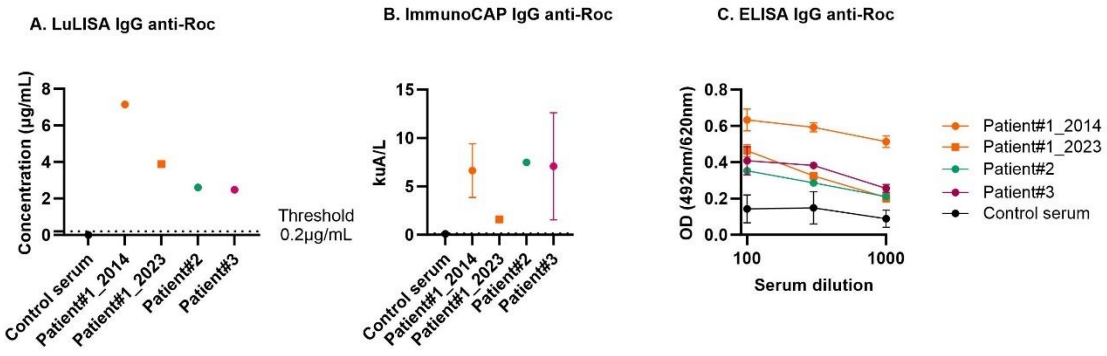

Supp. Fig. 1: **Screening for anti-rocuronium IgG in patient's sera.** IgG anti-rocuronium detection by (**A**) LuLISA with a cut-off level at 0.2 µg/mL (n=1), (**B**) ImmunoCAP with a cut-off level at 0.13 kUA/L (n=1) (**C**) ELISA performed in triplicates, in the serum of indicated patients or serum from five blood bank donors.

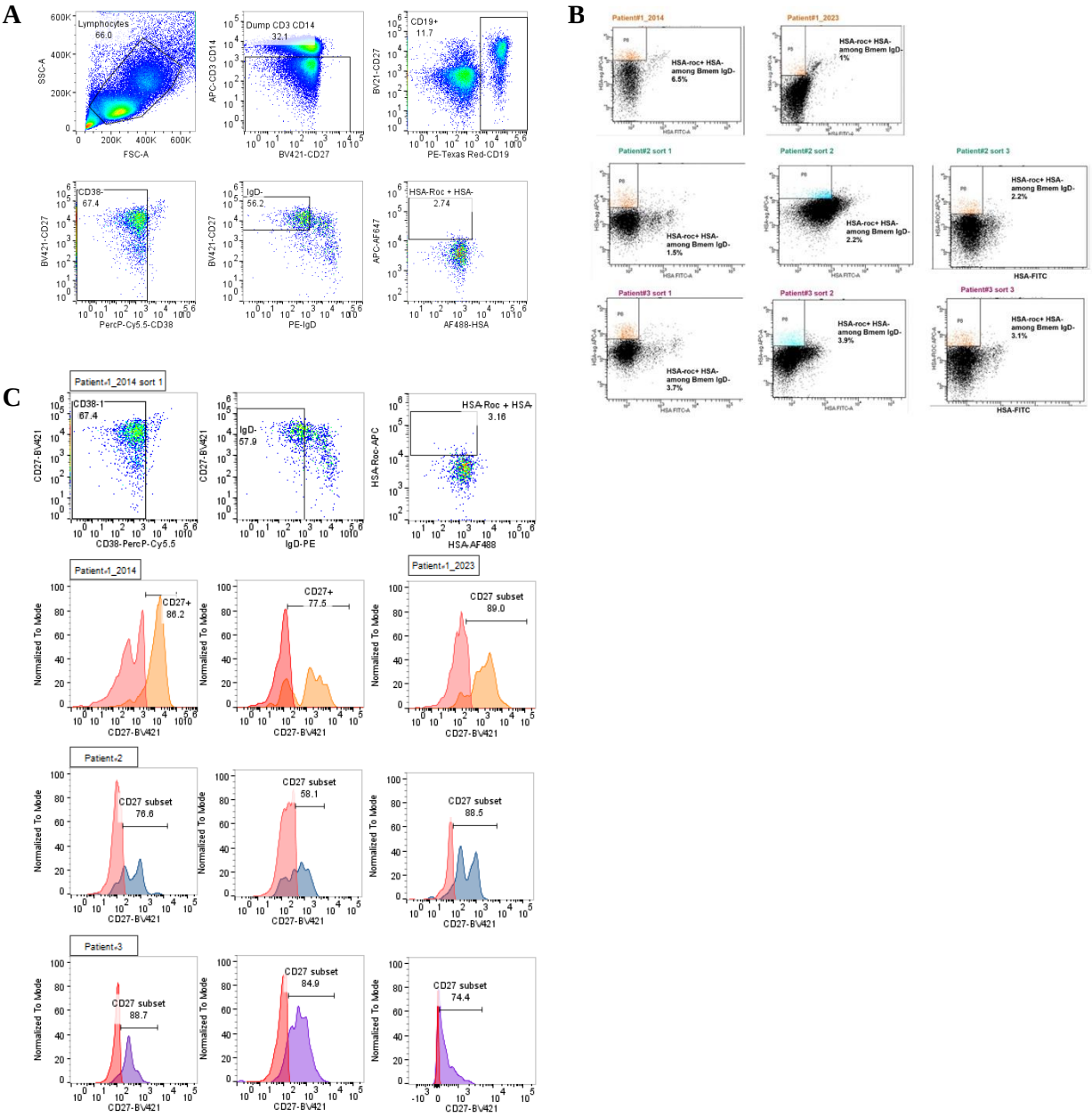

Supp. Fig. 2: **Gating strategy for the sorting of rocuronium-binding human memory B cells from human PBMCs**. (**A**) Full gating strategy for the single-cell sort of rocuronium-binding memory B cells ($CD3^-$ $CD14^-$ $CD19^+$ $CD38^-$ $CD27^+$ IgD^- $HSA\text{-}roc^+$ HSA^-) from the PBMCs of Patient#1_2014, as in Figure 1D. (**B**) Dot plots showing the final sorting gate for all the sorts with percentages of cells gated among the represented cells in each panel.(**C**) Back gating of the CD27+ population among CD3-, CD14-, CD38-, CD19+, HSA-Roc+, HSA-, IgD- cell populations. Histogram of the CD27+ population for Patient#1 (orange), Patient#2 (blue) and Patient#3 (purple) are superimposed on the histogram of the CD3-, CD14-, CD38-, and CD27- population. Percentage of CD27+ among antigen specific cells are calculated compared to the CD27- population.

A

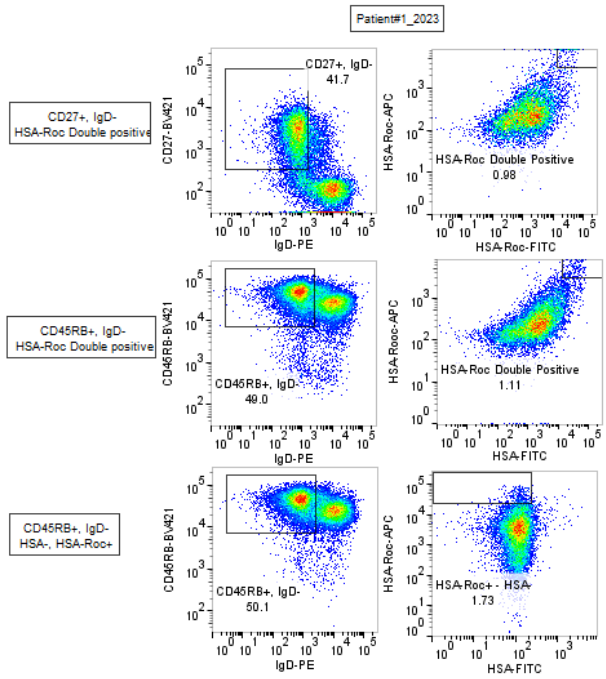

B

		Sorting data			Monoclonal cultures				
		IgD- among Bmem (%)	Antigen screen	Sorted cells among IgD- Bmem (%)	(A) cultured cells #	(B) Positive HSA-roc ELISA # (% among A)	(C) Not inhibited by free rocuronium # (% among B)	Total rocuronium-binding cultures # (% among A)	Strong binders among the latter # (%)
CD27+ typical memory B cells	**Patient#1_ 2023**	41.7%	HSA-rocuronium-APC *versus* HSA-rocuronium-FITC	0.98%	**768**	78 (9.9%)	9 (11%)	**69 (9%)**	57 (81%)
CD45RB+ atypical memory B cells		50.1%		1.73%	**672**	34 (5.0%)	2 (6%)	**32 (4.7%)**	18 (56%)
CD45RB+ atypical memory B cells		*49%*	HSA-rocuronium-APC versus HSA-FITC	*1.1%*	**672**	*38 (5.5%)*	*5 (13%)*	***33 (4.9%)***	16 *(48%)*

Supp. Fig. 3. (**A**) **Analysis of single-cell sorts of rocuronium-binding atypical and typical memory B cells.** $CD3^-$ $CD14^-$ $CD19^+$ $CD38^-$ PBMCs from Patient#1_2023 were gated for (top, left) CD27+ IgD- cells, or (middle, left and bottom, left) CD45RB+ IgD- cells, and immediately on their right for (top & middle) HSA-roc-APC+/HSA-roc-FITC+ ("HSA-roc double positive)"or HSA-roc-APC+/HSA-FITC- ("HSA-roc+ HSA-"). Numbers in the panels indicate the percentage of cells gated among the represented cells in each panel. The gates in the right column were used for single cell sorting. Numbers in the panels indicate the percentage of cells gated among the represented cells in each panel. (**B**) **Summary of sorting data and monoclonal cultures**. *Note*: Rocuronium specificity was assessed using competition ELISA for which free rocuronium inhibited a minimum of 50% of the OD value in the absence of free rocuronium. Strong versus weak binding (extreme right column) was determined by the ratio of the OD of the HSA-rocuronium ELISA on the OD of the IgG ELISA, with a ratio>1 being considered a strong binder.

A

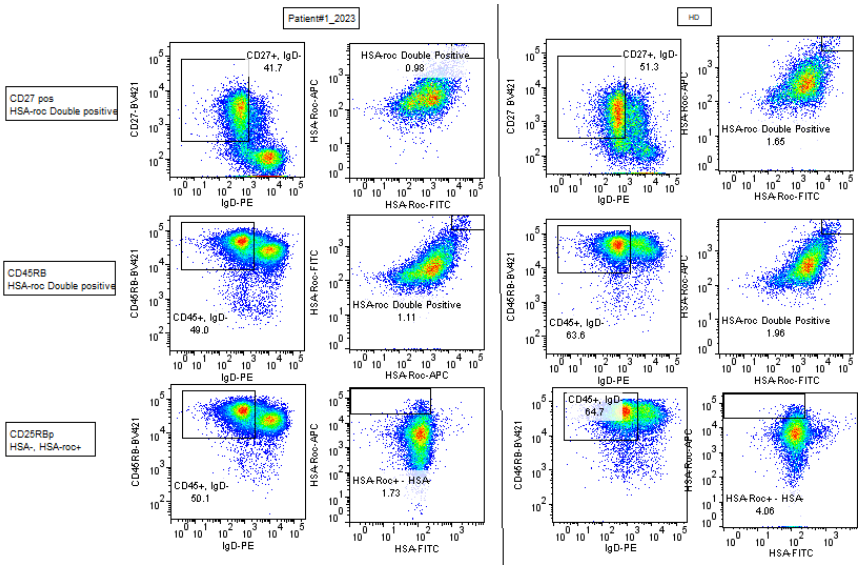

B

	Sorting data			Monoclonal cultures				
Patient	**Sort**	**CD27+ IgD- or CD45RB+ IgD- among Bmem cells** **%**	**Sorted cells** **%**	**(A) cultured cells** #	**(B) Positive HSA-roc ELISA** **# (% among A)**	**(C) Not inhibited by free rocuronium** **# (% among B)**	**Total rocuronium-binding cultures** **# (% among A)**	**Among the latter: Strong binders** **# (%)**
#1_2023	CD27+ double positive	41.7	0.98	768	78 (10%)	9 (12%)	69 (88%)	56 (**81**%)
HD		51.3	1.65	768	36 (4.7%)	0 (0%)	36 (100%)	22 (**61**%)
#1_2023	CD45RB+ double positive	50.1	1.73	672	34 (5.1%)	6 (18%)	28 (82%)	19 (**67**%)
HD		64.7	4.06	288	15 (5.2%)	2 (13%)	13 (87%)	5 (**38**%)
#1_2023	CD45RB+ HSA-roc+ HSA-	49	1.1	672	38 (5.6%)	13 (34%)	25 (66%)	21 (**84**%)
HD		63.6	1.96	288	14 (4.8%)	0 (0%)	14 (100%)	4 (**29**%)

Supp. Fig. 4. (**A**) **Analysis of single-cell sorts of rocuronium-binding typical and atypical memory B cells from Patient#1_2023 and a healthy donor (HD).** $CD3^-$ $CD14^-$ $CD19^+$ $CD38^-$ PBMCs from indicated individuals were gated for (top) CD27+ IgD- cells, or (middle and bottom) CD45RB+ IgD- cells, and immediately on their right for (top & middle) HSA-roc-APC+/HSA-roc-FITC+ ("HSA-roc double positive)"or HSA-roc-APC+/HSA-FITC- ("HSA-roc+ HSA-"). Numbers in the panels indicate the percentage of cells gated among the represented cells in each panel. The gates in the right column were used for single cell sorting. Numbers in the panels indicate the percentage of cells

gated among the represented cells in each panel. (**B**) **Summary of sorting data and monoclonal cultures**. *Note*: Rocuronium specificity was assessed using competition ELISA for which free rocuronium inhibited a minimum of 50% of the OD value in the absence of free rocuronium. Strong versus weak binding (extreme right column) was determined by the ratio of the OD of the HSA-rocuronium ELISA on the OD of the IgG ELISA, with a ratio>1 being considered a strong binder.

A

	VH mutations			VL mutations		
Patient	**mean**	median	standard deviation	**mean**	median	standard deviation
#1_2014	**16.9**	14	12.9	**9.2**	10	4.9
#1_2023	**11.5**	11	6.5	**5.0**	4	3.6
#2	**15.0**	15	8.4	**7.8**	8	4.8
#3	**6.0**	2	8.7	**2.9**	1	3.7
All	**13.0**	12	9.6	**6.3**	5.5	4.7

B

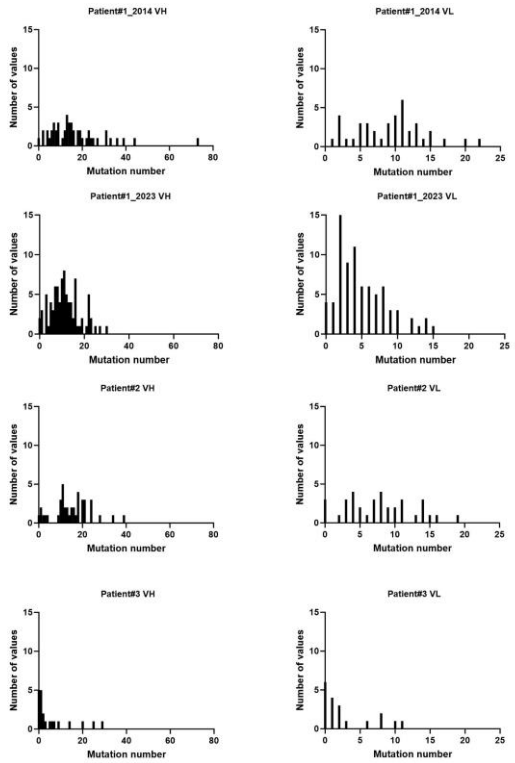

Supp. Fig. 5: **Anti-rocuronium human VH and VL nucleotidic mutation frequency**. (**A**) VH and VL mutation frequencies compared to germline among VH-VL pairs from each patient or VH-VL pairs from all patients pooled together (All). (**B**) Distribution of mutation frequency among (top) VH sequences and (bottom) VL sequences compared to germline in indicated patient samples and from all patients pooled together (All).

A

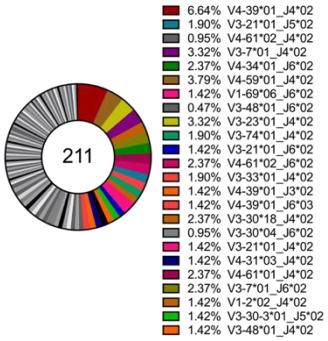
211
6.64% V4-39*01_J4*02
1.90% V3-21*01_J5*02
0.95% V4-61*02_J4*02
3.32% V3-7*01_J4*02
2.37% V4-34*01_J6*02
3.79% V4-59*01_J4*02
1.42% V1-69*06_J6*02
0.47% V3-48*01_J6*02
3.32% V3-23*01_J4*02
1.90% V3-74*01_J4*02
1.42% V3-21*01_J6*02
2.37% V4-61*02_J6*02
1.90% V3-33*01_J4*02
1.42% V4-39*01_J3*02
1.42% V4-39*01_J6*03
2.37% V3-30*18_J4*02
0.95% V3-30*04_J6*02
1.42% V3-21*01_J4*02
1.42% V4-31*03_J4*02
2.37% V4-61*01_J4*02
2.37% V3-7*01_J6*02
1.42% V1-2*02_J4*02
1.42% V3-30-3*01_J5*02
1.42% V3-48*01_J4*02

B

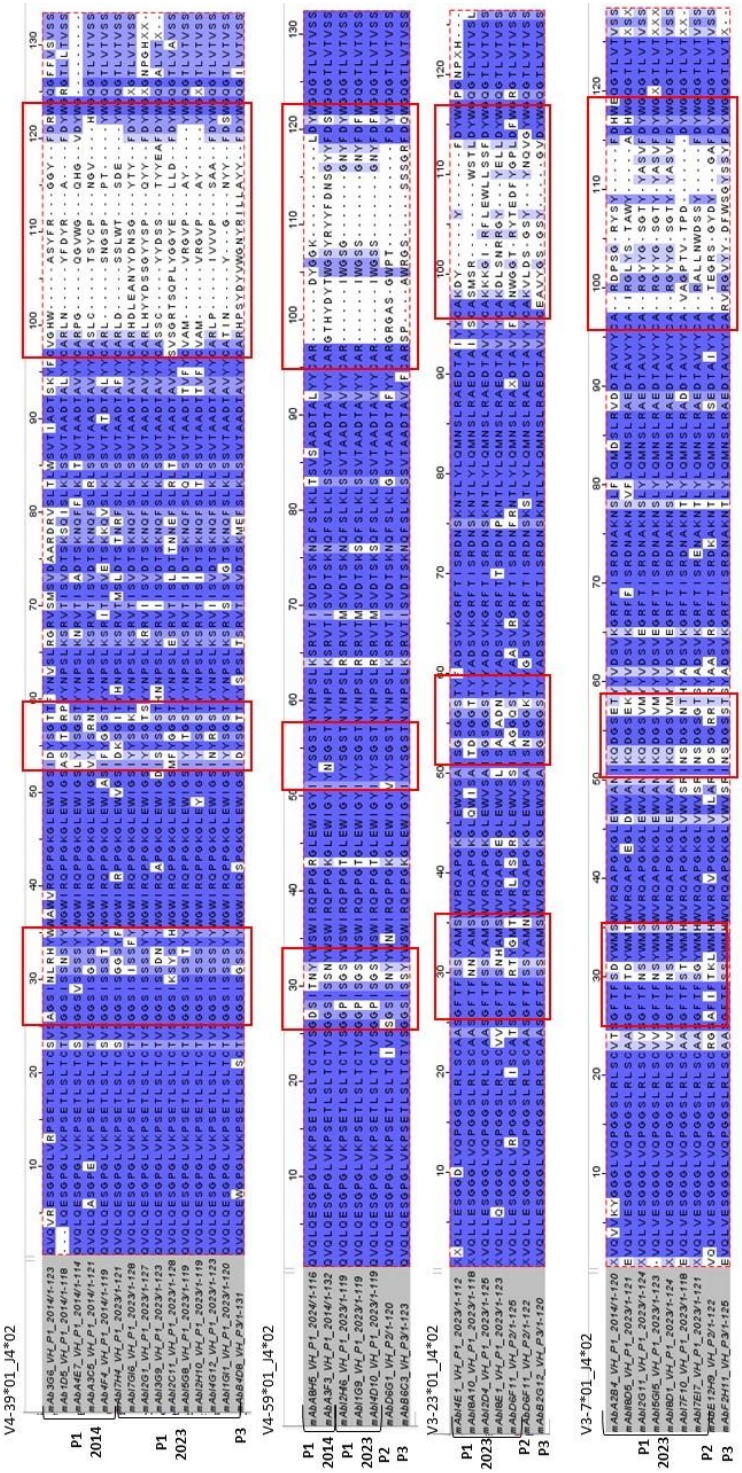
V4-39*01_J4*02
V4-59*01_J4*02
V3-23*01_J4*02
V3-7*01_J4*02
P1
2014
P1
2023
P2
P3

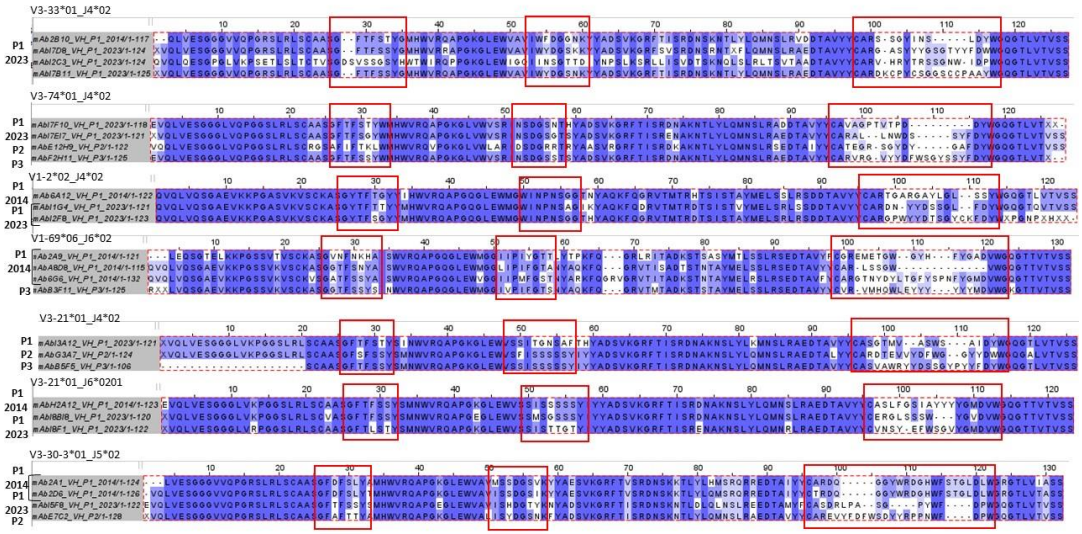
V3-33*01_J4*02
V3-74*01_J4*02
V1-2*02_J4*02
V1-69*06_J6*02
V3-21*01_J4*02
V3-21*01_J6*0201
V3-30-3*01_J5*02

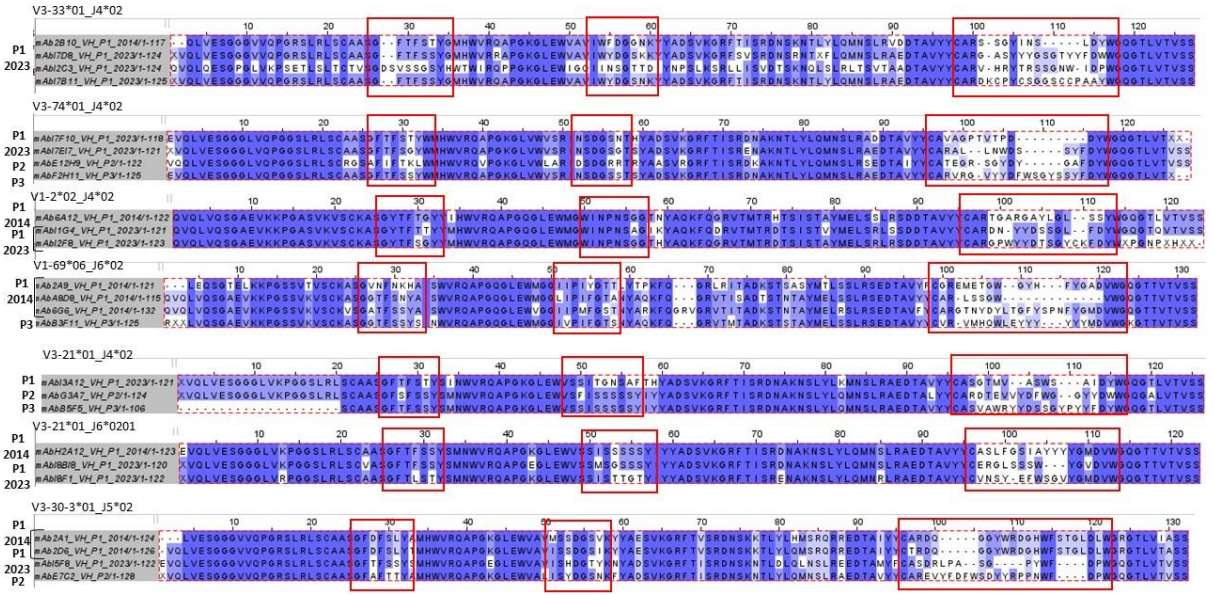
V3-33*01_J4*02
V3-74*01_J4*02
V1-2*02_J4*02
V1-69*06_J6*02
V3-21*01_J4*02
V3-21*01_J6*0201
V3-30-3*01_J5*02

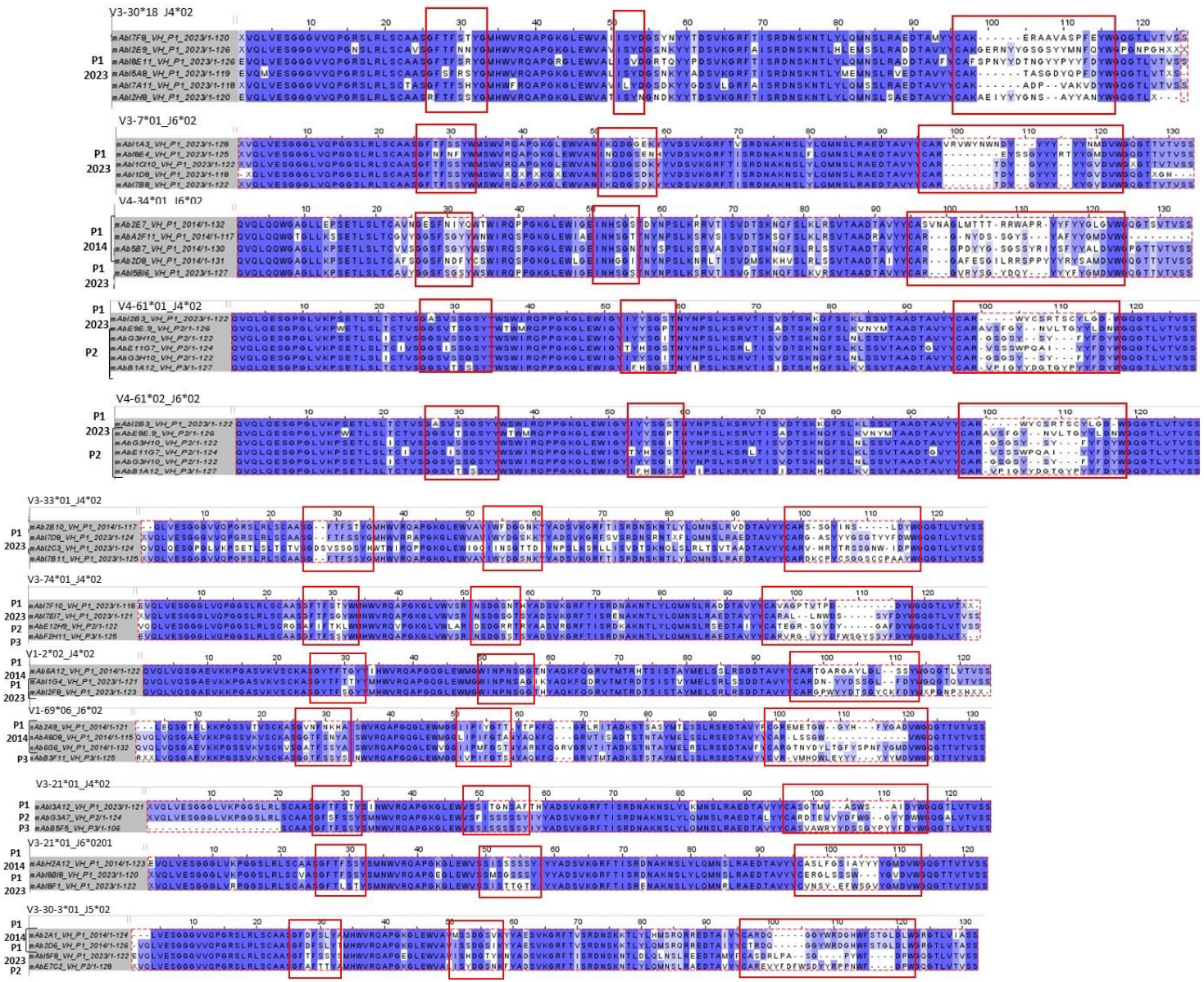
V3-30*18_J4*02
V3-7*01_J6*02
V4-34*01_J6*02
V4-61*01_J4*02
V4-61*02_J6*02
V3-33*01_J4*02
V3-74*01_J4*02
V1-2*02_J4*02
V1-69*06_J6*02
V3-21*01_J4*02
V3-21*01_J6*0201
V3-30-3*01_J5*02

Supp. Fig. 6: Antibody repertoire analysis of the different patients. (**A**) Donut plot of V(D)J gene usage among all the VH (n=211, indicated in the center of the donut) sequenced from monoclonal B cell cultures of the 3 patients. The major V-J recombinations and their frequency (in parentheses) are indicated in color. (**B**) Sequence alignment of the amino acid VH sequences from the 22 V-J families composed of at least 3 members using MUltiple Sequence Comparison by Log- Expectation (Muscle) and colored by percentage identity. CDRs are framed in red. Names of the V-J families are indicated over the alignments and colored in the donut plot.

A

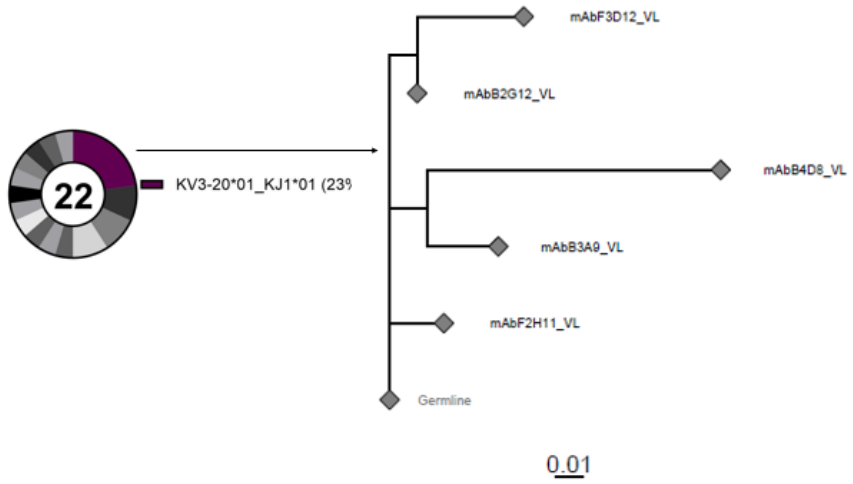

B

	VH (V gene)	VH (D gene)	VH (J gene)	CDR3
mAbF3D12_VH	IGHV1-3*01	IGHD3-3*01	IGHJ3*02	CARGAEYYDFWSGYSGGSDAFDIW
mAbB2G12_VH	IGHV3-23*01,IGHV3-23D*01	IGHD3-10*01	IGHJ4*02	CEAVYGSGSYGVDYW
mAbB4D8_VH	IGHV4-39*01	IGHD3-16*02	IGHJ4*02	CARHPSYDYVWGNYRILLAYYFDYW
mAbB3A9_VH	IGHV3-64D*06	IGHD6-19*01	IGHJ5*02	CVKDRSVAGKYNWFDPW
mABF2H11_VH	IGHV3-74*01	IGHD3-3*01	IGHJ4*02	CARVRGVYYDFWSGYSSYFDYW

C

	mAbF3D12	mAbB2G12	mAbB4D8	mAbB3A9	mABF2H11
mAbF3D12	-	48.30	44.62	50.39	55.47
mAbB2G12	-	-	50.76	83.61	79.2
mAbB4D8	-	-	-	50.76	49.24
mAbB3A9	-	-	-	-	78.4
mABF2H11	-	-	-	-	-

Supp. Fig. 7. Characteristics of the VL clonal group encoded by KV3-20*01_J1*01 from Patient#3. (**A**) Tree showing nucleotidic distances among the clonal group (identical V-J genes and CDR3 length) composed of the five VLs corresponding to a KV3-20*01_J1*01 rearrangement from Patient#3, and the GKV3−20_IGKJ1 germline sequence. (**B**) Heavy chain V-D-J gene identity, CDR3 amino acid sequence and (**C**) peptidic sequence homology of the antibodies belonging to the KV3-20*01_J1*01 clonal group from Patient#3.

A

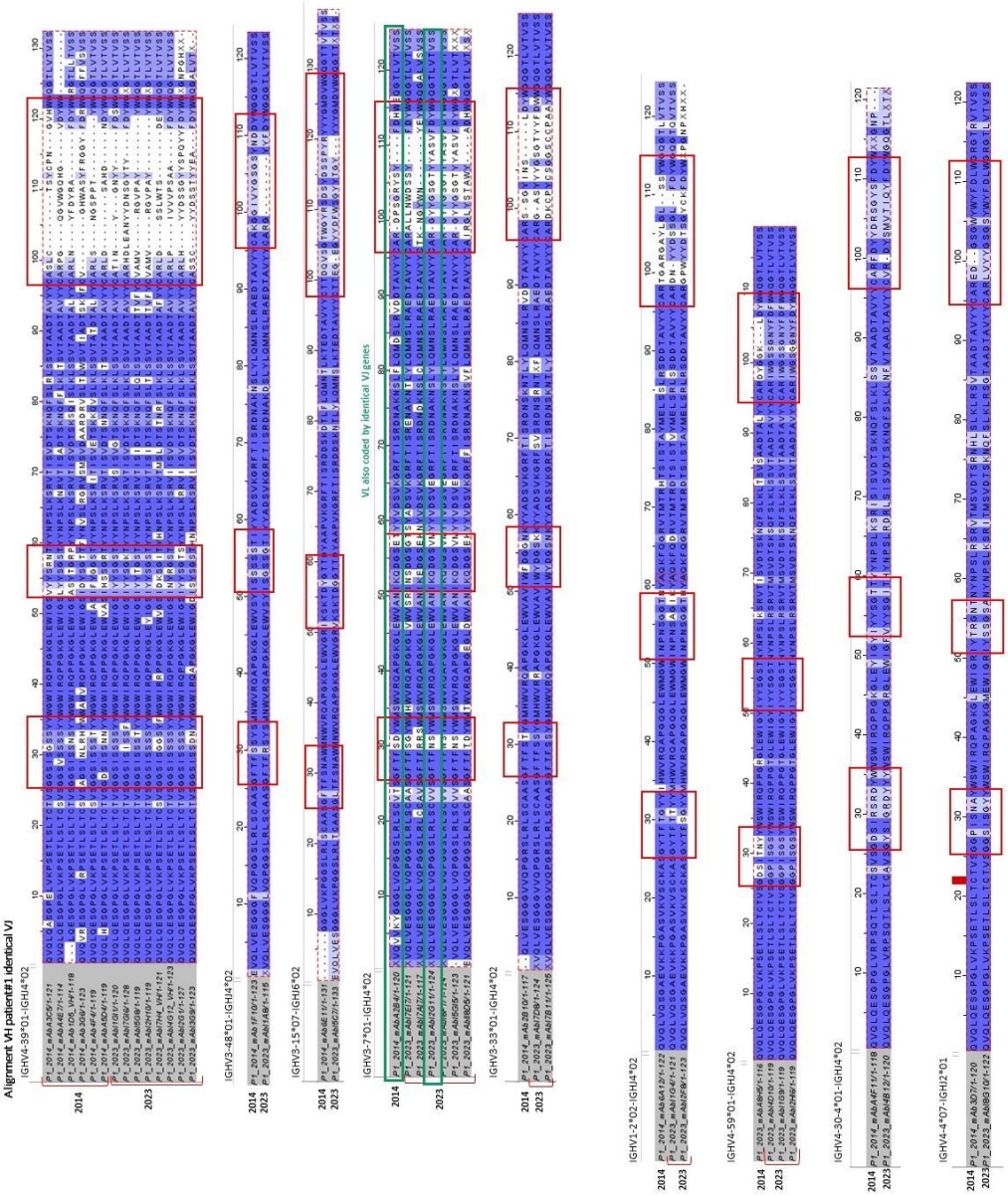
Alignment VH patient#1 identical VJ
IGHV4-39*01-IGHJ4*02
IGHV3-48*01-IGHJ4*02
IGHV3-15*07-IGHJ6*02
IGHV3-7*01-IGHJ4*02
VL also coded by identical VJ genes
IGHV3-33*01-IGHJ4*02
IGHV1-2*02-IGHJ4*02
IGHV4-59*01-IGHJ4*02
IGHV4-30-4*01-IGHJ4*02
IGHV4-4*07-IGHJ2*01

B

	VH CDR3	% ID VH	VL CDR3	% ID VL
mAb A2B4 Patient#1_2014	CARDPSGRYSYFDHW	81	CQQYYSIPPGTF	86
mAb I2G11 Patient#1_2023	CARGYYGSGTYYASVFDYW		CQQYYNTPWTF	

Supp. Fig. 8: Anti-rocuronium antibody repertoire comparison between Patient#1_2014 and Patient#1_2023. (**A**) Sequence alignment of the amino acid VH sequences coded by identical V-J genes using MUltiple Sequence Comparison by Log- Expectation (Muscle) and colored by percentage identity. CDRs are framed in red. Among those, two VH sequences also share the same light chain rearrangement and are highlighted in green. (**B**) Comparison of mAbs A2B4 and I2G11 with percentage similarities of pairwise alignment of the complete sequence.

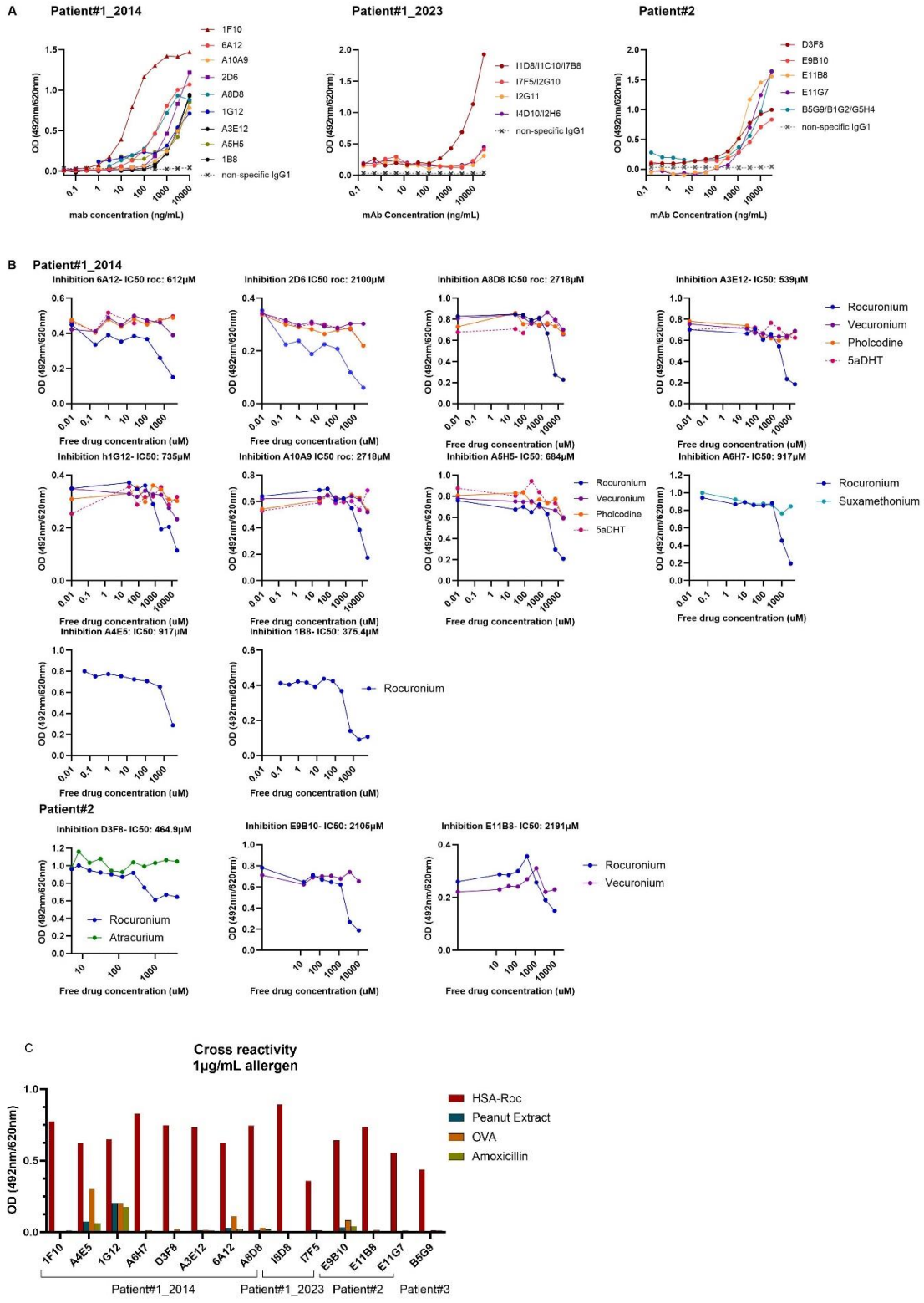

Supp. Fig. 9: Characterization of human anti-rocuronium mAbs. (**A**) Binding of human mAbs to rocuronium by ELISA. (**B**) "Competitive ELISA" of anti-IgG rocuronium ELISA from (**B**) Patient#1_2014 and Patient#2 at fixed mAb concentration (1.5 µg/mL) but increasing concentrations of indicated molecules free in solution. 5aDHT: 5-alpha-

Di-Hydro-Testosterone; IC50, Half-maximal inhibitory concentration. (C) Cross-reactivity test by ELISA of representative mAbs. Various allergens (peanut extract, amoxicillin, and ovalbumin) were coated at 1 µg/mL with mAb concentrations (2µg/mL - 0.03 ug/mL). For a fixed mAb concentration giving a signal ~OD0.7 the signal given for the representative allergen is represented.

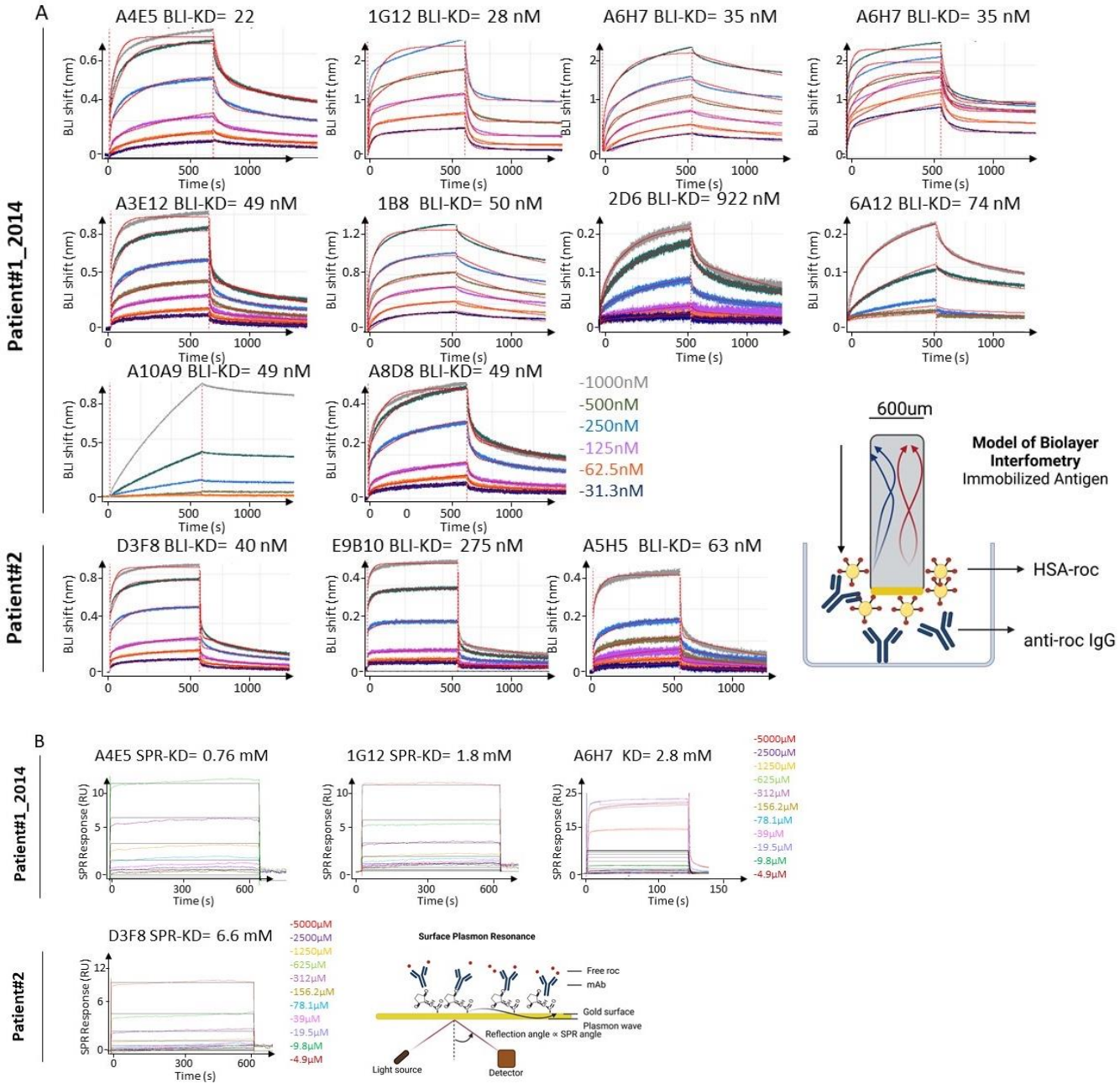

Supp. Fig. 10: Affinity of human anti-rocuronium mAbs for haptenized or free rocuronium. (**A**) Bio-layer interferometry affinity measurement of the interaction between immobilized HSA-roc and varying concentrations of human mAbs in solution. A scheme of the setup is provided. (**B**) Surface Plasmon Resonance affinity measurement of the interaction between immobilized human mAbs captured by an anti-Fc and varying concentrations of free rocuronium in solution. A scheme of the setup is provided. (A-B) The KD was obtained by fitting the curves using a heterogenous ligand model.

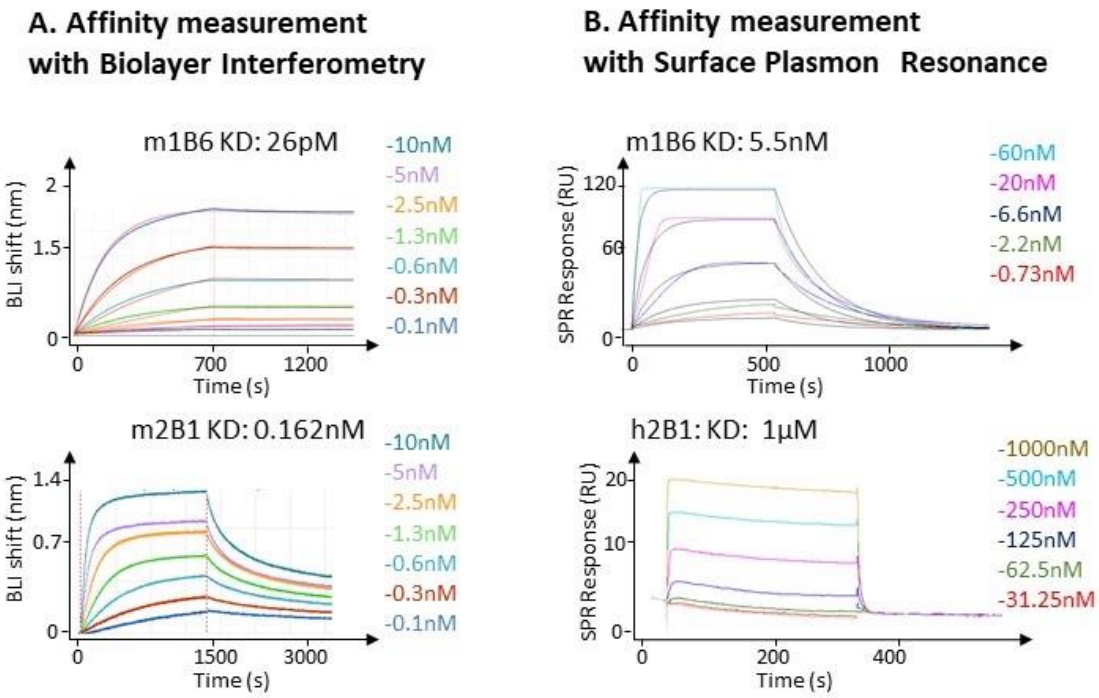

Supp. Fig. 11: Affinity of mouse anti-rocuronium mAbs for haptenized or free rocuronium. (**A**) Bio-layer interferometry affinity measurement of the interaction between immobilized HSA-roc and varying concentrations of mouse mAbs in solution. (**B**) Surface Plasmon Resonance affinity measurement of the interaction between immobilized mouse mAbs captured by an anti-Fc and varying concentrations of free rocuronium in solution. (A-B) Fitting was performed using kinetic analysis and 1:1 binding, and the K_D are indicated.

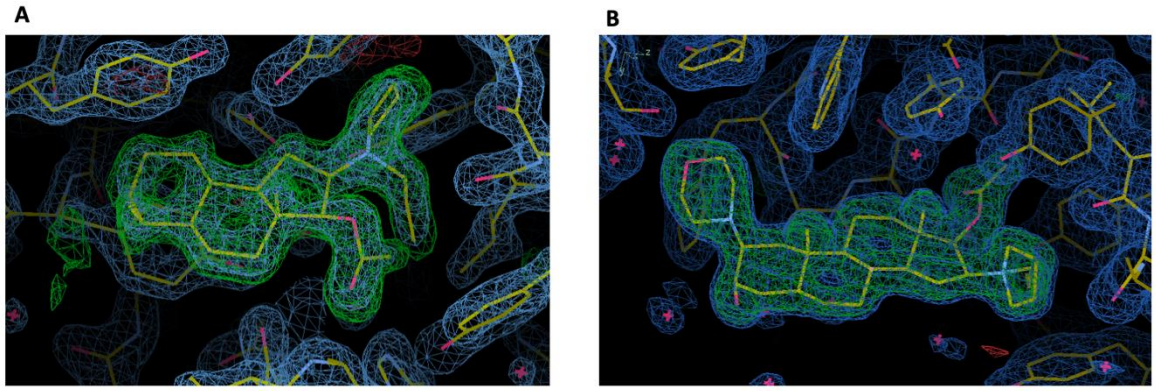

Supp. Fig. 12. Density map of rocuronium within the binding cleft of mAb m2B1 and mAb m1B6. 2Fo-Fc electron density omitmap contoured at 3.5σ of Fab-m2B1-rocuronium (**A**) and scFv-m1B6-rocuronium (**B**) showing the rocuronium molecule in the binding site of both antibodies.

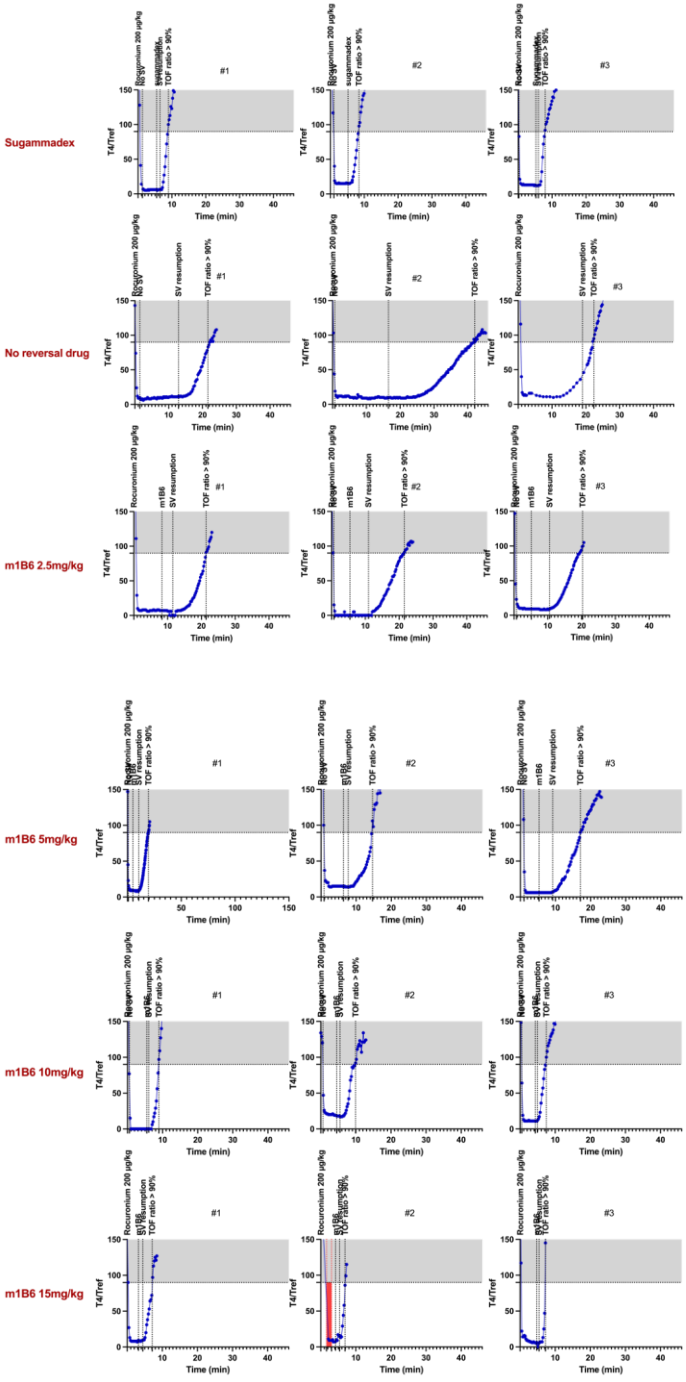

Supp. Fig. 13: TOF measurement in the non-human primate cohort. TOF measurement in macaques following rocuronium injection (200 µg/kg) to monitor neuromuscular reversal following injection of indicated compounds. The time points of rocuronium injection, compound injection, resumption of spontaneous ventilation (SV) and TOF ratio T4/Tref > 0.9 are indicated. Once deep neuromuscular blockade was established (absence of T1 response), indicated concentrations of (first row) sugammadex, (second row) vehicle, (third row) m1B6 at 2.5 mg/mL, (fourth row) m1B6 at 5 mg/mL, (fifth row) m1B6 at 10 mg/mL, (sixth row) m1B6 at 15 mg/mL were injected. The ID of each macaque is indicated. Red box illustrates the interruption of monitoring.

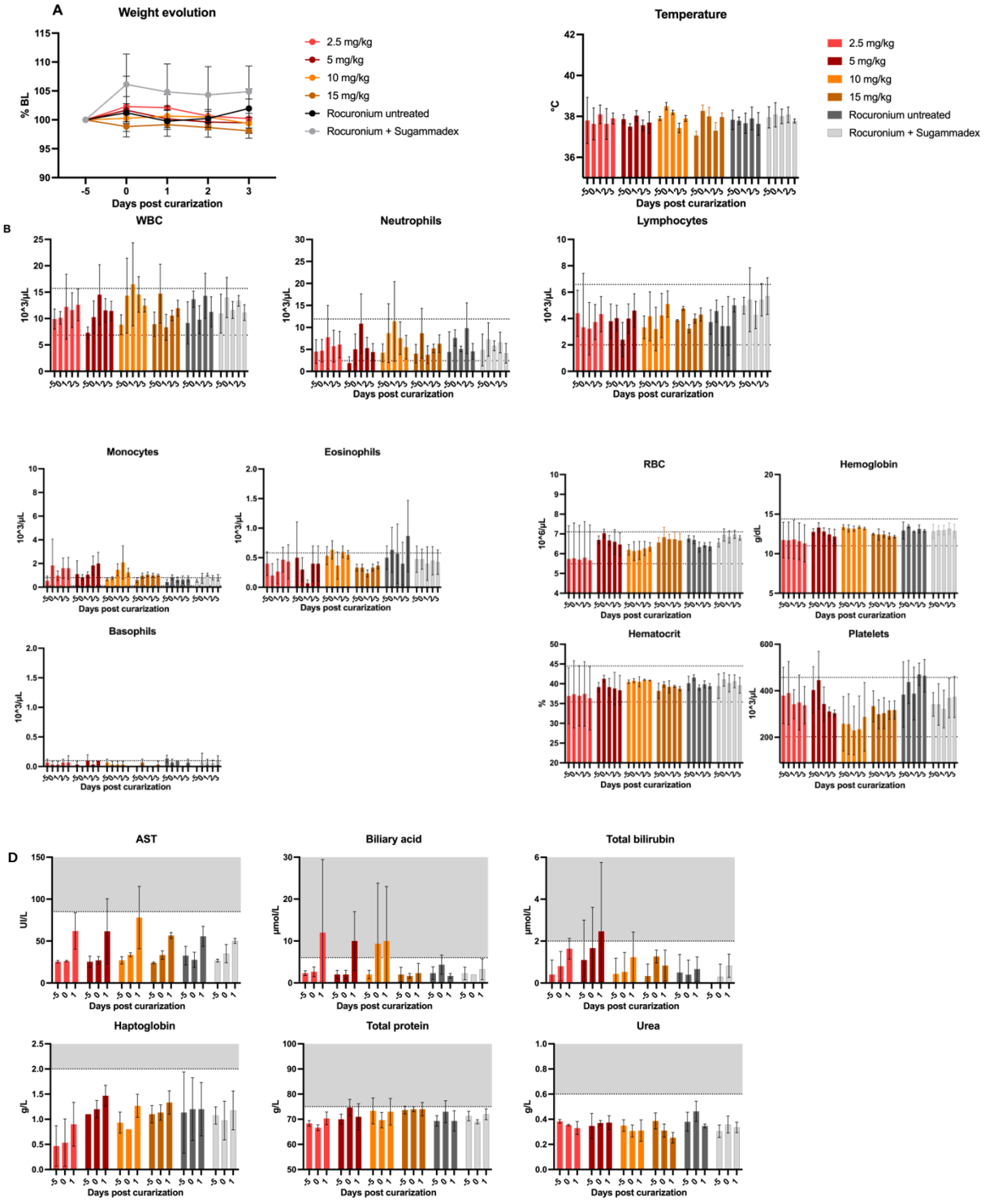

Supp. Fig. 14: Follow-up of physiological parameters in macaques. Median and standard deviation of the macaques (n=5 per group) (**A**) body weight and body temperature modification reported to the day of curare enhanced anesthesia. (**B**) Median and standard deviation of indicated cell populations and hematocrit in circulating blood reported to the day of curare enhanced anesthesia for each macaque (n=5 per group). (**D**) Blood biochemistry results for indicated parameters of the macaques (n=3 per group). (A-D) Blood drawing on day 0 was performed before curare injection. No statistical significance was found for any measurement or cell population count.

APPENDIX 2. Supplementary material from Article 2

SUPPLEMENTARY FIGURES

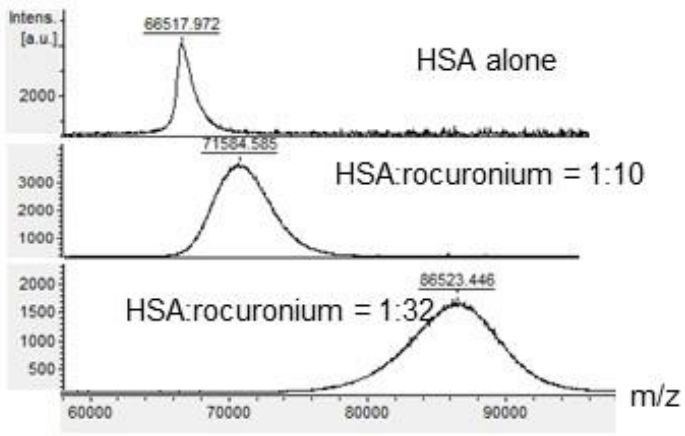

Sup. Fig. 1: Chemical conjugation of rocuronium derivatives to a carrier protein. MALDI-TOF spectra of HSA alone (top) and conjugated to rocuronium with molar ratios 1:10 (middle) and 1:32 (bottom). The light intensity according to the mass (m) on charge (z) ratio is represented.

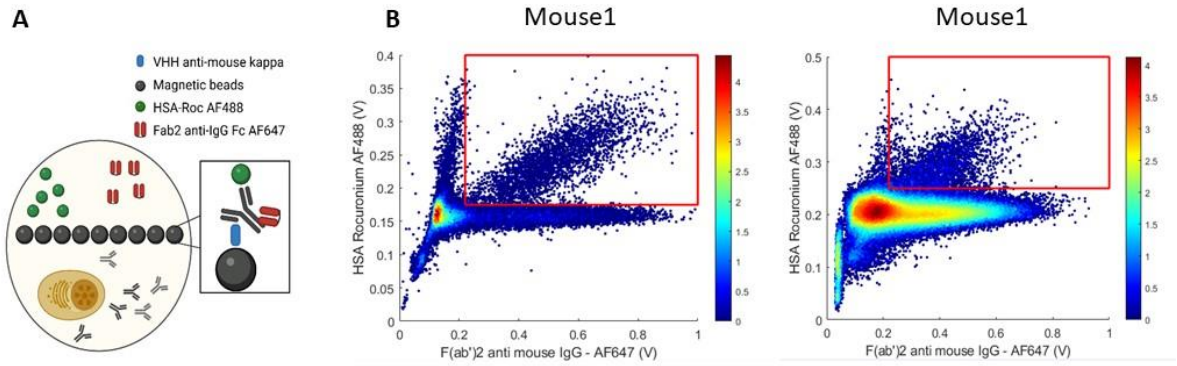

Sup. Fig. 2: Microfluidic droplet assay to detect rocuronium-specific IgG secreting cells. (**A**) Schematic of the in-droplet assay. Superparamagnetic nanoparticles pre-coated with a VHH anti-mouse kappa chain align into a beadline under the influence of a magnetic field applied to the microfluidic chip. If a kappa-light chain antibody-secreting cell is present in the droplet, its antibody will be captured by the VHH onto the beadline. If this antibody is an IgG it will be bound by the Alexa Fluor (AF) 647-labeled F(ab')$_2$ anti-mouse IgG Fc. If this antibody has affinity for rocuronium it will bind AF488-labeled HSA-rocuronium. This fluorescence relocation towards the beadline allows the generation of a fixed laser-induced signal to be captured by the photomultipliers (PMTs). The peak fluorescence intensity is acquired for each droplet. (**B**) Density plot representation of peak fluorescence intensity values for AF488 and AF647of all the droplets analyzed during the sort of cells from mouse#1. Droplets with peak fluorescence values contained in the red quadrant were sort

A

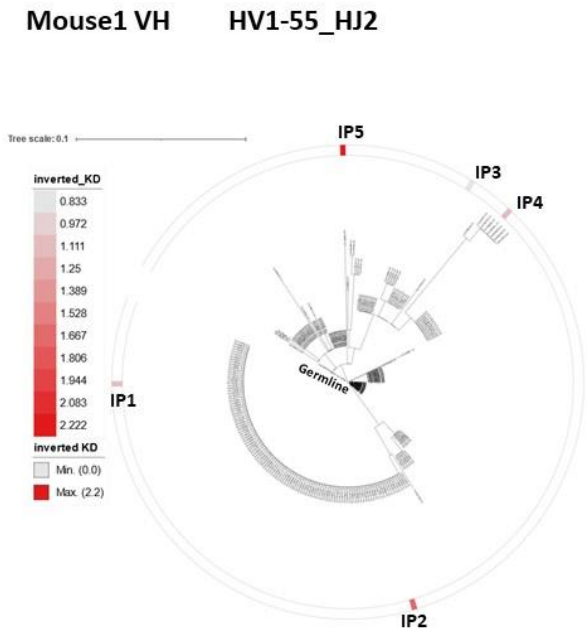
Mouse1 VH HV1-55_HJ2
Tree scale: 0.1
inverted_KD
0.833
0.972
1.111
1.25
1.389
1.528
1.667
1.806
1.944
2.083
2.222
inverted KD
Min. (0.0)
Max. (2.2)
IP5
IP3
IP4
IP1
IP2
Germline

B

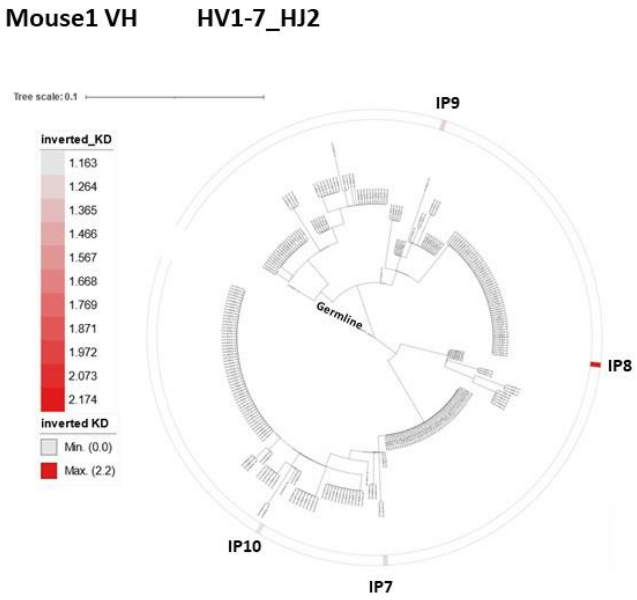
Mouse1 VH HV1-7_HJ2
Tree scale: 0.1
inverted_KD
1.163
1.264
1.365
1.466
1.567
1.668
1.769
1.871
1.972
2.073
2.174
inverted KD
Min. (0.0)
Max. (2.2)
IP9
IP8
IP10
IP7
Germline

C

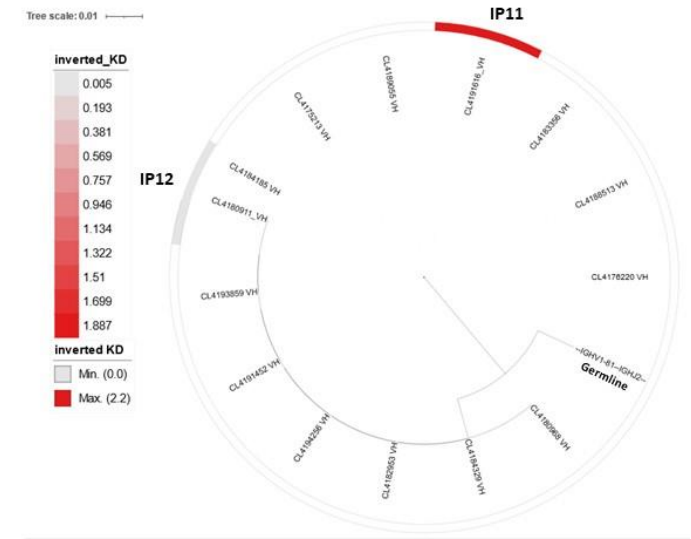
Mouse1 VH HV1-81_HJ2
Tree scale: 0.01
inverted_KD
0.005
0.193
0.381
0.569
0.757
0.946
1.134
1.322
1.51
1.699
1.887
inverted KD
Min. (0.0)
Max. (2.2)
IP11
IP12
Germline

D

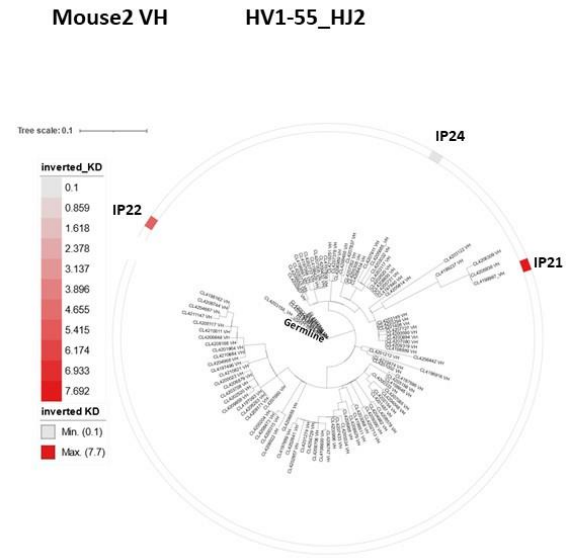

E

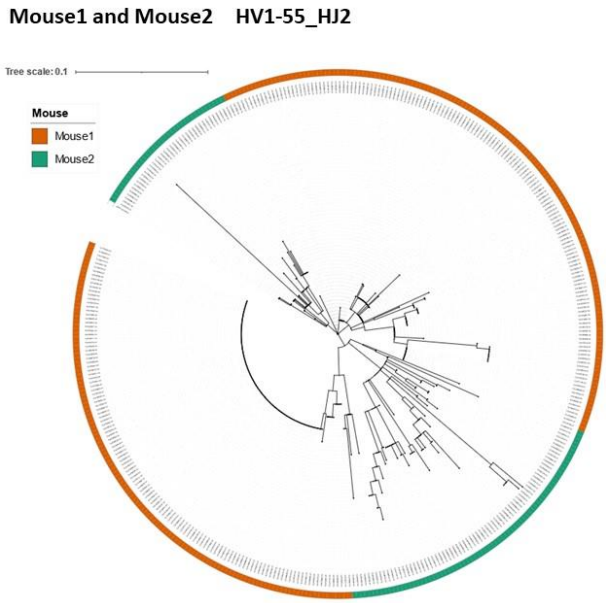

Supp. Fig. 3: Phylogenic analysis of the VH amino acid sequences of the "functional" antibody repertoire. Circular plot showing the VH amino acid distance of sequences coded by identical V-J genes of the "functional" repertoire i.e., with at least one family member having affinity for free rocuronium for each mouse (Fig A-D) and for two mice combined (FigE). Trees are rooted according to the germline sequence. NB: the length of a branch represents the number of mutations per residues as indicated by the scale (e.g., for a sequence length of 100 amino acids, a length of 0.01 corresponds to 1 amino acid mutation). Recombinantly produced and characterized mAbs for each family, and their affinity for free rocuronium indicated by an inverted K_D color scale i.e., the better the affinity, the darker the color.

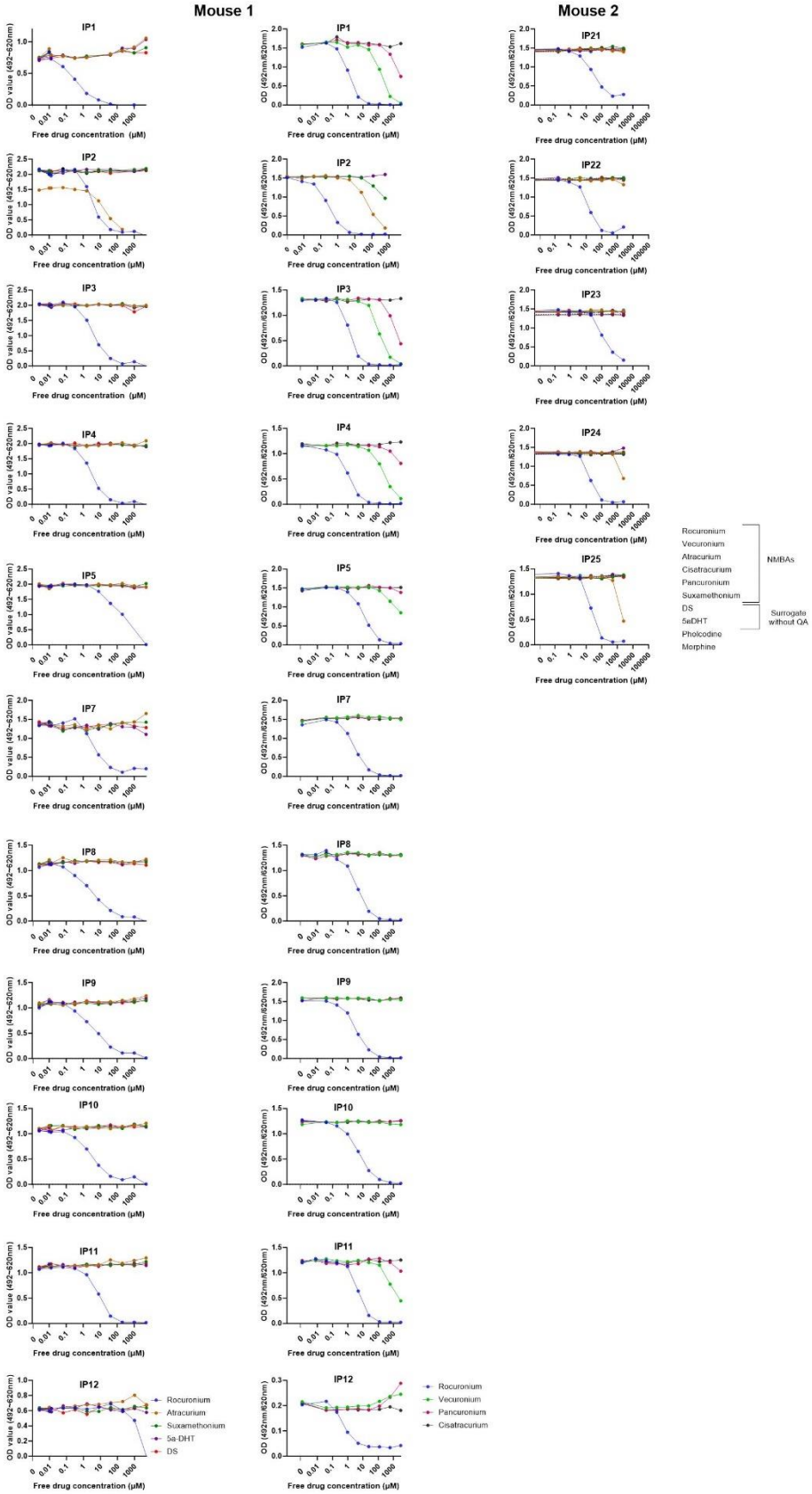
Mouse 1
Mouse 2
IP1
IP2
IP3
IP4
IP5
IP7
IP8
IP9
IP10
IP11
IP12
IP21
IP22
IP23
IP24
IP25
OD value (492-620nm)
OD (492nm/620nm)
Free drug concentration (μM)
Rocuronium
Vecuronium
Atracurium
Cisatracurium
Pancuronium
Suxamethonium
DS
5a-DHT
Pholcodine
Morphine
NMBAs
Surrogate without QA

Supp. Fig. 4: "Competition ELISA" of anti-IgG rocuronium ELISA. Fixed mouse mAbs concentration at 300ng/mL were used in these competitive anti-HSA-rocuronium ELISA with increasing concentrations of indicated molecules free in solution. 5a-DHT, 5-alpha-Di-Hydro-Testosterone; DS, Diisiopentyl succinate.

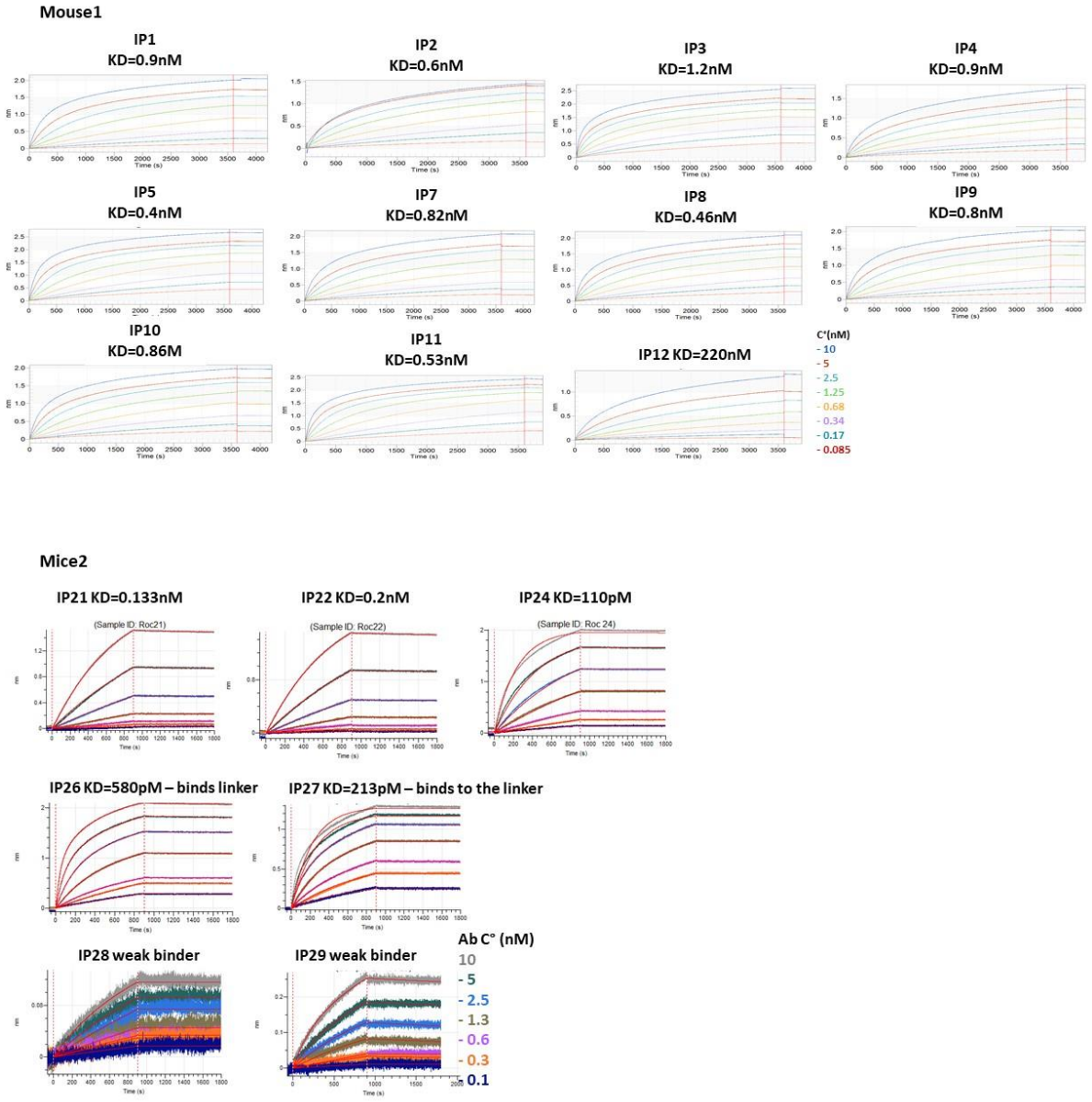

Supp. Fig. 5: Avidity of anti-rocuronium mAbs for haptenized rocuronium. Bio-layer interferometry affinity measurement of the interaction between immobilized HSA-rocuronium and varying concentrations of indicated mAbs in solution. The KD was obtained by fitting the curves using a heterogenous ligand model.

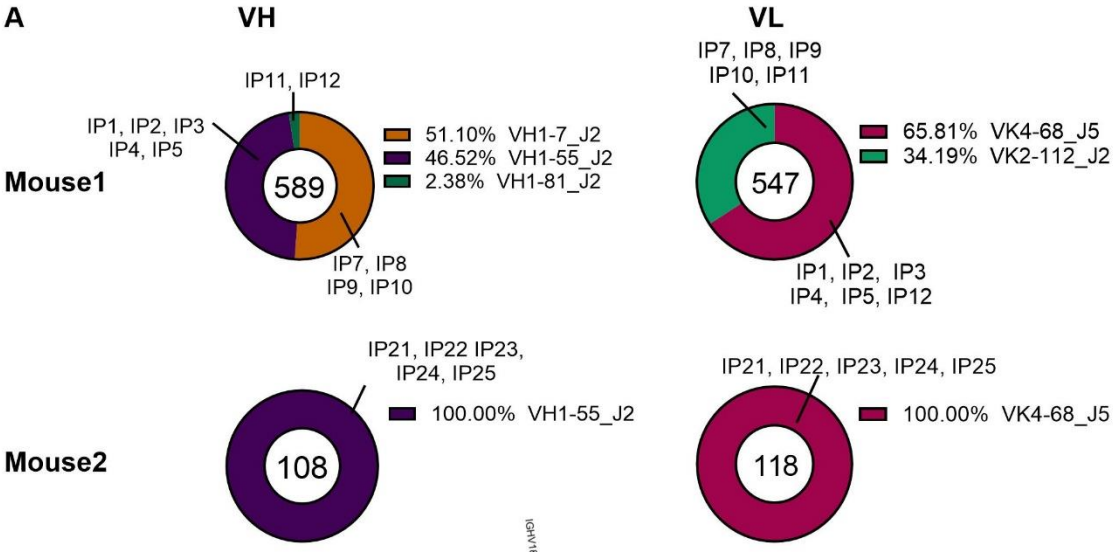
A
VH
VL
Mouse1
IP11, IP12
IP1, IP2, IP3
IP4, IP5
589
IP7, IP8
IP9, IP10
51.10% VH1-7_J2
46.52% VH1-55_J2
2.38% VH1-81_J2
IP7, IP8, IP9
IP10, IP11
547
IP1, IP2, IP3
IP4, IP5, IP12
65.81% VK4-68_J5
34.19% VK2-112_J2
Mouse2
IP21, IP22 IP23,
IP24, IP25
108
100.00% VH1-55_J2
IP21, IP22, IP23, IP24, IP25
118
100.00% VK4-68_J5

B

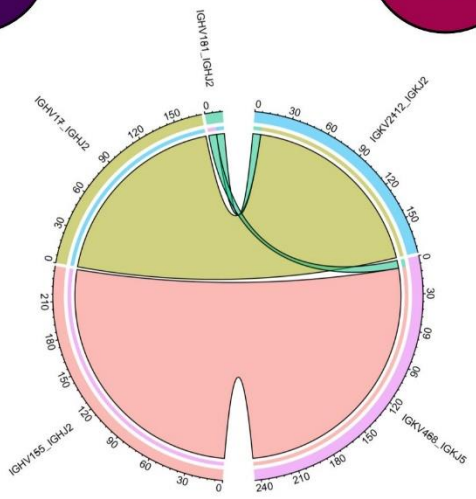
IGHV181_IGHJ2
IGKV2112_IGKJ2
IGKV468_IGKJ5
IGHV155_IGHJ2
IGHV117_IGHJ2

B

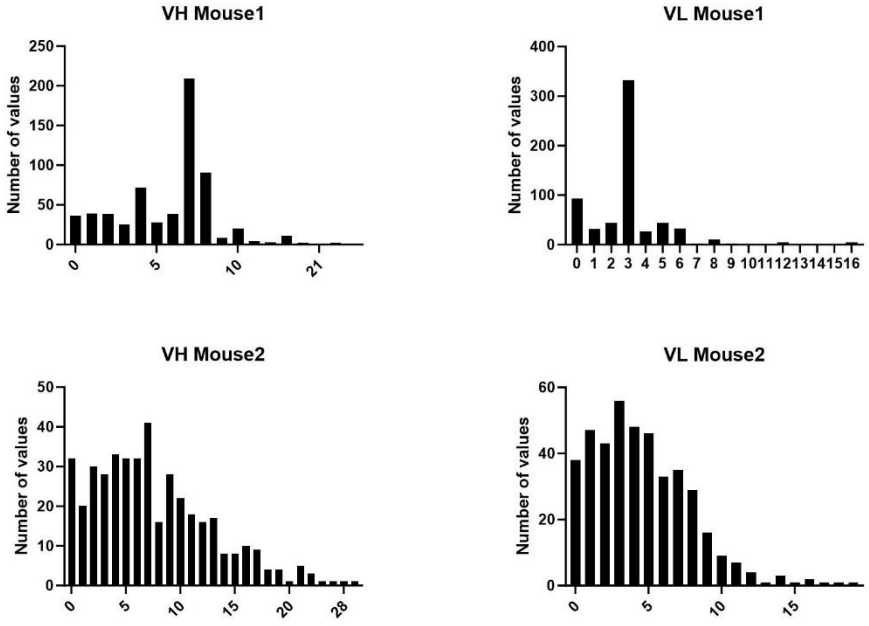
VH Mouse1
VL Mouse1
VH Mouse2
VL Mouse2
Number of values

	VH mutations			VL mutations		
	mean	median	standard deviation	**mean**	median	standard deviation
Mouse1	**5.8**	7	3.2	**3**	3	2.2
Mouse2	**7.4**	7	5.4	**4.5**	4	3.4

Supp. Fig. 6: Functional Antibody repertoire analysis of the mouse. (**A**) Donut plot of VJ gene usage for the VH and VL of the two mice. The name of a V-J rearrangement is indicated if at least one VH or one VL with the same V-J rearrangement has been identified as an anti-rocuronium antibody. (B) Circos plot of the functional antibody repertoire for mouse 1 thus showing the VH and VL rearrangements of VH1-7_J2, VH1-55_J2 and VH1-81_J2. (**C**) Distribution of nucleotidic mutation frequency among (top) VH sequences and (bottom) VL sequences compared to germline in Mouse1 and Mouse2.

APPENDIX 3. Review: Neuromuscular blocking agent induced hypersensitivity reaction exploration: an update

EJA

Eur J Anaesthesiol 2023; **40:**95–104

REVIEW ARTICLE

Neuromuscular blocking agent induced hypersensitivity reaction exploration: an update

Alice Dejoux, Luc de Chaisemartin, Pierre Bruhns, Dan Longrois and Aurélie Gouel-Chéron

Acute hypersensitivity reactions (AHRs) occurring in present-day anaesthesia can have severe, sometimes fatal, consequences and their incidence is increasing. The most frequent allergens responsible for AHR during anaesthesia are neuromuscular blocking agents (NMBAs) (70% of the cases) followed by antibiotics (18%), patent blue dye and methylene blue dye (5%), and latex (5%). Following an AHR, strategies for subsequent anaesthetic procedures (especially the choice of an NMBA) may be difficult to formulate due to inconclusive diagnostic analysis in up to 30% of AHRs. Current diagnosis of AHR relies on the detection of mast cell degranulation products and drug-specific type E immunoglobulins (IgE) in order to document an IgE-mediated anaphylaxis (IgE endotype). Nonetheless, other IgE-independent pathways can be involved in AHR, but their detection is not currently available in standard situations. The different mechanisms (endotypes) involved in peri-operative AHR may contribute to the inconclusive diagnostic work-up and this generates uncertainty concerning the culpable drug and strategy for subsequent anaesthetic procedures. This review provides details on the IgE endotype; an update on non-IgE related endotypes and the novel diagnostic tools that could characterise them. This detailed update is intended to provide explicit clinical reasoning tools to the anaesthesiologist faced with an incomplete AHR diagnostic work-up and to facilitate the decision-making process regarding anaesthetic procedures following an AHR to NMBAs.

Published online 18 October 2022

KEY POINTS

- Anaesthesiologists may be confronted with an inconclusive diagnostic work-up in up to 30% of AHR cases, thus impairing reliable selection of agents (mainly NMBA) for subsequent anaesthetic procedures.
- We suggest that part of the uncertainty concerning the mechanism and the culpable drug may be related to non-IgE mediated AHR. We present an update on potential mechanisms of AHR such as IgG-mediated and 'Mas-related G protein-coupled receptor X2' (MRGPRX2).
- We suggest explicit decision-making algorithms to help manage uncertainty regarding the choice of anaesthetic drugs for subsequent anaesthetic procedures following an AHR with an inconclusive diagnostic work-up.
- Potential new tests based on the detection of biomarkers may open novel perspectives to improve the diagnosis and guide anaesthesiologists to identify the endotype responsible for a peri-operative AHR event.

Glossary

Anaphylaxis: most severe form of AHR; can be fatal even in healthy individuals

Drug-induced AHR: acute reaction (phenotype) following exposure to a drug that does not refer to any specific endotype (such as IgE-mediated)

Endotype: refers to biomarkers (not available to clinical observation) that can characterise the sensitisation or the mediators of an AHR

From the Institut Pasteur, Université de Paris, Unit of Antibodies in Therapy and Pathology, Inserm UMR1222 (AD, LdC, PB, AGC), Immunology Department, DMU BIOGEM, Bichat Hospital, AP-HP (LdC), Université Paris-Saclay, Inserm, Inflammation, Microbiome and Immunosurveillance, Châtenay-Malabry (LdC), Anaesthesiology and Critical Care Medicine Department, DMU PARABOL, Bichat Hospital, AP-HP (DL, AGC), Université de Paris, FHU PROMICE (DL), Anaesthesiology and Critical Care Medicine Department, DMU PARABOL, Bichat-Claude Bernard and Louis Mourier Hospitals, APHP (DL), INSERM1148, Paris, France (DL), and Biostatistics Research Branch, Division of Clinical Research, National Institute of Allergy and Infectious Diseases, National Institutes of Health, Bethesda, Maryland, USA (AGC)

Correspondence to Aurélie Gouel-Chéron, Département d'Anesthésie-Réanimation, Hôpital Bichat – Claude Bernard, 46 rue Henri Huchard, Paris 75018, France
Tel: +33 140258355; fax: +33 140256309; e-mail: aurelie.gouel@aphp.fr

DOI:10.1097/EJA.0000000000001765

Sensitisation endotype: refers to all biomarkers and molecular mechanisms involved in the sensitisation step to the culprit agent

Mediators endotype: refers to biomarkers that induce the clinical signs (phenotype) of the AHR

Phenotype: clinical expression of the disease

Definitions and epidemiology

Allergies and atopy have become major public health problems, with a rapidly growing incidence over the past 20 years for reasons that are not yet fully understood.[1] Anaphylaxis is the most severe form of an acute hypersensitivity reaction (AHR) and has been defined in 2006 as 'a serious allergic reaction that is rapid in onset and may cause death'.[2] It can be fatal, even in healthy individuals. Drugs have become an increasingly identified cause of AHR in the practice of anaesthesia.[3] Peri-operative AHR is relatively rare (1 : 3000 to 1 : 20 000 patients who undergo anaesthesia)[4,5] but is associated with poor outcome (mortality rates of ~4% and sequelae in 34% of cases).[6,7] In France, the most frequent allergens responsible for AHR during anaesthesia are neuromuscular blocking agents (NMBAs) (70% of the cases) followed by antibiotics (18%), patent blue dye and methylene blue dye (5%), latex (5%), opioids (1%) and gelatins (<1%).[8] Chlorhexidine is also becoming increasingly recognised as a cause of peri-operative AHR.[9]

A major challenge during AHR is to identify the culpable allergen in order to avoid subsequent exposures. This identification relies on analysis of both clinical phenotypes and biological endotypes. The clinical phenotype represents the symptoms and signs of the disease (e.g. bronchospasm), whereas the biological endotype is the underlying pathological mechanism (e.g. IgE sensitisation or endotype mediators of anaphylaxis). Several endotypes can share the same phenotype, and *vice versa*. It may also be possible that a similar sensitisation endotype is associated with different endotypes of mediators. This could explain the differences in the severity of clinical manifestations for similar sensitisation endotypes. To date, no detailed endotypes have been described for allergic reactions, except for some asthma subtypes[10] and chronic rhinitis. Based on the first historical definition, the term 'allergy' often refers to the involvement of type E immunoglobulin (IgE) endotype. Here, we chose instead to use 'AHR', as this term does not refer to any specific endotype and only indicates the clinical manifestations that are visible.

The purpose of this article is to review the current knowledge about the pathophysiology of peri-operative AHR to assist anaesthesiologists in understanding biological investigations after an initial reaction to an NMBA and to guide their strategy for subsequent anaesthesia drug selection. We also provide insights into new investigations that might help to explore alternative pathways that are not IgE-dependent. A comprehensive search of Medline/PubMed, EMBASE, Scopus and Web of Science databases was performed by AD and AGC. Studies focusing on the pathophysiology of anaphylaxis were considered, in human and in animal models.

Details related to the classical immunoglobulin E mediated sensitisation endotype

Following an AHR, the World Allergy Organisation[11] recommends exploring the IgE-pathway[12] in determining the endotype, as it is the most common mechanism. This exploration includes immediate evaluation of blood histamine and tryptase concentrations, and delayed investigations (6 to 8 weeks following the AHR), such as skin tests, serum IgE quantification, which might be associated with basophil activation tests in some centres (Fig. 1).

The classical pathway of allergies involves IgE antibodies bound to their high-affinity IgE receptors (FcεRI), which are mainly expressed on the surface of mast cells and basophils (Fig. 2). When an antigen binds to its specific IgE (sIgE)/FcεRI complex, this enables cross-linking of FcεRI at the cell surface of mast cells in tissues and basophils in the circulation. This sIgE/FcεRI aggregation triggers degranulation and de-novo synthesis of inflammatory mediators including, but not limited to, histamine, tryptase, platelet-activating factor (PAF), prostaglandin D2 and leukotrienes. Histamine and tryptase are the only inflammatory mediators routinely measured to determine the endotype of an AHR. Histamine released by mast cells and basophils is believed to be the main cause of clinical symptoms and is detectable from 5 to 60 min after AHR onset.[13,14] Thus, the detection of histamine requires blood collection within the first 30 min after AHR onset.[15] Circulating histamine measurement is recommended by the French Society of Anaesthesiology and Intensive Care because peri-operative hypersensitivity diagnosis is highly probable when both histamine and tryptase concentrations are elevated.[16] Histamine can be measured by mass spectrometry or competitive ELISA. This assay, however, is not used in all countries because circulating histamine concentrations can be influenced by various AHR-unrelated factors such as pregnancy, haemolysis and circadian rhythm.

Tryptase is a specific biomarker of mast cell degranulation and, as such, is considered a marker of the IgE pathway involvement. A consensus equation has been defined to establish a significant rise of tryptase above baseline, a signature of mast cell activation: peak tryptase levels ($\mu g l^{-1}$) > 1.2 (baseline tryptase) + 2 ($\mu g l^{-1}$); with 78% sensitivity, 91% specificity, 98% positive predictive value and 44% negative predictive value.[17] Mast cell tryptase can be routinely measured in plasma or serum by fluorescence immunoassay (FEIA) method

Fig. 1 Diagnosis strategy of an immunoglobulin E endotype involvement based on the recommended allergist evaluation after a peri-operative acute hypersensitivity reaction.

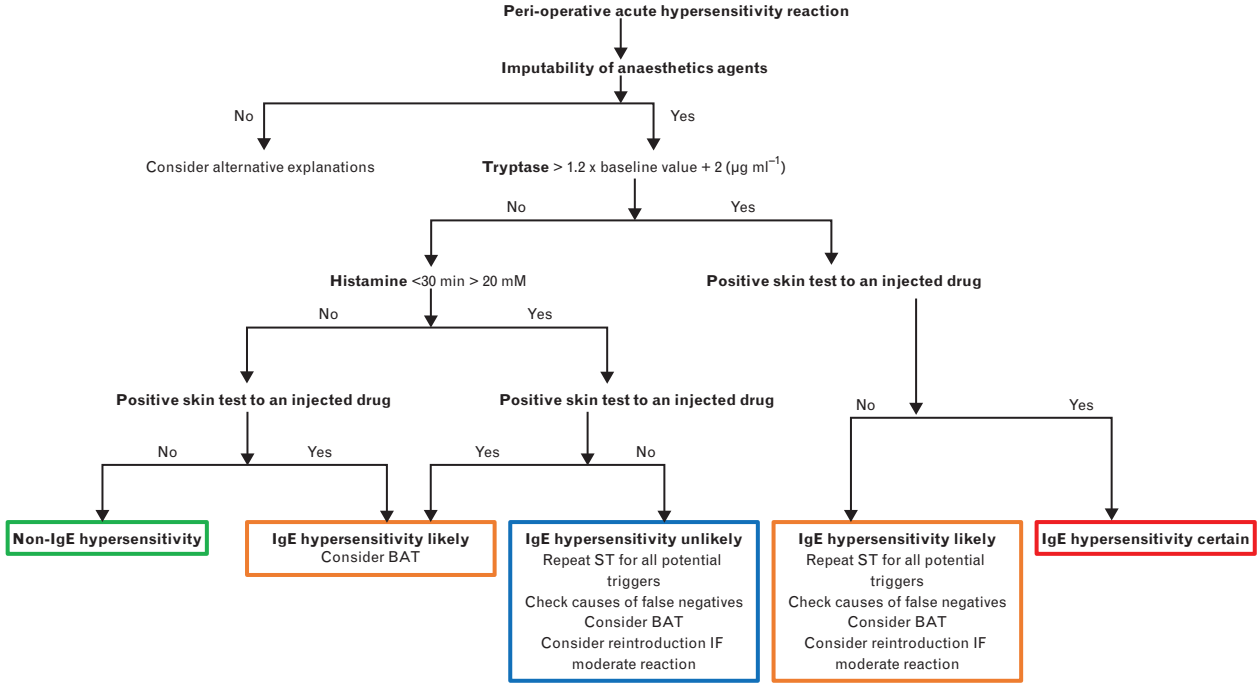

(ImmunoCAP Tryptase; ThermoFisher Scientific, Waltham, Massachusetts, USA).

Skin tests can identify the culpable agent through local injection of the diluted suspected allergen[13] that is expected to trigger sIgE/FcεRI on the surface of skin/dermal mast cells, providing evidence of the involvement of the IgE pathway in an individual. Skin tests mostly consist of skin prick tests, which should be performed first, and intradermal tests, which are performed if prick tests are negative or unconclusive. The tests are performed on the individual's forearm, including a positive and a negative control. Results are interpreted 15 min post injection, a wheal above 3 mm is considered a positive result and a confirmation of IgE-dependent activation of mast cells. Although skin tests are the recommended first-line tests in intra-anaesthetic AHR, interpretation should be cautious, as they can display false-positive (attributable to the drug-causing skin irritation) and false-negative results (if the drug concentration is too low). If performed in the conditions recommended by the European Academy of Allergy and Clinical Immunology (EAACI), their negative predictive value is above 95% for IgE-mediated AHR, and their positive predictive value is considered excellent; however, this is difficult to establish formally for ethical reasons. This is the gold standard, despite no categoric value, as no other appropriate techniques exist. As various factors can affect both specificity and sensitivity of the test, it must be performed and analysed by a trained physician.

There is debate on the nonirritant concentrations to use for NMBAs skin tests. Thus, an expert consensus has recently been published that defines concentrations for peri-operative drugs.[18] Technical procedures should be consistently followed to permit accuracy and reproducibility. The tests should be performed from 4 to 6 weeks until 4 months after the AHR, and after withdrawal of antihistamine drugs for at least 5 days prior to the test. Other drugs may have to be withdrawn, including corticosteroids, drugs with antihistaminergic effects such as some antidepressants and antipsychotics, beta-blockers and angiotensin-converting enzyme inhibitors. However, the latter drugs can only be temporarily withdrawn if deemed clinically well tolerated by relevant specialists, without increasing cardiovascular risks. The risk of anaphylaxis during skin tests, while feared, is extremely low, especially if drug concentration recommendations are strictly followed.[19,20] One major benefit of skin testing in an NMBA-suspected AHR is the evaluation of NMBA cross-reactivity, as recommendations allow reintroduction of NMBAs producing a negative skin testing, despite previous documentation of IgE-mediated NMBA allergies.[21] However, some authors recommend a cross-validation with other in-vitro tests, such as basophil activation tests (see below), to complement the assessment provided by skin tests.[22]

Fig. 2 Acute hypersensitivity reaction endotypes.

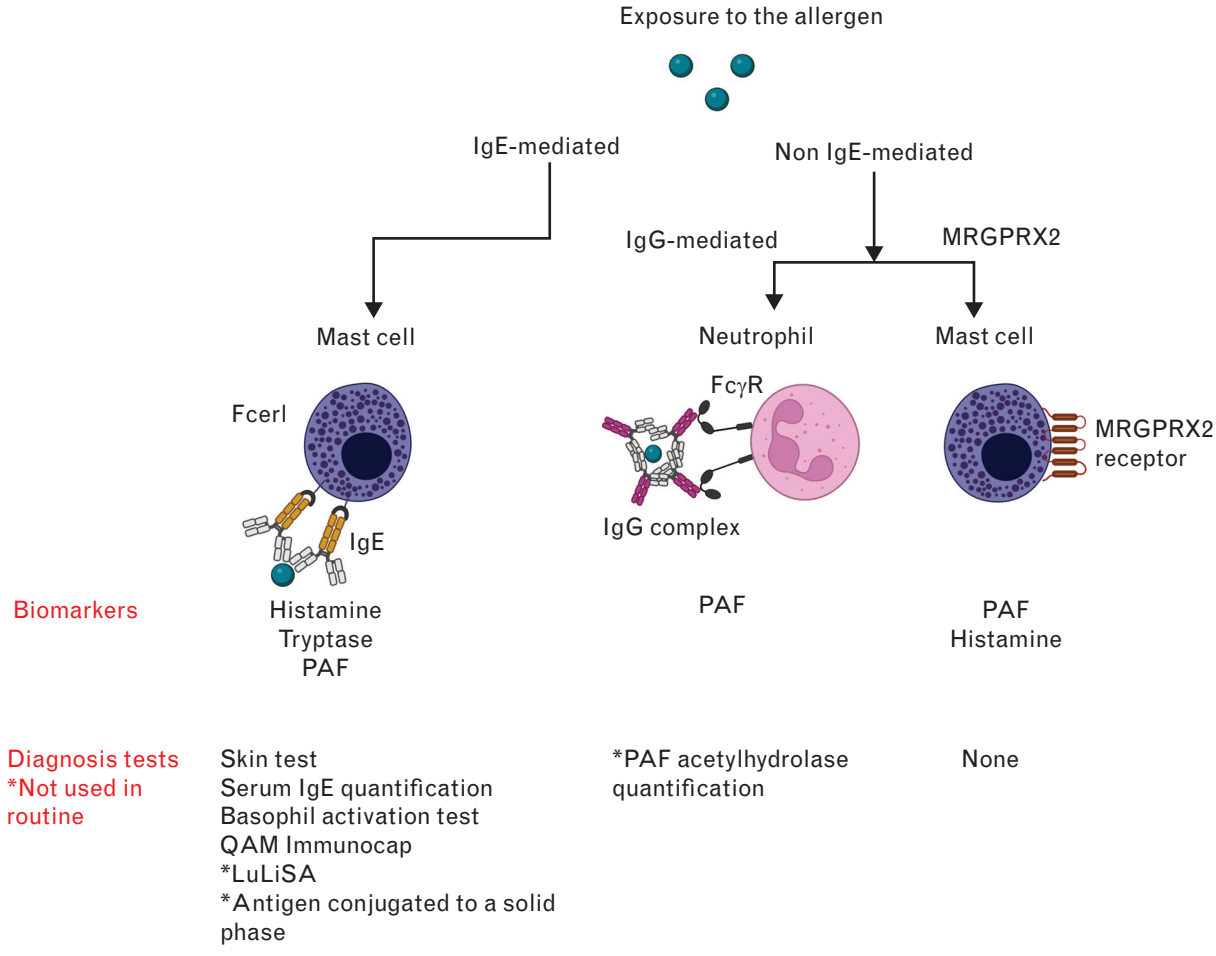

MRGPRX2, Mas-related G protein-coupled receptor X2; PAF, platelet activating factor.

One major cause of a false-positive skin test result is mastocytosis, which is a rare mast cell clonal disorder (prevalence 1 in 10 000, but underdiagnosed[23]) characterised by an abnormal increase in tissue mast cells, which can present in two forms: cutaneous mastocytosis, the most frequent phenotype, and systemic mastocytosis.[24,25] Patients with mastocytosis can develop nonallergic AHR, triggered by nonspecific stimuli such as histamine-releasing drugs, mechanical (skin irritation) and physical factors (hyperthermia). However, there is no evidence that there is a higher prevalence of either nonallergic or IgE-mediated drug-induced AHR in mastocytosis patients when compared with the general population.[26]

In addition, the quantification of sIgE in the plasma or serum of the patient is also used routinely in the diagnostic work-up following an AHR. The detection of sIgE for a specific antigen usually involves a solid phase to which the allergen is conjugated, and an anti-IgE antibody labelled with fluorescent or enzymatic tracer.[11] The sensitivity and negative predictive values of IgE testing are poor, probably in part because of the very low concentration of IgE in serum/plasma. The half-life of IgE in plasma is short and most IgE are captured and retained by the high-affinity IgE receptors on mast cells in the tissues and basophils which can preclude sIgE from being detectable in the circulation. Some tests detecting IgE against peri-operatively relevant allergens are available for routine testing, including latex, amoxicillin, chlorhexidine, protamine and suxamethonium. Quaternary ammonium moieties are present in all NMBAs and are hypothesised to be the immunogenic epitope (Fig. 3). Although the mechanisms are not fully understood, it is hypothesised that quaternary ammonium sensitisation is acquired through the environment as many compounds contain tertiary or quaternary substituted ammonium structures (e.g. detergents, cough syrups, cosmetics).[27,28] Therefore, to quantify IgE specific to the quaternary ammonium compound, an IgE-detection assay is available using a morphine surrogate possessing a quaternary ammonium (ThermoFisher, Waltham, Massachusetts, USA).[29] Although this test is not used routinely

Fig. 3 Chemical structures of three neuromuscular blocking agents and morphine.

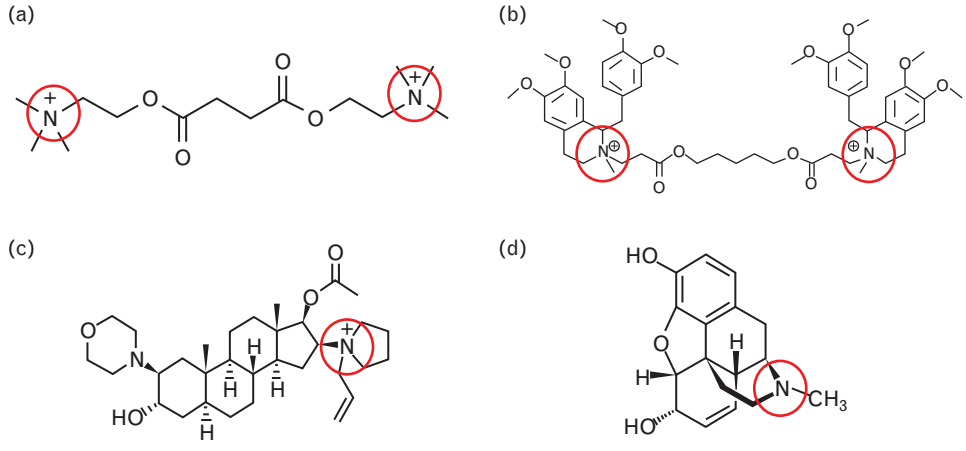

(a) Succinylcholine; (b) Atracurium; (c) Rocuronium and (d) the morphine compound used in the ImmunoCap assay. Quaternary ammonium compounds are circled in red.

worldwide, it can be valuable for detection of sensitisation to quaternary ammonium. It is supposed to detect specific antibodies to rocuronium (the chemical structure of which shares some similarities with morphine, in addition to the quaternary ammonium compounds) and suxamethonium; these two being the most allergenic NMBAs (Fig. 3). However, the detection of sIgE against quaternary ammonium morphine (QAM) should not be used in individuals to define a risk of NMBA hypersensitivity, as the pathogenic potential of sIgE without a relevant clinical history is not established. Thus, considered individually, the positive predictive value of the QAM-sIgE testing is low. This test does not represent anything definite and should always be considered with other investigations and a relevant clinical history.

In-vitro cellular activation tests can also be used, especially when uncertainty persists as to the culpable drug or when the results of different tests are discordant. Indeed, even though mast cell activation can be detected by flow cytometry,[30] the activation of these effector cells is difficult to assess in humans due to their confinement in tissues. Basophils circulating in peripheral blood are taken as surrogates of mast cells using the basophil activation test (BAT). During this test, several allergens are tested *in vitro* at different concentrations, allowing the detection of upregulated activation markers on the surface of basophils as well as intracellular markers by flow cytometry (when positive). BAT is a useful diagnostic tool that enables simultaneous testing of potentially cross-reactive NMBAs[31] and is an indicator of IgE-mediated reactions. Studies show that BAT cannot replace skin testing in the assessment of NMBA allergies but should be used as an additional tool.[32] In IgE-mediated AHR caused by a NMBA, BAT sensitivity and specificity varies, depending on the NMBA tested and the protocol used, from 38.5 to 92% and from 92 to 100%, respectively.[33] In NMBA-related AHR, the positive predictive value is high, whereas the negative predictive value is around 15–20%.

On the basis of the medical history of the patient, the clinical features of the reaction, and on the results of these tests, the allergist will draw conclusions and determine if suspected drugs could be safely used or not in a subsequent anaesthetic (Fig. 1).[34]

Anaesthetic strategy for subsequent procedure after an neuromuscular blocking agents induced acute hypersensitivity reactions

From the above, it is obvious that even the diagnostic work-up of a classical IgE-mediated endotype may still give uncertainty and inconsistent results, with both false-positive and false-negative results. When a single culpable agent is identified and it matches the clinical history, the decision-making process is straightforward. The situation becomes complex when several agents are implicated, when the identified agent does not match the clinical history, or when the investigations performed according to recommendations are inconsistent or discordant. In these situations, the allergist cannot draw any firm conclusion and recommends exclusion of all drugs administered before the AHR. Unfortunately, this may have important consequences for the patient's future anaesthesia procedures, as this decreases the choice of drugs available for these.

Recently, we had to treat a woman that presented a year ago with a grade III AHR related to atracurium. All skin tests were negative, histamine and tryptase levels were normal. For several medical reasons, she needed a rapid sequence induction to permit a hernia correction

Fig. 4 Anaesthetic strategy according to allergist work-up.

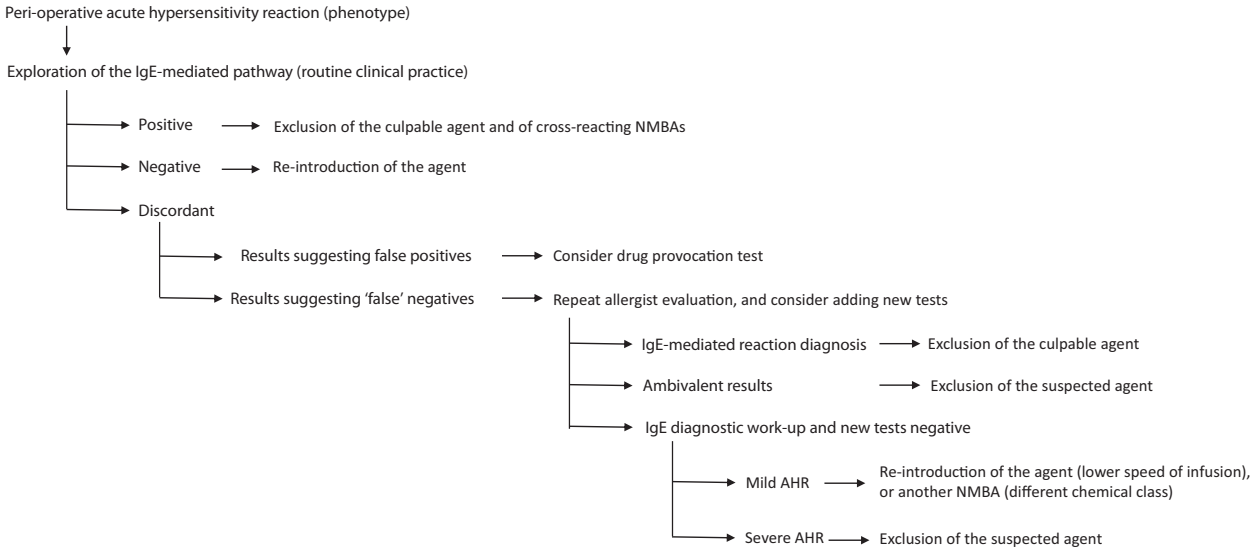

procedure. Several questions were raised in this situation. Should we consider that skin tests have a 100% negative predictive value (although non-IgE pathways have been described with atracurium) and permit the administration of all those NMBAs tested? Should we consider using cis-atracurium as the NMBA with the fewest reported cross-reactivities, although this would not be a good choice for a rapid sequence induction? Should we use rocuronium directly after a drug provocation test? Finally, should we perform a procedure without NMBAs, although the surgical procedure would be difficult without them?

Clinical reasoning should integrate all factors and should be an incentive for anaesthesiologists to anticipate the clinical consequences of false-positive and false-negative diagnoses. As such, we suggest an algorithm that could help anaesthesiologists to manage uncertainty and/or inconclusive allergology evaluations (Fig. 4).

Non immunoglobulin E mediated endotypes

Immunoglobulin G mediated anaphylaxis

IgG-dependent anaphylaxis has been described, mainly in animal models but also in humans. However, its biomarkers are not yet part of routine investigations.[35] This mechanism of anaphylaxis is mediated by an IgG/antigen complex forming in the circulation (i.e. an antibody-antigen immune complex), which can engage Fc gamma receptors (FcγRs) expressed on effector cells, including neutrophils, macrophages and monocytes, among other cells. IgG-mediated anaphylaxis has been described and manipulated in rodents, particularly in mouse models, and phenotypically resembles IgE-mediated anaphylaxis with severe hypothermia, respiratory distress and lethality at high allergen doses.[36,37] The model was validated in 'knock-in mice' humanised for the FcγR locus (i.e. mice expressing human IgG receptors, in place of mouse IgG receptors) that were susceptible to anaphylaxis.[36] IgG-dependent anaphylaxis in animal models relies on histamine and PAF as mediators.[38] Neutrophils are major producers of PAF that is released upon FcγR activation. Increased PAF levels have been strongly correlated with anaphylaxis severity in humans.[39,40] As PAF concentration is extremely difficult to measure, another marker of interest for this endotype is PAF acetylhydrolase activity, as this enzyme regulates PAF levels. A low PAF acetylhydrolase activity is correlated with increased severity of allergic reactions in humans.[39–41]

Jönsson *et al.*[39] showed that IgG-dependent anaphylaxis to NMBAs in humans is preferentially triggered via FcγR-mediated neutrophil activation and associated with the production of neutrophil extracellular traps (NETs). In this study, concentrations of anti-NMBA IgG, markers of FcγR activation, PAF release and neutrophil activation correlated with anaphylaxis severity. Interestingly, whereas some patients displayed both IgE and IgG endotypes, others in that cohort presented with only one endotype, either IgE or IgG. Thus, this work suggests that the IgG-dependent pathway may not only increase the severity of IgE-mediated hypersensitivity reactions but may also be triggered in the absence of activation of the classical IgE-dependent pathway, leading to potentially (more) severe anaphylactic reactions.

Platelets represent another cell type involved in the IgG endotype, as they express the activating IgG receptor FcγRIIA/CD32A on their surface. In human FcγR–expressing mouse models, platelet counts dropped

markedly within minutes of anaphylaxis induction and only when mice expressed the human IgG receptor FcγRIIA/CD32A. Platelet depletion prior to allergen challenge attenuated anaphylaxis, whereas thrombocythaemia substantially worsened its severity.[42] Serotonin released by activated platelets contributed to anaphylaxis severity in this model. These experimental observations were confirmed in data from a cohort of patients suffering from NMBA-induced anaphylaxis, wherein it was shown that platelet activation was associated with anaphylaxis severity and was accompanied by a reduction in circulating platelet numbers.[42] This suggests that platelets could have a critical role in IgG-dependent anaphylaxis and function as modulators of the reaction severity. Furthermore, this study demonstrates that serotonin, in addition to PAF, could be a biomarker of IgG-dependent anaphylaxis in humans.

Endotype of mediators responsible for an acute hypersensitivity reaction in the absence of previous exposure/sensitisation

It has recently been shown *in vitro* that some drugs can bypass the antibody-mediated activation pathway and trigger mast cell degranulation directly via a mast cell-specific receptor known as MRGPRX2. On the basis of in-vitro data, this pathway has been suggested to represent around 30% of AHR events[43] if the local concentration of the drug is high enough to allow MRGPRX2 activation, which remains a critical consideration for the importance of this pathway in human AHR. Indeed, the allergens identified as activators of MRGPRX2 *in vitro* usually include positively charged small drugs[44] that interact with human MRGPRX2 with very low affinities,[45,46] precluding MRGPRX2 activation at clinical doses of these drugs. The mouse ortholog of human MRGPRX2, Mrgprb2, has significantly higher affinity for most drugs tested so far,[44] generating confusion in the field. Nevertheless, several drugs used in the perioperative context have been proposed to trigger such a mechanism, including morphine, hydrocodone, fluoroquinolones (ciprofloxacin, moxifloxacin, levofloxacin, ofloxacin) and NMBAs, such as rocuronium,[47] atracurium, cisatracurium[48] and mivacurium.[49] Nonetheless, there are several controversies on the role of NMBAs on MRGPRX2-induced anaphylaxis reactions. For example, it has been suggested that hypersensitivity to rocuronium is mostly IgE-dependent and that it is only in a few patients that antirocuronium IgE could not be detected. In these patients, it has been proposed that their AHR could be due to off-target occupation of the MRGPRX2 receptor by rocuronium[50] even though the affinity of rocuronium for MRGPRX2 is very low.[44,46]

Several mysteries remain unsolved around MRGPRX2 activation. Although MRGPRX2 activation is well supported by in-vitro studies, to the best of our knowledge, it has never been identified in humans as the sole AHR pathway, as it is not possible to directly prove its activation. Furthermore, MRGPRX2 expression is particularly pronounced in human skin mast cells and is less pronounced in the gut and the lung. Thus, it might be expected that cutaneous symptoms may be predominant in MRGPRX2-dependent anaphylaxis, although this has never been formally reported. The phenotype of MRGPRX2-dependent AHR and initial biological results are expected to be similar between IgE endotypes and MRGPRX2 activation mechanisms, as they both lead to histamine and tryptase release.[51] Thus, a similar mediators endotype can result in similar phenotypes of AHR, in the absence or presence of a sensitisation (IgE and or IgG) endotype. Even if MRGRPX2 activation should only be suspected if the allergen concentrations are high enough to activate the receptor,[52] distinction between the two pathways might be especially challenging. Some researchers have suggested that BAT and sIgE could help to distinguish between IgE and MRGPRX2 endotypes.[30] However, both have a low sensitivity, making them unsuitable for that purpose.

Determination of the true involvement of MRGPRX2 in human AHR may be crucial in the future, as some authors have suggested that a MRGPRX2 blockade could be a potential treatment to prevent such episodes. Nonetheless, most of this work has only been reported in-vitro or in animal models.[53]

New diagnoses and explorations tests

To help anaesthesiologists to navigate through the uncertainty and to better understand the endotypes involved in AHRs, several strategies and assays may be of help in the upcoming years.

New sIgE diagnosis

Although the gold standard in NMBA AHR diagnosis and cross-reactivity assessment relies on skin testing, aminosteroids and some NMBAs (vecuronium, and rocuronium, cisatracurium and atracurium) have the potential to induce nonspecific skin reactivities in healthy volunteers.[54] To improve IgE pathway investigations and accurate diagnoses concerning NMBAs, new NMBA assays have recently been developed, in particular for sIgE detection of atracurium and rocuronium. These tests, that remain research tools only, would help to improve the skin testing performance if they were validated for clinical use.

For atracurium sIgE, Uyttebroek *et al.*[55] used a solid phase to bind a molecule chemically similar to the hemi-atracurium, named tetrahydropapaverine. This test is able to detect sIgE to atracurium with a 57% sensitivity and 100% specificity, but only in seven patients with positive sensitivity test to atracurium.[55] If this test can reproducibly identify sIgE in larger cohorts of patients who experienced atracurium-induced AHR, it would be of major importance. So far, there is no evidence of an IgE pathway in atracurium-induced AHR in human and

animal models, suggesting that this reaction might be related to alternative mechanisms, such as the ones described above (e.g. MRGPRX2-mediated).

For detection of rocuronium sIgE, two assays have been developed. The first one, a rocuronium-based radio immunoassay, failed in terms of diagnostic performances, as it was positive in only three of 13 patients with rocuronium-induced AHR.[56] The second one relies on an ImmunoCAP sIgE assay against rocuronium. In a cohort of 72 patients who presented with severe IgE-mediated AHR (established through skin test and BAT positivity), 80% of the positive patients had detectable IgE against-rocuronium. However, 24% of the patients with an AHR not related to a NMBA also had positive sIgE against rocuronium.[57] Another team evaluated this same assay in 25 rocuronium allergic patients (defined based on a positive skin-testing and a medical compatible history), and demonstrated sensitivity of 88% and specificity of 93%.[55] If this test were to be validated, one would first have to resolve the controversy on the threshold to apply. Indeed, the second team (Leysen *et al.*[57]) used the conventional threshold used for other ImmunoCAP assays (0.35 kUa l^{-1}), whereas the third team (Uyttebroek *et al.*[55]) suggested decreasing the threshold to 0.13 kUa l^{-1}. Of interest, in order to improve the sensitivity and specificity, Goyard *et al.*[58] created a highly sensitive ELISA method based on bioluminescent detection of IgE using a high-affinity anti-IgE nanobody coupled to an enhanced luciferase. This method, named luciferase-linked immunosorbent assay (LuLISA), has been validated clinically for the detection of anti-SARS-CoV-2 spike antibodies, and opens new perspectives for the diagnosis of drug-induced allergic diseases.[59]

Tests for immunoglobulin E and non-immunogloblin E endotypes

Hopefully, new tests will be introduced in the future to investigate the AHR endotype and identify the culpable drug(s). This would increase patients' safety and help anaesthesiologists to manage uncertainty. So far, PAF acetylhydrolase detection is not included in clinical routine but could be a truly useful tool to investigate the existence of an IgG endotype. Detection of specific IgG in sera of patients who suffered from drug-induced AHR could provide useful additional information on the pathway involved. The specific IgG levels can be measured by ImmunoCAP[60] or classical ELISA, and has been used in the French cohort on IgG-induced NMBA-anaphylaxis,[61] although in this context, the difference of levels between patients and controls was insufficient, precluding clinical use.

Novel biomarkers of anaphylaxis have recently been identified and could open perspectives to improve the diagnosis of anaphylaxis. Indeed, increasing levels of mast cell chymase in human serum measured by ELISA has been shown to correlate with anaphylaxis severity.[62] Moreover, mast cell carboxypeptidase A3 could also be a predictive biomarker in allergic reactions, as it has been shown to be higher in serum and saliva of patients after an anaphylactic episode, especially if they experienced severe symptoms.[63] A major advantage of using carboxypeptidase A3 as a biomarker of allergic reactions is its longer half-life compared with tryptase, thus increasing the time window for investigation. Two studies have looked into levels of dipeptidyl peptidase I (DPPI), another mast cell enzyme, during anaphylaxis in humans[62] and mice.[64] Both studies established that DDPI levels correlated with mast cell chymase levels and could be essential for their activation. The mouse study confirmed that DDPI, carboxypeptidase and chymase levels were correlated but did not correlate with tryptase levels.

In addition, serum levels of the chemokine CCL2 were measured in patients who experienced anaphylactic reactions to venom. The study reported elevated CCL2 levels correlating with reduced numbers of circulating basophils measured by flow cytometry in anaphylactic patients compared with controls.[65] Finally, another potential biomarker could be basogranulin as an indicator of basophil activation during IgE-dependent and IgE-independent anaphylaxis.[66]

To date, only one or two reports have been published for each of these latter biomarkers, making it difficult to confirm their sensitivity and specificity, or even the validity of each of these tests. The main limitation of these studies is the management of anaphylaxis that differs for each patient. The administration of corticoids, for example, can affect the levels of lymphocytes, basophils and neutrophils in the blood, thus introducing variability between patients and studies. Perhaps only the combination of several new biomarkers could improve AHR diagnostics and endotype identification. A larger study including biomarkers of the various endotypes is warranted to allow the comparison and validation of these additional explorations, and to report on the relative contributions of AHR endotypes in drug allergy.

Drug provocation tests

For allergies to food or antibiotics, the gold standard for identifying the culprit allergen is the provocation test, which consist of the administration of the suspected culpable agent (after a negative skin test). The absence of clinical symptoms confirms the absence of the IgE-pathway involvement. Although drug provocation tests (DPTs) are the gold standard for drug hypersensitivity diagnosis, no recommendations exist on DPT with perioperative drugs,[67] as many of them are only to be used in an operating room or in an intensive care unit. Performing some DPTs might even require intubation and mechanical ventilation such as test involving hypnotics or NMBAs. In that context, some centres in Denmark,[68] Spain, New Zealand and Australia[21] reported the

development of DPT procedures for NMBA-related AHR investigations. Controversies exist on the validity of such procedures, particularly regarding the patient's safety. However, if standardised protocols could be applicable under strict ICU surveillance and, without administering more than 10% of the clinically effective dose, it would firmly conclude the contribution of a particular drug to the AHR.

Conclusion

An AHR phenotype observed by the physician in the operating room may not correlate to a specific endotype (sensitisation or mediators) identified through routine biological and allergological evaluations as all of these clinically used tests rely on investigating the IgE-pathway, at least for the moment. According to the results, the allergist may not be able to draw firm conclusions on the culpable drug/substance and therefore formulate clear recommendations for the use/exclusion of specific drug(s) for subsequent anaesthetic procedures. When an IgE pathway has been diagnosed and a culpable drug identified, the strategy is straightforward. Uncertainty arises when the routine clinical diagnostic work-up is discordant with the clinical phenotype or when it is negative. Despite the recommendation that a NMBA producing a negative intradermal test and a negative skin prick test can be safely injected for subsequent anaesthesia procedures,[21,69] anaesthesiologists might be reluctant to do so. However, especially for drugs responsible for the activation of MRGPRX2 (notably atracurium),[21,44,70–72] reintroduction of the suspected agent might be possible if the dose and speed of administration are lower. There is an urgent need for validation, and adoption in clinical practice, of new biological tests/strategies that would decrease the level of uncertainty (but probably will never eliminate it). It is therefore necessary to formulate explicit decision algorithms that could help anaesthesiologists take into consideration the possible clinical consequences of false-positive and false-negative results.

Acknowledgements relating to this article

Assistance with the article: none declared.

Financial support and sponsorship: AD is a recipient of a PhD fellowship from Sorbonne Université, Paris, France. This work was supported by the French National Research Agency grant ANR 21 CE15 0015 0027 01 project CURAREP. P.B. acknowledges additional support from the Institut Pasteur and from the Institut National de la Santé et de la Recherche Médicale (INSERM). Luc de Chaisemartin reports lecture fees from MSD France. Other authors declare that they have no conflict of interest related to this manuscript.

All authors fulfil the ICJME criteria for authorship.

Conflicts of interest: none declared.

Presentation: none declared.

This manuscript was handled by Patrice Forget.

References

1 Miller RL, Shtessel M, Robinson LB, *et al.* Advances in drug allergy, urticaria, angioedema and anaphylaxis in 2018. *J Allergy Clin Immunol* 2019; **144**:381–392.
2 Turner PJ, Worm M, Ansotegui IJ, *et al.* Time to revisit the definition and clinical criteria for anaphylaxis? *World Allergy Organ J* 2019; **12**:100066.
3 Regateiro F, Marques M, Gomes E. Drug-induced anaphylaxis: an update on epidemiology and risk factors. *Int Arch Allergy Immunol* 2020; **181**:481–487.
4 Mertes PM, Alla F, Trechot P, *et al.* Anaphylaxis during anesthesia in France: an 8-year national survey. *J Allergy Clin Immunol* 2011; **128**:366–373.
5 Mertes PM, Ebo DG, Garcez T, *et al.* Comparative epidemiology of suspected perioperative hypersensitivity reactions. *Br J Anaesth* 2019; **123**:e16–e28.
6 Reitter M, Petitpain N, Latarche C, *et al.* Fatal anaphylaxis with neuromuscular blocking agents: a risk factor and management analysis. *Allergy* 2014; **69**:954–959.
7 Harper NJN, Cook TM, Garcez T, *et al.* Anaesthesia, surgery, and life-threatening allergic reactions: epidemiology and clinical features of perioperative anaphylaxis in the 6th National Audit Project (NAP6). *Br J Anaesth* 2018; **121**:159–171.
8 Tacquard C, Collange O, Gomis P, *et al.* Anaesthetic hypersensitivity reactions in France between 2011 and 2012: the 10th GERAP epidemiologic survey. *Acta Anaesthesiol Scand* 2017; **61**:290–299.
9 Abdallah C. Perioperative chlorhexidine allergy: is it serious? *J Anaesthesiol Clin Pharmacol* 2015; **31**:152–154.
10 Agache IO. From phenotypes to endotypes to asthma treatment. *Curr Opin Allergy Clin Immunol* 2013; **13**:249–256.
11 Ansotegui IJ, Melioli G, Canonica GW, *et al.* IgE allergy diagnostics and other relevant tests in allergy, a World Allergy Organization position paper. *World Allergy Organ J* 2020; **13**:100080.
12 Longrois D, Lejus C, Constant I, *et al.* Treatment of anaphylactic reactions occurring during anesthesia and in particular anaphylactic shock. *Ann Fr Anesth Reanim* 2011; **30**:312–322.
13 Aalberse RC, Kleine Budde I, Mulder M, *et al.* Differentiating the cellular and humoral components of neuromuscular blocking agent-induced anaphylactic reactions in patients undergoing anaesthesia. *Br J Anaesth* 2011; **106**:665–674.
14 Dybendal T, Guttormsen AB, Elsayed S, *et al.* Screening for mast cell tryptase and serum IgE antibodies in 18 patients with anaphylactic shock during general anaesthesia. *Acta Anaesthesiol Scand* 2003; **47**:1211–1218.
15 Laroche D, Vergnaud MC, Sillard B, *et al.* Biochemical markers of anaphylactoid reactions to drugs. Comparison of plasma histamine and tryptase. *Anesthesiology* 1991; **75**:945–949.
16 Shi R, Feng S, Park CY, *et al.* Fluorescence detection of histamine based on specific binding bioreceptors and carbon quantum dots. *Biosensors Bioelectron* 2020; **167**:112519.
17 Baretto RL, Beck S, Heslegrave J, *et al.* Validation of international consensus equation for acute serum total tryptase in mast cell activation: a perioperative perspective. *Allergy* 2017; **72**:2031–2034.
18 Garvey LH, Ebo DG, Mertes P-M, *et al.* An EAACI position paper on the investigation of perioperative immediate hypersensitivity reactions. *Allergy* 2019; **74**:1872–1884.
19 Brockow K, Romano A. Skin tests in the diagnosis of drug hypersensitivity reactions. *Curr Pharm Design* 2008; **14**:2778–2791.
20 Brockow K, Romano A, Blanca M, *et al.* General considerations for skin test procedures in the diagnosis of drug hypersensitivity. *Allergy* 2002; **57**:45–51.
21 Garvey LH, Ebo DG, Krøigaard M, *et al.* The use of drug provocation testing in the investigation of suspected immediate perioperative allergic reactions: current status. *Br J Anaesth* 2019; **123**:e126–e134.
22 Takazawa T, Sabato V, Ebo DG. In vitro diagnostic tests for perioperative hypersensitivity, a narrative review: potential, limitations, and perspectives. *Br J Anaesth* 2019; **123**:e117–e125.
23 Brockow K. Epidemiology, prognosis, and risk factors in mastocytosis. *Immunol Allergy Clin N Am* 2014; **34**:283–295.
24 Pardanani A. Systemic mastocytosis in adults: 2021 update on diagnosis, risk stratification and management. *Am J Hematol* 2021; **96**:508–525.
25 Bahri R, Custovic A, Korosec P, *et al.* Mast cell activation test in the diagnosis of allergic disease and anaphylaxis. *J Allergy Clin Immunol* 2018; **142**:485–496; e16.
26 Dewachter P, Castells MC, Hepner DL, *et al.* Perioperative management of patients with mastocytosis. *Anesthesiology* 2014; **120**:753–759.
27 Shane HL, Lukomska E, Kashon ML, *et al.* Topical application of the quaternary ammonium compound didecyldimethylammonium chloride activates Type 2 innate lymphoid cells and initiates a mixed-type allergic response. *Toxicol Sci* 2019; **168**:508–518.

28 LaKind JS, Goodman M. Methodological evaluation of human research on asthmagenicity and occupational cleaning: a case study of quaternary ammonium compounds ('quats'). *Allergy Asthma Clin Immunol* 2019; **15**:69.
29 Laroche D, Chollet-Martin S, Léturgie P, *et al.* Evaluation of a new routine diagnostic test for immunoglobulin E sensitization to neuromuscular blocking agents. *Anesthesiology* 2011; **114**:91–97.
30 Elst J, van der Poorten M-LM, Van Gasse AL, *et al.* Mast cell activation tests by flow cytometry: a new diagnostic asset? *Clin Exp Allergy* 2021; **51**:1482–1500.
31 Uyttebroek AP, Sabato V, Leysen J, *et al.* Flowcytometric diagnosis of atracurium-induced anaphylaxis. *Allergy* 2014; **69**:1324–1332.
32 Dewachter P, Chollet-Martin S, Mouton-Faivre C, *et al.* Comparison of basophil activation test and skin testing performances in NMBA allergy. *J Allergy Clin Immunol Pract* 2018; **6**:1681–1689.
33 Ebo DG, Faber M, Elst J, *et al.* In vitro diagnosis of immediate drug hypersensitivity during anesthesia: a review of the literature. *J Allergy Clin Immunol Pract* 2018; **6**:1176–1184.
34 Ebo DG, Fisher MM, Hagendorens MM, *et al.* Anaphylaxis during anaesthesia: diagnostic approach. *Allergy* 2007; **62**:471–487.
35 Bruhns P, Chollet-Martin S. Mechanisms of human drug-induced anaphylaxis. *J Allergy Clin Immunol* 2021; **147**:1133–1142.
36 Gillis CM, Jönsson F, Mancardi DA, *et al.* Mechanisms of anaphylaxis in human low-affinity IgG receptor locus knock-in mice. *J Allergy Clin Immunol* 2017; **139**:1253–1265; e14.
37 Finkelman FD, Khodoun MV, Strait R. Human IgE-independent systemic anaphylaxis. *J Allergy Clin Immunol* 2016; **137**:1674–1680.
38 Kow ASF, Chik A, Soo K-M, *et al.* Identification of soluble mediators in IgG-mediated anaphylaxis via Fcγ receptor: a meta-analysis. *Front Immunol* 2019; **10**:190.
39 Jönsson F, de Chaisemartin L, Granger V, *et al.* An IgG-induced neutrophil activation pathway contributes to human drug-induced anaphylaxis. *Sci Transl Med* 2019; **11**:eaat1479.
40 Vadas P, Perelman B, Liss G. Platelet-activating factor, histamine, and tryptase levels in human anaphylaxis. *J Allergy Clin Immunol* 2013; **131**:144–149.
41 Piwowarek ŘKL, Rzeszotarska A, Korsak ŘJL, *et al.* Clinical significance of plasma PAF acetylhydrolase activity measurements as a biomarker of anaphylaxis: cross-sectional study. *PLoS One* 2021; **16**:e0256168.
42 Beutier H, Hechler B, Godon O, *et al.* Platelets expressing IgG receptor Fc (RIIA/CD32A determine the severity of experimental anaphylaxis. *Sci Immunol* 2018; **3**:eaan5997.
43 Mackay GA, Fernandopulle NA, Ding J, *et al.* Antibody or anybody? Considering the role of MRGPRX2 in acute drug-induced anaphylaxis and as a therapeutic target. *Front Immunol* 2021; **12**:688930.
44 McNeil BD, Pundir P, Meeker S, *et al.* Identification of a mast-cell-specific receptor crucial for pseudo-allergic drug reactions. *Nature* 2015; **519**:237–241.
45 Varricchi G, Pecoraro A, Loffredo S, *et al.* Heterogeneity of human mast cells with respect to MRGPRX2 receptor expression and function. *Front Cell Neurosci* 2019; **13**:299.
46 Lansu K, Karpiak J, Liu J, *et al.* In silico design of novel probes for the atypical opioid receptor MRGPRX2. *Nat Chem Biol* 2017; **13**:529–536.
47 Elst J, Sabato V, Mertens C, *et al.* Association between mutated Mas-related G protein-coupled receptor-X2 and rocuronium-induced intraoperative anaphylaxis. Comment on Br J Anaesth 2020; 125: e446-e448. *Br J Anaesth* 2020; **125**:e448–e450.
48 Che D, Rui L, Cao J, *et al.* Cisatracurium induces mast cell activation and pseudo-allergic reactions via MRGPRX2. *Int Immunopharmacol* 2018; **62**:244–250.
49 Che D, Wang J, Ding Y, *et al.* Mivacurium induce mast cell activation and pseudo-allergic reactions via MAS-related G protein coupled receptor-X2. *Cell Immunol* 2018; **332**:121–128.
50 Van Gasse AL, Elst J, Bridts CH, *et al.* Rocuronium hypersensitivity: does off-target occupation of the MRGPRX2 receptor play a role? *J Allergy Clin Immunol Pract* 2019; **7**:998–1003.
51 Ebo DG, Van der Poorten M-L, Elst J, *et al.* Immunoglobulin E cross-linking or MRGPRX2 activation: clinical insights from rocuronium hypersensitivity. *Br J Anaesth* 2021; **126**:e27–e29.
52 McNeil BD. MRGPRX2 and adverse drug reactions. *Front Immunol* 2021; **12**:2594.
53 Azimi E, Reddy VB, Shade K-TC, *et al.* Dual action of neurokinin-1 antagonists on Mas-related GPCRs. *JCI Insight* 2016; **1**:e89362.
54 Mertes PM, Moneret-Vautrin DA, Leynadier F, *et al.* Skin reactions to intradermal neuromuscular blocking agent injections: a randomized multicenter trial in healthy volunteers. *Anesthesiology* 2007; **107**:245–252.
55 Uyttebroek AP, Sabato V, Bridts CH, *et al.* Immunoglobulin E antibodies to atracurium: a new diagnostic tool? *Clin Exp Allergy* 2015; **45**:485–487.
56 Anon. Anaesthesia and intensive care, 2000. Correspondence 2000; 28:167–168.
57 Leysen J, Bridts CH, De Clerck LS, *et al.* Allergy to rocuronium: from clinical suspicion to correct diagnosis. *Allergy* 2011; **66**:1014–1019.
58 Goyard S, Balbino B, Chinthrajah RS, *et al.* A highly sensitive bioluminescent method for measuring allergen-specific IgE in microliter samples. *Allergy* 2020; **75**:2952–2956.
59 Anna F, Goyard S, Lalanne AI, *et al.* High seroprevalence but short-lived immune response to SARS-CoV-2 infection in Paris. *Eur J Immunol* 2021; **51**:180–190.
60 Movérare R, Blume K, Lind P, *et al.* Human allergen-specific IgG subclass antibodies measured using ImmunoCAP technology. *Int Arch Allergy Immunol* 2017; **172**:1–10.
61 De Chaisemartin L, Jönsson F, Granger V, *et al.* Presence of an IgG-induced neutrophil activation mechanism in drug related anaphylaxis. *Rev Fr Allergol* 2018; **58**:264.
62 Zhou X, Whitworth HS, E-K M, *et al.* Mast cell chymase: a useful serum marker in anaphylaxis. *J Allergy Clin Immunol* 2011; **127**:AB143.
63 Brown TA, Whitworth HS, Zhou XY, *et al.* Mast cell carboxypeptidase as a confirmatory and predictive marker in allergic reactions to drugs. *J Allergy Clin Immunol* 2011; **127**:AB143.
64 Wolters PJ, Pham CTN, Muilenburg DJ, *et al.* Dipeptidyl peptidase I is essential for activation of mast cell chymases, but not tryptases, in mice*. *J Biol Chem* 2001; **276**:18551–18556.
65 Korosec P, Turner PJ, Silar M, *et al.* Basophils, high-affinity IgE receptors, and CCL2 in human anaphylaxis. *J Allergy Clin Immunol* 2017; **140**:750–758; e15.
66 Mochizuki A, McEuen AR, Buckley MG, *et al.* The release of basogranulin in response to IgE-dependent and IgE-independent stimuli: validity of basogranulin measurement as an indicator of basophil activation. *J Allergy Clin Immunol* 2003; **112**:102–108.
67 Garvey LH, Dewachter P, Hepner DL, *et al.* Management of suspected immediate perioperative allergic reactions: an international overview and consensus recommendations. *Br J Anaesth* 2019; **123**:e50–e64.
68 Cuilenborg VRvan, Hermanides J, Bos EME, *et al.* Awake intravenous provocation with small doses of neuromuscular blocking agent in patients with suspected allergy: experiences from the Dutch Perioperative Allergy Centre. *Br J Anaesth* 2019; **123**:e153–e155.
69 Chiriac AM, Tacquard C, Fadhel NB, *et al.* Safety of subsequent general anaesthesia in patients allergic to neuromuscular blocking agents: value of allergy skin testing. *Br J Anaesth* 2018; **120**:1437–1440.
70 Navinés-Ferrer A, Serrano-Candelas E, Lafuente A, *et al.* MRGPRX2-mediated mast cell response to drugs used in perioperative procedures and anaesthesia. *Sci Rep* 2018; **8**:11628.
71 Porebski G, Kwiecien K, Pawica M, *et al.* Mas-related G protein-coupled receptor-X2 (MRGPRX2) in drug hypersensitivity reactions. *Front Immunol* 2018; **9**:3027.
72 Subramanian H, Gupta K, Ali H. Roles of Mas-related G protein-coupled receptor X2 on mast cell-mediated host defense, pseudoallergic drug reactions, and chronic inflammatory diseases. *J Allergy Clin Immunol* 2016; **138**:700–710.

APPENDIX 4. Review: Animal Models of IgE Anaphylaxis

biology

MDPI

Review

Animal Models of IgE Anaphylaxis

Aurélie Gouel-Chéron [1,2,3,*], Alice Dejoux [3,4], Emma Lamanna [3,5] and Pierre Bruhns [3]

[1] Université Paris Cité, 75010 Paris, France
[2] Anaesthesiology and Critical Care Medicine Department, DMU Parabol, Bichat-Claude Bernard Hospital, AP-HP, 75018 Paris, France
[3] Institut Pasteur, Université de Paris Cité, INSERM UMR1222, Antibodies in Therapy and Pathology, 75015 Paris, France
[4] Sorbonne Université, Collège Doctoral, 75005 Paris, France
[5] Neovacs SA, 92150 Suresnes, France
* Correspondence: aurelie.gouel@aphp.fr; Tel.: +33-140258355

Simple Summary: Anaphylaxis is the most severe form of allergic reactions and can be life-threatening. It is very difficult to study the mechanisms underlying anaphylaxis in humans since these events are rare and often lethal. Therefore, animal models have been established. Mice and rats are mostly used since their biological parameters, such as temperature drop, behavioral changes, and blood or cell biomarkers, can be easily measured in the laboratory. These animals can also be genetically modified to express human proteins and cell functions. Different animal models have been established to replicate as closely as possible the natural route of sensitization to the allergen and to trigger anaphylaxis in animals. These animal models have deepened our knowledge on human anaphylaxis with certain limitations, as discussed in this review.

Abstract: Allergies and atopy have emerged as significant public health concerns, with a progressively increasing incidence over the last two decades. Anaphylaxis is the most severe form of allergic reactions, characterized by a rapid onset and potentially fatal outcome, even in healthy individuals. Due to the unpredictable nature and potential lethality of anaphylaxis and the wide range of allergens involved, clinical studies in human patients have proven to be challenging. Diagnosis is further complicated by the lack of reliable laboratory biomarkers to confirm clinical suspicion. Thus, animal models have been developed to replicate human anaphylaxis and explore its pathophysiology. Whereas results obtained from animal models may not always be directly translatable to humans, they serve as a foundation for understanding the underlying mechanisms. Animal models are an essential tool for investigating new biomarkers that could be incorporated into the allergy workup for patients, as well as for the development of novel treatments. Two primary pathways have been described in animals and humans: classic, predominantly involving IgE and histamine, and alternative, reliant on IgG and the platelet-activating factor. This review will focus essentially on the former and aims to describe the most utilized IgE-mediated anaphylaxis animal models, including their respective advantages and limitations.

Keywords: allergy; anaphylaxis; IgE; animal models

Citation: Gouel-Chéron, A.; Dejoux, A.; Lamanna, E.; Bruhns, P. Animal Models of IgE Anaphylaxis. *Biology* **2023**, *12*, 931. https://doi.org/10.3390/biology12070931

Academic Editor: Abdelouahab Bellou

Received: 29 April 2023
Revised: 16 June 2023
Accepted: 21 June 2023
Published: 29 June 2023

1. Introduction

Allergies and atopy have emerged as significant public health concerns with a growing incidence over the last two decades, for reasons not yet entirely understood [1]. Anaphylaxis, the most severe form of acute hypersensitivity reaction, has been defined as a "serious allergic reaction that is rapid in onset and may result in death" [2]. It can be fatal, even in healthy individuals, with food and drugs being the most widely recognized culprit agents [3]. There are different definitions of anaphylaxis in the literature: some require a systemic and generalized reaction, whereas other definitions require symptoms in one

organ system [4]. Typical symptoms (also called phenotype) of anaphylaxis include skin rash, respiratory symptoms with bronchospasm, cardiovascular symptoms with arterial hypotension, tachy/bradycardia and cardiac arrest in the most severe form, and gastrointestinal difficulties [5]. According to the World Allergy Organization, anaphylaxis is diagnosed when one of the following criteria is fulfilled: (1) an acute onset of an illness with the involvement of the skin or mucosal tissues, or (2) an acute onset of hypotension or bronchospasm even in the absence of skin involvement.

In human patients, studies of anaphylaxis are challenging because of the rapid onset and potential lethality of the reaction. For obvious ethical reasons, inducing anaphylaxis in humans is not acceptable. Most of the time, the reaction takes place outside the hospital, making it difficult to study the early stage of the reaction. Epinephrine is the predominant treatment against anaphylaxis since it counteracts the physiologic changes induced by anaphylaxis through the activation of adrenergic receptors by inducing, among other effects, vasoconstriction and bronchodilation. Because of this context and the lethality of the reaction, randomized control trials analyzing epinephrine compared to another treatment, such as methylene blue, vasopressin, or norepinephrine, would not be acceptable without strong animal evidence of efficacy. Most data in humans have so far relied on clinical case series [6,7]. Additionally, the type and quantity of allergens, as well as the route of exposure, may vary greatly between patients. Symptoms can occur within seconds to a few hours after allergen exposure and can affect multiple organ systems, although not all may be affected in a single allergic reaction. Early intervention is essential, and it has been identified as a positive prognostic factor [8]. The lack of reliable biomarkers to confirm the clinical prognosis and the difficulties in diagnosis further impede research into anaphylaxis in the clinic.

Due to these challenges, animal models have been established to reproduce as faithfully as possible the pathophysiology of human anaphylaxis [9]. Such tools include genetically modified strains that can express humanized proteins (i.e., receptors and ligands) or suppress the expression of murine genes. Although findings obtained from animal models may not completely replicate human anaphylaxis, they provide a framework for comprehending the mechanisms at work [10]. Furthermore, they are an invaluable tool for exploring potential new biomarkers that could be included in the allergy work-up for patients and new treatments.

The classical pathway of anaphylaxis involves immunoglobulin (Ig) E antibodies, but other alternative pathways have been described in humans. The non-IgE mediated pathways include the formation of IgG/antigen complexes that can activate effector cells such as neutrophils, macrophages, and monocytes [11]. This review aims to outline the most used IgE-mediated anaphylaxis animal models and their respective advantages and limitations.

2. Physiopathology

2.1. Antibodies in IgE-Mediated Anaphylaxis

Two independent mechanisms have been described in animal models of anaphylaxis, each of them involving antibodies of a distinct isotype (IgE or IgG); the first of these, referred to as the classical pathway, is the subject of this review [11]. Ig is a symmetrical protein composed of two identical heavy and light chains that possesses a variable and a constant region. The amino acids forming the variable region are involved in antigen binding and define the specificity of the antibody for a unique antigen. The constant region is responsible for mediating effector functions by binding to receptors expressed on the cell surface. This determines the underlying mechanisms activated in response to the presence of antibodies recognizing the antigen. Such mechanisms can include cell activation, endocytosis, release of inflammatory mediators, and complement activation. The heavy-chain constant region also determines the antibody isotype: IgG, IgA, IgM, IgD, or IgE, each possessing a distinct role [12].

The binding of Ig to antibody Fc receptors (FcR) expressed on the surface of effector cells triggers a biological response that can include activating or inhibitory signals. The formation of an antibody–antigen complex is necessary to trigger the cellular response by causing receptor aggregation or cross-linking. FcRs possess different affinities for their respective Ig isotypes, which can vary from one species to another [13]. Most FcRs, however, are of low affinity and only retain Ig if present as an immune complex, opsonized on a surface, or aggregated. Rare high-affinity receptors exist that can bind and retain Ig, such as the IgE receptor FcεRI. In humans, FcεRI and FcεRII (CD23) are IgE receptors, FcγRs are IgG receptors, and FcαRI (CD89) is an IgA receptor. Mice do not express FcαRI, and most of their IgG receptors bind IgE with low affinity (inhibitory mouse FcγRIIB and activating mouse FcγRIII and FcγRIV) [14,15]. FcεRI, the high-affinity IgE receptor, is composed of α, β, and γ subunits ($\alpha\beta\gamma_2$ tetramers) in human and mouse mast cells and basophils, whereas it is composed of only α and γ subunits ($\alpha\gamma_2$ trimers) in human macrophages and Langerhans cells [15]. These differences in the cell expression pattern might alter the translation of mouse experimental results to humans. The β subunit enhances signaling through FcεRI but is not required for binding; indeed, it has been shown that the α subunit of the hIgE receptor is sufficient for high-affinity IgE binding [16].

2.2. Mechanisms of IgE-Mediated Anaphylaxis

Although other mechanisms have been described, the classical pathway of anaphylaxis involves IgE antibodies bound to their high-affinity receptors (FcεRI), which are mainly expressed on the surface of mast cells in tissues and basophils in circulation. This pathway requires a two-step process. First the sensitization phase: pre-exposure to the antigen that leads to the synthesis of a specific IgE (sIgE) that binds on the surface of the effector cells in a T-cell helper type 2 (Th2) environment. Activated Th2 lymphocytes secrete cytokines IL-4, IL-5, and IL-13, which induce IgE class switch recombination in B cells and their differentiation into IgE-secreting plasma cells. This secreted IgE binds to FcεRI on mast cells forming IgE/FcεRI complexes. The second phase occurs following a second antigen exposure, during which antigens bind to at least two IgE/FcεRI complexes enabling the cross-linking of the receptor and the induction of signal transduction by the γ and β chains. This sIgE/FcεRI aggregation triggers the degranulation of pre-stored and de novo synthesized inflammatory mediators such as histamine (primarily responsible for the development of the reaction), tryptase, platelet-activating factor (PAF), prostaglandin D2, and leukotrienes, leading to clinical signs of anaphylaxis (Figure 1) [17]. Mast cells are key players in allergic disease and have been recognized as the main cell responsible for anaphylaxis events for more than 50 years [18]. Indeed, their activation by the antigen-induced IgE crosslinking of FcεRI induces a feed-back loop stimulating mast cell survival and, in B cells, a mechanism of immunoglobulin class switch to IgE, further promoting Th2-type immunity [19]. Mast cell mediators can be released by either sIgE/FcεRI aggregation in the presence of the specific antigen or by IgE-independent degranulation. Indeed, some drugs can directly trigger mast cell degranulation in vitro via the activation of the mast cell receptor 'Mas-related G protein-coupled receptor X2' (MRGPRX2) [20], although no formal proof has been reported *in vivo* in humans so far. Finally, human cardiac mast cells are also suspected to be involved in cardiac anaphylaxis phenotypes, such as the type 1 Kounis syndrome, which is characterized by vasospasm in healthy coronary arteries [21].

Whereas the nature of the allergen and the route of sensitization are usually well known in food or venom anaphylaxis, this is not usually the case for drug allergies, since some molecules are non-immunogenic and drug-induced anaphylaxis occurs frequently upon the first exposure to the patient. The mechanism of drug sensitization has been the subject of intense research in recent years [22]. The leading theory is that some drugs can form a complex with a carrier protein (the hapten theory) that will be recognized as a neo-antigen.

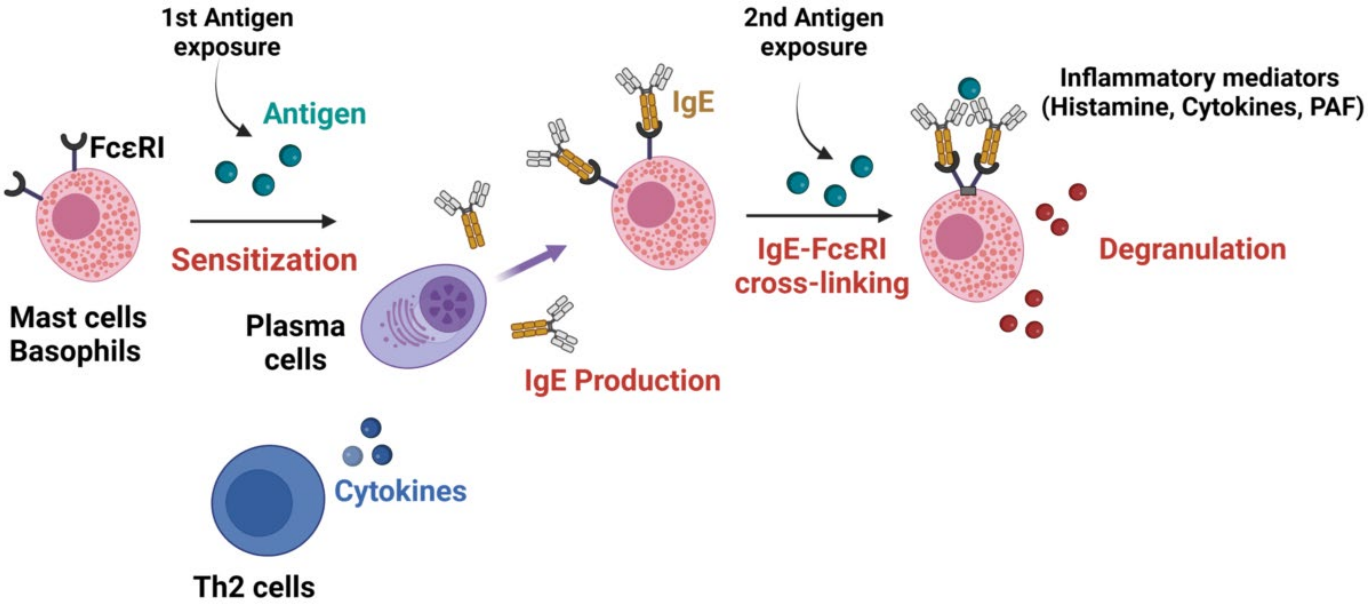

Figure 1. Pathway of IgE-mediated anaphylaxis. A first antigen exposure is required for specific IgE synthesis by plasma cells in a Th2 environment. The second antigen exposure enables the cross-linking of FcεRI by the binding of the antigen on the specific sIgE/FcεRI complex. The sIgE/FcεRI aggregation triggers mast cell and basophil degranulation, which releases inflammatory mediators responsible for the clinical symptoms of anaphylaxis.

3. Anaphylaxis Monitoring in Animal Models

The use of animals in research requires approval from an ethical committee and compliance with the Guiding Principles for Research Involving Animals, regardless of the species involved. Whereas animal models have been predominantly established in mice and rats, reports have also been published for other species such as rabbits [8], guinea pigs [23], dogs [24], sheep [25], pigs, and swine [26]. These have been largely described elsewhere and are not the subject of this review [27,28].

Anaphylactic reactions can include a large range of symptoms in humans, such as arterial hypotension, vasodilation, bronchoconstriction, erythema, and arrhythmia as previously described [4]. To model anaphylaxis in animals, the consequences of the induced reaction on the hemodynamic and respiratory system must be measured. In mouse models, invasive monitoring can present challenges because of the small size of the animal. Although feasible, it requires specific equipment, and surgery which is time-consuming to setup and therefore not often used. To replace this approach, clinical noninvasive tools are thus required. Hypothermia, measured by rectal temperature, is widely used to evaluate anaphylaxis severity in mice, as it is considered a surrogate marker of cardiac output. Other monitoring tools can include a quantitative mouse activity scale (3, normal activity; 2, slow movement after prodding; 1, no movement in response to prodding; and 0, inability to right itself after being turned on its side) and diarrhea occurrence, which is thought to positively correlate with levels of intestinal mast cells [29]. To the best of our knowledge, most of the anaphylaxis mouse models reported so far relied on these measures to assess anaphylaxis.

As opposed to mice, all anaphylaxis models on rats have used invasive measurements to assess the impacts of anaphylaxis on the respiratory and hemodynamic system. As rats are larger in size compared to mice, certain procedures are easier to perform, such as tracheal intubation or tracheotomy; artery and vein line placement (femoral, jugular, or carotid); and the insertion of tissue oxygen pressure (PtiO2) and microdialysis probes. These procedures enable the monitoring of mean arterial pressure, blood flow velocity, vascular peripheral resistance, and muscular interstitial lactate concentration. They also allow biological sampling such as arterial blood gases and hematologic measurements. A precise evaluation of the decreased vascular resistance, fluid loss, and hemodynamic impairment

induced by a reaction can be performed with these monitoring devices (Table 1). Respiratory resistance and elastance, microvascular leakage in the airways [30], and extensive cerebral monitoring [31] can also be more easily performed in rats, including measurements of cerebral cortical blood flow, carotid artery blood flow, cerebral oxygen partial pressure, cerebral interstitial lactate/pyruvate ratio, and PtiO2 via electrode insertion after craniotomy into the right cerebral cortex [32–34]. The objectives are to evaluate the consequences of the hemodynamic failure induced by anaphylaxis on the cerebral oxygenation (Table 1). Hemodynamic measurements (micro- and macro-circulation), including cardiac output, skeletal muscular oxygen partial pressure, skeletal muscular interstitial lactate/pyruvate ratio, and PtiO2, can also be extended using perivascular ultrasonic flow probes placed around the upper abdominal aorta or by inserting an electrode into muscles, among other techniques [32]. Left-ventricular function can be assessed by inserting a catheter into the left ventricle to measure direct pressure. Similarly, as performed in humans, cardiac echography enables left-ventricular end-diastolic and systolic diameter measurements, allowing for the calculation of the left-ventricular shortening fraction [35]. Although these measures have been reported in mice, they have never been assessed in anaphylaxis models [36].

Table 1. Summary of the different monitoring approaches available in mice or rats to evaluate physiological parameters during anaphylaxis experiments.

Animal	Physiological Parameter	Probes for Measurement
Mice/rats	Drop in core body temperature	Rectal temperature
	Level of intestinal mast cells	Occurrence of diarrhea
	Reduced physical activity	Activity scale
	Decreased vascular resistance, fluid loss, and hemodynamic impairment	Tracheal intubation, vein line placement
	Muscular interstitial lactate concentration	PtiO2 and micro-dialysis probes in the quadriceps muscle
Mostly rats	Hemodynamic failure of cerebral oxygenation	Measurements of cerebral cortical blood flow and oxygen partial pressure
	Hemodynamic failure	Perivascular ultrasonic flow probes
	Left-ventricular function impairment	Catheter insertion
	Vascular leakage due to histamine release	Hematocrit measurement

Acute hemoconcentration, as assessed by an increase in the hemoglobin concentration in the absence of acute diuresis, has been suggested as a highly indicative marker of anaphylaxis occurrence and vascular leak. Hematocrit measurement and, consequently, the correction of hemoconcentration can attest to the efficacy of volume expansion and have been suggested as a monitoring tool in animal studies [37]. However, performing blood draws on a mouse during an anaphylactic reaction is hardly feasible, if not impossible, as the blood pressure is too low. However, animals are often sacrificed at the end of the anaphylaxis experiments, allowing for blood sampling and tissue collection for biomarker measurement, cytometry, and histological analyses [38,39].

In most mouse anaphylaxis models reported so far, clinical surrogate measurements have been used (rectal temperature, behavior scale), whereas the use of larger animals, such as rats, enables the measurement of particular outcomes such as hemodynamic changes, particularly in assessing treatment efficacy and its effects on cerebral oxygenation, cardiac output, and vascular leakage [40,41].

4. Animal Models

In immunization procedures, the use of adjuvants is imperative to bypass the phenomenon of oral tolerance to proteins observed in most animal species. The goal is to induce clinical responses that closely resemble IgE-mediated food and drug allergies in

humans. The extent of sensitization depends on various factors, including antigen concentration, administration route and duration, animal age and strain, Th1/Th2 polarization (which is more distinct in mice compared to humans), and use of adjuvants.

4.1. Sensitization Routes

Sensitization success varies considerably according to the route of administration, dose, and frequency of injections. Various routes of immunization can be used to induce sensitization, including oral gavage; epicutaneous, subcutaneous, or intradermal exposure; and intraperitoneal or intravenous injections.

It is generally accepted that among adjuvants, alum favors the production of IgG1 and IgE antibodies in wild-type mice, whereas Complete Freund's Adjuvant (CFA) favors IgG2 antibodies, even if mice with different genetic backgrounds can display different responses to immunization with these adjuvants [42]. In both cases, however, IgG1 antibodies are the most abundant and IgE the least abundant.

The route of sensitization chosen should depend on the allergen used and the human disease studied. In food-driven anaphylaxis, oral sensitization is predominantly used [43]. This model emphasizes the effect of digestion on sensitization and stimulate the interactions of the epithelia with the allergens. Indeed, it has been shown that the intestinal epithelial barrier regulates protein antigen passage and guides mucosal immune responses. One protocol example is intragastric feeding once a week for 7 weeks with the allergen and cholera toxin using a ball-ended feeding needle [44]. It was established in a mouse model of anaphylaxis sensitized with different doses of peanut protein via intragastric gavage that lower doses of peanut protein induced the highest IgE levels and a more severe anaphylactic reaction [45]. This suggested that lower doses of allergen could induce a stronger sensitization compared to higher allergen doses.

Sensitization via the skin can be performed epicutaneously or subcutanesouly. Epicutaneous sensitization is performed on abraded skin. There are various methods to perform this type of sensitization: (1) calcipotriol application on a specific skin area for 14 consecutive days, which inhibits keratinocyte proliferation and generates an atopic-dermatitis-like skin lesion [46,47]; (2) the application of the allergen directly on a shaved skin area under a transparent bio-occlusive dressing for 7 days, with the same treatment being applied at the same site for a total of three 1-week exposures, separated by a 14-day period [48–51]; and (3) the induction of a skin injury to mimic the mechanical injury caused by scratching. This route of sensitization is very useful to mimic skin-driven allergies but is also justified for other antigens such as peanut proteins. Indeed, a human study demonstrated that peanut sensitization occurs as a result of environmental household exposures rather than maternal peanut consumption during pregnancy [52]. Most animal studies support the evidence that subcutaneous sensitization is the most effective in mouse asthma models. In a study comparing intraperitoneal, subcutaneous, and aerosol sensitization using the major birch pollen allergen Bet v 1, the subcutaneous route elicited higher IgE levels and the preferential production of Th2 cytokines in spleen cells [53].

A fourth sensitization route relies on intraperitoneal injections. Several strategies can be mixed. Jonsson et al. [54] reported three intraperitoneal injections on days 0, 14, and 28 using BSA as the antigen either with CFA for the first injection followed twice by Incomplete Freund's Adjuvant; or three times with alum; or three times with alum plus Pertussis toxin. The challenge performed 10 days after the last immunization induced a strong anaphylaxis reaction in mice with high lethality [54]. This route has been shown to be more efficient than other routes of sensitization in some animal studies. For instance, Liu et al. [55] sensitized mice with wheat gluten via intraperitoneal, transdermal, and oral gavage sensitization routes. They showed that all three methods could induce allergic symptoms (increased serum antibodies, Th2 secretion, and inflammatory factors). Nonetheless, levels of serum antibodies were higher in mice sensitized intraperitoneally, and the bacterial species diversity in the intestinal flora was more significantly decreased in this group of mice as well [55]. The comparison of oral, intraperitoneal, and subcutaneous sen-

sitization in ovalbumin (OVA) anaphylaxis led to the generation of OVA IgE-epitopes in all models, with more binding epitopes in intraperitoneal compared to oral immunization [56]. However, the answer is not straight forward, as epicutaneous sensitization can elicit a stronger immune response than the intraperitoneal route in some cases. Several mouse studies supported this hypothesis, with higher OVA-specific serum IgE and IgG antibody responses after epicutaneous compared to intraperitoneal sensitization. They suggested that epicutaneous sensitization may be more prone to inducing a Th2 response [48].

Combining sensitization routes could also be of interest, as the combination of intraperitoneal and epicutaneous sensitization has been shown to be more effective than epicutaneous alone in a mouse model of skin disease (atopic dermatitis) [57].

Intradermal sensitization is mostly used for passive cutaneous anaphylaxis (PCA) (Section 4.2) by injecting the antigen under the epidermis. This route of injection has the longest absorption time and the advantage of being easily visualized.

Intravenous allergen injection in mouse is mostly used for antigen challenge after a prior sensitization. This route of allergen administration is useful to closely mimic drug-induced anaphylactic reactions in humans, which are often triggered by the intravenous injection of high doses of drugs. However, it might be used for sensitization when the mice need to be passively sensitized with an antibody before the antigen challenge during passive systemic anaphylaxis (PSA) (Section 4.3). The antibody administered intravenously can directly bind the receptors at the surface of effector cells prior to allergen exposure.

As there has been a lot of variation in the choice of route, immunization frequency, and the concentration of antigen sensitization across different studies, it is crucial to carefully optimize these parameters when implementing animal models of anaphylaxis.

4.2. Passive Cutaneous Anaphylaxis

PCA was among the earliest models described, and, consequently, it played a significant role in the comprehension of anaphylaxis pathophysiology. The model involves the intradermal injection of allergen-specific IgE antibodies into mice, followed by intravenous challenge with the corresponding allergen [58,59]. Mouse IgE monoclonal antibodies (mAbs) can be used in mice expressing endogenous FcεRI (mFcεRI), whereas human IgE mAbs or serum from an allergic patient can be used in transgenic mice expressing human FcεRI (hFcεRI).

Evans Blue dye can be administered with or closely following antigen challenge to determine changes in vascular permeability as demonstrated by the leakage of the dye into the reaction site. This method provides a visual representation of the hypersensitivity reaction, as well as a quantitative result when extracting postmortem the dye from the skin and measuring its optical density.

4.3. Passive Systemic Anaphylaxis

Passive systemic anaphylaxis (PSA) induced by IgE is an established model for the study of anaphylaxis. The model involves the systemic injection of specific IgE antibodies in mice, followed 24–48 h later by challenge with the corresponding antigen. Passive sensitization can be performed with monoclonal antibodies (mouse or human if mouse express human FcεRI) or with a pool of immunized human or mouse sera [60,61]. Anaphylactic shock develops within minutes and can be assessed as described in Section 3, most practically by recording hypothermia. In the case of oral administration, mice should fast for 3 to 4 h prior induction. This model has been instrumental in the understanding of the IgE-dependent classical pathway mediated by mast cells and the release of histamine [62].

Dombrowicz et al. [59]. demonstrated that mice deficient in mFcεRI were protected from developing anaphylaxis, showing that FcεRI is necessary for the induction of IgE-mediated anaphylaxis. In addition, IgE-induced PSA was abrogated in mast-cell-deficient W/W^v mice [63] and after the injection of anti-IgE mAbs [64].

The role of histamine and mast cells in PSA has been demonstrated in studies with mice lacking histamine (using histidine decarboxylase-deficient mice) or mice injected with

histamine receptor antagonists to prevent anaphylaxis [65]. All the studies performed using this model demonstrated the importance of mFcεRI and mast cells in IgE-induced PSA, as they release histamine following the crosslinking of IgE molecules bound to the mast cell surface via mFcεRI.

4.4. Active Systemic Anaphylaxis

The active systemic anaphylaxis (ASA) model differs from the PSA model as it involves sensitization to a specific allergen using the allergen itself rather than bypassing the immunization phase by providing passively specific antibodies against the allergen. The purpose of this process is to mimic the sensitization process that occurs in humans prior to IgE- or IgG-dependent anaphylaxis and requires antibodies to be produced by the host.

Although ASA and PSA present similar symptoms, a higher mortality rate is observed in ASA, and the results obtained from these models do not always correlate [66]. ASA is frequently used in research on alternative pathways of anaphylaxis, as it highlights the indispensable role of IgG and IgG receptors in ASA and the downstream production of PAF, which mediates the physiological symptoms of ASA [54,67].

4.5. Intestinal Models of Anaphylaxis

Several animal models have been described to study food-allergy-induced diarrhea and shock. In the model, mice were sensitized via intraperitoneal injection with ovalbumin emulsified in alum, twice and two weeks apart [68,69]. In the second model, mice were sensitized through the ingestion of an allergen, such as peanut extract, with cholera toxin as a mucosal adjuvant [45]. In the third model, mice were sensitized through epicutaneous exposure to hazelnut extract, where the allergen was applied to the mouse's clipped back skin and covered with a bandage for three days [70,71].

Challenges with the appropriate allergen were performed through intra-gastric gavage after depriving mice of food for 3–4 h. Interestingly, the ovalbumin model only induced diarrhea, whereas the peanut and hazelnut models induced both diarrhea and shock. The reason for this difference was not immediately clear and may be related to the allergen nature, molecular structure, and dose, which could lead to differences in allergen absorption or activate different pathways.

These studies have played a crucial part in elucidating the role of the classical mast-cell- and IgE-mediated mechanisms in allergic manifestations with gastrointestinal symptoms, including diarrhea, in response to food allergens. A mouse model of oral antigen-induced anaphylaxis with intestinal and systemic symptoms revealed that diarrhea and hypothermia were mitigated in mFcεRI-deficient mice following challenge compared to controls [29]. Intestinal mast cell levels were also found to be correlated with the severity of these symptoms.

4.6. Transgenic Mice and Humanized Mouse Models

Transgenic mouse models have been developed to investigate the involvement of specific cytokines, such as IL-4 and IL-13, in anaphylaxis [72], as well as the roles of various effector cells, antibodies, and receptors. For example, mice deficient in cytokine IL-9 and its receptor were used to study the role of IL-9 in intestinal anaphylaxis [73], whereas mice deficient in the IL-33 receptor (ST2) were used to evaluate the role of IL-33 in IgE production and mast cell degranulation [74]. Mice deficient in CC chemokine receptor 4 (CCR4), which is expressed on skin-homing T cells, showed the involvement of T-cells during oral sensitization [44], whereas platelet endothelial cell adhesion molecule-1-deficient mice demonstrated its properties as a counter regulatory mechanism in allergic disease susceptibility and severity [75].

To precisely analyze the effect of a single human effector cell, antibody, or receptor, several "humanized" models of anaphylaxis have been developed and can be used in PCA, PSA, ASA, and intestinal anaphylaxis models. They were established to study anaphylaxis in a manner that more closely mimics human physiology. These models include mice expressing hFcεRI and mice deficient in various or all FcRs.

Mice expressing hFcεRI instead of mFcεRI display a similar cell expression profile of hFcεRI to humans [76]. Whereas mouse IgE can bind to human FcεRI, human IgE cannot bind to mouse FcεRI. To investigate the role of hFcεRI in anaphylaxis, these transgenic mice were used in PSA [59] and PCA [58] models. mIgEs are able to bind not only to the high-affinity IgE-receptor mFcεRI but also to low-affinity IgG-receptors, such as mFcγRIIB and mFcγRIII. The use of knock-out mice has revealed that IgE-mediated anaphylaxis can be modulated by IgG receptors, such as mFcγRIIB (the IgG inhibitory receptor) (with an enhanced reaction in mFcγRIIB-deficient mice) and mFcγRIII (an IgG activating receptor, leading to an attenuated reaction in mFcγRIII-deficient mice). Both receptors are present on mast cells and can act as regulators of IgE-mediated anaphylaxis in mice [77]. Transgenic mice with a gain-of-function mutation in the immunoreceptor tyrosine-based inhibitory motif (ITIM) at position 709 (Y→F) of the IL-4 receptor (IL-4Rα) displayed elevated IgE levels and increased susceptibility to allergen-induced airway inflammation, similar to atopic individuals. In these mice, the amplification of IL-4Rα signals facilitated allergic sensitization to ingested antigens and drove IgE-dependent anaphylactic responses [78–80]. These mice could also be useful in experiment setup in which robust allergic sensitization cannot be achieved due to tolerizing effects. Finally, highly immunodeficient NOD-scid $\gamma c^{-/-}$ (NSG) mice could be engrafted with human hematopoietic stem cells to study hIgE-mediated reactions and were used for PCA and ASA peanut allergic models [81–83]. Following engraftment, NSG mice developed large numbers of human mast cells in the peritoneal cavity and peripheral tissues, were able to produce hIgEs and hIgGs in response to sensitization, and could develop anaphylaxis after challenge.

Other mouse models have been developed to investigate the role of IgG in anaphylaxis and the importance of the IgG pathway compared to the IgE-mediated pathway. Indeed, the generation of an anti-allergen IgE response requires an initial IgG response and the switching of IgG B cells to IgE B cells. Anti-allergen IgG may thus positively or negatively regulate the IgE pathway in anaphylaxis and hence anaphylaxis symptoms and severity. Indeed, mice deficient in both IgE receptors, FcεRI and FcεRII (CD23), developed ASA similarly to wild-type mice. However, mice deficient in all activating FcRs (IgG and IgE receptors) were protected from ASA [54], suggesting that mouse IgG receptors are sufficient to induce anaphylaxis. The same was demonstrated using transgenic mice for human IgG receptors: in mice deficient in all endogenous mouse FcRs, the expression of hFcγRIIA was found to be sufficient to induce fatal ASA [84], and the expression of hFcγRI was sufficient to induce mild ASA [85]. More recent mouse models expressing all human low-affinity IgG receptors as knock-ins demonstrated the predominance of hFcγRIIA in PSA (using human IgG antibodies) and ASA (based on endogenous mouse IgG production) models, leading to neutrophil activation and PAF release [86]. Mice expressing all hFcγRs as transgenes showed that hFcγRs can induce PSA when injected with heat-aggregated IVIG [87].

Overall, these models offer a powerful set of tools for investigating potential new human treatments for anaphylaxis, such as histamine receptor 1 antagonists, omalizumab (an anti-IgE-capture antibody) [82], anti-FcγRIIA blocking antibodies, and PAF receptor antagonists [86]. More models are currently being developed that aim to reconstitute the expression of both human IgE receptors, hFcεRI and hFcεRII, and the production of human IgE for the study of the human IgE pathway in in vivo models.

5. Animal Strain Influence

The use of mouse models to study anaphylaxis is complicated by the differences in responses to sensitization and challenge exhibited by mice of different genetic backgrounds. Strains such as BALB/c, DBA/2, C3H/HeJ, BDF-1, A/J, 129S5, and C57BL/6 have been employed. BALB/c strain mice are the most commonly used, presumably because BALB/c strain mice favor Th2 over Th1 responses, and because of their ability to develop airway responsiveness during lung challenge. However, they do not systematically develop anaphylaxis compared to other mouse strains. Indeed, in a peanut allergy model using intramuscular immunization with DNA encoding for an allergen, C3H/HeSn

mice displayed anaphylaxis after challenge at weeks 3 and 5 after immunization, whereas AKR/J and BALB/c mice did not. All three strains displayed increased specific IgG2a, but increased specific IgG1 or IgE was only detected in C3H mice [88]. Similarly, in an active sensitization model using intraperitoneal injections of peanut extract or purified Ara h 2, C3H/HenHsd mice, but not BALB/C and C57BL/6 mice, experienced clinical symptoms of anaphylaxis and temperature loss following antigen challenge [61,78]. Furthermore, 129S5 mice also demonstrated an increased susceptibility to anaphylaxis compared to BALB/c mice [89]. In a recent study in our laboratory, we found that BALB/c and C57BL/6 mice produced different subclasses of IgG in response to the same allergen in alum, leading to the retention of the allergen in the lungs of BALB/c, but not C57BL/6, mice during anaphylaxis challenge [42].

Regarding rats, the Brown Norway rat is a high-IgE-responder strain that does not require an adjuvant for sensitization to an allergen and has been widely used. Other strains such as Wistar, Hooded Lister, and Piebald Virol Glaxo have also been studied, but their inability to produce antigen-specific IgE make them less suitable for anaphylaxis models [90–92].

Careful animal strain selection is mandatory to adapt the strain to the sensitization and challenge method (or vice-versa) and should be considered in the context of results obtained using other animal strains to draw conclusions on allergen-induced reactions in humans.

6. Limits of Animal Models in Anaphylaxis

Rodents, particularly mice and rats, are widely used in laboratory models due to their availability; low cost; and well-understood metabolism, physiology, and biochemistry pathways. However, their distinct antibody and receptor profiles compared to humans must be considered when interpreting study results and extrapolating findings to human patients. Whereas these species share some pathophysiological similarities, such as in sepsis models [93], the time-course of anaphylaxis development, the lack of supportive therapeutic interventions, and the relatively allergen-free environment of laboratory facilities limit the translation of animal models to human anaphylaxis. Indeed, human medical intervention usually takes place minutes (in the peri-operative setting) to hours (when anaphylaxis occurs outside the hospital or following oral intake) after the reaction, whereas animal models focus on seconds to minutes after induction. Humans develop in an environment full of allergens, whereas animals are only sensitized to one defined antigen, which might modify the immune/antibody response in animals compared to humans. This will undeniably affect biomarker dynamics and therapeutic efficacy. Animal models typically use young adult animals with similar genetic backgrounds, age, gender, weight, and nutritional status, whereas human anaphylaxis occurs in patients with diverse ethnicities/genetics, food diets, gender, age, weight, and potential ongoing medical treatments and comorbidities. Moreover, most animal models rely on high antigen quantities for immunization and challenge, which may involve different pathways compared to human pathways leading to anaphylaxis [67]. The immune systems of animals and humans differ in antibody subclasses and the distribution of antibody receptors. As discussed previously, FcεRI, for example, is more widely expressed in human subjects, including on macrophages and dendritic cells, whereas in mice, it is only expressed on mast cells and basophils [66].

Therefore, translating animal model findings to human clinical practice is highly challenging. Despite these limitations, animal models remain valuable tools to enhance our understanding of anaphylaxis pathophysiology and treatment, as long as their advantages and limitations are considered in the study design and result interpretation.

7. Perspectives

One missing aspect in anaphylaxis animal models is the translation of results obtained in small rodents to larger mammals that are more relevant in terms of physiology to humans. As illustrated in this review, published mouse and rat models have not focused on the same

aspects. Whereas rat models have mostly been used so far to investigate treatment efficacy and physiological changes after anaphylaxis induction and treatment, mouse models have mostly focused on sensitization and the cellular and molecular physiopathology of anaphylaxis. Small animals are easier and cheaper to manage and reproduce and therefore represent a useful tool for developing models of anaphylaxis. However, large animals might better reproduce human physiopathology and might be considered for result validation before translation into clinical practice. An ideal animal model should display the same level of tolerance to antigens as humans, with a similar allergenicity profile; require the same amount of allergen to induce sensitization via the same route and duration of exposure; and present the same Th1/Th2 polarization and the same antibody profile as humans. It should also allow the realization of skin tests or in vitro tests, as performed in clinical practice. From this perspective, dogs, neonatal swine, and monkeys might represent particularly interesting species because of their similarity to humans in terms of physiopathology and immune response. Dogs and swine have demonstrated a natural tendency for allergic reactions with similar immunopathogenic consequences and therapeutic interventions as in humans. To the best of our knowledge, these latter species have mostly been used to investigate food allergies so far. Considering a final validation of results established in rodent models in the abovementioned animals, especially for treatment efficacy, might be useful before translation into clinical practice.

From a clinical point of view, anaphylaxis remains a mystery in terms of many aspects. The first is the immunization step: why does one individual develop an allergy but not another? Which route is responsible for the sensitization? What are the key factors associated with this? Animal models bred in pathogen-free environments cannot provide answers to these questions, as the experimental conditions do not reflect the complex and changing environments in which humans develop for many years before noticing symptoms. The second is the endotype of the reaction and the mediators involved. In this regard, animal models might be particularly useful, especially for improving basic molecular knowledge, the analysis of the different pathways involved, and evaluating how receptor polymorphisms and genetic variations can modulate the reaction. For instance, knockout mouse models are useful to study the importance of specific genes in different pathways (IgE/IgG-mediated) and to conduct investigations at the cellular and molecular level (e.g., mast cell activation and the quantification of histamine/PAF release).

Finally, evaluating new treatments for anaphylaxis is particularly challenging in humans as anaphylaxis events are rare and mostly unpredictable, and because treatment must be administered in a life-threatening emergency setting. Controversies also remain as to the use of adjuvant vasopressors [94], such as methylene blue [32] or vasopressin, in humans [33], which can be of major help in patients presenting with refractory anaphylaxis.

8. Conclusions

Given the challenges of analyzing the mechanisms involved in human anaphylaxis, animal models have been established to replicate human anaphylaxis and reproduce its pathophysiology. In mouse models, monitoring tools such as rectal temperature, quantitative activity scales, and diarrhea occurrence are routinely used to assess an allergic response. Rats offer an ease of invasive measurements, especially regarding hemodynamic, respiratory, and cerebral oxygenation evaluation. Their use is crucial particularly in assessing treatment efficacy and its effects on cerebral oxygenation, cardiac output, and vascular leakage. Sensitization procedures in animal models depend on various factors, including the administration route, antigen concentration, use of adjuvants, and genetic background, to induce clinical responses that resemble IgE-mediated food and drug allergies in humans. Overall, animal models provide valuable insights into the pathophysiology of anaphylaxis and are essential for testing potential therapies and developing preventive measures for this life-threatening condition.

Author Contributions: All authors performed the literature research, the study conceptualization, and the review and editing of the manuscript. A.G.-C. performed the original draft writing. All authors have read and agreed to the published version of the manuscript.

Funding: This research received no external funding.

Institutional Review Board Statement: Not applicable.

Informed Consent Statement: Not applicable.

Data Availability Statement: Not applicable.

Acknowledgments: A.D. is a recipient of a doctoral fellowship from Sorbonne Université, Paris, France.

Conflicts of Interest: P.B. is a paid consultant for Regeneron Pharmaceuticals. The other authors have no financial conflicts of interest.

References

1. Miller, R.L.; Shtessel, M.; Robinson, L.B.; Banerji, A. Advances in Drug Allergy, Urticaria, Angioedema and Anaphylaxis in 2018. *J. Allergy Clin. Immunol.* **2019**, *144*, 381–392. [CrossRef] [PubMed]
2. Turner, P.J.; Worm, M.; Ansotegui, I.J.; El-Gamal, Y.; Rivas, M.F.; Fineman, S.; Geller, M.; Gonzalez-Estrada, A.; Greenberger, P.A.; Tanno, L.K.; et al. Time to revisit the definition and clinical criteria for anaphylaxis? *World Allergy Organ. J.* **2019**, *12*, 100066. [CrossRef] [PubMed]
3. Sampson, H.A. Anaphylaxis and emergency treatment. *Pediatrics* **2003**, *111*, 1601–1608. [CrossRef] [PubMed]
4. Cardona, V.; Ansotegui, I.J.; Ebisawa, M.; El-Gamal, Y.; Rivas, M.F.; Fineman, S.; Geller, M.; Gonzalez-Estrada, A.; Greenberger, P.A.; Borges, M.S.; et al. World Allergy Organization Anaphylaxis Guidance 2020. *World Allergy Organ. J.* **2020**, *13*, 100472. [CrossRef]
5. Hanschmann, T.; Francuzik, W.; Dölle-Bierke, S.; Hofmeier, K.S.; Grabenhenrich, L.; Ruëff, F.; Renaudin, J.-M.; Pföhler, C.; Treudler, R.; Bilò, M.B.; et al. Different phenotypes of drug-induced anaphylaxis-Data from the European Anaphylaxis Registry. *Allergy* **2023**, *78*, 1615–1627. [CrossRef]
6. Evora, P.R.; Simon, M.R. Role of nitric oxide production in anaphylaxis and its relevance for the treatment of anaphylactic hypotension with methylene blue. *Ann. Allergy Asthma Immunol.* **2007**, *99*, 306–313. [CrossRef]
7. Dünser, M.W.; Mayr, A.J.; Ulmer, H.; Ritsch, N.; Knotzer, H.; Pajk, W.; Luckner, G.; Mutz, N.J.; Hasibeder, W.R. The effects of vasopressin on systemic hemodynamics in catecholamine-resistant septic and postcardiotomy shock: A retrospective analysis. *Anesth Analg* **2001**, *93*, 7–13. [CrossRef]
8. Guerci, P.; Tacquard, C.; Chenard, L.; Millard, D.; Soufir, L.; Malinovsky, J.-M.; Garot, M.; Lalot, J.-M.; Besch, G.; Louis, G.; et al. Epidemiology and outcome of patients admitted to intensive care after anaphylaxis in France: A retrospective multicentre study. *Br. J. Anaesth.* **2020**, *125*, 1025–1033. [CrossRef]
9. Finkelman, F.D. Anaphylaxis: Lessons from mouse models. *J. Allergy Clin. Immunol.* **2007**, *120*, 506–515. [CrossRef]
10. Strait, R.T.; Morris, S.C.; Yang, M.; Qu, X.-W.; Finkelman, F.D. Pathways of anaphylaxis in the mouse. *J. Allergy Clin. Immunol.* **2002**, *109*, 658–668. [CrossRef]
11. Jönsson, F.; de Chaisemartin, L.; Granger, V.; Gouel-Chéron, A.; Gillis, C.M.; Zhu, Q.; Dib, F.; Nicaise-Roland, P.; Ganneau, C.; Hurtado-Nedelec, M.; et al. An IgG-induced neutrophil activation pathway contributes to human drug-induced anaphylaxis. *Sci. Transl. Med.* **2019**, *11*, eaat1479. [CrossRef] [PubMed]
12. Padlan, E.A. Anatomy of the antibody molecule. *Mol. Immunol.* **1994**, *31*, 169–217. [CrossRef] [PubMed]
13. Wang, Y.; Krémer, V.; Iannascoli, B.; Goff, O.R.-L.; Mancardi, D.A.; Ramke, L.; de Chaisemartin, L.; Bruhns, P.; Jönsson, F. Specificity of mouse and human Fcgamma receptors and their polymorphic variants for IgG subclasses of different species. *Eur. J. Immunol.* **2022**, *52*, 753–759. [CrossRef] [PubMed]
14. Mancardi, D.A.; Iannascoli, B.; Hoos, S.; England, P.; Daeron, M.; Bruhns, P. FcgammaRIV is a mouse IgE receptor that resembles macrophage FcepsilonRI in humans and promotes IgE-induced lung inflammation. *J. Clin. Investig.* **2008**, *118*, 3738–3750. [CrossRef] [PubMed]
15. Bruhns, P.; Jönsson, F. Mouse and human FcR effector functions. *Immunol. Rev.* **2015**, *268*, 25–51. [CrossRef]
16. Hakimi, J.; Seals, C.; Kondas, J.A.; Pettine, L.; Danho, W.; Kochan, J. The alpha subunit of the human IgE receptor (FcERI) is sufficient for high affinity IgE binding. *J. Biol. Chem.* **1990**, *265*, 22079–22081. [CrossRef]
17. Dejoux, A.; de Chaisemartin, L.; Bruhns, P.; Longrois, D.; Gouel-Chéron, A. Neuromuscular blocking agent induced hypersensitivity reaction exploration: An update. *Eur. J. Anaesthesiol.* **2022**, *40*, 95–104. [CrossRef]
18. Lieberman, P.; Garvey, L.H. Mast Cells and Anaphylaxis. *Curr. Allergy Asthma Rep.* **2016**, *16*, 20. [CrossRef]
19. Galli, S.J.; Tsai, M. IgE and mast cells in allergic disease. *Nat. Med.* **2012**, *18*, 693–704. [CrossRef] [PubMed]
20. Mackay, G.A.; Fernandopulle, N.A.; Ding, J.; McComish, J.; Soeding, P.F. Antibody or Anybody? Considering the Role of MRGPRX2 in Acute Drug-Induced Anaphylaxis and as a Therapeutic Target. *Front. Immunol.* **2021**, *12*, 688930. [CrossRef]

21. Kounis, N.G.; Mazarakis, A.; Bardousis, C.; Patsouras, N. The heart and coronary arteries as primary target in severe allergic reactions: Cardiac troponins and the Kounis hypersensitivity-associated acute coronary syndrome. *Int. J. Cardiol.* **2015**, *198*, 83–84. [CrossRef]
22. Pichler, W.J. Immune pathomechanism and classification of drug hypersensitivity. *Allergy* **2019**, *74*, 1457–1471. [CrossRef]
23. Piacentini, G.L.; Bertolini, A.; Spezia, E.; Piscione, T.; Boner, A.L. Ability of a new infant formula prepared from partially hydrolyzed bovine whey to induce anaphylactic sensitization: Evaluation in a guinea pig model. *Allergy* **1994**, *49*, 361–364. [CrossRef]
24. Buchanan, B.B.; Frick, O.L. The dog as a model for food allergy. *Ann. N. Y. Acad. Sci.* **2002**, *964*, 173–183. [CrossRef] [PubMed]
25. Ladics, G.S.; Knippels, L.M.J.; Penninks, A.H.; Bannon, G.A.; Goodman, R.E.; Herouet-Guicheney, C. Review of animal models designed to predict the potential allergenicity of novel proteins in genetically modified crops. *Regul. Toxicol. Pharmacol.* **2010**, *56*, 212–224. [CrossRef] [PubMed]
26. Helm, R.M.; Furuta, G.T.; Stanley, J.S.; Ye, J.; Cockrell, G.; Connaughton, C.; Simpson, P.; Bannon, G.A.; Burks, A.W. A neonatal swine model for peanut allergy. *J. Allergy Clin. Immunol.* **2002**, *109*, 136–142. [CrossRef] [PubMed]
27. Helm, R.M.; Ermel, R.W.; Frick, O.L. Nonmurine animal models of food allergy. *Environ. Health Perspect.* **2003**, *111*, 239–244. [CrossRef] [PubMed]
28. McClain, S.; Bannon, G.A. Animal models of food allergy: Opportunities and barriers. *Curr. Allergy Asthma Rep.* **2006**, *6*, 141–144. [CrossRef] [PubMed]
29. Ahrens, R.; Osterfeld, H.; Wu, D.; Chen, C.-Y.; Arumugam, M.; Groschwitz, K.; Strait, R.; Wang, Y.-H.; Finkelman, F.D.; Hogan, S.P. Intestinal mast cell levels control severity of oral antigen-induced anaphylaxis in mice. *Am. J. Pathol.* **2012**, *180*, 1535–1546. [CrossRef]
30. Zheng, F.; Copotoiu, R.; Tacquard, C.; Demoulin, B.; Malinovsky, J.M.; Levy, B.; Longrois, D.; Barthel, G.; Mertes, P.M.; Marchal, F.; et al. Epinephrine but not vasopressin attenuates the airway response to anaphylactic shock in rats. *Exp. Lung Res.* **2017**, *43*, 158–166. [CrossRef]
31. Davidson, J.; Zheng, F.; Tajima, K.; Barthel, G.; Alb, I.; Tabarna, A.; Thornton, S.N.; Lambert, M.; Longrois, D.; Audibert, G.; et al. Anaphylactic Shock Decreases Cerebral Blood Flow More Than What Would Be Expected from Severe Arterial Hypotension. *Shock* **2012**, *38*, 429–435. [CrossRef] [PubMed]
32. Zheng, F.; Barthel, G.; Collange, O.; Montémont, C.; Thornton, S.N.; Longrois, D.; Levy, B.; Audibert, G.; Malinovsky, J.-M.; Mertes, P.-M. Methylene blue and epinephrine: A synergetic association for anaphylactic shock treatment. *Crit. Care Med.* **2013**, *41*, 195–204. [CrossRef]
33. Zheng, F.; Collange, O.; Davidson, J.; Barthel, G.; Oulehri, W.; Thornton, S.N.; Longrois, D.; Levy, B.; Audibert, G.; Malinovsky, J.-M.; et al. Epinephrine, compared with arginine vasopressin, is associated with similar haemodynamic effects but significantly improved brain oxygenation in the early phase of anaphylactic shock in rats: An experimental study. *Eur. J. Anaesthesiol.* **2015**, *32*, 563–570. [CrossRef] [PubMed]
34. Dewachter, P.; Jouan-Hureaux, V.; Franck, P.; Menu, P.; de Talancé, N.; Zannad, F.; Laxenaire, M.-C.; Longrois, D.; Mertes, P.M. Anaphylactic Shock: A Form of Distributive Shock without Inhibition of Oxygen Consumption. *Anesthesiology* **2005**, *103*, 40–49. [CrossRef] [PubMed]
35. Tacquard, C.; Oulehri, W.; Collange, O.; Garvey, L.H.; Nicoll, S.; Tuzin, N.; Geny, B.; Mertes, P.M. Treatment with a platelet-activating factor receptor antagonist improves hemodynamics and reduces epinephrine requirements, in a lethal rodent model of anaphylactic shock. *Clin. Exp. Allergy* **2020**, *50*, 383–390. [CrossRef] [PubMed]
36. Lips, D.J.; van der Nagel, T.; Steendijk, P.; Palmen, M.; Janssen, B.J.; van Dantzig, J.-M.; de Windt, L.J.; Doevendans, P.A. Left ventricular pressure-volume measurements in mice: Comparison of closed-chest versus open-chest approach. *Basic Res. Cardiol.* **2004**, *99*, 351–359. [CrossRef]
37. Boura, C.; Caron, A.; Longrois, D.; Mertes, P.M.; Labrude, P.; Menu, P. Volume Expansion with Modified Hemoglobin Solution, Colloids, or Crystalloid After Hemorrhagic Shock in Rabbits: Effects in Skeletal Muscle Oxygen Pressure and Use Versus Arterial Blood Velocity and Resistance. *Shock* **2003**, *19*, 176–182. [CrossRef]
38. Osterfeld, H.; Ahrens, R.; Strait, R.; Finkelman, F.D.; Renauld, J.-C.; Hogan, S.P. Differential roles for the IL-9/IL-9 receptor alpha-chain pathway in systemic and oral antigen-induced anaphylaxis. *J. Allergy Clin. Immunol.* **2010**, *125*, 469–476.e2. [CrossRef]
39. Tomar, S.; Ganesan, V.; Sharma, A.; Zeng, C.; Waggoner, L.; Smith, A.; Kim, C.H.; Licona-Limón, P.; Reinhardt, R.L.; Flavell, R.A.; et al. IL-4-BATF signaling directly modulates IL-9 producing mucosal mast cell (MMC9) function in experimental food allergy. *J. Allergy Clin. Immunol.* **2021**, *147*, 280–295. [CrossRef]
40. Dewachter, P.; Jouan-Hureaux, V.; Lartaud, I.; Bello, G.; de Talancé, N.; Longrois, D.; Mertes, P.M. Comparison of Arginine Vasopressin, Terlipressin, or Epinephrine to Correct Hypotension in a Model of Anaphylactic Shock in Anesthetized Brown Norway Rats. *Anesthesiology* **2006**, *104*, 734–741. [CrossRef]
41. Bellou, A.; Lambert, H.; Gillois, P.; Montémont, C.; Gerard, P.; Vauthier, E.; Sainte-Laudy, J.; Longrois, D.; Guéant, J.L.; Mallié, J.P. Constitutive nitric oxide synthase inhibition combined with histamine and serotonin receptor blockade improves the initial ovalbumin-induced arterial hypotension but decreases the survival time in brown norway rats anaphylactic shock. *Shock* **2003**, *19*, 71–78. [CrossRef]

42. Todorova, B.; Godon, O.; Conde, E.; Gillis, C.M.; Iannascoli, B.; Richard-Le Goff, O.; Fiole, D.; Roumenina, L.T.; Leusen, J.H.W.; Murphy, A.J.; et al. IgG Subclass-Dependent Pulmonary Antigen Retention during Acute IgG-Dependent Systemic Anaphylaxis in Mice. *J. Immunol.* **2022**, *209*, 1243–1251. [CrossRef]
43. McDole, J.R.; Wheeler, L.W.; McDonald, K.G.; Wang, B.; Konjufca, V.; Knoop, K.A.; Newberry, R.D.; Miller, M.J. Goblet cells deliver luminal antigen to CD103+ dendritic cells in the small intestine. *Nature* **2012**, *483*, 345–349. [CrossRef] [PubMed]
44. Oyoshi, M.K.; Elkhal, A.; Scott, J.E.; Wurbel, M.-A.; Hornick, J.L.; Campbell, J.J.; Geha, R.S. Epicutaneous challenge of orally immunized mice redirects antigen-specific gut-homing T cells to the skin. *J. Clin. Investig.* **2011**, *121*, 2210–2220. [CrossRef] [PubMed]
45. Li, X.-M.; Serebrisky, D.; Lee, S.-Y.; Huang, C.-K.; Bardina, L.; Schofield, B.H.; Stanley, J.S.; Burks, A.W.; Bannon, G.A.; Sampson, H.A. A murine model of peanut anaphylaxis: T- and B-cell responses to a major peanut allergen mimic human responses. *J. Allergy Clin. Immunol.* **2000**, *106*, 150–158. [CrossRef] [PubMed]
46. Hussain, M.; Borcard, L.; Walsh, K.P.; Pena Rodriguez, M.; Mueller, C.; Kim, B.S.; Kubo, M.; Artis, D.; Noti, M. Basophil-derived IL-4 promotes epicutaneous antigen sensitization concomitant with the development of food allergy. *J. Allergy Clin. Immunol.* **2018**, *141*, 223–234.e5. [CrossRef] [PubMed]
47. Noti, M.; Kim, B.S.; Siracusa, M.C.; Rak, G.D.; Kubo, M.; Moghaddam, A.E.; Sattentau, Q.A.; Comeau, M.R.; Spergel, J.M.; Artis, D. Exposure to food allergens through inflamed skin promotes intestinal food allergy through the thymic stromal lymphopoietin–basophil axis. *J. Allergy Clin. Immunol.* **2014**, *133*, 1390–1399.e6. [CrossRef] [PubMed]
48. Spergel, J.M.; Mizoguchi, E.; Brewer, J.P.; Martin, T.R.; Bhan, A.K.; Geha, R.S. Epicutaneous sensitization with protein antigen induces localized allergic dermatitis and hyperresponsiveness to methacholine after single exposure to aerosolized antigen in mice. *J. Clin. Investig.* **1998**, *101*, 1614–1622. [CrossRef]
49. Bartnikas, L.M.; Gurish, M.F.; Burton, O.T.; Leisten, S.; Janssen, E.; Oettgen, H.C.; Beaupré, J.; Lewis, C.N.; Austen, K.F.; Schulte, S.; et al. Epicutaneous sensitization results in IgE-dependent intestinal mast cell expansion and food-induced anaphylaxis. *J. Allergy Clin. Immunol.* **2013**, *131*, 451–460.e6. [CrossRef]
50. Yu, R.; Igawa, K.; Handa, Y.; Munetsugu, T.; Satoh, T.; Yokozeki, H. Basophils and mast cells are crucial for reactions due to epicutaneous sensitization to ovalbumin. *Exp. Dermatol.* **2017**, *26*, 778–784. [CrossRef]
51. Muto, T.; Fukuoka, A.; Kabashima, K.; Ziegler, S.F.; Nakanishi, K.; Matsushita, K.; Yoshimoto, T. The role of basophils and proallergic cytokines, TSLP and IL-33, in cutaneously sensitized food allergy. *Int. Immunol.* **2014**, *26*, 539–549. [CrossRef] [PubMed]
52. Fox, A.T.; Sasieni, P.; Du, T.G.; Syed, H.; Lack, G. Household peanut consumption as a risk factor for the development of peanut allergy. *J. Allergy Clin. Immunol.* **2009**, *123*, 417–423. [CrossRef] [PubMed]
53. Repa, A.; Wild, C.; Hufnagl, K.; Winkler, B.; Bohle, B.; Pollak, A.; Wiedermann, U. Influence of the route of sensitization on local and systemic immune responses in a murine model of type I allergy. *Clin. Exp. Immunol.* **2004**, *137*, 12–18. [CrossRef] [PubMed]
54. Jonsson, F.; Mancardi, D.A.; Kita, Y.; Karasuyama, H.; Iannascoli, B.; Van Rooijen, N.; Shimizu, T.; Daeron, M.; Bruhns, P. Mouse and human neutrophils induce anaphylaxis. *J. Clin. Investig.* **2011**, *121*, 1484–1496. [CrossRef]
55. Liu, C.; Chen, C.; Yan, X.; Gu, S.; Jia, X.; Fu, W.; Meng, X.; Xue, W. Assessment of immune responses and intestinal flora in BALB/c mice model of wheat food allergy via different sensitization methods. *Food Sci. Hum. Wellness* **2023**, *12*, 871–881. [CrossRef]
56. Mine, Y.; Yang, M. Epitope characterization of ovalbumin in BALB/c mice using different entry routes. *Biochim. Biophys. Acta* **2007**, *1774*, 200–212. [CrossRef]
57. Yoo, J.; Manicone, A.M.; McGuire, J.K.; Wang, Y.; Parks, W.C. Systemic sensitization with the protein allergen ovalbumin augments local sensitization in atopic dermatitis. *J. Inflamm. Res.* **2014**, *7*, 29–38. [CrossRef]
58. Liu, Y.; Sun, Y.; Chang, L.-J.; Li, N.; Li, H.; Yu, Y.; Bryce, P.J.; Grammer, L.C.; Schleimer, R.P.; Zhu, D. Blockade of peanut allergy with a novel Ara h 2-Fcγ fusion protein in mice. *J. Allergy Clin. Immunol.* **2013**, *131*, 213–221.e5. [CrossRef]
59. Dombrowicz, D.; Flamand, V.; Brigman, K.K.; Koller, B.H.; Kinet, J.P. Abolition of anaphylaxis by targeted disruption of the high affinity immunoglobulin E receptor alpha chain gene. *Cell* **1993**, *75*, 969–976. [CrossRef]
60. Jo, S.K.; Ahn, B.-E.; Choi, E.H.; Kang, J.E.; An, H.; Oh, M.; Rhie, G. Evaluation of the protective efficacy of recombinant protective antigen vaccine (GC1109)-immunized human sera using passive immunization in a mouse model. *Vaccine* **2020**, *38*, 1586–1588. [CrossRef]
61. Paolucci, M.; Homère, V.; Waeckerle-Men, Y.; Wuillemin, N.; Bieli, D.; Pengo, N.; Sonati, T.; Kündig, T.M.; Johansen, P. Strain matters in mouse models of peanut-allergic anaphylaxis: Systemic IgE-dependent and Ara h 2-dominant sensitization in C3H mice. *Clin. Exp. Allergy* **2023**, *53*, 550–560. [CrossRef] [PubMed]
62. Galli, S.J. Pathogenesis and management of anaphylaxis: Current status and future challenges. *J. Allergy Clin. Immunol.* **2005**, *115*, 571–574. [CrossRef]
63. Miyajima, I.; Dombrowicz, D.; Martin, T.R.; Ravetch, J.V.; Kinet, J.P.; Galli, S.J. Systemic anaphylaxis in the mouse can be mediated largely through IgG1 and Fc gammaRIII. Assessment of the cardiopulmonary changes, mast cell degranulation, and death associated with active or IgE- or IgG1-dependent passive anaphylaxis. *J. Clin. Investig.* **1997**, *99*, 901–914. [CrossRef]
64. Baniyash, M.; Eshhar, Z. Inhibition of IgE binding to mast cells and basophils by monoclonal antibodies to murine IgE. *Eur. J. Immunol.* **1984**, *14*, 799–807. [CrossRef]
65. Ohtsu, H. Histamine synthesis and lessons learned from histidine decarboxylase deficient mice. *Adv. Exp. Med. Biol.* **2010**, *709*, 21–31. [CrossRef]

66. Bruhns, P. Properties of mouse and human IgG receptors and their contribution to disease models. *Blood* **2012**, *119*, 5640–5649. [CrossRef] [PubMed]
67. Tsujimura, Y.; Obata, K.; Mukai, K.; Shindou, H.; Yoshida, M.; Nishikado, H.; Kawano, Y.; Minegishi, Y.; Shimizu, T.; Karasuyama, H. Basophils play a pivotal role in immunoglobulin-G-mediated but not immunoglobulin-E-mediated systemic anaphylaxis. *Immunity* **2008**, *28*, 581–589. [CrossRef]
68. Forbes, E.E.; Groschwitz, K.; Abonia, J.P.; Brandt, E.B.; Cohen, E.; Blanchard, C.; Ahrens, R.; Seidu, L.; McKenzie, A.; Strait, R.; et al. IL-9- and mast cell-mediated intestinal permeability predisposes to oral antigen hypersensitivity. *J. Exp. Med.* **2008**, *205*, 897–913. [CrossRef] [PubMed]
69. Brandt, E.B.; Strait, R.T.; Hershko, D.; Wang, Q.; Muntel, E.E.; Scribner, T.A.; Zimmermann, N.; Finkelman, F.D.; Rothenberg, M.E. Mast cells are required for experimental oral allergen-induced diarrhea. *J. Clin. Investig.* **2003**, *112*, 1666–1677. [CrossRef] [PubMed]
70. Birmingham, N.P.; Parvataneni, S.; Hassan, H.M.A.; Harkema, J.; Samineni, S.; Navuluri, L.; Kelly, C.J.; Gangur, V. An adjuvant-free mouse model of tree nut allergy using hazelnut as a model tree nut. *Int. Arch. Allergy Immunol.* **2007**, *144*, 203–210. [CrossRef]
71. Birmingham, N.; Gangur, V.; Samineni, S.; Navuluri, L.; Kelly, C. Hazelnut Allergy: Evidence that hazelnut can directly elicit specific IgE antibody response via activating type 2 cytokines in mice. *Int. Arch. Allergy Immunol.* **2005**, *137*, 295–302. [CrossRef] [PubMed]
72. Fish, S.C.; Donaldson, D.D.; Goldman, S.J.; Williams, C.M.M.; Kasaian, M.T. IgE generation and mast cell effector function in mice deficient in IL-4 and IL-13. *J. Immunol.* **2005**, *174*, 7716–7724. [CrossRef]
73. Chen, C.-Y.; Lee, J.-B.; Liu, B.; Ohta, S.; Wang, P.-Y.; Kartashov, A.V.; Mugge, L.; Abonia, J.P.; Barski, A.; Izuhara, K.; et al. Induction of Interleukin-9-Producing Mucosal Mast Cells Promotes Susceptibility to IgE-Mediated Experimental Food Allergy. *Immunity* **2015**, *43*, 788–802. [CrossRef] [PubMed]
74. Komai-Koma, M.; Brombacher, F.; Pushparaj, P.N.; Arendse, B.; McSharry, C.; Alexander, J.; Chaudhuri, R.; Thomson, N.C.; McKenzie, A.N.J.; McInnes, I.; et al. Interleukin-33 amplifies IgE synthesis and triggers mast cell degranulation via interleukin-4 in naïve mice. *Allergy* **2012**, *67*, 1118–1126. [CrossRef] [PubMed]
75. Wong, M.-X.; Roberts, D.; Bartley, P.A.; Jackson, D.E. Absence of platelet endothelial cell adhesion molecule-1 (CD31) leads to increased severity of local and systemic IgE-mediated anaphylaxis and modulation of mast cell activation. *J. Immunol.* **2002**, *168*, 6455–6462. [CrossRef]
76. Fung-Leung, W.P.; De Sousa-Hitzler, J.; Ishaque, A.; Zhou, L.; Pang, J.; Ngo, K.; Panakos, J.A.; Chourmouzis, E.; Liu, F.T.; Lau, C.Y. Transgenic mice expressing the human high-affinity immunoglobulin (Ig) E receptor alpha chain respond to human IgE in mast cell degranulation and in allergic reactions. *J. Exp. Med.* **1996**, *183*, 49–56. [CrossRef]
77. Ujike, A.; Ishikawa, Y.; Ono, M.; Yuasa, T.; Yoshino, T.; Fukumoto, M.; Ravetch, J.V.; Takai, T. Modulation of immunoglobulin (Ig)E-mediated systemic anaphylaxis by low-affinity Fc receptors for IgG. *J. Exp. Med.* **1999**, *189*, 1573–1579. [CrossRef]
78. Mathias, C.B.; Hobson, S.A.; Garcia-Lloret, M.; Lawson, G.; Poddighe, D.; Freyschmidt, E.-J.; Xing, W.; Gurish, M.F.; Chatila, T.A.; Oettgen, H.C. IgE-mediated systemic anaphylaxis and impaired tolerance to food antigens in mice with enhanced IL-4 receptor signaling. *J. Allergy Clin. Immunol.* **2011**, *127*, 795–805.e6. [CrossRef]
79. Rivas, M.N.; Burton, O.T.; Wise, P.; Zhang, Y.; Hobson, S.A.; Lloret, M.G.; Chehoud, C.; Kuczynski, J.; DeSantis, T.; Warrington, J.; et al. A microbiota signature associated with experimental food allergy promotes allergic sensitization and anaphylaxis. *J. Allergy Clin. Immunol.* **2013**, *131*, 201–212. [CrossRef]
80. Zhou, J.S.; Sandomenico, A.; Severino, V.; Burton, O.T.; Darling, A.; Oettgen, H.C.; Ruvo, M. An IgE receptor mimetic peptide (PepE) protects mice from IgE mediated anaphylaxis. *Mol. Biosyst.* **2013**, *9*, 2853–2859. [CrossRef]
81. Burton, O.T.; Stranks, A.J.; Tamayo, J.M.; Koleoglou, K.J.; Schwartz, L.B.; Oettgen, H.C. A humanized mouse model of anaphylactic peanut allergy. *J. Allergy Clin. Immunol.* **2017**, *139*, 314–322.e9. [CrossRef]
82. Pagovich, O.E.; Wang, B.; Chiuchiolo, M.J.; Kaminsky, S.M.; Sondhi, D.; Jose, C.L.; Price, C.C.; Brooks, S.F.; Mezey, J.G.; Crystal, R.G. Anti-hIgE gene therapy of peanut-induced anaphylaxis in a humanized murine model of peanut allergy. *J. Allergy Clin. Immunol.* **2016**, *138*, 1652–1662. [CrossRef]
83. Bryce, P.J.; Falahati, R.; Kenney, L.L.; Leung, J.; Bebbington, C.; Tomasevic, N.; Krier, R.A.; Hsu, C.-L.; Shultz, L.D.; Greiner, D.L.; et al. Humanized mouse model of mast cell-mediated passive cutaneous anaphylaxis and passive systemic anaphylaxis. *J. Allergy Clin. Immunol.* **2016**, *138*, 769–779. [CrossRef]
84. Jonsson, F.; Mancardi, D.A.; Zhao, W.; Kita, Y.; Iannascoli, B.; Khun, H.; van Rooijen, N.; Shimizu, T.; Schwartz, L.B.; Daeron, M.; et al. Human FcgammaRIIA induces anaphylactic and allergic reactions. *Blood* **2012**, *119*, 2533–2544. [CrossRef] [PubMed]
85. Mancardi, D.A.; Albanesi, M.; Jonsson, F.; Iannascoli, B.; Van Rooijen, N.; Kang, X.; England, P.; Daeron, M.; Bruhns, P. The high-affinity human IgG receptor FcgammaRI (CD64) promotes IgG-mediated inflammation, anaphylaxis, and antitumor immunotherapy. *Blood* **2013**, *121*, 1563–1573. [CrossRef] [PubMed]
86. Gillis, C.M.; Jönsson, F.; Mancardi, D.A.; Tu, N.; Beutier, H.; Van Rooijen, N.; Macdonald, L.E.; Murphy, A.J.; Bruhns, P. Mechanisms of anaphylaxis in human low-affinity IgG receptor locus knock-in mice. *J. Allergy Clin. Immunol.* **2017**, *139*, 1253–1265.e14. [CrossRef] [PubMed]
87. Smith, P.; DiLillo, D.J.; Bournazos, S.; Li, F.; Ravetch, J.V. Mouse model recapitulating human Fcγ receptor structural and functional diversity. *Proc. Natl. Acad. Sci. USA* **2012**, *109*, 6181–6186. [CrossRef]

88. Li, X.; Huang, C.K.; Schofield, B.H.; Burks, A.W.; Bannon, G.A.; Kim, K.H.; Huang, S.K.; Sampson, H.A. Strain-dependent induction of allergic sensitization caused by peanut allergen DNA immunization in mice. *J. Immunol.* **1999**, *162*, 3045–3052. [CrossRef]
89. Arumugam, M.; Ahrens, R.; Osterfeld, H.; Kottyan, L.C.; Shang, X.; Maclennan, J.A.; Zimmermann, N.; Zheng, Y.; Finkelman, F.D.; Hogan, S.P. Increased susceptibility of 129SvEvBrd mice to IgE-Mast cell mediated anaphylaxis. *BMC Immunol.* **2011**, *12*, 14. [CrossRef]
90. Kreis, M.E.; Mueller, M.H.; Reber, D.; Glatzle, J.; Enck, P.; Grundy, D. Stress-induced attenuation of brain stem activation following intestinal anaphylaxis in the rat. *Neurosci Lett.* **2003**, *345*, 187–191. [CrossRef]
91. Sun, N.; Zhou, C.; Pu, Q.; Wang, J.; Huang, K.; Che, H. Allergic reactions compared between BN and Wistar rats after oral exposure to ovalbumin. *J. Immunotoxicol* **2013**, *10*, 67–74. [CrossRef] [PubMed]
92. Wex, E.; Thaler, E.; Blum, S.; Lamb, D. A novel model of IgE-mediated passive pulmonary anaphylaxis in rats. *PLoS ONE* **2014**, *9*, e116166. [CrossRef] [PubMed]
93. Buras, J.A.; Holzmann, B.; Sitkovsky, M. Animal Models of sepsis: Setting the stage. *Nat. Rev. Drug. Discov.* **2005**, *4*, 854–865. [CrossRef] [PubMed]
94. Garvey, L.H.; Dewachter, P.; Hepner, D.L.; Mertes, P.M.; Voltolini, S.; Clarke, R.; Cooke, P.; Garcez, T.; Guttormsen, A.B.; Ebo, D.G.; et al. Management of suspected immediate perioperative allergic reactions: An international overview and consensus recommendations. *Br. J. Anaesth.* **2019**, *123*, e50–e64. [CrossRef] [PubMed]